Beyond the white

BEYOND THE WHITE

Effects of the titanium dioxide food additive E171
on the development of colorectal cancer

Héloïse Proquin

Layout: Héloïse Proquin

Cover design: Héloïse Proquin & Chloë Romengas

Printed by: Gildeprint

ISBN: 978-94-9301-461-9

BEYOND THE WHITE

Effects of the titanium dioxide food additive E171 on the development of colorectal cancer

DISSERTATION

to obtain the degree of Doctor at Maastricht University,
on the authority of the Rector Magnificus, Prof. dr. Rianne M. Letschert
with the decision of the Board of Deans, to be defended in public on
Friday 2nd November 2018 at 10 hours

by

Héloïse Audrey Adélaïde Proquin

born on 7th September 1988, in La Roche-sur-Yon (France)

Promotors

Prof. Dr. H. van Loveren

Prof. Dr. T.M.C.M. de Kok

Co-promotor

Dr. J.J. Briedé

Assessment committee

Prof. dr. C.T.A. Evelo (UM; chairman)

Prof. dr. A. Opperhuizen (UM)

Dr. M. Heringa (RIVM)

Prof. dr. J.C.S. Kleinjans (UM)

Dr. A.A. van Bodegraven (Zuyderland hospital)

The research described in this thesis was conducted at GROW School of Oncology and Developmental Biology of Maastricht University.

Contents

Chapter 1

Introduction and aim of the thesis

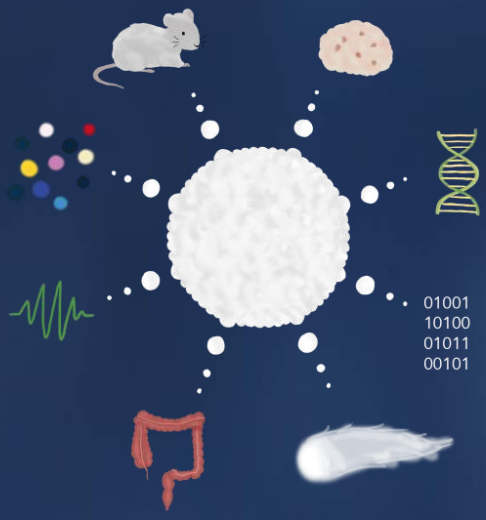

I- What is titanium dioxide

I-1- Chemical characteristics and manufacturing of titanium dioxide

The titanium element was discovered in 1791 by William Gregor but its final name was given 4 years later by Martin H. Klaproth in analogy with the titans of the Greek mythology (1). While Martin H. Klaproth was not able to produce the pure element of titanium, he was able to manufacture TiO_2, or titanium dioxide. TiO_2 was first used as a white pigment in oil paints and started to be mass produced in the beginning of the 20th century.

The main existing crystalline forms of TiO_2 are rutile, anatase, and brookite. Rutile is the most stable form, however, anatase and brookite are stable at normal temperature but convert to rutile at a temperature above 550°C and 750°C respectively (2). Anatase is the major form used due to its lower production costs as compared to rutile. After being mined, purification of TiO_2 occurs via 2 main manufacture methods: the sulphate process and the chloride route. Anatase pigments can only be produced by the sulphate process. This process consists of digesting ilmenite ($FeTiO_3$) with sulfuric acid to produce $TiOSO_4$. The titanium oxygen sulphate produced is then hydrolysed, resulting in sulfuric acid waste and a precipitate gel containing hydrated TiO_2 ($TiO_2.nH_2O$). Finally, water is removed and the crystals of TiO_2 left are heated at a temperature of 800-850°C to form anatase or at 900−930°C to form rutile (2).

I-2- Use and market value

TiO_2 is used for its unique properties. It is a very stable pigment, has a high refractive index and is resistant to UV radiation (3-6). These properties makes TiO_2 the most used white pigment in many products including paint, food, and personal care products (3,4,6,7). Paints and coatings for housing and industry, commercial printing inks, plastics, and paper contribute to 94% of the total demand for TiO_2 in the European Union (EU). The remaining 6% are the use of TiO_2 in food products, pharmaceuticals, cosmetics, and others. The market value of TiO_2 is € 3 billion with an economic growth of € 560 billion in 2017 with around 8,150 million workers (5). The production is of 33% sold outside of the European Economic Area (5).

In food, TiO_2 is the main white pigment used under the name of E171. Rutile and anatase forms are allowed in food products. The main commercial reasons for its use is that consumers are more likely to buy and eat products that are brighter or more vibrant in colour as they look fresher (5). In addition, TiO_2 delivers exceptional whiteness, opacity, and creamy effects (8). The number of companies using TiO_2 as an ingredient form the largest in food industry in EU with 289,000 companies, 4.25 million workers, and a € 1,048 billion of annual turnover (5).

I-3- Types of food products in which TiO_2 is used

Table 1 shows the variety of products in which TiO_2 is used, ranging from sweets, cookies, sauces to dairy products (3,4,6,9). In dairy products, TiO_2 is authorised by EU in flavoured fermented milk products including heat-treated products (10) and is used to boost natural whiteness and give a milkier structure (8). However, it is not permitted in unflavoured pasteurised and sterilised (including UHT) milk and unflavoured plain pasteurised cream (excluding reduced fat cream) (10). In sweets, TiO_2 has been detected in M&M's®, Skittles®, Mentos®, and many chewing-gums, in cookies in their icing, and in sauces such as mayonnaise. As a non-food product, toothpaste is an additional source of human oral exposure to TiO_2 only considered for children under 6 years old (9). Concentrations of TiO_2 in toothpaste ranged from 0.7 to 5.9 mg/g of product (4,6).

The highest concentrations of TiO_2 were found in milk substitutes, dressings and food supplements, but in some cases, e.g. milk substitutes, sweets, and cheese, high differences in concentrations were detected between the different studies. This might be due to the brand used, as explained in the above studies (3,4,6,9). Differences in concentrations can be very important between the generic and name brand but can also differ between countries.

Table 1: Quantity of TiO_2 in food and food related products found in literature.

Product	Food item	Concentration of mg TiO_2/g product			
		Lomer et al (3)	**Weir et al (6)**	**Peters et al. (4)**	**Rompelberg et al. (9)**
Milk	Raw (cow) milk		$0.25x10^{-3}$		$0.51x10^{-3}$
	Soy milk		$0.29x10^{-3}$		$0.55x10^{-3}$
Milk substitutes/ whiteners	Coffee	2	0. 067		2.739
	Tea	7.5	0.067		
Cheeses	Cottage Cheese	1	0. 001		
Desserts	Ice Cream	1	1		
	Yogurt	1	1		$0.79x10^{-3}$
	Icing for cakes	2	1		$0.38x10^{-3}$
	Sorbet				$0.26x10^{-3}$
	Other dairy	1	1		$0.21x10^{-3}$
Chocolate	Chocolate	2	0. 005	1	
Sweets	Hard, soft and chewing gums	2	2	1.7	$0.42x10^{-3}$
Dressings and sauces	Salad	5	0.2	0.5	$0.72x10^{-3}$
Drinks	Energy drinks (containing caffeine)				$0.11x10^{-3}$
	Soft drink				$0.11x10^{-3}$
	Sports drink				$0.14x10^{-3}$
	Syrup				$0.28x10^{-3}$
Food supplements	Multivitamins				1.242

II- Differences between E171 and TiO_2 nanoparticles (NPs) and microparticles (MPs)

II-1- Size range

The size range of TiO_2 particles found in E171 has been evaluated from material purchased directly from manufacturers or extracted from food products. The assessment was performed by Scanning Electron Microscopy (SEM) or Transmission Electron Microscopy (TEM) and demonstrated a NPs (<100 nm) fraction of 25 to 40% of all material, the remainder being MPs (>100 nm) (6,11-13).

Due to the increasing use of nanomaterials, a definition of NPs was created by the EU in 2011. A commission of recommendation has defined that a nanomaterial is "a natural, incidental or manufactured material containing particles, in an unbound state or as an aggregate or as an agglomerate and where, for 50 % or more of the particles in the number size distribution, one or more external dimensions is in the size range 1 nm-100 nm" (14). Therefore, E171 is not considered as a nanomaterial but it contains a large fraction of NPs.

II-2- Properties of TiO_2 particles

II-2-1- Surface area

One of particularities of the NPs is the higher surface area than the MPs. The surface area is "the total area on the surface of a three-dimensional figure" (15). Consequently, for a given quantity, a decrease in size results in an increase in surface area. For example, for a given cube of 1 cm, the surface area is 6 cm^2, if this cube is filled with little cubes of 1 µm, it would need $1x10^{12}$ cubes and the surface area would be 6.000 cm^2. Furthermore, if this 1 cm cube was filled with 1 nm cubes, it would need $1x10^{21}$ cubes and the surface area would be 60.000.000 cm^2 (600km^2). The small size and the high surface area of the NPs allow more physical contact with any other surface including cellular and subcellular structures and biomolecules.

II-2-2- Agglomeration and aggregation

Attraction between particles can lead to agglomeration and aggregation. By sonication, which agitates the particles with ultrasonic frequencies (>20 kHz), agglomeration is reversible. In contrast, aggregation is an irreversible process by which the particles create a new dense mass of fused particles (16). It is impossible to distinguish between agglomeration and aggregation via conventional techniques such as electron microscopy imaging (SEM, TEM), or dynamic light scattering (DLS), because these techniques only identify the presence and the size of large particle clusters.

Several factors may influence the agglomeration and aggregation of TiO_2 (17). The first factor is the particle properties like the crystallinity, anatase or rutile (18). The second factor is the concentration of these particles; the increase of the concentration increases the size of agglomerates and aggregates (19). The third factor is the properties of cell medium (like ionic strength, composition, pH, viscosity, electrolyte specificity, ion valence, and hydrophobicity) (20) and the amount of foetal bovine serum (FBS); the higher the concentration of FBS, the less aggregation and agglomeration (21,22). The fourth factor is the dispersion protocol; some authors suggest that the increasing collision frequency promotes a low level of agglomeration and aggregation (23).

III- Exposure and kinetics

III-1- Types of exposure

Humans can be exposed to TiO_2 by dermal contact, inhalation, and ingestion. The effects of TiO_2 have been mainly studied after exposure via inhalation. TiO_2 particles were both found to be tumorigenic and genotoxic. In rats, non-malignant tumours were observed after chronic inhalation of ultrafine TiO_2 (24). Furthermore, inhalation of NPs of TiO_2 was found to be tumorigenic in rat lungs after a chronic exposure of 2 years (25).

Skin contact to TiO_2 occurs after using personal care products, such as face cream or sunscreens (6). Sunscreens containing TiO_2 NPs provide an effective barrier against ultraviolet B (UVB) damage to the skin (26). Several studies showed a cytotoxic and inflammatory effect of TiO_2 NPs exposure of keratinocytes (27,28).

Ingestion of TiO_2 occurs every day due to the high number of products to which it is added (Table 1). The quantities ingested by humans were estimated by several studies depending on the UK, US, and Dutch diets (6,9). The authors discriminated exposure of children under 10 years old from adult exposure because the concentrations of TiO_2 in sweets and toothpaste, which are mostly ingested by children, are higher. Measurements in the USA and the Netherlands showed comparable ranges of exposure. The exposure in US children <10 years old is on average estimated at 1-2 mg TiO_2/kg_{bw}/day and above 10 years 0.2-0.7 mg TiO_2/kg_{bw}/day (6). In the Netherlands, the authors estimated a mean average exposure to be 0.67 mg TiO_2/kg_{bw}/day between 2-6 years old, 0.17 mg TiO_2/kg_{bw}/day between 7-69 years old, and 0.06 mg TiO_2/kg_{bw}/day above 70 years old (9). These concentrations are exceeded by children under the age of 10 years in the UK who are on average exposed to 2-3 mg TiO_2/kg_{bw}/day and above 10 years old to 1 mg TiO_2/kg_{bw}/day (6). In addition, in the re-evaluation of TiO_2 as a food additive performed by the European Food Safety Authority (EFSA) in 2016, a new estimation of average ingestion was performed (29). This estimation was based on a non-brand-loyal scenario which assumes that the population is exposed to the mean reported use/analytical levels of TiO_2 in 14 food categories for a long period of time. In this scenario validated by the EFSA, it has been estimated that the mean exposure ranged from 0.2 mg/kg_{bw}/day for infants (from 12 weeks to 11 months) and elderly (>65 years old) to 5.5 mg/kg_{bw}/day for children (3 to 9 years old). At the 95th percentile, EFSA estimates the exposure ranged from 0.5 mg/kg_{bw}/day for the elderly to 14.8 mg/kg_{bw}/day for children.

III-2- Gastrointestinal uptake of TiO_2

After ingestion, TiO_2 reaches the gastrointestinal track and exposure occurs on the constituent cells like enterocytes, mucus-secreting goblet cells, and microfold cells (M-cells). In a monoculture of Caco-2 cells, accumulation of TiO_2 NPs was observed after 2h exposure and reach saturation after 8h (30). In addition, the presence of TiO_2 NPs in the cytoplasm of the cell as well as the nucleus was observed in human epidermal cells (A431) (31). Accumulation in the cytoplasm and in vesicles was also observed in human amnion epithelial (WISH) cells (32). A higher accumulation of TiO_2 was observed in a co-culture of Caco-2 (enterocytes) with goblet cells or Caco-2 with M-cells, a 50-fold increase and a 100-fold increase of accumulation in the cells of TiO_2 NPs was observed respectively as compared to a monoculture of Caco-2 cells (33). The uptake of TiO_2 by these cells mainly occurs through M-cells and goblet cells.

III-3- Translocation to the blood stream after ingestion

After ingestion in rodents, translocation of TiO_2 to the blood stream and other organs has been observed. A majority of these studies have been performed with TiO_2 NPs, the minor part of E171. After ingestion, TiO_2 NPs have been found in liver, spleen, testis, thyroid, lungs as well as plasma (33-39). Three studies describe the presence of TiO_2 NPs in the liver after oral administration of 250 and 500 mg/kg_{bw}/day for 14 days in mice (34), 2 weeks after a single dose of 5 g/kg in mice (35), and in rats after 2, 10 and 50 mg/kg_{bw}/day for 30 and 90 days (36). Accumulation in the liver as well as in the spleen has been observed post-mortem in 15 humans (38). In rats, accumulation in the spleen has been identified after TiO_2 NPs ingestion of 1 and 2 mg/kg_{bw}/day for 5 days (37). The latter study also found accumulation of NPs in ovaries and testis. Another study described accumulation of NPs in testis after intravenous injection of 5, 25, and 50 mg/kg for 30 days (39). Biodistribution of TiO_2 MPs has been assessed *in vivo* in mice. Two weeks after a single dose of 5 g/kg, the particles were found in brain, kidney, and liver (35). Evidence of absorption and translocation of TiO_2 in the form of E171 in the blood stream have also been shown by Bettini et al. in rats (40). They detected E171 in the liver after one week of treatment exhibiting a systemic absorption of E171 as previously shown for the MPs and NPs fraction. In humans, translocation to the blood stream has been observed 6h after ingestion of 100 mg of pharmaceutical/food-grade TiO_2 (41).

IV- Evidence of adverse effects

TiO_2 is shown to be taken up by gastrointestinal cells and translocated to the blood stream. Consequently, the cells come in contact with the particles and adverse effects can ensue from this interaction such as inflammation, DNA damage, effects on the immune system, and development of cancer. These observed effects after exposure to different sizes of TiO_2 are described below.

IV-1- In vivo

IV-1-1- Inflammation and oxidative stress

Potential adverse effects of ingestion of TiO_2 *in vivo* have been studied in rodents, generally focussing on the anatase NPs fraction of E171. After ingestion of 50 and 100 mg/kg_{bw} of TiO_2 NPs in male Wistar rats for 14 days, changes in the serum parameters (total protein, glucose, AST, ALT, and ALP) indicated an induced hepatic damage (42). Inflammatory response via cytokine production or NLRP3 inflammasome in the gut was also observed after exposure of TiO_2 NPs and MPs (100 mg/kg_{bw}/day) for 10 days in mice (43). Another study showed that orally administered TiO_2 NPs worsen colitis in mice through the activation of NLRP3 inflammasome. These results were obtained after ingestion of 50 or 500 mg/kg_{bw}/day of TiO_2 NPs (rutile) in WT and Nlrp3$^{-/-}$ mice; after 8 days WT mice presented a more severe colitis than the Nlrp3$^{-/-}$ mice. In addition, long term oral exposure to 10 mg/kg_{bw}/day of E171 in rats for 100 days showed low-grade inflammation in the colon (40). Increased inflammation in the intestines after exposure to TiO_2 can increase the occurrence of diseases in susceptible persons and exacerbate the symptoms of existing diseases like inflammatory bowel diseases (40,44).

IV-1-2- DNA damage

Studies demonstrate that TiO_2 NPs and MPs can damage DNA directly or indirectly via oxidative stress and/or inflammatory responses (20). Therefore, DNA damage was also assessed in organs after exposure to TiO_2 NPs or MPs, however, this has not been demonstrated after E171 ingestion yet. After ingestion in mice of TiO_2 NPs or MPs from a concentration of 40 to 2000 mg/kg_{bw}/day for 5 to 7 days, single-strand DNA damage was found in liver (200, 500, 1000, and 2000 mg/kg_{bw}/day of TiO_2 NPs) (45-47), bone marrow (40 and 200 mg/kg_{bw}/day of TiO_2 NPs and MPs) (47), and kidneys (500, 1000, and 2000 mg/kg_{bw}/day of TiO_2 NPs) (46). In addition, micronuclei formation was observed in the bone marrow of mice after ingestion of 1000 mg/kg_{bw}/day of TiO_2 MPs for 7 days (47) and in red blood cells after ingestion of 500 mg/kg_{bw}/day of TiO_2 NPs for 5 days (45).

IV-1-3- Immune response

Stimulation of inflammatory processes in the gut can also lead to an immune response from the innate and adaptive immune system. Results indicating a potential reduction of the immune capacity in the gut after TiO_2 ingestion have been reported in one study. This study demonstrated the impact of TiO_2 NPs on the immune response via a potent Th1/Th17 immune response after exposure to 10 mg/kg_{bw}/day in rats (40). Similar results have been observed after ingestion of 10 mg/kg_{bw}/day of TiO_2 in the form of E171 (40).

IV-1-4- Colon cancer

Enhancement of tumour formation in a colorectal cancer model with azoxymethane (AOM) and dextran sodium sulphate (DSS) has been demonstrated after ingestion of 5 mg/kg_{bw}/day of TiO_2 in the form of E171 for 10 weeks in mice (48). In addition, E171 in combination AOM/DSS increased the expression of markers of tumour progression including COX2, Ki67, and β-catenin. In the same study, exposure to E171 solely in normal mice did not develop tumours but induced dysplastic changes in colonic epithelium and a decrease of goblet cells. Another study showed, in a chemically induced carcinogenesis model in rats induced by treatment with 1,2-dimethylhydrazine , that exposure to E171 for 100 days induced preneoplastic lesions as well as the growth of aberrant crypt foci (40).

IV-2- In vitro

IV-2-1- Inflammation and oxidative stress

The capacity of TiO_2 to produce reactive oxygen species (ROS) *in vitro* is well documented for the NPs. ROS production by TiO_2 NPs has been identified in many different cell lines like mouse fibroblast, mouse peritoneal macrophage (RAW 264), goldfish skin cells (GFSk-S1), Caco-2, Caco-2/HT29-MTX, human bronchial epithelial (BEAS-2B), human bronchial fibroblasts (IMR 90) osteoblast, human amnion epithelial (WISH), glial, brain microglia, and human epidermal cells (11,31,32,49-57). The concentrations used for this ROS identification range from 0.5 µg/mL in RAW 264.7 cells (57) to 50 µg/mL in Caco-2 cells (11). The majority of the observations were done after 6h exposure (11,31,51,53), others were done after 20 min (52), 2h (54,56), 4h (57), 24h (11,32,50), and 48h (49,55). MPs of TiO_2 were also found to induce oxidative stress in RAW 264 cells after 4h of exposure (57). ROS formation by TiO_2 in the form of E171 was also observed in Caco-2 and Caco-2/HT29-MTX cells after exposure to 10 µg/mL for 48h and 50 µg/mL for 6h respectively (11) but the contribution of the MPs fraction to identify the most active and potentially the fraction that gives the most adverse effects has not been evaluated.

IV-2-2- DNA damage

In vitro, DNA damage after exposure to TiO_2 NPs has been observed in different cell lines i.e. HepG2, BEAS-2B cells, and WISH cells (32,46,56,58,59). The concentrations used for this identification range from 10 µg/mL in HepG2 and GFSk-S1 cells (46,56) to 100 µg/mL in bone marrow cells (58). There results were observed after 2h (56), 6h (32,46,59), and 24h (58). The capacity of TiO_2 in the form of E171 to induce DNA damage *in vitro* was also determined in Caco-2 and Caco-2/HT29-MTX cells after exposure to 10 µg/mL and 50 µg/mL respectively (11). As for the evaluation of ROS formation, all the different size-ranges were not tested, therefore the contribution of each fraction could not be assessed. Furthermore, Charles et al. evaluated, in a regulatory framework, a number of *in vitro* studies of exposure to anatase TiO_2 NPs with an appropriate level of confidence. These studies must comply with the following criteria: adequate characterization of TiO_2, adequate description of the dispersion and genotoxicity protocols, evidence of cytotoxicity, inclusion of positive and negative results, and use of replicates or independent experiments (20). The 36 studies assessed showed that 58% of the comet assays reported positive results as well as 56% of the micronucleus assay.

IV-2-3- Immune response

As observed *in vivo*, the immune system is one of the mechanisms affected by TiO_2. These adverse effects have been studied on the NPs of TiO_2. Increased levels of TNF-α and IL-6 cytokines were determined on Jurkat and RAW 246.7 cells after exposure to 25 µg/mL for 24h (60). Sukwong et al. suggest that the NPs of TiO_2 interact with the adaptive and innate immune system via T-cell receptors and TLR respectively. Another study showed that TiO_2 NPs (128 µg/mL; 48h) induced an increased expression of CD83 and CD86 and a higher production of IL-12p40 suggesting that TiO_2 NPs induce dendritic cell maturation (61). In addition, increased production of IL-8 was also observed in A549 human lung epithelial cells after exposure to 300 µg/mL for 48h (62).

IV-2-4- Cancer related effects

Many different factors can lead to development of cancer such as inflammation, DNA damage, impairment of the immune system but also cell proliferation, decreased apoptosis. After exposure to 150 µg/mL TiO_2 NPs for 24h, Bothelho et al. observed an increase of both proliferation and overall survival in gastric epithelial cancer (AGS) cells (63). In addition, a significant decrease of apoptosis was observed with 4 different sizes of NPs on osteoblasts cells after exposure to 150 µg/mL for 72h (64). No information was found on TiO_2 in the form of E171 or MPs.

V- Mode of action

Three different mode of action leading to translocation to the blood stream as well as exposure to the different colon cells can be retrieved based on the findings described above. The modes of action are endocytosis through the epithelial cells, persorption which is a concept introduced by Volkheimer of a passage in a gap at the top of the villous right after the loss of enterocytes, and putative paracellular uptake which is a passage between the cellular junctions when they are damaged by drugs, diet, and disease allowing influx of small NPs (44).

A number of molecular responses to TiO_2 can be suggested to explain the advanced tumour formation in mice observed by Urrutia-Ortega (48). First of all, TiO_2 may induce ROS which can lead to local inflammation. ROS formation is known to induce oxidative stress and inflammation which may lead to non-selective DNA damage (55) including the formation of double-strand breaks. These breaks can lead to high rates of mutations in favour of loss of functional p53 which, when combined with inflammation, creates a potent tumour-promoting mechanism (65). As a consequence of DNA damage and inflammation, the innate immune system can be activated and the cytoplasmic inflammasome in the intestinal epithelium cells starts producing IL-18 and IL-1β (66). The inflammasome-processed cytokines like IL-1β can also recruit the adaptive immune system. The activation of the immune system allows the tumour cells to be destroyed. An impairment of the immune system creates a favourable environment for cancer development. We therefore hypothesise that ingestion of TiO_2 induces ROS, DNA damage and impairs the immune system which creates a favourable environment for tumour development as demonstrated previously in a colon cancer mouse model (48).

VI- Evaluation of potential health effects of TiO_2 by international organizations

VI-1-Evaluation by Joint WHO/FAO Expert Committee of Food Additives (JECFA)

In Europe, manufacturers are allowed to use TiO_2 in food since 1969 after an assessment made by the JECFA. The evaluation was performed based on 5 published studies in 1927, 1928, 1950, 1955 and 1962 and one unpublished study in 1963 assessing TiO_2 absorption and toxicity in animals and humans after TiO_2 ingestion (67). The first study, published in 1927, is a long term exposure study on 2 guinea-pigs, 2 rabbits, 2 cats and one dog exposed to 9 g/day for the dogs, 3 g/day for the rabbits and cats, and 0.6 g/day for the guinea-pigs of technical grade TiO_2 for 390 days (68). The technical grade TiO_2 used for this experiment was not pure and contained 1% of sodium sulphate and 0.1% of ferric oxide. Two additional cats were added to the experiment to which 3 g/day of technical grade TiO_2 was given for 175 and 300 days respectively. Researcher observed no toxic effects during the experiment nor any abnormalities during histological investigations made upon these animals. In addition, examination for the presence of TiO_2 using an assay method sensitive to 5 mg of titanium in liver, bile, heart, spleen and skeletal muscle were shown to be negative.

The second study, published in 1928, involved 3 groups of 2 dogs to which 0.05, 0.1, and 0.15 g of TiO_2 was given orally (69). Every 5 days, the dose was doubled. In each group, 1 dog received the particular diet for 1 month and the other one for 2 months. Researchers concluded that no toxic effects were observed. The little number of animals and the fact that both test and control dogs lost weight during the experiment raise concern about validity of the study. In the second part of this study, 3 dogs received subcutaneous injections of a suspension TiO_2 in oil. The initial dose was 500 mg rising up to 3 g after 7 weeks of exposure. One dog died of a cause unconnected with the administration of TiO_2. The conclusion of this part of the study was that the three dogs survived with no adverse effects.

The third study, published in 1950, was based on the comparison of digestibility of TiO_2 with calcium in rats and the translocation in other organs (70). After ingestion of 1% of the weight of a rat of TiO_2 for 15 days, no traces of TiO_2 was found in blood, liver, kidneys, and urine with a sensitivity of 10 µg. In the second part of the study, the passage of TiO_2 through the gastro-intestinal track was studied. Rats were administered 0.42 g of calcium together with 0.2, 1 or 2 g of TiO_2 per 100g of food. The hypothesis of the study was that if the speed of digestion was different between TiO_2 and Ca^{2+}, different Ca^{2+}/TiO_2

ratios would be found from the stomach to the colon. No different ratios were found, therefore it was concluded that no translocation through the gastrointestinal track to the blood stream was observed. Incomplete information was given about the methods such as the total number of rats used (only the Ca^{2+}/TiO_2 ratio of rats number 1, 2, 7, 8 and 11) as well as the type, size and purity of the TiO_2 and the type of assays performed.

The fourth study, published in 1955, evaluated the digestibility of TiO_2 in albinos male rats (n=30) (71). These rats were given 0.25% of TiO_2 (equivalent to around 295 mg TiO_2/kg_{bw}/day) in the diet for a week. The faeces were collected up to 13 days after initial consumption and 92% of TiO_2 was recovered in the faeces. The authors concluded that no absorption took place and hypothesised that delayed excretion of the 8% left could be due to accumulation of titanium in some part of the gastrointestinal tract. No information was given on the purity or the size of the TiO_2.

The fifth study, published in 1962, determined a LD50 in rats. LD50 was determined at 120 g/kg_{bw} (72). To determine this LD50, rats were orally given up to 120 g/kg_{bw} of barium titanate, bismuth titanate, calcium titanate, and lead titanate for 2 weeks. No more details on the experiment could be retrieved.

Part of the data of the unpublished study performed in 1963 was described in the re-evaluation of the EFSA (73). This study was also based on digestibility and on translocation (74). The first part of the study was performed with 5 human volunteers. After ingestion of 5 g of TiO_2 for 3 days, no TiO_2 was found in urine in the next 5 consecutive days. The authors concluded that no significant absorption could be observed. The second part of the study was performed in rats (10 males and 10 females) which were given 10% TiO_2 (equivalent to 100 mg TiO_2/kg diet) for 30-34 days. Results showed no change in weight compared to control as well as no relevant gross pathology. No evidence of an increase in titanium content was found in any of the seven different tissues analysed (liver, spleen, kidney, bone, plasma or erythrocytes) except a presence of 0.1 ppm of TiO_2 in muscle. No details were given on the strain of rats, purity and size of TiO_2 as well as how TiO_2 content in organs was analysed along with the detection limit.

Based on the results of these studies, JECFA concluded that TiO_2 was free from toxic effects on account of its insolubility and inertness (75). Therefore, TiO_2 was approved as a food additive in 1969 by the EU under the name of E171 (76). E171 was classified in the food additives from the group II, food colours authorized at *quantum satis*, meaning that there are no maximum intake levels for ingestion specified.

VI-2- Food and Drug Administration (FDA)

In the United States, the FDA is also using the evaluation of JEFCA for regulatory purposes (77). Food additive TiO_2 was allowed in 1966 based on the evaluation of JEFCA in 1964 (78). This evaluation precedes the one described above, so one can assume that no more studies than the ones described in the evaluation in 1969 were used for the 1964 evaluation. TiO_2 is authorised in food products as long as it does not exceed 1% by total weight of the product.

VI-3- International Agency for Research in Cancer (IARC)

Since the approval by the EU in 1969, the outcome of animal and human studies as well as insight regarding the potential mechanisms by which TiO_2 might cause cancer in humans have raised concern about the safe use of TiO_2. Therefore, in 2010, the IARC evaluated these new findings (79). As only a few studies were available on increased cancer risk in human population studies, the IARC concluded that there was inadequate evidence from epidemiological studies whether or not TiO_2 causes cancer in humans. Animal studies in rats after inhalation of TiO_2 showed an increase incidence of lung tumours. Other routes of administration (ingestion and dermal contact) did not show an increase incidence of tumours. Subsequent to new inhalation studies in animals on effects of exposure to MPs and NPs of TiO_2, the IARC classified TiO_2 as possible carcinogen to humans in 2010 (Group 2B). Modes of action by which TiO_2 may cause cancer like kinetics, *in vivo* and *in vitro* genotoxicity, cytotoxicity, presence of inflammation, and penetration of TiO_2 through the skin were also considered in the evaluation. The IARC considered that available mechanistic evidence was not strong enough to warrant classification other than Group 2B.

VI-4- Re-evaluation of TiO_2 as a food additive by the EFSA

With regard to the new evidence acquired on the potential adverse effects of E171, the EFSA decided in 2016 to re-evaluate TiO_2 as a food additive (73). A large number of studies regarding potential adverse effects of TiO_2 were encountered, however, according to the EFSA, most of these data were not considered relevant to the evaluation of TiO_2 as a food additive. Data regarding inhalation and dermal exposure were not considered in the final risk assessment. In addition, a total of 80 studies describing adverse effects of TiO_2 NPs in various organ systems from the medical college of Soochow University (China) were disregarded because of deficiencies in statistical analysis. The deficiencies were the use of the same 5% standard deviation or standard error for all measured values. Thus, the EFSA concluded that the real variation and statistical

significance of the results could not be established. Another study describing an increased number of tumours in the colon of mice after E171 ingestion (5 mg/kg_{bw}/day) in a chemically induced colorectal cancer model as well as an increased expression of tumour markers including COX2, Ki67 and β-catenin (48) was not used for final risk assessment because more research was deemed necessary.

Based on a carcinogenicity study performed by the National Cancer Institute (NCI) in 1979 on rats and mice, the EFSA chose a lowest no observed adverse effects level (NOAEL) of 2.25 g TiO_2/kg_{bw}/day. During this experiment, B6C3F1 mice (50 animals/sex), were administrated 0, 25, and 50 g of TiO_2/kg diet (equivalent to 0, 3.25, 6.50 g TiO_2/kg_{bw}/day for males and 0, 4.175, 8.35 g TiO_2/kg_{bw}/day for females) for 103 weeks with an additional week of observation afterwards. At the end of the study, the survival rates were of 80% in males compared to 64% in controls and 66% in females compared to 90% in controls in the highest doses. A slight increase of hepatocellular carcinomas was observed in the higher dose compared to control but no increase was found compared to historical data. During the second part of the experiment, 344 Fischer rats (50 animals/sex) were administrated TiO_2 in diet at concentrations of 0, 25, and 50 g/kg diet (equivalent to 0, 1.125, 2.25 g TiO_2/kg_{bw}/day in males and 0, 1.45, 2.90 g TiO_2/kg_{bw}/day in females) for 103 weeks with an additional week of observation afterwards. Exposure to TiO_2 did not affect survival rates and no significant increase of tumours was observed. Consequently, exposure lower than the NOAEL was not considered of concern in the re-evaluation of EFSA.

After evaluating a large number of studies, only the 2 aforementioned carcinogenicity studies were validated by the EFSA for risk assessment. The outcome of these oral *in vivo* studies, one in rats and one in mice, were reported to be negative. Therefore, based on these data and the earlier data reported in the JECFA (75) evaluation, EFSA concluded that E171 is not carcinogenic after ingestion.

VII- Research objectives and outline of the thesis

The majority of the studies on the potential adverse effects of TiO_2 were performed in relation to inhalation exposure. Since the IARC classified TiO_2 as possibly carcinogen to humans, the question was also raised if ingestion may also lead to increased cancer risk. This has initiated several studies investigating the effects of oral exposure, mainly focussing on the NPs fraction of the food additive E171. The potential adverse effects of ingestion of E171 itself as well as the mechanisms by which E171 enhance tumour remain unknown.

Therefore, the aim of the work presented in this thesis is to confirm the induction of histopathological changes and facilitation of colon cancer development after ingestion of E171 as observed previously in mice (48). In addition, this thesis aims to expand the current knowledge about the molecular mechanisms that may underlie these effects. To this end, we performed studies in different mouse models and *in vitro* studies using colon epithelial cells with a particular emphasis on the analysis of gene expression changes. As E171 is composed of different particle sizes of TiO_2, effects of separate size fractions (NPs and MPs) were investigated *in vitro*. The purpose of these studies is to determine the relative importance of the different size fractions and to identify possible mechanisms of E171-induced effects in terms of facilitation of colon cancer. The outcome of these studies may strengthen the basis for the evaluation cancer risk associated with the ingestion of E171 in humans.

First, in **Chapter 2**, we aim to understand the molecular mechanisms affected after E171 ingestion as well as histopathological changes in normal mice. BALB/c mice underwent exposure to 5 mg/kg_{bw}/day for 2, 7, 14, and 21 days. The molecular mechanisms were studied by whole genome microarrays on the distal colon of the mice and histopathological changes by staining.

In **Chapter 3**, we investigate the mechanisms of facilitation of colon cancer after E171 ingestion in a chemically induced colorectal cancer model before the tumours arise. BALB/c mice underwent exposure to 5 mg/kg_{bw}/day for 2, 7, 14, and 21 days in combination with AOM/DSS. Gene expression changes in the distal colon were analysed by microarray technology and compared to the normal BALB/c mouse model.

In **Chapter 4**, we aim to confirm facilitation of colon cancer formation that was found in earlier studies (48) and the underlying mechanisms in a model that spontaneously develop tumours without the addition of AOM/DSS. For this purpose, we used a transgenic mouse model with the Cre-LoxP system to generate a tissue specific knockout mouse model. A tumour formation study was first performed to verify the ability of the model to develop tumours and to establish if E171 enhances the occurrence of these tumours by exposing these mice to 5 mg/kg_{bw}/day of E171 for 1, 3, 5, 7, and 9 weeks. Secondly, a gene expression study was performed to confirm the mechanisms observed in the chemically induced colorectal cancer model (**Chapter 3**) and the normal BALB/c mouse model (**Chapter 2**). The same time points as in these chapters were used and a total of 3 concentrations of E171 were used: 5, 2, and 1 mg/kg_{bw}/day. The results of the whole gene microarray analysis on the mice colons were compared to the chemically induced colorectal cancer model and the normal BALB/c mouse model.

Chapter 5 and **Chapter 6** aim to investigate the differential effects of the MPs and NPs fraction *in vitro*. **Chapter 5** describes the capacity of E171, NPs, and MPs to induce oxidative stress, DNA damage and induction of the micronuclei, while **Chapter 6** describes the gene expression changes after exposure to E171, NPs, and MPs.

Finally, **Chapter 7** summarises and discusses the major findings of the studies presented in this thesis and focuses on the general mechanisms affected after E171 ingestion in the context of the work from other researchers. Based on this, proposals are made for further work necessary to perform an adequate risk assessment.

References

1. OCCA (1983) Titanium Dioxide Pigments. In Oil and Colour Chemists' Association, A. (ed.), *Surface Coatings: Vol I-Raw Materials and Their Usage*. Springer Netherlands, Dordrecht, pp. 305-312.
2. Middlemas, S., Fang, Z.Z., and Fan, P. (2013) A new method for production of titanium dioxide pigment. *Hydrometallurgy*, **131**, 107-113.
3. Lomer, M.C.E., Thompson, R.P.H., Commisso, J., Keen, C.L., and Powell, J.J. (2000) Determination of titanium dioxide in foods using inductively coupled plasma optical emission spectrometry. *Analyst*, **125**, 2339-2343.
4. Peters, R.J., van Bemmel, G., Herrera-Rivera, Z., Helsper, H.P., Marvin, H.J., Weigel, S., Tromp, P.C., Oomen, A.G., Rietveld, A.G., and Bouwmeester, H. (2014) Characterization of titanium dioxide nanoparticles in food products: analytical methods to define nanoparticles. *J Agric Food Chem*, **62**, 6285-6293.
5. TDMA (2018) Titanium Dioxide Manufacturers Association website
6. Weir, A., Westerhoff, P., Fabricius, L., Hristovski, K., and von Goetz, N. (2012) Titanium dioxide nanoparticles in food and personal care products. *Environmental science & technology*, **46**, 2242-2250.
7. Shi, H., Magaye, R., Castranova, V., and Zhao, J. (2013) Titanium dioxide nanoparticles: a review of current toxicological data. *Particle and fibre toxicology*, **10**, 15.
8. Venator (2018) Venator Materials PLC website.
9. Rompelberg, C., Heringa, M.B., van Donkersgoed, G., Drijvers, J., Roos, A., Westenbrink, S., Peters, R., van Bemmel, G., Brand, W., and Oomen, A.G. (2016) Oral intake of added titanium dioxide and its nanofraction from food products, food supplements and toothpaste by the Dutch population. *Nanotoxicology*, **10**, 1404-1414.
10. EU (2015) REGULATION (EC) No 1333/2008 OF THE EUROPEAN PARLIAMENT AND OF THE COUNCIL on food additives. *Official Journal of the European Union*
11. Dorier, M., Beal, D., Marie-Desvergne, C., Dubosson, M., Barreau, F., Houdeau, E., Herlin-Boime, N., and Carriere, M. (2017) Continuous in vitro exposure of intestinal epithelial cells to E171 food additive causes oxidative stress, inducing oxidation of DNA bases but no endoplasmic reticulum stress. *Nanotoxicology*, 1-54.
12. Dudefoi, W., Moniz, K., Allen-Vercoe, E., Ropers, M.H., and Walker, V.K. (2017) Impact of food grade and nano-TiO2 particles on a human intestinal community. *Food Chem Toxicol*, **106**, 242-249.
13. Yang, Y., Doudrick, K., Bi, X.Y., Hristovski, K., Herckes, P., Westerhoff, P., and Kaegi, R. (2014) Characterization of Food-Grade Titanium Dioxide: The Presence of Nanosized Particles. *Environmental science & technology*, **48**, 6391-6400.
14. EU (2011) COMMISSION RECOMMENDATION of 18 Oct 2011 of the definition of nanomaterial (2011/696/EU). *Official Journal of the European Union*
15. Collins (2018) Collins Dictionnary website. https://www.collinsdictionary.com/.
16. Sokolov, S.V., Tschulik, K., Batchelor-McAuley, C., Jurkschat, K., and Compton, R.G. (2015) Reversible or not? Distinguishing agglomeration and aggregation at the nanoscale. *Anal Chem*, **87**, 10033-10039.
17. Min, Y., Akbulut, M., Kristiansen, K., Golan, Y., and Israelachvili, J. (2008) The role of interparticle and external forces in nanoparticle assembly. *Nat Mater*, **7**, 527-538.
18. Numano, T., Xu, J., Futakuchi, M., Fukamachi, K., Alexander, D.B., Furukawa, F., Kanno, J., Hirose, A., Tsuda, H., and Suzui, M. (2014) Comparative study of toxic effects of anatase and rutile type nanosized titanium dioxide particles in vivo and in vitro. *Asian Pac J Cancer Prev*, **15**, 929-935.

19. Prasad, R.Y., Wallace, K., Daniel, K.M., Tennant, A.H., Zucker, R.M., Strickland, J., Dreher, K., Kligerman, A.D., Blackman, C.F., and Demarini, D.M. (2013) Effect of treatment media on the agglomeration of titanium dioxide nanoparticles: impact on genotoxicity, cellular interaction, and cell cycle. *ACS Nano*, **7**, 1929-1942.
20. Charles, S., Jomini, S., Fessard, V., Bigorgne-Vizade, E., Rousselle, C., and Michel, C. (2018) Assessment of the in vitro genotoxicity of TiO2 nanoparticles in a regulatory context. *Nanotoxicology*, 1-18.
21. Freyre-Fonseca, V., Téllez-Medina, D.I., Medina-Reyes, E.I., Cornejo-Mazón, M., López-Villegas, E.O., Alamilla-Beltrán, L., Ocotlán-Flores, J., Chirino, Y.I., and Gutiérrez-López, G.F. (2016) Morphological and Physicochemical Characterization of Agglomerates of Titanium Dioxide Nanoparticles in Cell Culture Media. *J Nanomater*, **2016**, 1-19.
22. Lankoff, A., Sandberg, W.J., Wegierek-Ciuk, A., Lisowska, H., Refsnes, M., Sartowska, B., Schwarze, P.E., Meczynska-Wielgosz, S., Wojewodzka, M., and Kruszewski, M. (2012) The effect of agglomeration state of silver and titanium dioxide nanoparticles on cellular response of HepG2, A549 and THP-1 cells. *Toxicology letters*, **208**, 197-213.
23. Taurozzi, J.S., Hackley, V.A., and Wiesner, M.R. (2011) Ultrasonic dispersion of nanoparticles for environmental, health and safety assessment--issues and recommendations. *Nanotoxicology*, **5**, 711-729.
24. Hext, P.M., Tomenson, J.A., and Thompson, P. (2005) Titanium dioxide: inhalation toxicology and epidemiology. *Ann Occup Hyg*, **49**, 461-472.
25. Dankovic, D., Kuempel, E., and Wheeler, M. (2007) An approach to risk assessment for TiO2. *Inhal Toxicol*, **19 Suppl 1**, 205-212.
26. Monteiro-Riviere, N.A., Wiench, K., Landsiedel, R., Schulte, S., Inman, A.O., and Riviere, J.E. (2011) Safety evaluation of sunscreen formulations containing titanium dioxide and zinc oxide nanoparticles in UVB sunburned skin: an in vitro and in vivo study. *Toxicol Sci*, **123**, 264-280.
27. Hiroike, M., Sakabe, J., Kobayashi, M., Shimauchi, T., Ito, T., Hirakawa, S., Inoh, A., and Tokura, Y. (2013) Acicular, but not globular, titanium dioxide nanoparticles stimulate keratinocytes to produce pro-inflammatory cytokines. *J Dermatol*, **40**, 357-362.
28. Crosera, M., Prodi, A., Mauro, M., Pelin, M., Florio, C., Bellomo, F., Adami, G., Apostoli, P., De Palma, G., Bovenzi, M., Campanini, M., and Filon, F.L. (2015) Titanium Dioxide Nanoparticle Penetration into the Skin and Effects on HaCaT Cells. *Int J Environ Res Public Health*, **12**, 9282-9297.
29. EFSA (2016) Re-evaluation of titanium dioxide (E 171) as a food additive. *EFSA Journal*, **14**, e04545-n/a.
30. Gitrowski, C., Al-Jubory, A.R., and Handy, R.D. (2014) Uptake of different crystal structures of TiO2 nanoparticles by Caco-2 intestinal cells. *Toxicology letters*, **226**, 264-276.
31. Shukla, R.K., Sharma, V., Pandey, A.K., Singh, S., Sultana, S., and Dhawan, A. (2011) ROS-mediated genotoxicity induced by titanium dioxide nanoparticles in human epidermal cells. *Toxicol In Vitro*, **25**, 231-241.
32. Saquib, Q., Al-Khedhairy, A.A., Siddiqui, M.A., Abou-Tarboush, F.M., Azam, A., and Musarrat, J. (2012) Titanium dioxide nanoparticles induced cytotoxicity, oxidative stress and DNA damage in human amnion epithelial (WISH) cells. *Toxicol In Vitro*, **26**, 351-361.
33. Brun, E., Barreau, F., Veronesi, G., Fayard, B., Sorieul, S., Chaneac, C., Carapito, C., Rabilloud, T., Mabondzo, A., Herlin-Boime, N., and Carriere, M. (2014) Titanium dioxide nanoparticle impact and translocation through ex vivo, in vivo and in vitro gut epithelia. *Particle and fibre toxicology*, **11**, 13.
34. Yang, J., Luo, M., Tan, Z., Dai, M., Xie, M., Lin, J., Hua, H., Ma, Q., Zhao, J., and Liu, A. (2017) Oral administration of nano-titanium dioxide particle disrupts hepatic metabolic functions in a mouse model. *Environ Toxicol Pharmacol*, **49**, 112-118.

35. Wang, J., Zhou, G., Chen, C., Yu, H., Wang, T., Ma, Y., Jia, G., Gao, Y., Li, B., Sun, J., Li, Y., Jiao, F., Zhao, Y., and Chai, Z. (2007) Acute toxicity and biodistribution of different sized titanium dioxide particles in mice after oral administration. *Toxicology letters*, **168**, 176-185.
36. Chen, Z., Wang, Y., Wang, X., Zhuo, L., Chen, S., Tang, S., Zhao, L., Luan, X., and Jia, G. (2018) Effect of titanium dioxide nanoparticles on glucose homeostasis after oral administration. *J Appl Toxicol*.
37. Tassinari, R., Cubadda, F., Moracci, G., Aureli, F., D'Amato, M., Valeri, M., De Berardis, B., Raggi, A., Mantovani, A., Passeri, D., Rossi, M., and Maranghi, F. (2014) Oral, short-term exposure to titanium dioxide nanoparticles in Sprague-Dawley rat: focus on reproductive and endocrine systems and spleen. *Nanotoxicology*, **8**, 654-662.
38. Heringa, M.B., Peters, R.J.B., Bleys, R., van der Lee, M.K., Tromp, P.C., van Kesteren, P.C.E., van Eijkeren, J.C.H., Undas, A.K., Oomen, A.G., and Bouwmeester, H. (2018) Detection of titanium particles in human liver and spleen and possible health implications. *Particle and fibre toxicology*, **15**, 15.
39. Meena, R., Kajal, K., and R., P. (2015) Cytotoxic and Genotoxic Effects of Titanium Dioxide Nanoparticles in Testicular Cells of Male Wistar Rat. *Applied Biochemistry and Biotechnology*, **175**, 825-840.
40. Bettini, S., Boutet-Robinet, E., Cartier, C., Comera, C., Gaultier, E., Dupuy, J., Naud, N., Tache, S., Grysan, P., Reguer, S., Thieriet, N., Refregiers, M., Thiaudiere, D., Cravedi, J.P., Carriere, M., Audinot, J.N., Pierre, F.H., Guzylack-Piriou, L., and Houdeau, E. (2017) Food-grade TiO2 impairs intestinal and systemic immune homeostasis, initiates preneoplastic lesions and promotes aberrant crypt development in the rat colon. *Sci Rep*, **7**, 40373.
41. Pele, L.C., Thoree, V., Bruggraber, S.F.A., Koller, D., Thompson, R.P.H., Lomer, M.C., and Powell, J.J. (2015) Pharmaceutical/food grade titanium dioxide particles are absorbed into the bloodstream of human volunteers. *Particle and fibre toxicology*, **12**.
42. Vasantharaja, D., Ramalingam, V., and Aadinaath Reddy, G. (2015) Oral toxic exposure of titanium dioxide nanoparticles on serum biochemical changes in adult male Wistar rats. *Nanomedicine Journal*, **2**, 46-53.
43. Nogueira, C.M., de Azevedo, W.M., Dagli, M.L., Toma, S.H., Leite, A.Z., Lordello, M.L., Nishitokukado, I., Ortiz-Agostinho, C.L., Duarte, M.I., Ferreira, M.A., and Sipahi, A.M. (2012) Titanium dioxide induced inflammation in the small intestine. *World J Gastroenterol*, **18**, 4729-4735.
44. Powell, J.J., Faria, N., Thomas-McKay, E., and Pele, L.C. (2010) Origin and fate of dietary nanoparticles and microparticles in the gastrointestinal tract. *J Autoimmun*, **34**, J226-233.
45. Trouiller, B., Reliene, R., Westbrook, A., Solaimani, P., and Schiestl, R.H. (2009) Titanium dioxide nanoparticles induce DNA damage and genetic instability in vivo in mice. *Cancer research*, **69**, 8784-8789.
46. Shi, Z.Q., Niu, Y.J., Wang, Q., Shi, L., Guo, H.C., Liu, Y., Zhu, Y., Liu, S.F., Liu, C., Chen, X., and Zhang, R. (2015) Reduction of DNA damage induced by titanium dioxide nanoparticles through Nrf2 in vitro and in vivo. *Journal of Hazardous Materials*, **298**, 310-319.
47. Sycheva, L.P., Zhurkov, V.S., Iurchenko, V.V., Daugel-Dauge, N.O., Kovalenko, M.A., Krivtsova, E.K., and Durnev, A.D. (2011) Investigation of genotoxic and cytotoxic effects of micro- and nanosized titanium dioxide in six organs of mice in vivo. *Mutation research*, **726**, 8-14.
48. Urrutia-Ortega, I.M., Garduno-Balderas, L.G., Delgado-Buenrostro, N.L., Freyre-Fonseca, V., Flores-Flores, J.O., Gonzalez-Robles, A., Pedraza-Chaverri, J., Hernandez-Pando, R., Rodriguez-Sosa, M., Leon-Cabrera, S., Terrazas, L.I., van Loveren, H., and Chirino, Y.I. (2016) Food-grade titanium dioxide exposure exacerbates tumor formation in colitis associated cancer model. *Food Chem Toxicol*, **93**, 20-31.
49. Jin, C.Y., Zhu, B.S., Wang, X.F., and Lu, Q.H. (2008) Cytotoxicity of titanium dioxide nanoparticles in mouse fibroblast cells. *Chem Res Toxicol*, **21**, 1871-1877.

50. Park, E.J., Yi, J., Chung, K.H., Ryu, D.Y., Choi, J., and Park, K. (2008) Oxidative stress and apoptosis induced by titanium dioxide nanoparticles in cultured BEAS-2B cells. *Toxicology letters*, **180**, 222-229.
51. De Angelis, I., Barone, F., Zijno, A., Bizzarri, L., Russo, M.T., Pozzi, R., Franchini, F., Giudetti, G., Uboldi, C., Ponti, J., Rossi, F., and De Berardis, B. (2013) Comparative study of ZnO and TiO(2) nanoparticles: physicochemical characterisation and toxicological effects on human colon carcinoma cells. *Nanotoxicology*, **7**, 1361-1372.
52. Long, T.C., Saleh, N., Tilton, R.D., Lowry, G.V., and Veronesi, B. (2006) Titanium dioxide (P25) produces reactive oxygen species in immortalized brain microglia (BV2): implications for nanoparticle neurotoxicity. *Environmental science & technology*, **40**, 4346-4352.
53. Bhattacharya, K., Davoren, M., Boertz, J., Schins, R.P., Hoffmann, E., and Dopp, E. (2009) Titanium dioxide nanoparticles induce oxidative stress and DNA-adduct formation but not DNA-breakage in human lung cells. *Particle and fibre toxicology*, **6**, 17.
54. Huerta-Garcia, E., Perez-Arizti, J.A., Marquez-Ramirez, S.G., Delgado-Buenrostro, N.L., Chirino, Y.I., Iglesias, G.G., and Lopez-Marure, R. (2014) Titanium dioxide nanoparticles induce strong oxidative stress and mitochondrial damage in glial cells. *Free Radic Biol Med*, **73**, 84-94.
55. Niska, K., Pyszka, K., Tukaj, C., Wozniak, M., Radomski, M.W., and Inkielewicz-Stepniak, I. (2015) Titanium dioxide nanoparticles enhance production of superoxide anion and alter the antioxidant system in human osteoblast cells. *Int J Nanomed*, **10**, 1095-1107.
56. Reeves, J.F., Davies, S.J., Dodd, N.J., and Jha, A.N. (2008) Hydroxyl radicals (*OH) are associated with titanium dioxide (TiO(2)) nanoparticle-induced cytotoxicity and oxidative DNA damage in fish cells. *Mutation research*, **640**, 113-122.
57. Kang, J.L., Moon, C., Lee, H.S., Lee, H.W., Park, E.M., Kim, H.S., and Castranova, V. (2008) Comparison of the biological activity between ultrafine and fine titanium dioxide particles in RAW 264.7 cells associated with oxidative stress. *J Toxicol Env Heal A*, **71**, 478-485.
58. Chen, Z., Wang, Y., Ba, T., Li, Y., Pu, J., Chen, T., Song, Y., Gu, Y., Qian, Q., Yang, J., and Jia, G. (2014) Genotoxic evaluation of titanium dioxide nanoparticles in vivo and in vitro. *Toxicology letters*, **226**, 314-319.
59. Zijno, A., De Angelis, I., De Berardis, B., Andreoli, C., Russo, M.T., Pietraforte, D., Scorza, G., Degan, P., Ponti, J., Rossi, F., and Barone, F. (2015) Different mechanisms are involved in oxidative DNA damage and genotoxicity induction by ZnO and TiO nanoparticles in human colon carcinoma cells. *Toxicol In Vitro*, **29**, 1503-1512.
60. Sukwong, P., Kongseng, S., Chaicherd, S., Yoovathaworn, K., Tubtimkuna, S., and Pissuwan, D. (2017) Comparison effects of titanium dioxide nanoparticles on immune cells in adaptive and innate immune system. *Iet Nanobiotechnology*, **11**, 759-765.
61. Vandebriel, R.J., Vermeulen, J.P., van Engelen, L.B., de Jong, B., Verhagen, L.M., de la Fonteyne-Blankestijn, L.J., Hoonakker, M.E., and de Jong, W.H. (2018) The crystal structure of titanium dioxide nanoparticles influences immune activity in vitro and in vivo. *Particle and fibre toxicology*, **15**, 9.
62. Sayes, C.M., Wahi, R., Kurian, P.A., Liu, Y., West, J.L., Ausman, K.D., Warheit, D.B., and Colvin, V.L. (2006) Correlating nanoscale titania structure with toxicity: a cytotoxicity and inflammatory response study with human dermal fibroblasts and human lung epithelial cells. *Toxicol Sci*, **92**, 174-185.
63. Botelho, M.C., Costa, C., Silva, S., Costa, S., Dhawan, A., Oliveira, P.A., and Teixeira, J.P. (2014) Effects of titanium dioxide nanoparticles in human gastric epithelial cells in vitro. *Biomedicine & pharmacotherapy = Biomedecine & pharmacotherapie*, **68**, 59-64.
64. Cai, K., Hou, Y., Hu, Y., Zhao, L., Luo, Z., Shi, Y., Lai, M., Yang, W., and Liu, P. (2011) Correlation of the cytotoxicity of TiO2 nanoparticles with different particle sizes on a sub-200-nm scale. *Small*, **7**, 3026-3031.

65. Pribluda, A., Elyada, E., Wiener, Z., Hamza, H., Goldstein, R.E., Biton, M., Burstain, I., Morgenstern, Y., Brachya, G., Billauer, H., Biton, S., Snir-Alkalay, I., Vucic, D., Schlereth, K., Mernberger, M., Stiewe, T., Oren, M., Alitalo, K., Pikarsky, E., and Ben-Neriah, Y. (2013) A senescence-inflammatory switch from cancer-inhibitory to cancer-promoting mechanism. *Cancer Cell*, **24**, 242-256.
66. Lasry, A., Zinger, A., and Ben-Neriah, Y. (2016) Inflammatory networks underlying colorectal cancer. *Nat Immunol*, **17**, 230-240.
67. FAO, and WHO (1969) TOXICOLOGICAL EVALUATION OF SOME FOOD COLOURS, EMULSIFIERS, STABILIZERS, ANTI-CAKING AGENTS AND CERTAIN OTHER SUBSTANCES. *FAO Nutrition Meetings Report Series* **No. 46A WHO/FOOD ADD/70.36**.
68. Lehmann, K.P., and Herget, L. (1927) Studies on the hygienic manufacture of titanium dioxide and titanium white. *Chem. Ztg*, **51**, 793-794.
69. Vernetti-Blina, L. (1928) Clinical research and experiments on the oxides of titanium. *Riforma Med*, **44**, 1516-1525.
70. Fournier, P. (1950) De l'emploi de l'oxyde de titane pour l'étude quantitative de l'absorption intestinale. *Comptes rendus hebdomadaires des scéances de l'Académie des sciences*, **231**, 1343-1345.
71. Lloyd, L.E., Rutherford, B.E., and Crampton, E.W. (1955) A comparison of titanic oxide and chromic oxide as index materials for determining apparent digestibility. *J. Nutrition*, **56**, 535-537.
72. Brown, J.R., and Mastromatteo, E. (1962) Acute oral and parenteral toxicity of four titanate compounds in the rat. *Indust Med Surg*, **31**, 302–304.
73. EFSA (2016) Scientific Opinion on the re-evaluation of titanium dioxide (E 171) as a food additive. *EFSA Journal*, **14**, 4545-4638.
74. West, B., and Wyzan, H. (1963) Investigations of the possible absorption of titanium dioxide from the gastrointestinal tract. *Unpublished report*, **American Cyanamid Company, Central Medical Department, New Jersey,**.
75. FAO, and WHO (1970) Specification for the identity and purity of food additives and their toxicological evaluation. *World Health Organization technical report series No. 445, FAO nutrition meetings report series No. 46*.
76. EU (2012) Regulation No 231-2012 on food additives. *Official Journal of the European Union*, **83**, 1-295.
77. Lehto, S., Buchweitz, M., Klimm, A., Strassburger, R., Bechtold, C., and Ulberth, F. (2017) Comparison of food colour regulations in the EU and the US: a review of current provisions. *Food Addit Contam A*, **34**, 335-355.
78. [USFDA] (2016) US Food and Drug Administration regulation on Titanium dioxide. *Code of Federal Regulations*, **Title 21, Section 73.575.**
79. IARC (2010) IARC MONOGRAPHS ON THE EVALUATION OF CARCINOGENIC RISKS TO HUMANS: Carbon Black, Titanium dioxide and Talc. **Volume 93**.

Chapter 2

Gene expression profiling in colon of mice exposed to food additive titanium dioxide (E171)

Food and Chemical Toxicology, Volume 111, January 2018, Pages 153-165

Data of this article published as

Time course gene expression data in colon of mice after exposure to food-grade E171

Data in Brief, Volume 16, February 2018, Pages 531-600

Héloïse Proquin,

Marlon J. Jetten,

Marloes C.M. Jonkhout,

Luis G. Garduño-Balderas,

Jacob J. Briedé,

Theo M. de Kok,

Yolanda I. Chirino,

Henk van Loveren

Abstract

Dietary factors that may influence the risks of colorectal cancer, including specific supplements, are under investigation. Previous studies showed the capacity of food additive titanium dioxide (E171) to induce DNA damage *in vitro* and facilitate growth of colorectal tumours *in vivo*. This study aimed to investigate the molecular mechanisms behind these effects after E171 exposure. BALB/c mice were exposed by gavage to 5 mg/kg_{bw}/day of E171 for 2, 7, 14, and 21 days. Transcriptome changes were studied by whole genome mRNA microarray analysis on the mice's distal colons. In addition, histopathological changes as well as a proliferation marker were analysed. The results showed significant gene expression changes in the olfactory/GPCR receptor family, oxidative stress, the immune system, and of cancer related genes. Transcriptome analysis also identified genes that thus far have not been included in known biological pathways and can induce functional changes by interacting with other genes involved in different biological pathways. Histopathological analysis showed alteration and disruption in the normal structure of crypts inducing a hyperplastic epithelium. At cell proliferation level, no consistent increase over time was observed. These results may offer a mechanistic framework for the enhanced tumour growth after ingestion of E171 in BALB/c mice.

I- Introduction

Colorectal cancer (CRC) in industrialized countries is the 3rd cancer in men and the 2nd in women with a total of 694,000 deceased people in 2012 (8.5% of all cancer deaths that year) (1). Obesity, alcohol, and tobacco smoking are factors that may increase the risk of developing CRC whereas fruits and vegetables have been shown to be associated with decreased risk of CRC. Most likely as a consequence of their high fibre content and the presence of a wide range of bioactive compounds, including antioxidant (2,3). The increased incidence of CRC has been observed particularly in industrialized countries over the last decades and could potentially be explained by specific dietary patterns such as Western types of diets (1).

Colouring agents are used in many different types of food. Titanium dioxide (TiO_2) is used as a colouring agent (4), it gives a white colour to food products such as salad dressings, chewing gum, icing, cookies, and candies (5,6). Following a risk assessment performed by the joint Food and Agriculture Organization/World Health Organization (FAO/WHO), TiO_2 was approved as a food additive in 1969 by the European Union under the name of E171 (4). It is permitted in food at *quantum satis*, which indicates that there is no maximum level specified. In 2010, the International Agency for Research in Cancer (IARC) classified TiO_2 as possible carcinogen to humans (Group 2B) mainly based on inhalation studies *in vivo* as well as epidemiological studies on effects of exposure to microparticles (MPs) and nanoparticles (NPs) of TiO_2 (7).

E171 consists of approximately 40% of TiO_2 NPs (<100 nm) and 60% of TiO_2 MPs (>100 nm) (6,8,9). In the USA, the estimated average exposure of children below 10 years of age was 1-2 mg TiO_2/kg_{bw}/day and above 10 years old, 0.2-0.7 mg TiO_2/kg_{bw}/day. In the UK, the estimated exposure was on average 2-3 mg TiO_2/kg_{bw}/day for children younger than 10 years and 1 mg TiO_2/kg_{bw}/day for children over 10 years of age (6). Another study performed in the Netherlands showed an intake of TiO_2 in the same range as in the USA (10). This study, published in 2016, estimated the mean average exposure to be 0.67 mg TiO_2/kg_{bw}/day between 2-6 years old, 0.17 mg TiO_2/kg_{bw}/day between 7-69 years old, and 0.06 mg TiO_2/kg_{bw}/day above 70 years old. Furthermore, in June 2016, a new evaluation from the European Food Safety Authority (EFSA) on TiO_2 in food was published (11). In the non-brand-loyal scenario validated by the EFSA, it has been estimated that the mean exposure ranged from 0.2 mg/kg_{bw}/day for infants and the elderly to 5.5 mg/kg_{bw}/day for children. At the 95th percentile, EFSA estimates the exposure ranged from 0.5 mg/kg_{bw}/day for the elderly to 14.8 mg/kg_{bw}/day for children.

Although some studies report no adverse effects of TiO_2 (12), many others indicate adverse effects of MPs and NPs of TiO_2. These effects are diverse and have been observed *in vivo* as well as *in vitro*. It includes gene expression changes related to immune response and inflammation in mice exposed intragastrically to 10 mg/kg_{bw} for 90 days (13). After whole genome microarray analysis in mice livers, Cui et al. observed the generation of inflammation and a reduction in immune capacity by the downregulation of genes involved in the complement system. These results are in line with a recent study on the effects of ingestion of 10 mg/kg_{bw} of E171 for 7 and 100 days in rats (14). In the rats' Peyer's Patches, a significant decreased frequency of immunoregulatory Tregs and $CD4^+CD25^+$ T helpers was observed after 7 and 100 days. Furthermore, induction of inflammatory markers such as TNF-α, IL-8 and IL-10 was measured in aberrant crypts after 100 days of exposure to E171. A potent Th1/Th17 immune response was detected via an increased production of IFN-γ in Peyer's Patches and IFN-γ and IL-17 in the spleen after 7 days of exposure. Another *in vivo* study observed a reduction in both non-specific and specific immune responses in rats' primary pulmonary alveolar macrophages exposed by inhalation to TiO_2 NPs (5 and 200 nm; 0.5, 5, or 50 mg/kg_{bw}) (15). Additionally, TiO_2 NPs have an impact on the bacterial ratio of the human intestinal community *in vitro* which can affect the immune response (16). Inflammation is enhanced via the production of reactive oxygen species (ROS). In an *in vitro* study, oxidative stress was produced by E171 and TiO_2 NPs in a cell-free environment whereas MPs induced ROS formation in the presence of Caco-2 cells (8). These results confirmed previous studies in which ROS production was observed in mouse fibroblasts and fish cells with fibroblast-like morphology (17,18) and *in vivo* in mice exposed intragastrically to TiO_2 NPs for 60 days (19). The findings of this mouse study showed a significant increase of $O_2^{\bullet-}$ and H_2O_2 in the liver starting at a concentration of 10 mg/kg_{bw}. ROS production can lead to DNA damage in mice but also in human cells like liver hepatocellular cells (HepG2) and bronchial epithelial cells (BEAS-2B) (20-23). Recently we have demonstrated that E171 as well as NPs and MPs of TiO_2 possess the capacity to induce single-strand DNA damage in Caco-2 cells and induce micronuclei in HCT116 cells (8).

A reduction of the immune capacity, induction of inflammation and DNA damage can increase the risk of developing cancer. An *in vivo* study performed in BALB/c mice in which CRC was chemically induced by a combination of azoxymethane (AOM) and dextran sodium sulphate (DSS) showed, after 10 weeks of ingestion of 5 mg/kg_{bw}/day of E171, a significantly increased number of tumours in the colon as compared to the control (AOM/DSS) (24). It was concluded that E171 exacerbates the number of tumours induced by a genotoxic insult in addition to an irritant. In absence of AOM/DSS, mice did not develop tumours. However, the exposure of mice to E171 only induced hyperplastic epithelium with dysplastic changes with an increase of crypts size and number, and a decrease in the number of goblet cells in the colon of mice. In addition, staining for tumour progression markers showed a significant increase of COX2, Ki67 and β-catenin markers.

In order to understand the molecular changes behind these phenotypical modifications, and behind the production of ROS and DNA damage *in vitro*, a new experiment was designed. Physiological changes were previously observed from 4 weeks on (24), therefore the exposure time was limited to 3 weeks. To establish responses to E171 exposure at the mRNA level in the colon of BALB/c mice, mice ingested 5 mg/kg_{bw}/day of E171 for 2, 7, 14, and 21 days. Transcriptome changes were determined by whole genome mRNA microarrays. Moreover, histological changes were studied by Hematoxylin & Eosin (H&E) and a proliferation marker (Ki67) staining. We hypothesized that the exposure to E171 induces inflammatory, immunological, and specific cancer-related pathways in colon tissue that may explain the facilitated development of CRC by E171 reported previously.

II- Materials and Methods

II-1- E171 particle characterization

E171 was kindly donated by the Sensient Technologies Company in Mexico. E171 was previously characterized by electron microscopy with Scios DualBeam FIB/SEM (SEM, 20 KV, The Netherlands) at 150,000x magnification to evaluate the size and morphology. To evaluate the hydrodynamic size distribution and the zeta potential a Malvern Nano ZS (Malvern Instruments, UK) dynamic light scattering instrument was used. Results have been previously published (8). E171 comprises 2 fractions of different sizes with a ratio of 39% NPs and 61% MPs. E171 contains slightly to fully rounded particles. At non cytotoxic concentration, the dynamic size of E171 was 316.8 ± 282.4 d.nm and the zeta potential −12.78 ± 0.52 mV.

II-2- Mouse model

BALB/c mice underwent exposure to E171 by ingestion at the Unidad de Biomedicina, Facultad de Estudios Superiores Iztacala, Universidad Nacional Autónoma de México, Mexico. Experiment was approved by the Comité de Ética de la Facultad de Estudios Superiores Iztacala de la Universidad Nacional Autónoma de México under the number: FESI-ICY-I151. Experimental work followed the guidelines of Norma Oficial Mexicana (NOM-062-ZOO-1999, NOM-087-ECOL-1995) and the Protocol for the Care and Use of Laboratory Animals (PICUAL). Thirty-two BALB/c mice (16 males, 16 females) of 4-6 weeks old (Harlan Laboratories, Mexico) were housed in polycarbonate cages and kept in a housing room (21°C, 50-60% relative humidity, 12 h light/dark cycles, air filtered until 5 µm particles and was exchanged 18 times/h). The number of animals was determined with a power calculation. The calculation was performed with a web-based source named Power Atlas (http://poweratlas.ssg.uab.edu/). It was created by Gadbury et al. and Page et al. to assist researchers in the planning and design of microarray and expression based experiments (25,26). This software is currently aimed at estimating the power and sample size for a two groups comparison based upon pilot data. The results of this calculation showed that with 16 animals per exposure group and an alpha at 0.1, the power of the experiment is over 80%. Standard commercial rat chow diet from Harland Teklad (Madison, WI, USA) was given *ad libitum* as well as water. After one week of acclimation, the mice were randomly divided in the following groups: a) control (8 males, 8 females), b) E171 group (8 males, 8 females). Both the control and exposure groups received a single intraperitoneal injection of 500 µL of sterile saline solution a week before the start of the experiment and water *ad libitum* between day 1 and 5 respectively. This was to mimic

comparable conditions but now without an AOM injection and the supply of DSS in drinking water given in the CRC model. One milligram of E171 was sterilized, resuspended in 1 mL of water and sonicated for 30 min at 60 Hz. The E171 group of mice received an intragastric administration of 5 mg/kg body weight of E171 by a gavage from Monday to Friday during 21 days according to the scheme (Figure 1). The control group received 100 µL of sterile sonicated water (30 min at 60 Hz) by intragastric gavage from Monday to Friday during 21 days according to the scheme. After 2, 7, 14, and 21 days, 4 mice (2 males, 2 females) were sacrificed in a humid chamber with sevoflurane and colon was collected. Colons were directly put in a tube containing RNA*later®* (Thermofischer, The Netherlands) and left overnight at 4°C. Next day the remaining RNA*later®* was discarded. The organs were stored at -80°C until RNA isolation. The samples have been transported in dry ice at -80°C for 2 days. The temperature of the samples has been monitored throughout the shipping process with a thermometer provided by the shipping company to ensure stable freezing conditions and optimal sample quality. Samples have been put at -80°C in the freezer immediately upon arrival. RNA isolation and further procedures were performed at the Department of Toxicogenomics, Maastricht University, Maastricht, the Netherlands.

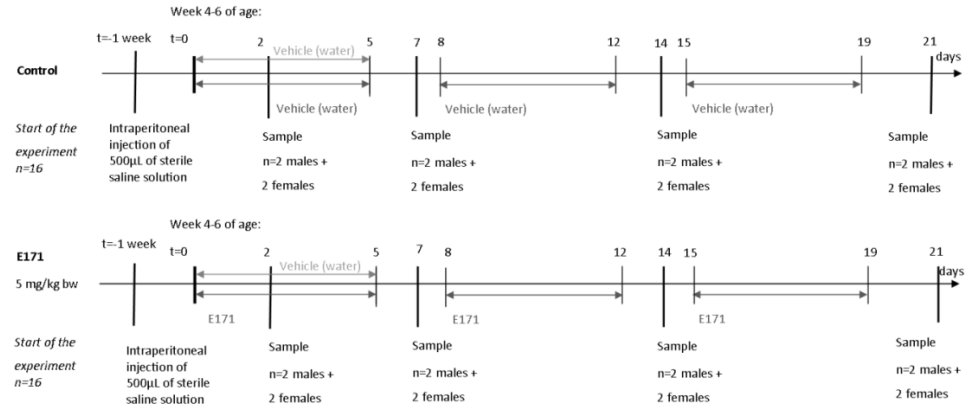

Figure 1: Scheme of exposure of experimental mouse model.

BALB/c mice (n = 32) were randomly distributed in 2 groups: one control group with water as a vehicle (dark grey line) and one exposure group with E171 (dark grey line). Both groups received a single intraperitoneal injection of 500µL of sterile saline solution a week before the start of the experiment (t= -1 week vertical line) and water *ad libitum* between day 1 and 5 respectively (light grey line). Vertical lines correspond to the sampling times at 2, 7, 14, and 21 days.

II-3- mRNA isolation from distal colons

The previous study from our group showed an increased numbers of tumours in the distal colon of BALB/c mice (24), therefore it was chosen to isolate total RNA from this part of the colon. Before RNA isolation, the distal colon was submerged in Qiazol (Qiagen, The Netherlands) and subsequently disrupted and homogenized using a Mini Bead Beater (BioSpec Products, The Netherlands) on a speed of 48 beats per second for 30 seconds. Isolation of RNA was performed using the miRNeasy Mini Kit (Qiagen, The Netherlands) including a DNase treatment, according to the manufacturer's protocols for "Animal Cells and Animal Tissues" (27). The concentration of total RNA was measured on a Nanodrop® ND-1000 spectrophotometer (Thermofischer, The Netherlands). The integrity of total RNA was checked using RNA Nanochips on a 2100 Bioanalyzer (Agilent Technologies, The Netherlands). Only samples with an RNA Integrity Number (RIN) higher than 6 were used for microarray analysis which was the case for all samples with an average of 8.8 ± 0.7.

II-4- cRNA synthesis, labelling and hybridization

Total RNA was synthesized into cRNA and labelled according to the One-Color Microarray-Based Gene Expression Analysis protocol version 6.6 (Agilent Technologies, The Netherlands). The procedure was performed as described by the manufacturer's protocol (28). The RNeasy Mini Kit (Qiagen, The Netherlands) was used to purify the amplified cRNA samples according to the manufacturer's protocol of Agilent. Subsequently, the cRNA was quantified using a Nanodrop® ND-1000 spectrophotometer with a Microarray Measurement. The yield and specific efficiency of the labelling of the cRNA was determined using the formulas in the protocol of Agilent.

Hybridization was performed according to the Agilent's protocol on SurePrint G3 mouse Gene exp 60kv2 microarrays slides (Agilent Technologies, The Netherlands). After hybridization, the microarray slides were scanned using an Agilent DNA Microarray Scanner with Surescan High-resolution Technology (Agilent Technologies, The Netherlands) with scanner settings to Dye Channel: G, Profile: AgilentG3_GX_1Color, Scan region: Agilent HD (61 x 21.3 mm), Scan resolution 3 µm, Tiff file dynamic range: 20 bit, Red PMT gain: 100%, Green PMT gain: 100%.

II-5- Pre-processing and data analysis of microarrays

The methods for pre-processing were performed as previously described (29). In short, first the quality of the microarrays was checked by the quality control pipeline provided by Agilent (Feature extraction software (FES) version 10.7.3.1). All samples met the quality criteria of the FES. In order to have a thorough quality check and normalize the data with local background correction, flagging of bad spots, controls and spots with too low intensity, log2 transformation and quantile normalization an in-house QC pipeline was developed and is publically available (github.com/BiGCAT-UM/arrayQC_Module). All samples met the in-house quality check. Raw data with expression values and genes were selected for data analysis based on flags and missing values (GEO accession: GSE92563). Height groups were defined: E171 2 days, 7 days, 14 days, 21 days for the exposed samples and control 2 days, 7 days, 14 days, 21 days for the controls. Within each group, at least 66% of the samples had to have a pass for the spot. Also, within each group, unique spot identifiers passed when there were less than 40% of missing values. The unique spot identifiers with an average expression less than four in all of the groups were omitted. The missing values were pre-processed using the GenePattern ImputeMissingValues.KNN module v13 (30), with standard settings. Unique spot identifiers were removed and identical Agilent probe identifiers were merged with Babelomics 5 (31), using the median method for pre-processing data. Next, the data was re-annotated from Agilent probe identifiers to EntrezGene identifiers (EntrezGeneIDs). The expression data for all genes with an identical EntrezGeneIDs were subsequently merged with Babelomics 5, using the median method for pre-processing data. Using an R-script, a Linear Mixed Model Analysis for Microarrays (LIMMA) (32) (version 1.0) was performed to extract differentially expressed genes (DEG) (33). The data of each control time point (control) was subtracted from the time-matched exposed mice to E171. The standard cut-off values of a fold-change (FC) of 1.5 and a p-value of 0.05 were used in LIMMA. Furthermore, the false discovery rate was calculated according to the Benjamini-Hochberg method with a threshold at 0.05.

II-6- Pathway and network analyses

The DEG for each time point were subsequently used in Consensus Pathway Database (CPDB) for an over-representation gene set analysis (ORA) (34,35). CPDB is an aggregate of 16 different databases developed by the Max Planck institute (35). With respect to content, CPDB has a focus on molecular interactions, and it provides deep exploration of the interactome network, protein complexes and pathway resources. All the available databases from CPDB were used (release MM9, 11 Oct. 2013) with settings in the “pathways as defined by pathway databases” with a minimum overlap of input list

of 2 and a p-value cut-off of $p<0.01$. For computing the significance of the over-representation of the annotation sets with respect to user-input molecules, CPDB applies Fisher's exact test. For each annotation set, the p-value is calculated. As many annotation sets are tested, CPBD corrects for multiple hypothesis testing using the false discovery rate procedure within each type of annotation set (34,35).

To validate the ORA method, a gene set enrichment analysis (GSEA) was performed. The GSEA method performed by CPDB carries out a paired Wilcoxon signed-rank test for each pathway based on the measurement values of each DEG per time point (34,35). All available databases from CPDB were used with settings in the “pathways as defined by pathway databases” with a minimum number of measured genes of 4 and a p-value cut-off of $p<0.01$.

A network analysis was performed using Cytoscape (version 3.4.0) (36) with the software application GeneMANIA (version 3.4.1). The GeneMANIA plugin in Cytoscape is based on a guilt-by-association approach to derive predictions from a combination of potentially heterogeneous data sources. The integration of an association of networks from multiple sources into a single composite network using a conjugate gradient optimization algorithm as described in Mostafavi et al. (37). Networks are weighted according to query dependent criteria. This compact matrix representation is used directly by the conjugate gradient algorithm. GeneMANIA allows the connection of genes in a network based on information on their function and expression found in literature (38), all DEG per time point were used and compared to the GEO database of *Mus musculus* for co-expression. The network was built using the EntrezGeneID. Among the 417 DEG at 2 days of exposure, 196 could not be recognized by GeneMANIA, 221 could be included in the network and 20 were added by GeneMANIA to improve the connections between the genes. Among the 971 DEG at 7 days of exposure, 271 could not be recognized by GeneMANIA, 700 could be included in the network and 20 were added by GeneMANIA. Among the 1512 DEG at 14 days of exposure, 336 could not be recognized by GeneMANIA, 1176 could be included in the network and 20 were added by GeneMANIA. Among the 229 DEG at 21 days of exposure, 90 could not be recognized by GeneMANIA, 140 could be included in the network and 19 were added by GeneMANIA. DEG belonging to a known pathway were extracted from the network, separated per biological processes (e.g. signalling, immune response) and coloured. All genes added by GeneMANIA to improve the network by linking some genes together were labelled with a different symbol and colour and were also extracted from the network.

II-7- Colorectal histology and Ki67 proliferative cell marker

The distal part of the colon was dissected, extensively washed with PBS and fixed with 4% paraformaldehyde. After fixation, colons were dehydrated in ethanol and embedded in paraffin. Cuts of 5 µm thickness were stained with Hematoxylin (Sigma-Aldrich, Mexico) & Eosin (Sigma-Aldrich, Mexico).

Ki67 immunostaining was used as a proliferative cell marker. Briefly, tissue section of 5 µm thickness were permeabilized and incubated overnight with primary antibody (dilution 1:300). Samples were then washed with PBS and incubated with the secondary antibody (dilution 1:100; IgG-FITC, Santa Cruz) for 1.5 hours at 37°C. Samples were analysed using a LEICA TCS SP2 confocal microscope. In each sample, 20 fields of 50 square millimetres were randomly used for fluorescence quantification. Data are described as mean ± standard error. Statistical analysis was performed with a Student t-test.

III- Results

III-1- Differently Expressed Genes (DEG)

DEG were observed per time point after correction by the time-matched control, indicating the impact of E171 on the gene expression levels in the distal colon. The number of genes that passed the pre-processing in all time points was 21,106 genes, of which 417 were significantly different ($p<0.05$ and $FC>1.5$) after 2 days of exposure, 971 after 7 days, 1512 after 14 days and 229 after 21 days (Table 1). Using an adjusted p-value, no DEG were observed at 2 and 21 days, therefore, the criteria for DEG used for further analysis are $p<0.05$ and $FC>1.5$.

Table 1: Summary of results of DEG after LIMMA analysis

	2 days	7 days	14 days	21 days
|FC| >= 1.5	1593	2638	3057	1305
Upregulated	776	717	823	520
Downregulated	817	1921	2234	785
p.val < 0.05	922	1918	3395	545
adj.p.val < 0.05	0	8	385	0
|FC| and p.val	417	971	1512	229
|FC| and adj.p.val	0	7	289	0

The majority of the genes was time specific, whereas a small number was in common between several time points (Figure 2) and only one gene was significantly upregulated at all time points: Cyfip1 (Supplementary Figure 1). In total 32 DEG were in common between 3 out of 4 time points. Of these, 11 DEG were in common between time points 2, 7, and 14 days however only 6 had a known biological function, others were cDNA or genes without a known function. This was also observed in the cluster with 7, 14, and 21 days where 13 DEG out of 14 had a known function. The 2, 7, and 21 days cluster contained 1 known DEG out of 3. The 2, 14, and 21 days cluster had 2 known DEG out of 4. Finally, there was a total of 23 DEG with a known biological function in 3 out of 4 time points and 1 common in the 4 time points. The gene names and direction of expression of the genes are shown in Supplementary Figure 1.

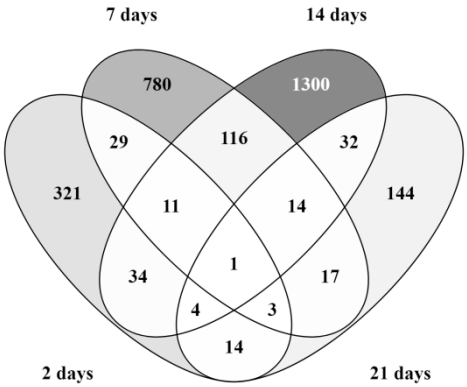

Figure 2: Venn diagram showing the overlap of DEG (p<0.05 and FC>1.5) between the different time points (2, 7, 14, and 21 days) after exposure to E171 in colon of mice.
Grey scale indicates the number of genes in the different parts of the Venn diagram.

III-2- Pathway and network analyses per time point

To gain insight in biological mechanisms of effects of E171, pathways were identified based on the CPDB as described in the Materials and Methods section. Only a relatively low proportion of the full list of DEG was involved in specific molecular pathways and could be identified by CPDB. Therefore, a network analysis with co-expression of genes was performed in order to observe the connection between genes in pathways and those that are as yet not included in these pathways. This allows for an improved and more complete biological interpretation of the effect of E171 in the colon. Below, first the results of the pathways analysis are described, followed by the network analysis.

III-2-1- Pathway analysis
III-2-1-1- 2 days of exposure

In Table 2, pathways identified per time point after ORA in CPDB are presented. After 2 days of exposure, signalling pathways such as signalling by GPCR, GPCR downstream signalling and signal transduction were observed. Furthermore in the same family as GPCRs, DEG were regulated in molecular pathways such as olfactory signalling, olfactory transduction, and odorant GPCRs. More details about the fold change and the direction of expression of the genes are presented in Table 5, in ref (39). A second group of pathways corresponded to an immune response with pathways such as Epstein-Barr virus infection and antigen processing and presentation. These 2 pathways contained genes such as H2-M9, Hspa1b and Hspa1a, Polr2d which were downregulated whereas Ikbkb, Cdkn1a and H2-M11 were upregulated. In a third group of pathways, cancer signalling group, 2 pathways were modulated: MAPK signalling pathway and

destabilization of mRNA by AUF1 (hnRNP D0). In the last group, metabolism, the Protein processing in endoplasmic reticulum pathway consisted of only down-regulated DEG such as Dnaja1, Dnajb1 and Ube2g2 (Table 5, in ref (39)).

The activation of signalling genes was confirmed by GSEA which resulted in 5 signalling pathways after 2 days of exposure (Supplementary Table 1). All pathways were common to the ORA and contained the same genes.

III-2-1-2- 7 days of exposure

The results after ORA showed that at day 7 of exposure and comparable to 2 days of exposure, signalling pathways were observed such as olfactory, GPCR, and signal transduction pathways, and insulin events with downregulated genes such as Ins1, Prkag3 and Trib3. The p-values of the signalling pathways were from 10^{-4} to 10^{-15} (Table 2). In the identical signalling pathways between 2 and 7 days, the number of DEG at 7 days was increased compared to 2 days. Also the ratio up- and -downregulated genes was increased towards up-regulation. More details about the genes can be found in Table 6, in ref (39). As at day 2 of exposure, after 7 days, a group of pathways related to cancer signalling was observed and contained a pathway linked to the MAPK pathway; p38MAPK event. Other pathways in cancer signalling at 7 days were no longer common to 2 days and contained some interesting upregulated genes such as Trp53, Mapkap3, Hist4h4Apc, Fzd5, and Patch1. Compared to 2 days, new pathways were related to oxidative stress. These pathways contained upregulated genes such as Phc1, Tpr3 (synonym of Tp53) and histone clusters. A second newly identified group of pathways named cell cycle with pathways such as RNA Polymerase I Promoter Opening pathway contained upregulated histone cluster genes. Furthermore, a neuronal system group of pathways contained amyloids and meiotic synapsis pathways with some upregulated histone genes. In addition, genes in metabolism pathways were modulated and ranging from vitamin C metabolism to protein citrunillation. The latter contained 2 downregulated DEG; Padi1 and Padi2.

As well as at day 2, at day 7, the activation of signalling genes was confirmed by using the GSEA method. Five of the 7 olfactory pathways were also observed and contained the same genes (Supplementary Table 1). In relation to the RNA polymerase pathway, mRNA processing pathway was present after using the GSEA method. This pathway contained genes related to the translation of mRNA with genes such as Eif4g3, Taf15, Papolg, and Rbm6. A pathway related to the transmembrane transport of small molecules was observed only after GSEA, with 14 genes from the solute carrier family.

Table 2: Result of the pathway over-representation analysis of the DEG in the distal colon of BALB/c mice after exposure to E171.

Time of exposure	Group of pathways	Name of pathway	p-value	Database
2 days	Signalling	- Olfactory transduction	7.36E-10	KEGG
		- Olfactory Signalling Pathway	9.95E-06	Reactome
		- Odorant GPCRs	8.67E-05	Wikipathways
		- Signalling by GPCR	0.000288	Reactome
		- GPCR downstream signalling	0.00052	Reactome
		- Signal Transduction	0.00745	Reactome
	Immune response	- Epstein-Barr virus infection	0.00632	KEGG
		- Antigen processing and presentation	0.00673	KEGG
	Cancer signalling	- Destabilization of mRNA by AUF1 (hnRNP D0)	0.00239	Reactome
		- MAPK signalling pathway	0.00473	KEGG
	Metabolism	- Protein processing in endoplasmic reticulum	0.00848	KEGG
7 days	Signalling	- Olfactory transduction	1.03E-15	KEGG
		- Olfactory Signalling Pathway	1.86E-12	Reactome
		- GPCR downstream signalling	3.99E-10	Reactome
		- Signalling by GPCR	1.39E-09	Reactome
		- Signal Transduction	1.03E-07	Reactome
		- Odorant GPCRs	0.000703	Wikipathways
		- GPCRs, Other	0.000938	Wikipathways
		- IRS-related events	0.00283	Reactome
		- Insulin receptor signalling cascade	0.00439	Reactome
		- SHC activation	0.00463	Reactome

	Cancer signalling	-	Cellular Senescence	0.00301	Reactome
		-	Basal cell carcinoma	0.0043	KEGG
		-	p38MAPK events	0.00817	Reactome
		-	Activation of PKB	0.00902	Reactome
		-	Formation of Senescence-Associated Heterochromatin Foci (SAHF)	0.00902	Reactome
	Cell cycle	-	Meiosis	0.00361	Reactome
		-	Meiotic Recombination	0.00488	Reactome
		-	RNA Polymerase I Promoter Opening	0.00599	Reactome
	Oxidative stress	-	Oxidative Stress Induced Senescence	0.00409	Reactome
		-	Cellular responses to stress	0.00826	Reactome
	Neuronal system	-	Amyloids	0.00488	Reactome
		-	Meiotic Synapsis	0.00272	Reactome
	Metabolism	-	Vitamin C (ascorbate) metabolism	0.00195	Reactome
		-	protein citrullination	0.00902	MouseCyc
14 days	Cancer signalling	-	GAB1 signalosome	0.0029	Reactome
		-	PIP3 activates AKT signalling	0.00535	Reactome
		-	PI-3K cascade	0.00535	Reactome
		-	PI3K events in ERBB2 signalling	0.00535	Reactome
		-	PI3K events in ERBB4 signalling	0.00535	Reactome
		-	PI3K/AKT Signalling in Cancer	0.00535	Reactome
		-	PI3K/AKT activation	0.00723	Reactome
		-	Glioma	0.00777	KEGG
		-	Melanoma	0.00868	KEGG
		-	Constitutive PI3K/AKT signalling in Cancer	0.00882	Reactome
	Cell cycle	-	Caspase-mediated cleavage of cytoskeletal proteins	0.00608	Reactome
		-	Signalling by ERBB4	0.00795	Reactome
		-	PERK regulated gene expression	0.00435	Reactome

	Oxidative stress	-	Mitochondrial Uncoupling Proteins	0.00435	Reactome
		-	The fatty acid cycling model	0.00435	Reactome
		-	The proton buffering model	0.00435	Reactome
	Immune response	-	Role of LAT2/NTAL/LAB on calcium mobilization	0.00359	Reactome
		-	Chemokine signalling pathway	0.00829	KEGG
		-	Role of phospholipids in phagocytosis	0.00392	Reactome
	Bone development	-	Chondroitin sulfate biosynthesis	0.00514	Reactome
		-	Chondroitin sulfate/dermatan sulfate metabolism	0.00844	Reactome
	Neuronal system	-	Serotonin receptors	0.00493	Reactome
21 days	Signalling	-	Olfactory Signalling Pathway	0.00035	Reactome
		-	Olfactory transduction	0.000556	KEGG
		-	GPCR downstream signalling	0.00162	Reactome
		-	Signal Transduction	0.00453	Reactome
		-	Signalling by GPCR	0.00543	Reactome
	Oxidative stress	-	Mitochondrial Uncoupling Proteins	7.71E-05	Reactome
		-	The fatty acid cycling model	7.71E-05	Reactome
		-	The proton buffering model	7.71E-05	Reactome
	Metabolism of proteins	-	Synthesis of glycosylphosphatidylinositol (GPI)	0.00655	Reactome

III-2-1-3- 14 days of exposure

The ORA showed that, after 14 days of exposure, 22 pathways illustrated the effect of E171 (Table 2). More details about the genes can be found in Table 7, in ref (39). Like at day 2 and 7, at day 14 a group of cancer signalling pathways was identified although the pathways included in that group were not identical. The pathways at day 14 were mostly related to the PI3K/AKT activation but also Glioma, Melanoma and GAB1 signalosome. Some of these genes were of interest such as downregulation of Pten or upregulation of Pik3r2, Akt1s1, Pik3r1, Foxo3, Src, Cdkn1a, Trp53 and Akt2.Immune related genes were expressed in the same direction as at day 2 with different pathways such as role of LAT2/NTAL/LAB on calcium mobilization, chemokine signalling pathway and role of phospholipids in phagocytosis. Modulation of genes in the group of cell cycle pathway was common to 7 days of exposure with different pathways such as caspase-mediated cleavage of cytoskeletal proteins, signalling by ERBB4 and PERK regulated gene expression. In the cell cycle group and the immune system group approximately 1/3 of the DEG were upregulated. Oxidative stress genes were activated as well as after 7 days of exposure but different pathways were involved in this activation. Interestingly, the oxidative stress group included the upregulation of Ucp2 and Ucp3 which were also upregulated at 21 days of exposure. As well as after 7 days of exposure, genes related to a neuronal response were also activated but with a different pathway serotonin receptors. An additional process with genes related to bone development was activated after 14 days of exposure, with 2 pathways being affected.

When the GSEA method was applied, similar results to the ORA were observed which confirms previously observed results. As well as at 7 days of exposure, GSEA displayed the modulation of signalling genes with 7 pathways. Among these 7 pathways, 2 were common to 2 and 7 days of exposure: signal transduction and signalling by GPCR. A similar but stronger immune response was observed with 7 pathways and 96 DEG involved in innate and adaptive immune system. Among the 96 DEG, 78% of them were down-regulated (Supplementary Table 1). As after 7 days of exposure, at day 14, GSEA showed an activation of genes related to the mRNA processing pathway. In addition, 2 extra pathways related to cellular processes were present, phagosome and endocytosis (Supplementary Table 1). Two additional processes were observed after 14 days, metabolism, metabolism of proteins and metabolism of diseases with 2, 2, and 14 pathways respectively. In the metabolism of diseases pathways, 13 pathways contained the same 12 genes as these pathways were all related to Mucopolysaccharidoses diseases.

III-2-1-4- 21 days of exposure

The results after ORA showed that at day 21 of exposure, fewer pathways were modulated (Table 2) compared to 14 days of exposure. Nine pathways were modulated and can be clustered into 3 groups. First, oxidative stress, common to 7 and 14 days, contained 3 pathways with the same 2 upregulated genes: Ucp2 and Ucp3 which were already observed at 14 days. Secondly, signalling pathways were significantly affected like at 2 and 7 days of exposure with the activation of pathways such as olfactory, GPCR and signal transduction pathways. Interesting genes in these pathways include Cxcl10 and Ccl27a which were also involved in an immune response. All these signalling pathways had more upregulated genes than downregulated ones as seen in Table 8, in ref (39). Last, metabolism of proteins contained one pathway, synthesis of glycosylphosphatidylinositol (GPI) pathway with 2 upregulated DEG. After 21 days of exposure, no pathways were observed using GSEA, the response is more subtle.

III-2-2- Network analysis

A relatively small fraction of the full gene list of DEG was involved in molecular pathways; therefore the next approach was to perform a network analysis with GeneMANIA on Cytoscape for each time point with co-expression of genes (Figure 3). Indeed, genes that were not directly in the pathways described above were now visualized, including the connection with the genes in pathways. With all DEG of each time point (2, 7, 14, and 21 days) networks analyses were performed. For every time point, more than 50% of all DEG could not be connected to a molecular pathway but could be connected with the genes in these pathways via co-expression. In addition, almost all genes in pathways were directly or indirectly connected via genes added by GeneMANIA to genes that are not known to be involved in pathways. Strong interactions between the genes related to molecular pathways and the other DEG can be observed. As these DEG have yet been linked to pathways, the interpretation of the effect of E171 in the colon is limited to the current knowledge about genes included in pathways.

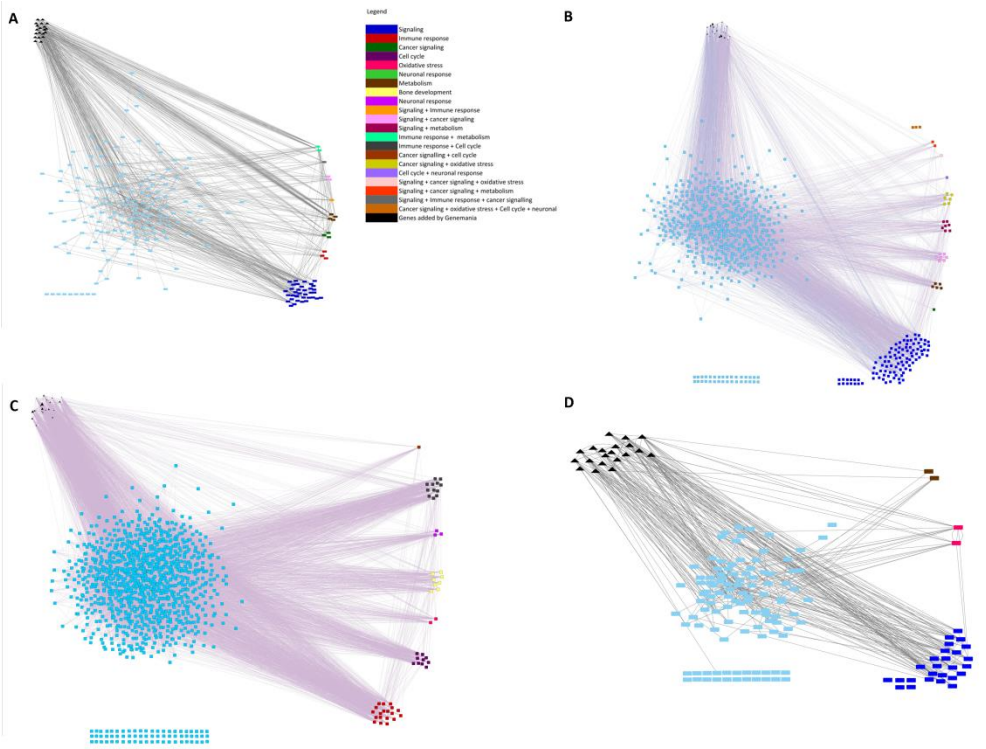

Figure 3: Linkage of pathway related genes to non-pathway related genes after (A) 2 days, (B) 7 days, (C) 14 days, (D) 21 days of exposure with all pathways p<0.01.

All the genes involved in a molecular pathway identified by CPDB after ORA were moved in a half-circle on the right side. Each group of gene has its own colour (see legend) and corresponds to genes involved in one or several biological processes. Genes not included in pathways are in the centre of the figure (light blue rectangles). All the added genes by the GeneMANIA application were displayed in the upper part of the network (black triangles). Genes that could not be linked in the network are aligned in the bottom left part of the figure (light blue rectangles).

III-3- Colorectal histology and proliferative cell marker

Histological changes were studied after H&E staining on the distal colon of the control group and the group exposed to E171 for all time points (Figure 4A). The distal colon of control groups showed typical epithelium with normal crypts after 2, 7, 14, and 21 days. Typical structure was also observed in the distal colon of mice treated with E171 for 2 days. However, after 7 days, colon tissue shows seldom alteration of the crypt architecture (green rectangles) and, at a later time point, 14 and 21 days, the exposure to E171 induced disruption in the normal structure of crypts with a hyperplastic epithelium (blue squares).

Expression of Ki67 was analysed in the control group as well as the group exposed to E171 for all the time points (Figure 4B and 4C). Results showed that, after 2 days, levels of Ki67 expression is 18% lower in the E171 treated mice compared to its time-matched control (Control: 164.2 ± 40.03 AU, E171: 134.03 ± 26.1 AU, $p<0.01$). After 7 day of exposure, the Ki67 expression was similar in control and exposed groups. Higher expression of Ki67, increase of 30%, was observed after 14 days in the E171 group compared to the control (Control: 108.27 ± 29.54 AU, E171: 141.4 ± 49.44 AU, $p< 0.01$). As well as at day 7, no differences at day 21 were seen.

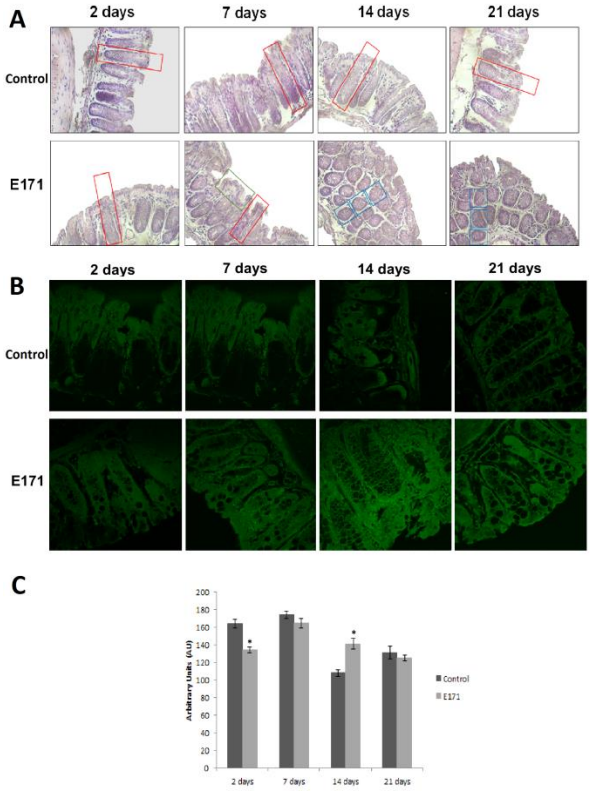

Figure 4: Representative images of colon after oral exposure to 5 mg/kg_{bw}/day of E171 for 2, 7, 14, and 21 days.

A) Representative images of histology using H&E staining. Red rectangles show a typical crypt structure in control tissue and also in group exposed to E171 for 2 days. In the exposed group to E171 for 7 days, colon tissue shows seldom alteration of the crypt architecture (green rectangles). Groups from 14 and 21 days of E171 exposure showed hyperplastic epithelium (blue squares). B) Representative images of Ki67 immunodetection of colon tissue of mice exposed to E171 for 2, 7, 14, and 21 days. Images were taken under 63X magnification. C) Arbitrary values of Ki67 immunodetection of colon tissue of control mice and mice exposed to E171. * Significant at $p<0.01$

IV- Discussion

The presented study shows that the food additive E171 induces gene expression changes in the colon of mice that were intragastrically exposed to this compound. Modulations of genes were observed in many different pathways from signalling to metabolism. However, these findings point towards inflammatory, immune, and carcinogenic processes and may offer a mechanistic framework for the enhanced tumour growth after ingestion of E171 in mice treated with AOM and DSS, as observed earlier by our group (24).

Consequent to the early molecular changes detected, seldom alteration of the crypt architecture after exposure to E171 for 7 days and hyperplastic alterations were observed at 14 and 21 days in the distal colon of mice. These results are consistent with the results of a previous study with an identical mouse model performed by our group in which hyperplastic alterations in the colon of mice were observed from 4 weeks of E171 ingestion (24). Histopathological changes in the colon occurred from 7 days on in this study and, in the identical mouse model, an increase of crypts size and number, and a decrease in the number of goblet cells was found from 4 weeks (24). Thus, our results confirm previous studies on the appearance of gene expression alterations before histopathological changes (40,41). At the level of cell proliferation after E171 exposure, no consistent increase over time is observed.

With regard to the molecular changes, the common response that we observed over time from 2 to 21 days of exposure (except at 14 days in the ORA) lies in the modulation of genes involved in GPCR and olfactory receptors (Table 2, Supplementary Table 1). GPCR are cell membranes associated receptors that transduce extracellular signals into intracellular effector pathways and are activated by a large number of endogenous and exogenous ligands and stimuli (42-45). In our data signature, several genes were not only GPCR/olfactory genes but were also involved in other known mechanisms which may influence cancer development in the gastro-intestinal tract. First, several genes were related to the activation of inflammation and chemokines. Ccl3 is a pro-inflammatory chemokine that modulates osteoclast differentiation by binding to GPCR (CCR1 and CCR5), and activates ERK and AKT signalling pathways (46). It was regulated at day 2 and 14 in our data. Furthermore, Cxcl10 gene was modulated after 21 days of exposure to E171 which is in line with Krüger at al. who showed that *in vitro* exposure to TiO_2 NPs induced gene expression changes in inflammatory genes like Cxcl10 (47). Moreover, Gpr75 activated by the chemokine Ccl5/Rantes (48) and Ptgdr2 has a role in the

eosinophils migration and mediates the pro-inflammatory chemotaxis of eosinophils, basophils, and Th2 lymphocytes generated during allergic inflammation (49,50). These were both regulated after 2 days. The second main known other function of these GPCR/olfactory and signalling genes is the activation of cancer related genes such as Ptch1 a tumour suppressor. Ghrhr is also involved in the growth of cancers such as breast and lung cancer (51). In our study, it was differentially expressed at 2, 7, and 14 days of exposure. Furthermore, cancer related DEG were also observed in signal transduction pathways at all time points. These DEG include fzd5 (frizzled homolog), Akt2, Ptch1 and Rous sarcoma oncogene (Src). Src, a member of the tyrosine kinase family, was up-regulated from 7 days of exposure. It has been shown that over-expression of this gene in colon cancer cells increases cell adhesion, invasion, and migration but not cell proliferation (52,53).

The effect of E171 on cancer related genes was observed from 7 days of exposure onwards. This effect might also have been induced indirectly via the immune system, as suggested by the activation of genes such as Trp53 (synonym of Tp53) and Pad. These are involved in regulating p53 and nuclear receptor target genes and play a role in the formation of NETs and antibacterial innate immunity (Table 6, in ref (39)) (54). After 14 days, cancer related genes and their related pathways were activated with 8 DEG involved in cell death upon oxidative stress and activation of cancer (52,55-57) (Table 7, in ref (39)). Over time, a total of 11 DEG have been identified that play a role in cancer and of which 7 are known to be specifically involved in CRC via various mechanisms such as the activation of cancer signalling or via the immune response (Supplementary Figure 1). This can be observed by the upregulation of Src gene which activates the PI3K/Akt (observed after 14 days of exposure), MAPK (observed at 2 days), Stat3, IL-8, and VEGF pathways from 7 days onwards. Enhancement of intestinal epithelial cell proliferation and protection from apoptosis is associated with the downregulation of the P2rx7. These effects are linked to an increased production of TGFβ1 (58). Related mechanisms such as survival of stem cells in the gut were activated by the upregulation from 7 days of Lgr4 and Flywch1. These genes cause overexpression of E-cadherin and both cell migration and defects that mimic the canonical Wnt loss-of-function (59). Another type of mechanism is induced by the mutation of Ptch1, its mutation in CRC induces a upregulation of the Hedgehog downstream gene Gli1 (53). In our study, this gene was significantly up-regulated from 2 to 14 days. Other genes over time are associated with CRC such as Diaph1 which was up-regulated from 7 days. Lin et al. have shown a significant correlation between colon cancer metastasis and expression of Diaph1; it is not detectable in normal colon cells but significantly upregulated in colon cancer metastasis (60). Chd7 gene was significantly up-

regulated from 2 to 14 days in our experiment. Its mutation is found in many subtypes of CRC (61,62). Finally, a suggested biomarker for breast cancer and colorectal cancer, Dyx1c1 (63,64) was activated at 2 days and downregulated at 7 and 14 days of exposure in our study.

Other genes showing over-expression after 7 days of exposure are involved in different type of cancers but not specifically in CRC like Ghrhr in breast and lung cancer (51), L1cam which supports metastasis and plays a major role in the malignancy of human tumours (65), and Eno1 which is often overexpressed in various human cancers and has been shown to play a critical role in glycolysis and in oncogenesis (66). Furthermore, DEG at multiple time points in cell cycle may have a direct and indirect impact on the development of cancer by several mechanisms. First mechanism is the inhibition cell death and growth cell arrest with the upregulation of growth arrest-specific 2 like 1 (Gas2l1) gene (67). A second mechanism is the effect on several translation factors such as the Cyfip1. Its protein binds to the translation initiation factor eIF4E and mediates translational repression in mammalian cells and its upregulation affects general mRNA translation (68,69). This effect can be observed at day 7 and 14 (after GSEA) with in the modulation of mRNA processing pathway. Another affected translation factor is the Transcription elongation factor A protein-like 5 (Tceal5) gene. It regulates transcription from RNA polymerase II promoter and transcription. In our data, it was downregulated from 2 to 14 days of exposure. A third mechanism involves the induction of RNA methylation with the upregulation from 7 days of tRNA methyltransferase 1 (Trmt1) gene (70).

Genes involved in the immune system were also affected by the presence of E171. This might also have an impact on the development of cancer. After 2 and 7 days of exposure, we observed a significant down-regulation of Hspa genes that are known to be active in the inflammation of the intestinal mucosa (71). At day 2 and 14, genes involved in the MHC class I & II presentation (H2-M9, H2-M11 and H2-Ea-ps), mice HLA genes, were up- and down-regulated. According to Pernot et al., a downregulation but not complete loss of MHC class I expression could contribute to an escape from NK-cell and T-cell mediated surveillance (72). In addition, after 14 days, 2 genes involved in the activation of the complement were downregulated. Our data is in line with previous findings where a systemic disturbance of cellular immune function after ingestion of food-grade TiO_2 in rats was also measured (14). In the rats' Peyer's Patches, a significant decreased frequency of immunoregulatory Tregs and $CD4^+CD25^+$ T helpers was observed after 7 and 100 days. Furthermore, an inhibition of the immune response (73) and a reduction in immune

capacity by the downregulation of genes involved in the activation of the complement (13) were observed in mice liver after ingestion of TiO_2 NPs. Immune responses can also be mediated by the activation of serotonin receptor genes. At day 14 and 21, serotonin or 5-hydroxytryptamine (5-HT) genes were regulated (Table 7 and 8, in ref (39)). These genes encode for a neurotransmitter and hormone that contributes to the regulation of various physiological functions by its actions in the central nervous system and in other organ systems (74). Enterochromaffin cells in the gastrointestinal tract are the main producers of peripheral 5-HT, and form the main source of serotonin in the human body (74,75). Peripheral 5-HT is a potent immune modulator and affects various immune cells such as dendritic cells through its receptors and via the process of serotonylation (75,76). Alterations in 5-HT signalling have been associated with tumour progression in prostate as well as breast cancer (77), regulation of genes involved in bone development (observed at 14 days) (78) and described in inflammatory conditions of the gut, such as inflammatory bowel disease (74). Hence, the activation of serotonin receptors may lead to a chain reaction where immune related genes are modulated, as well as inflammation.

Oxidative stress related genes were also induced by E171 starting from 7 days of exposure with an upregulation of DEG such as Trp53, Cabin1 and Mapkapk3. Furthermore, Ucp2 and Ucp3 were upregulated at 14 and 21 days and are activated when oxidative stress occurs. Their uncoupling activities of the oxidative phosphorylation in the mitochondria can be stimulated by superoxide anions, limiting ROS production by the mitochondrial respiratory chain (79,80). Previous studies suggested that Ucp2 may interact with oncogenes and tumour suppressor genes, providing a potential new mechanism of how Ucp2 contributes to cancer (80). These results showed that oxidative stress may be a constantly deregulated process over time and increases during prolonged exposure to E171. Possibly as a consequence of oxidative stress, pathways involved in DNA repair mechanisms were observed to be activated after 7 days of exposure. In total 7 pathways were identified after using the ORA method. All these pathways contain upregulated histone genes which have a crucial role in transcription regulation, DNA repair, DNA replication and chromosomal stability (81,82). Furthermore, Cdkn1a/p21 is activated at 2, 14 and 21 days. It inhibits cell cycle progression and allows DNA repair to proceed while inhibiting apoptosis (83). This confirms previous finding where TiO_2 NPs was found to induce oxidative stress and DNA damage *in vitro* in different cell lines like HepG2 (from 0.1 µg/mL) or Caco-2 (from 10 or 20 µg/mL) (8,22,84) and also *in vivo* in other mouse models where oxidative stress as well as inflammation and DNA damage after intragastric administration was observed (85-87). In addition to DNA repair, deregulation

of the genes in the metabolism of proteins like post-translational protein modification indicate an effect of E171 towards development of cancer.

ROS production also induces changes in metabolic pathways. At 2 days, cellular stress regulates the mRNA stability of genes coding for heat shock proteins (Hsp) (88). Indeed, in the protein processing in endoplasmic reticulum pathway, 5 Hsp genes and 1 ubiquitin-conjugating enzyme gene were down-regulated. Furthermore, at day 7, after using the ORA method, insulin related signalling pathway genes were activated. A previous study reported an increase of plasma glucose in mice after exposure to TiO_2 via the activation of MAPK pathways by production of ROS (89). We also observed modulation of MAPK genes at 2 days of exposure causing a deregulation of MAPK signalling pathway (Table 2). At day 7 after ORA, the vitamin C metabolism pathway, contained genes such as glutathione S-transferase omega 2 (Gsto2) and 1 solute carrier family gene (Table 6, in ref (39)). Solute carrier genes were also observed after GSEA at day 7 with the SLC-mediated transmembrane transport pathway (Supplementary Table 1). Glutathione gene expression was downregulated which is in line with a previous study where they observed a significant reduction of cellular GSH content in human epidermal cells due to the radicals produced by the TiO_2 NPs (90). Other genes such as genes involved in the synthesis of glycosylphosphatidylinositol (GPI) were also present in metabolism pathways and downregulated. These genes are involved in anchoring protein and glycoprotein to the cell surface in response to a stimuli (91) and genes are activated with the presence of oxidative stress (92). One GPI genes Pigb was activated at day 2, 7 and 21 (Supplementary Figure 1).

In order to conclude with respect to the effect of E171 over time, a network has been created in order to visualize the effect of exposure to E171 in the colon of mice (Figure 5). This network shows that via different mechanisms, E171 activates the immune response, inflammation, GPCR/olfactory receptors, cell cycle, DNA repair, cancer related genes, metabolism, and also serotonin receptors genes. This molecular response to the presence of E171 is very diverse and points towards an induction of inflammatory, immunological and specific cancer-related pathways in colon tissue that may explain the facilitated development of CRC by E171 reported previously (24). The histopathological modifications observed at 14 and 21 days are resulting from these molecular changes.

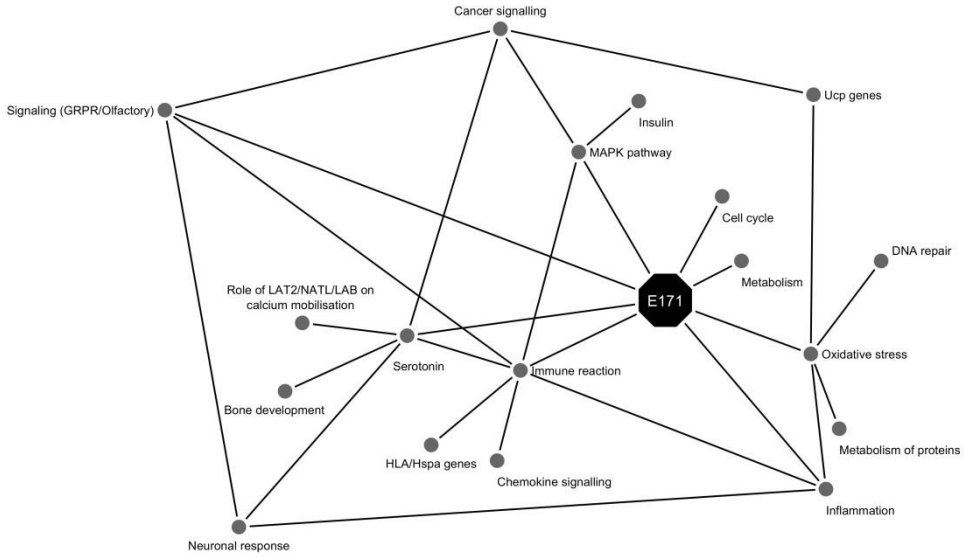

Figure 5: Network created with Cytoscape to visualize the interaction between the different biological processes (circles) regulated after exposure to E171 (octagon) for 2, 7, 14, and 21 days.

Not all DEG could be related to molecular pathways by CPDB, therefore a network analysis was performed with GeneMANIA. This network analysis showed, after all genes known to be in pathways were extracted (after ORA), that the number of genes present in the pathway analysis was low (Figure 3). This indicates that probably more genes, especially GPCR genes or olfactory genes, could be added in the corresponding pathways. At all investigated time points, the links by co-expression between the genes in molecular pathways and the centre of the network showed that the reaction after exposure to E171 in the colon was more extensive that what is actually known. Furthermore, most of the common genes between the different time points were contained in the centre of the network. The response of the colon cells to E171 was surely stronger than what can be observed by the current pathway classification. All the genes that could not directly be linked to pathways are of major interest for further studies since these might be related to yet unknown (biological) processes activated by exposure to E171.

V- Conclusion

In this study we observed gene expression changes in the distal colon of BALB/c mice after intragastric exposure to E171. We observed that E171 regulated GPCR/olfactory and serotonin gene receptors, induced oxidative stress and immune response pathways, activated genes for DNA repair and both up- and down-regulated genes involved in development of cancer, for instance colon cancer (Figure 5). Furthermore, we identified responses to E171 on the expression of genes that thus far have not been defined as being involved in any pathway but may be functionally related to genes which have been assigned to biologically relevant pathways. Although no consistent effect of cell proliferation was observed, histology showed a hyperplastic epithelium in colonic crypts after 14 and 21 days of E171 ingestion. To the best of our knowledge this is the first time that a full genome analysis indicating biological effects induced by exposure to E171 in the colon of mice are described at the mRNA level. The results are in line with our previous study in which oxidative stress and DNA damage was observed *in vitro* in colon epithelial cells after E171 exposure (8) and could explain in part the facilitation by E171 of tumour growth in the colon of the BALB/c mouse model for CRC (24). These results emphasize that the potentially harmful effects of E171 observed in the colon after oral exposure should be further investigated in order to guarantee the safe use of this food additive.

Supplementary materials

Supplementary Figure 1: Heat map of DEG (p<0.05 and FC>1.5) common in 3 out of 4 time points or in all time points after exposure to E171 in colon of mice for 2, 7, 14 and 21 days.

ftp://web.tgx.unimaas.nl/hproquin/Chapter_2a/Supplementary_figure_1.tif

Supplementary Table 1: Results of the pathway GSEA on the DEG in the distal colon of BALB/c mice after exposure to E171.

ftp://web.tgx.unimaas.nl/hproquin/Chapter_2a/Supplementary_table_1_enrichment_analysis.docx

Table 1 in ref (39): Differentially expressed genes (DEG) in the colon of mice after 2 days of exposure to E171

ftp://web.tgx.unimaas.nl/hproquin/Chapter_2b/Table_1_DEG_2_days.docx

Table 2 in ref (39): Differentially expressed genes (DEG) in the colon of mice after 7 days of exposure to E171

ftp://web.tgx.unimaas.nl/hproquin/Chapter_2b/Table_2_DEG_7_days.docx

Table 3 in ref (39): Differentially expressed genes (DEG) in the colon of mice after 14 days of exposure to E171

ftp://web.tgx.unimaas.nl/hproquin/Chapter_2b/Table_3_DEG_14_days.docx

Table 4 in ref (39): Differentially expressed genes (DEG) in the colon of mice after 21 days of exposure to E171

ftp://web.tgx.unimaas.nl/hproquin/Chapter_2b/Table_4_DEG_21_days.docx

Table 5 in ref (39): Group of pathways, pathways, genes related to this pathways and log2FC values after 2 days of exposure to E171 in BALB/c mice.
Numbers in bold are upregulated genes. Log2FC= Log2 fold change obtained with LIMMA script with correction for its own time-matched control.

ftp://web.tgx.unimaas.nl/hproquin/Chapter_2b/Table_5_pathways_and_genes_2_days.docx

Table 6 in ref (39): Group of pathways, pathways, genes related to this pathways and log2FC values after 7 days of exposure to E171 in BALB/c mice.
Numbers in bold are upregulated genes. Log2FC= Log2 fold change obtained with LIMMA script with correction for its own time-matched control.

ftp://web.tgx.unimaas.nl/hproquin/Chapter_2b/Table_6_pathways_and_genes_7_days.docx

Table 7 in ref (39): Group of pathways, pathways, genes related to this pathways and log2FC values after 14 days of exposure to E171 in BALB/c mice. Numbers in bold are upregulated genes. Log2FC= Log2 fold change obtained with LIMMA script with correction for its own time-matched control.

ftp://web.tgx.unimaas.nl/hproquin/Chapter_2b/Table_7_pathways_and_genes_14_days.docx

Table 8 in ref (39): Group of pathways, pathways, genes related to this pathways and log2FC values after 21 days of exposure to E171 in BALB/c mice.
Numbers in bold are upregulated genes. Log2FC= Log2 fold change obtained with LIMMA script with correction for its own time-matched control.

ftp://web.tgx.unimaas.nl/hproquin/Chapter_2b/Table_8_pathways_and_genes_21_days.docx

References

1. Globocan (2012) CANCER FACT SHEETS: COLORECTAL CANCER.
2. Haggar, F.A., and Boushey, R.P. (2009) Colorectal cancer epidemiology: incidence, mortality, survival, and risk factors. *Clin Colon Rectal Surg*, **22**, 191-197.
3. de Kok, T.M., de Waard, P., Wilms, L.C., and van Breda, S.G. (2010) Antioxidative and antigenotoxic properties of vegetables and dietary phytochemicals: the value of genomics biomarkers in molecular epidemiology. *Mol Nutr Food Res*, **54**, 208-217.
4. EU (2012) Regulation No 231-2012 on food additives. *Official Journal of the European Union*, **83**, 1-295.
5. Peters, R.J., van Bemmel, G., Herrera-Rivera, Z., Helsper, H.P., Marvin, H.J., Weigel, S., Tromp, P.C., Oomen, A.G., Rietveld, A.G., and Bouwmeester, H. (2014) Characterization of titanium dioxide nanoparticles in food products: analytical methods to define nanoparticles. *J Agric Food Chem*, **62**, 6285-6293.
6. Weir, A., Westerhoff, P., Fabricius, L., Hristovski, K., and von Goetz, N. (2012) Titanium dioxide nanoparticles in food and personal care products. *Environmental science & technology*, **46**, 2242-2250.
7. IARC (2010) IARC MONOGRAPHS ON THE EVALUATION OF CARCINOGENIC RISKS TO HUMANS: Carbon Black, Titanium dioxide and Talc. **Volume 93**.
8. Proquin, H., Rodriguez-Ibarra, C., Moonen, C.G., Urrutia Ortega, I.M., Briede, J.J., de Kok, T.M., van Loveren, H., and Chirino, Y.I. (2017) Titanium dioxide food additive (E171) induces ROS formation and genotoxicity: contribution of micro and nano-sized fractions. *Mutagenesis*, **32**, 139-149.
9. Dorier, M., Beal, D., Marie-Desvergne, C., Dubosson, M., Barreau, F., Houdeau, E., Herlin-Boime, N., and Carriere, M. (2017) Continuous in vitro exposure of intestinal epithelial cells to E171 food additive causes oxidative stress, inducing oxidation of DNA bases but no endoplasmic reticulum stress. *Nanotoxicology*, 1-54.
10. Rompelberg, C., Heringa, M.B., van Donkersgoed, G., Drijvers, J., Roos, A., Westenbrink, S., Peters, R., van Bemmel, G., Brand, W., and Oomen, A.G. (2016) Oral intake of added titanium dioxide and its nanofraction from food products, food supplements and toothpaste by the Dutch population. *Nanotoxicology*, **10**, 1404-1414.
11. EFSA (2016) Re-evaluation of titanium dioxide (E 171) as a food additive. *EFSA Journal*, **14**, e04545-n/a.
12. Macwan, D.P., Dave, P.N., and Chaturvedi, S. (2011) A review on nano-TiO2 sol-gel type syntheses and its applications. *J Mater Sci*, **46**, 3669-3686.
13. Cui, Y., Liu, H., Ze, Y., Zhang, Z., Hu, Y., Cheng, Z., Cheng, J., Hu, R., Gao, G., Wang, L., Tang, M., and Hong, F. (2015) Corrigendum: Gene Expression in Liver Injury Caused by Long-Term Exposure to Titanium Dioxide Nanoparticles in Mice. *Toxicol Sci*, **146**, 202.
14. Bettini, S., Boutet-Robinet, E., Cartier, C., Comera, C., Gaultier, E., Dupuy, J., Naud, N., Tache, S., Grysan, P., Reguer, S., Thieriet, N., Refregiers, M., Thiaudiere, D., Cravedi, J.P., Carriere, M., Audinot, J.N., Pierre, F.H., Guzylack-Piriou, L., and Houdeau, E. (2017) Food-grade TiO2 impairs intestinal and systemic immune homeostasis, initiates preneoplastic lesions and promotes aberrant crypt development in the rat colon. *Sci Rep*, **7**, 40373.
15. Liu, R., Yin, L.H., Pu, Y.P., Li, Y.H., Zhang, X.Q., Liang, G.Y., Li, X.B., Zhang, J., Li, Y.F., and Zhang, X.Y. (2010) The immune toxicity of titanium dioxide on primary pulmonary alveolar macrophages relies on their surface area and crystal structure. *J Nanosci Nanotechnol*, **10**, 8491-8499.
16. Dudefoi, W., Moniz, K., Allen-Vercoe, E., Ropers, M.H., and Walker, V.K. (2017) Impact of food grade and nano-TiO2 particles on a human intestinal community. *Food Chem Toxicol*, **106**, 242-249.
17. Jin, C.Y., Zhu, B.S., Wang, X.F., and Lu, Q.H. (2008) Cytotoxicity of titanium dioxide nanoparticles in mouse fibroblast cells. *Chem Res Toxicol*, **21**, 1871-1877.
18. Reeves, J.F., Davies, S.J., Dodd, N.J., and Jha, A.N. (2008) Hydroxyl radicals (*OH) are associated with titanium dioxide (TiO(2)) nanoparticle-induced cytotoxicity and oxidative DNA damage in fish cells. *Mutation research*, **640**, 113-122.

19. Cui, Y., Gong, X., Duan, Y., Li, N., Hu, R., Liu, H., Hong, M., Zhou, M., Wang, L., Wang, H., and Hong, F. (2010) Hepatocyte apoptosis and its molecular mechanisms in mice caused by titanium dioxide nanoparticles. *J Hazard Mater*, **183**, 874-880.
20. Park, E.J., Yi, J., Chung, K.H., Ryu, D.Y., Choi, J., and Park, K. (2008) Oxidative stress and apoptosis induced by titanium dioxide nanoparticles in cultured BEAS-2B cells. *Toxicology letters*, **180**, 222-229.
21. Chen, Z., Wang, Y., Ba, T., Li, Y., Pu, J., Chen, T., Song, Y., Gu, Y., Qian, Q., Yang, J., and Jia, G. (2014) Genotoxic evaluation of titanium dioxide nanoparticles in vivo and in vitro. *Toxicology letters*, **226**, 314-319.
22. Shi, Z.Q., Niu, Y.J., Wang, Q., Shi, L., Guo, H.C., Liu, Y., Zhu, Y., Liu, S.F., Liu, C., Chen, X., and Zhang, R. (2015) Reduction of DNA damage induced by titanium dioxide nanoparticles through Nrf2 in vitro and in vivo. *Journal of Hazardous Materials*, **298**, 310-319.
23. Zijno, A., De Angelis, I., De Berardis, B., Andreoli, C., Russo, M.T., Pietraforte, D., Scorza, G., Degan, P., Ponti, J., Rossi, F., and Barone, F. (2015) Different mechanisms are involved in oxidative DNA damage and genotoxicity induction by ZnO and TiO nanoparticles in human colon carcinoma cells. *Toxicol In Vitro*, **29**, 1503-1512.
24. Urrutia-Ortega, I.M., Garduno-Balderas, L.G., Delgado-Buenrostro, N.L., Freyre-Fonseca, V., Flores-Flores, J.O., Gonzalez-Robles, A., Pedraza-Chaverri, J., Hernandez-Pando, R., Rodriguez-Sosa, M., Leon-Cabrera, S., Terrazas, L.I., van Loveren, H., and Chirino, Y.I. (2016) Food-grade titanium dioxide exposure exacerbates tumor formation in colitis associated cancer model. *Food Chem Toxicol*, **93**, 20-31.
25. Gadbury, G.L., Page, G.P., Edwards, J., Kayo, T., Prolla, T.A., Weindruch, R., Permana, P.A., Mountz, J.D., and Allison, D.B. (2004) Power and sample size estimation in high dimensional biology. *Stat Methods Med Res*, **13**, 325-338.
26. Page, G.P., Edwards, J.W., Gadbury, G.L., Yelisetti, P., Wang, J., Trivedi, P., and Allison, D.B. (2006) The PowerAtlas: a power and sample size atlas for microarray experimental design and research. *Bmc Bioinformatics*, **7**, 84.
27. Qiagen (2012) RNeasy Mini Handbook. *https://www.qiagen.com/us/resources/resourcedetail?id=14e7cf6e-521a-4cf7-8cbc-bf9f6fa33e24&lang=en*.
28. Agilent (2015) One-Color Microarray-Based Gene Expression Analysis. *http://www.agilent.com/cs/library/usermanuals/Public/G4140-90040_GeneExpression_OneColor_6.9.pdf*.
29. Espin-Perez, A., de Kok, T.M., Jennen, D.G., Hendrickx, D.M., De Coster, S., Schoeters, G., Baeyens, W., van Larebeke, N., and Kleinjans, J.C. (2015) Distinct genotype-dependent differences in transcriptome responses in humans exposed to environmental carcinogens. *Carcinogenesis*, **36**, 1154-1161.
30. Reich, M., Liefeld, T., Gould, J., Lerner, J., Tamayo, P., and Mesirov, J.P. (2006) GenePattern 2.0. *Nature genetics*, **38**, 500-501.
31. Alonso, R., Salavert, F., Garcia-Garcia, F., Carbonell-Caballero, J., Bleda, M., Garcia-Alonso, L., Sanchis-Juan, A., Perez-Gil, D., Marin-Garcia, P., Sanchez, R., Cubuk, C., Hidalgo, M.R., Amadoz, A., Hernansaiz-Ballesteros, R.D., Aleman, A., Tarraga, J., Montaner, D., Medina, I., and Dopazo, J. (2015) Babelomics 5.0: functional interpretation for new generations of genomic data. *Nucleic Acids Res*, **43**, W117-121.
32. Smyth, G. (2017) Linear Models for Microarray Data. https://www.bioconductor.org/packages/devel/bioc/manuals/limma/man/limma.pdf.
33. Smyth, G.K. (2005) Limma: linear models for microarray data. *Bioinformatics and computational biology solutions using R and Bioconductor*. Springer, pp. 397-420.
34. Kamburov, A., Stelzl, U., Lehrach, H., and Herwig, R. (2013) The ConsensusPathDB interaction database: 2013 update. *Nucleic Acids Res*, **41**, D793-800.
35. Herwig, R., Hardt, C., Lienhard, M., and Kamburov, A. (2016) Analyzing and interpreting genome data at the network level with ConsensusPathDB. *Nat Protoc*, **11**, 1889-1907.

36. Cline, M.S., Smoot, M., Cerami, E., Kuchinsky, A., Landys, N., Workman, C., Christmas, R., Avila-Campilo, I., Creech, M., Gross, B., Hanspers, K., Isserlin, R., Kelley, R., Killcoyne, S., Lotia, S., Maere, S., Morris, J., Ono, K., Pavlovic, V., Pico, A.R., Vailaya, A., Wang, P.L., Adler, A., Conklin, B.R., Hood, L., Kuiper, M., Sander, C., Schmulevich, I., Schwikowski, B., Warner, G.J., Ideker, T., and Bader, G.D. (2007) Integration of biological networks and gene expression data using Cytoscape. *Nature Protocols*, **2**, 2366-2382.
37. Mostafavi, S., Ray, D., Warde-Farley, D., Grouios, C., and Morris, Q. (2008) GeneMANIA: a real-time multiple association network integration algorithm for predicting gene function. *Genome Biol*, **9 Suppl 1**, S4.
38. Montojo, J., Zuberi, K., Rodriguez, H., Kazi, F., Wright, G., Donaldson, S.L., Morris, Q., and Bader, G.D. (2010) GeneMANIA Cytoscape plugin: fast gene function predictions on the desktop. *Bioinformatics*, **26**, 2927-2928.
39. Proquin, H., Jetten, M.J., Jonkhout, M.C.M., Garduno-Balderas, L.G., Briede, J.J., de Kok, T.M., Chirino, Y.I., and van Loveren, H. (2017) Time course gene expression data in colon of mice after exposure to food-grade E171. *Data in Brief,* **16,** 531-600.
40. Waters, M.D., and Fostel, J.M. (2004) Toxicogenomics and systems toxicology: aims and prospects. *Nat Rev Genet*, **5**, 936-948.
41. Castro, N.P., Osorio, C.A., Torres, C., Bastos, E.P., Mourao-Neto, M., Soares, F.A., Brentani, H.P., and Carraro, D.M. (2008) Evidence that molecular changes in cells occur before morphological alterations during the progression of breast ductal carcinoma. *Breast Cancer Res*, **10**, R87.
42. Busnelli, M., Mauri, M., Parenti, M., and Chini, B. (2013) Analysis of GPCR dimerization using acceptor photobleaching resonance energy transfer techniques. *Methods Enzymol*, **521**, 311-327.
43. Lappano, R., and Maggiolini, M. (2012) GPCRs and cancer. *Acta Pharmacol Sin*, **33**, 351-362.
44. Kroeze, W.K., Sheffler, D.J., and Roth, B.L. (2003) G-protein-coupled receptors at a glance. *J Cell Sci*, **116**, 4867-4869.
45. Perez, D.M. (2005) From plants to man: the GPCR "tree of life". *Mol Pharmacol*, **67**, 1383-1384.
46. Vallet, S., Pozzi, S., Patel, K., Vaghela, N., Fulciniti, M.T., Veiby, P., Hideshima, T., Santo, L., Cirstea, D., Scadden, D.T., Anderson, K.C., and Raje, N. (2011) A novel role for CCL3 (MIP-1alpha) in myeloma-induced bone disease via osteocalcin downregulation and inhibition of osteoblast function. *Leukemia*, **25**, 1174-1181.
47. Kruger, K., Schrader, K., and Klempt, M. (2017) Cellular Response to Titanium Dioxide Nanoparticles in Intestinal Epithelial Caco-2 Cells is Dependent on Endocytosis-Associated Structures and Mediated by EGFR. *Nanomaterials (Basel)*, **7**.
48. Liu, B., Hassan, Z., Amisten, S., King, A.J., Bowe, J.E., Huang, G.C., Jones, P.M., and Persaud, S.J. (2013) The novel chemokine receptor, G-protein-coupled receptor 75, is expressed by islets and is coupled to stimulation of insulin secretion and improved glucose homeostasis. *Diabetologia*, **56**, 2467-2476.
49. Monneret, G., Gravel, S., Diamond, M., Rokach, J., and Powell, W.S. (2001) Prostaglandin D-2 is a potent chemoattractant for human eosinophils that acts via a novel DIP receptor. *Blood*, **98**, 1942-1948.
50. Hirai, H., Tanaka, K., Yoshie, O., Ogawa, K., Kenmotsu, K., Takamori, Y., Ichimasa, M., Sugamura, K., Nakamura, M., Takano, S., and Nagata, K. (2001) Prostaglandin D2 selectively induces chemotaxis in T helper type 2 cells, eosinophils, and basophils via seven-transmembrane receptor CRTH2. *J Exp Med*, **193**, 255-261.
51. Barabutis, N., Tsellou, E., Schally, A.V., Kouloheri, S., Kalofoutis, A., and Kiaris, H. (2007) Stimulation of proliferation of MCF-7 breast cancer cells by a transfected splice variant of growth hormone-releasing hormone receptor. *Proc Natl Acad Sci U S A*, **104**, 5575-5579.
52. Playford, M.P., and Schaller, M.D. (2004) The interplay between Src and integrins in normal and tumor biology. *Oncogene*, **23**, 7928-7946.
53. Chung, J.H., and Bunz, F. (2013) A loss-of-function mutation in PTCH1 suggests a role for autocrine hedgehog signaling in colorectal tumorigenesis. *Oncotarget*, **4**, 2208-2211.
54. Wang, S., and Wang, Y. (2013) Peptidylarginine deiminases in citrullination, gene regulation, health and pathogenesis. *Biochim Biophys Acta*, **1829**, 1126-1135.

55. Futreal, P.A., Coin, L., Marshall, M., Down, T., Hubbard, T., Wooster, R., Rahman, N., and Stratton, M.R. (2004) A census of human cancer genes. *Nat Rev Cancer*, **4**, 177-183.
56. Ortega-Molina, A., and Serrano, M. (2013) PTEN in cancer, metabolism, and aging. *Trends Endocrinol Metab*, **24**, 184-189.
57. Firat, E., and Niedermann, G. (2016) FoxO proteins or loss of functional p53 maintain stemness of glioblastoma stem cells and survival after ionizing radiation plus PI3K/mTOR inhibition. *Oncotarget*.
58. Hofman, P., Cherfils-Vicini, J., Bazin, M., Ilie, M., Juhel, T., Hebuterne, X., Gilson, E., Schmid-Alliana, A., Boyer, O., Adriouch, S., and Vouret-Craviari, V. (2015) Genetic and pharmacological inactivation of the purinergic P2RX7 receptor dampens inflammation but increases tumor incidence in a mouse model of colitis-associated cancer. *Cancer research*, **75**, 835-845.
59. Muhammad, B., Saadeddin, A., Spencer, B., Ibrahim, E.-S., Ilyas, M., and Nater, A. (2013) Identification, characterisation and functional analyses of novel beta-catenin associated protein, FLYWCH1. *PhD thesis, University of Nottingham*.
60. Lin, Y.N., Izbicki, J.R., Konig, A., Habermann, J.K., Blechner, C., Lange, T., Schumacher, U., and Windhorst, S. (2014) Expression of DIAPH1 is up-regulated in colorectal cancer and its down-regulation strongly reduces the metastatic capacity of colon carcinoma cells. *International journal of cancer. Journal international du cancer*, **134**, 1571-1582.
61. Kim, M.S., Chung, N.G., Kang, M.R., Yoo, N.J., and Lee, S.H. (2011) Genetic and expressional alterations of CHD genes in gastric and colorectal cancers. *Histopathology*, **58**, 660-668.
62. Tahara, T., Yamamoto, E., Madireddi, P., Suzuki, H., Maruyama, R., Chung, W., Garriga, J., Jelinek, J., Yamano, H.O., Sugai, T., Kondo, Y., Toyota, M., Issa, J.P., and Estecio, M.R. (2014) Colorectal carcinomas with CpG island methylator phenotype 1 frequently contain mutations in chromatin regulators. *Gastroenterology*, **146**, 530-538 e535.
63. Rosin, G., Hannelius, U., Lindstrom, L., Hall, P., Bergh, J., Hartman, J., and Kere, J. (2012) The dyslexia candidate gene DYX1C1 is a potential marker of poor survival in breast cancer. *BMC Cancer*, **12**, 79.
64. Kim, Y.J., Huh, J.W., Kim, D.S., Bae, M.I., Lee, J.R., Ha, H.S., Ahn, K., Kim, T.O., Song, G.A., and Kim, H.S. (2009) Molecular characterization of the DYX1C1 gene and its application as a cancer biomarker. *J Cancer Res Clin Oncol*, **135**, 265-270.
65. Kiefel, H., Bondong, S., Hazin, J., Ridinger, J., Schirmer, U., Riedle, S., and Altevogt, P. (2012) L1CAM: a major driver for tumor cell invasion and motility. *Cell Adh Migr*, **6**, 374-384.
66. Zhan, P., Wang, Y., Zhao, S., Liu, C., Wang, Y., Wen, M., Mao, J.H., Wei, G., and Zhang, P. (2015) FBXW7 negatively regulates ENO1 expression and function in colorectal cancer. *Lab Invest*, **95**, 995-1004.
67. Benetti, R., Del Sal, G., Monte, M., Paroni, G., Brancolini, C., and Schneider, C. (2001) The death substrate Gas2 binds m-calpain and increases susceptibility to p53-dependent apoptosis. *EMBO J*, **20**, 2702-2714.
68. De Rubeis, S., Pasciuto, E., Li, K.W., Fernandez, E., Di Marino, D., Buzzi, A., Ostroff, L.E., Klann, E., Zwartkruis, F.J., Komiyama, N.H., Grant, S.G., Poujol, C., Choquet, D., Achsel, T., Posthuma, D., Smit, A.B., and Bagni, C. (2013) CYFIP1 coordinates mRNA translation and cytoskeleton remodeling to ensure proper dendritic spine formation. *Neuron*, **79**, 1169-1182.
69. Napoli, I., Mercaldo, V., Boyl, P.P., Eleuteri, B., Zalfa, F., De Rubeis, S., Di Marino, D., Mohr, E., Massimi, M., Falconi, M., Witke, W., Costa-Mattioli, M., Sonenberg, N., Achsel, T., and Bagni, C. (2008) The fragile X syndrome protein represses activity-dependent translation through CYFIP1, a new 4E-BP. *Cell*, **134**, 1042-1054.
70. Davarniya, B., Hu, H., Kahrizi, K., Musante, L., Fattahi, Z., Hosseini, M., Maqsoud, F., Farajollahi, R., Wienker, T.F., Ropers, H.H., and Najmabadi, H. (2015) The Role of a Novel TRMT1 Gene Mutation and Rare GRM1 Gene Defect in Intellectual Disability in Two Azeri Families. *PLoS One*, **10**, e0129631.
71. Scieglinska, D., Piglowski, W., Chekan, M., Mazurek, A., and Krawczyk, Z. (2011) Differential expression of HSPA1 and HSPA2 proteins in human tissues; tissue microarray-based immunohistochemical study. *Histochem Cell Biol*, **135**, 337-350.
72. Pernot, S., Terme, M., Voron, T., Colussi, O., Marcheteau, E., Tartour, E., and Taieb, J. (2014) Colorectal cancer and immunity: what we know and perspectives. *World J Gastroentero*, **20**, 3738-3750.

73. Duan, Y., Liu, J., Ma, L., Li, N., Liu, H., Wang, J., Zheng, L., Liu, C., Wang, X., Zhao, X., Yan, J., Wang, S., Wang, H., Zhang, X., and Hong, F. (2010) Toxicological characteristics of nanoparticulate anatase titanium dioxide in mice. *Biomaterials*, **31**, 894-899.
74. Gershon, M.D., and Tack, J. (2007) The serotonin signaling system: from basic understanding to drug development for functional GI disorders. *Gastroenterology*, **132**, 397-414.
75. Shajib, M.S., and Khan, W.I. (2015) The role of serotonin and its receptors in activation of immune responses and inflammation. *Acta Physiol (Oxf)*, **213**, 561-574.
76. Idzko, M., Panther, E., Stratz, C., Muller, T., Bayer, H., Zissel, G., Durk, T., Sorichter, S., Di Virgilio, F., Geissler, M., Fiebich, B., Herouy, Y., Elsner, P., Norgauer, J., and Ferrari, D. (2004) The serotoninergic receptors of human dendritic cells: identification and coupling to cytokine release. *J Immunol*, **172**, 6011-6019.
77. Dizeyi, N., Bjartell, A., Nilsson, E., Hansson, J., Gadaleanu, V., Cross, N., and Abrahamsson, P.A. (2004) Expression of serotonin receptors and role of serotonin in human prostate cancer tissue and cell lines. *Prostate*, **59**, 328-336.
78. Yano, J.M., Yu, K., Donaldson, G.P., Shastri, G.G., Ann, P., Ma, L., Nagler, C.R., Ismagilov, R.F., Mazmanian, S.K., and Hsiao, E.Y. (2015) Indigenous bacteria from the gut microbiota regulate host serotonin biosynthesis. *Cell*, **161**, 264-276.
79. Rial, E., and Zardoya, R. (2009) Oxidative stress, thermogenesis and evolution of uncoupling proteins. *J Biol*, **8**, 58.
80. Robbins, D., and Zhao, Y. (2011) New aspects of mitochondrial Uncoupling Proteins (UCPs) and their roles in tumorigenesis. *Int J Mol Sci*, **12**, 5285-5293.
81. Hunt, C.R., Ramnarain, D., Horikoshi, N., Iyengar, P., Pandita, R.K., Shay, J.W., and Pandita, T.K. (2013) Histone modifications and DNA double-strand break repair after exposure to ionizing radiations. *Radiat Res*, **179**, 383-392.
82. Rossetto, D., Avvakumov, N., and Cote, J. (2012) Histone phosphorylation: a chromatin modification involved in diverse nuclear events. *Epigenetics*, **7**, 1098-1108.
83. Abbas, T., and Dutta, A. (2009) p21 in cancer: intricate networks and multiple activities. *Nat Rev Cancer*, **9**, 400-414.
84. Gerloff, K., Albrecht, C., Boots, A.W., Forster, I., and Schins, R.P.F. (2009) Cytotoxicity and oxidative DNA damage by nanoparticles in human intestinal Caco-2 cells. *Nanotoxicology*, **3**, 355-364.
85. Trouiller, B., Reliene, R., Westbrook, A., Solaimani, P., and Schiestl, R.H. (2009) Titanium dioxide nanoparticles induce DNA damage and genetic instability in vivo in mice. *Cancer research*, **69**, 8784-8789.
86. Iavicoli, I., Leso, V., and Bergamaschi, A. (2012) Toxicological Effects of Titanium Dioxide Nanoparticles: A Review of In Vivo Studies. *J Nanomater*.
87. Wang, J., Li, N., Zheng, L., Wang, S., Wang, Y., Zhao, X., Duan, Y., Cui, Y., Zhou, M., Cai, J., Gong, S., Wang, H., and Hong, F. (2011) P38-Nrf-2 signaling pathway of oxidative stress in mice caused by nanoparticulate TiO2. *Biol Trace Elem Res*, **140**, 186-197.
88. Deka, K., Singh, A., Chakraborty, S., Mukhopadhyay, R., and Saha, S. (2016) Protein arginylation regulates cellular stress response by stabilizing HSP70 and HSP40 transcripts. *Cell Death Discov*, **2**, 16074.
89. Hu, H., Li, L., Guo, Q., Jin, S., Zhou, Y., Oh, Y., Feng, Y., Wu, Q., and Gu, N. (2016) A mechanistic study to increase understanding of titanium dioxide nanoparticles-increased plasma glucose in mice. *Food Chem Toxicol*, **95**, 175-187.
90. Shukla, R.K., Sharma, V., Pandey, A.K., Singh, S., Sultana, S., and Dhawan, A. (2011) ROS-mediated genotoxicity induced by titanium dioxide nanoparticles in human epidermal cells. *Toxicol In Vitro*, **25**, 231-241.
91. Swarts, B.M., and Guo, Z. (2012) Chemical synthesis of glycosylphosphatidylinositol anchors. *Adv Carbohydr Chem Biochem*, **67**, 137-219.
92. Okada, N., Ogawa, J., and Shima, J. (2014) Comprehensive analysis of genes involved in the oxidative stress tolerance using yeast heterozygous deletion collection. *Fems Yeast Res*, **14**, 425-434.

Chapter 3

Transcriptomics analysis reveals new insights in E171-induced molecular alterations in a mouse model of colon cancer

Scientific Reports, December 2018, Volume 8 (1):9738

Héloïse Proquin

Marlon J. Jetten

Marloes C.M. Jonkhout

Luis Guillermo Garduño-Balderas

Jacob J. Briedé

Theo M. de Kok

Henk van Loveren

Yolanda I. Chirino

Abstract

Titanium dioxide as a food additive (E171) has been demonstrated to facilitate growth of chemically induced colorectal tumours *in vivo* and induce transcriptomic changes suggestive of an immune system impairment and cancer development. The present study aimed to investigate the molecular mechanisms behind the tumour stimulatory effects of E171 in combination with azoxymethane (AOM)/dextran sodium sulphate (DSS) and compare these results to a recent study performed under the same conditions with E171 only. BALB/c mice underwent exposure to 5 mg/kg_{bw}/day of E171 by gavage for 2, 7, 14, and 21 days. Whole genome mRNA microarray analyses on the distal colon were performed. The results show that E171 induced a downregulation of genes involved in the innate and adaptive immune system, suggesting impairment of this system. In addition, over time, signalling genes involved in colorectal cancer and other types of cancers were modulated. In relation to cancer development, effects potentially associated with oxidative stress were observed through modulation of genes related to antioxidant production. E171 affected genes involved in biotransformation of xenobiotics which can form reactive intermediates resulting in toxicological effects. These transcriptomics data reflect the early biological responses induced by E171 which precede tumour formation in an AOM/DSS mouse model.

I- Introduction

Titanium dioxide (TiO_2) is the most produced mineral worldwide (1) and is used for its white colouring properties and stability over time (2). One of the main applications of TiO_2 is its use as a food additive in processed food such as cookies, sweets, toppings and coffee creamer (1-3). TiO_2 was accepted as a food colorant and registered under the code of E171 by the European Union (EU) in 1969 (4). This approval followed a risk assessment made earlier that year by the joint Food Agriculture Organisation and World Health Organisation (FAO/WHO) that identified no risk concerning the ingestion of TiO_2 (4). Therefore, E171 is permitted by the EU in food at *quantum satis*, which means that there are no maximum intake levels for ingestion. In the USA, the regulation by the food and drug administration limits titanium dioxide to a maximum of 1% of the weight of the food (5).

Over the past decade, characteristics have been studied in order to assess possible adverse effects. The shape and size of E171 have been measured by several groups. E171 consist of approximately 40% of nanoparticles (NPs) (<100 nm) and 60% of microparticles (MPs) (>100 nm) (3,6,7). Studies on possible adverse effects have primarily been focused on inhalation of TiO_2. Based on the outcome of these studies, the International Agency for Research in Cancer (IARC) changed in 2010 the classification of TiO_2 from non-carcinogenic to probable carcinogenic to humans (Group 2B) (8).

More recently, there are increasing number of studies to detect and quantify E171 in foods for human consumption (9), pharmaceutical products (10), to distinguish between NPs and MPs in foods, and to estimate the daily intake in adults and children (11). In addition, a number of both *in vivo* and *in vitro* studies report on the adverse effects of exposure to TiO_2 by the oral route and the biological mechanisms involved. *In vitro* studies have identified induction of DNA damage and oxidative stress by the production of reactive oxygen species (ROS) in colon cell lines such as Caco-2 and HCT116 cells (6,7,12). Inflammation has also been observed *in vivo* with a significant increase of superoxide anion ($O_2^{\bullet -}$) and hydrogen peroxide (H_2O_2) in the liver after ingestion of 10 mg/kg_{bw} of TiO_2 NPs for 60 days in rats (13). The same group observed after ingestion of 10 mg/kg_{bw} of TiO_2 NPs for 90 days an induced inflammation and a reduction of the immune capacity in liver (14). A more recent study performed by our group showed a significant increase of the number of colonic tumours after ingestion of E171 for 10 weeks in a murine colorectal cancer (CRC) model, in which colorectal tumours were chemically induced by azoxymethane (AOM)/dextran sodium sulphate (DSS) (15). In addition, we

identified that a decrease in number of goblet cells and neoplastic alterations in distal colon of mice began after 4 weeks of exposure to TiO_2 (15). We also investigated initial transcriptome changes in colon tissue before the neoplastic alterations appeared and found that intragastric exposure to 5 mg/kg_{bw}/day of E171 for 2, 7, 14 and 21 days led to the up-regulation of genes involved in activation of inflammation, reduction of immune capacity and up-regulation of genes related in the development of CRC (16). In line with our data, Bettini et al. observed, after ingestion of E171 in rats, a potent Th1/Th17 immune response via an increased production of IFN-γ in Peyer's Patches and IFN-γ and IL-17 in the spleen after 7 days of exposure (17). In addition, Bettini et al. showed that E171 exposure for 100 days in a chemically induced carcinogenesis model induced a release of inflammatory molecules at a low level in the colon, preneoplastic lesions as well as the growth of aberrant crypt foci.

Based on the previous studies on the effects of E171 in the colon, we raised the hypothesis that ingestion of E171 induces gene expression changes in colon that are related to inflammation, deregulation of cancer-related genes and impairment of the immune system before tumours are detectable. To test this hypothesis, mice were co-exposed to AOM/DSS and to 5 mg/kg_{bw}/day of E171 for 2, 7, 14 and 21 days and transcriptome changes in the colon were determined by whole genome mRNA microarrays.

II- Materials and Methods

II-1- E171 particle characterisation

E171 was generously donated by the Sensient Technologies Company in Mexico. Characterisation of E171 was performed previously by electron microscopy with Scios DualBeam FIB/SEM (SEM, 20 KV, the Netherlands) at 150,000x magnification to evaluate the size and morphology of the particles (6). E171 contains slightly to fully rounded particles with a proportion of 39% NPs and 61% MPs.

II-2- Mouse model

Exposure of BALB/c mice to E171 by ingestion was performed at the Unidad de Biomedicina, Facultad de Estudios Superiores Iztacala, Universidad Nacional Autónoma de México, Mexico. Ethical approval was given by the Comité de Ética de la Facultad de Estudios Superiores Iztacala de la Universidad Nacional Autónoma de México under the number: FESI-ICY-I151. Guidelines of Norma Oficial Mexicana (NOM-062-ZOO-1999, NOM-087-ECOL-1995) were followed as well as the Protocol for the Care and Use of Laboratory Animals (PICUAL). The exposure of BALB/c mice was performed at the same time as a similar experiment (16) with a few changes as described below. After one week of acclimatisation, 32 BALB/c mice (16 males, 16 females) of 4-6 weeks of age (Harlan Laboratories, Mexico) were randomly placed into 2 groups: a) control group (AOM/DSS) (8 males, 8 females) named CRC and b) E171 group with AOM/DSS (8 males, 8 females) named CRC + E171 (Figure 1). One week before the start of the experiment, both groups received a single intraperitoneal injection of 12.5 mg/kg_{bw} of AOM (Sigma, USA) as described in the chemically colitis-associated colorectal cancer mouse model of Tanaka et al. (18). The first 5 days of the experiment, both groups were given 2% DSS (MW 35000-50000, MP Biomedicals, Solon OH, USA) dissolved in water and filtered *ad libitum*. In addition, the E171 group received an intragastric administration of 5 mg/kg_{bw} of E171 dispersed in drinking water and sonicated 30 min at 60 Hz by a gavage feeding 5 days per week for 21 days according to the scheme (Figure 5). The control group received 100 µL of sterile sonicated water (30 min at 60 Hz) by intragastric gavage 5 days per week during 21 days according to the scheme.

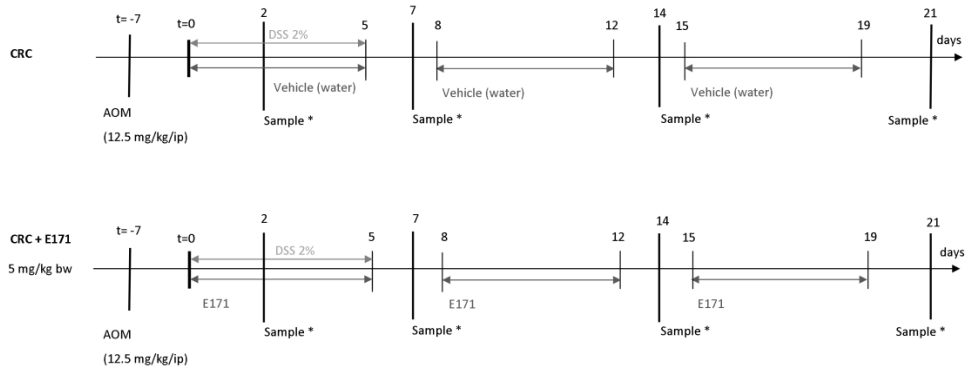

Figure 1: Scheme of exposure of experimental mouse model.

BALB/c mice (n = 32) were randomly distributed in 2 groups (16 per group) and were kept one week under acclimation conditions. Both the control and exposure group received a single intraperitoneal injection 12.5 mg/kg of AOM a week before the start of the experiment and DSS 2% dissolved in water *ad libitum* between day 1 and 5 respectively (light grey line). From day 1 to 21, E171 group received 5 mg/kg body weight by oral gavage of E171 dispersed in water 5 days per week (black line). The control group kept on receiving a vehicle (sterile water). *2 males and 2 females were sampled.

II-3- mRNA isolation from colonic tissues

mRNA extraction from the distal colons followed the same protocol as the previous study (16). In short, mRNA was isolated according to the manufacturer's protocols for "Animal Cells and Animal Tissues" (19), the miRNeasy Mini Kit (Qiagen, The Netherlands) with DNase treatment (Qiagen, The Netherlands). Total RNA yield as well as the 260/230 and the 260/280 were measured on a Nanodrop® ND-1000 spectrophotometer (ThermoFischer). Samples with a 260/230 ratio between 1.8 and 2.0 and a 260/280 ratio between 1.9 and 2.1 were checked for their integrity. The integrity of total RNA was checked using RNA Nanochips on a 2100 Bioanalyzer using manufacturer's protocol (Agilent Technologies, The Netherlands). All samples had an RNA integrity number (RIN) above 6, the number at which the sample is approved for microarray analysis. The average of all was 8.8 ± 0.7.

II-4- cRNA synthesis, labelling and hybridization

Preparation of the samples for microarray analysis was also performed with the exact same conditions as previously (16). In short, according to the One-Color Microarray-Based Gene Expression Analysis protocol version 6.6 (20), 200 ng of total RNA was synthesized into cRNA and labelled. The procedure was performed as described by the manufacturer's protocol. Purification of the amplified cRNA samples was performed with the RNeasy Mini Kit (Qiagen, The Netherlands) according to the manufacturer's protocol of Agilent. cRNA samples were quantified using a Nanodrop® ND-1000 spectrophotometer with a Microarray Measurement.

A quantity of 600 ng of labelled cRNA was hybridized on the microarray slide. Hybridization was performed according to the Agilent's protocol on SurePrint G3 mouse Gene exp 60kv2 microarrays slides (Agilent Technologies, The Netherlands). Furthermore microarray slides were scanned using an Agilent DNA Microarray Scanner with Surescan High-resolution Technology (Agilent Technologies, The Netherlands).

II-5- Pre-processing and data analysis of microarrays

Pre-processing methods were described previously (16). In short, the quality of the microarrays was first verified by the quality control pipeline provided by Agilent (Feature extraction software (FES) version 10.7.3.1). All samples met the quality criteria of the FES. All samples met the in-house quality check pipeline previously published (github.com/BiGCAT-UM/arrayQC_Module). Raw data with both expression values and genes were selected for data analysis based on flags and missing values. Eight groups were defined: E171 + AOM/DSS (CRC + E171) 2 days, 7 days, 14 days, and 21 days for the exposed samples and control AOM/DSS (CRC) 2 days, 7 days, 14 days, and 21 days for the controls. Within each group, spot identifiers were removed if flagged by the in-house quality control. Spot identifiers were deleted when more than 40% of samples in each group have a missing value and when the average expression was less than four in all groups. Pre-processing of missing values was performed using the standard settings of the GenePattern ImputeMissingValues.KNN module v13 (21). Spot identifiers were annotated to Agilent probe identifiers and merged with Babelomics 5 (22). Next, Agilent probe identifiers were re-annotated to EntrezGeneIDs and merged with Babelomics 5. By using LIMMA (version 1.0), data of the exposed samples (CRC + E171) were compared to their time matched control sample (CRC) and DEG were identified. The standard cut-off values of a fold-change (Log2FC) of 1.5 and a p-value of 0.05 were used (23). In addition, the false discovery rate was calculated according to the Benjamini-Hochberg method with a threshold at 0.05.

II-6- Pathway analyses

ORA was performed in CPDB with the DEG of each time point (24). For each annotation set, the p-value was calculated. Within each type of annotation set CPBD corrects for multiple hypothesis testing using the false discovery rate procedure (24,25). All available databases from CPDB were used (release 31, 1 sept. 2015) with settings in the "pathways as defined by pathway databases" with a minimum overlap of input list of 2 and a p-value cut-off of $p<0.01$.

With regard to the pathway analyses applied in the previous study, as second pathway analysis, a gene-set enrichment analysis (GSEA), was performed. Like the ORA, the GSEA was performed using CPDB. All the available databases from CPDB were used with settings in the "pathways as defined by pathway databases" with a minimum number of measured genes of 4 and a p-value cut-off of $p<0.01$.

II-7- Pathway construction

Biotransformation of compound pathway Phase I and II *Mus musculus* (WP702(r29945)) was downloaded from the WikiPathway database (August 2016) as an analogue of the *Homo sapiens* pathway with a 64% conversion rate (26) and uploaded on the Pathvisio software (version 3.2.4) (27). The gene list of this pathway was adapted to the DEG present in the dataset across all time points. Expression data from the DEG of all time points was imported and coloured according to the Log2FC values obtained after LIMMA. Genes coloured in blue are down-regulated and genes coloured in red are up-regulated.

II-8- Network construction

Summary network of the effects of E171 and its comparison to a previous mouse model in which mice were exposed to E171 only (16) was performed with Cytoscape (version 3.4) (28). All nodes and edges were added according to the biological effects observed at the pathway and gene levels. The biological processes only seen in the CRC mouse model in combination with E171 are in red, the ones only seen in the mice solely exposed to E171 are in blue. Common biological effects with the previous mouse model were in red and blue.

II-9- STEM analysis

STEM analysis was performed with the tool Short Time-series Expression Miner developed by Ernst and Bar-Joseph to analyse the expression pattern over time of short time series, below 8 time points (29). For the analysis, all genes passing the pre-processing were used which includes the non-differentially expressed genes. The gene annotation source was the mouse (EBI), no cross reference, no gene location, and no normalization were used. The clustering method was the STEM clustering method with a maximum of 50 models of profiles. Each expression of a gene is compared to the previous time point and the maximum unit change in model profiles between time points was 2. Significance is calculated by comparing actual number of genes per cluster to expected number of genes.

II-10- Data availability

The datasets generated and analysed during the current study are available in the Gene Expression Omnibus (GEO) repository (GEO accession: GSE109520), https://www.ncbi.nlm.nih.gov/geo/.

III- Results

III-1- Differentially expressed genes (DEG)

Gene expression values from samples of the distal colon of mice exposed to E171 (CRC + E171) were corrected for their own time-matched control (CRC) samples. In total, 21,106 genes passed the pre-processing. After using a Linear Mixed Model Analysis for Microarrays (LIMMA), the genes with a Log2FC>1.5 and a p<0.05 were selected. This selection resulted in 411 DEG after 2 days, 3506 DEG after 7 days of exposure, 2553 DEG after 14 days and 1178 DEG after 21 days (Table 1). With an adjusted p-value also called false discovery rate (FDR), there were only 2 DEG after 21 days and none after 2 days. Therefore, analysis will be performed with the DEG having a Log2FC>1.5 and a p<0.05 and stronger effects will be highlighted by indicating in the DEG with a Log2FC>1.5 and a p<0.05 which ones were also significant after FDR correction. The majority of changes in gene expression were time-point specific (Figure 1). From day 2 to 21, between 10 and 30% of the DEG were common to the other time point(s).

Table 1: Summary results of DEG after LIMMA analysis
Differently Expressed Genes after LIMMA analysis on the microarray data of chemically induced CRC BALB/c mice exposed to 5 mg/kgbw/day of E171. |FC|= Log2 fold change, p.val = p-value, adj.p.val = adjusted p-value.

	2 days	7 days	14 days	21 days
|FC| >= 1.5	2128	5277	4671	3387
Up-regulated	1203	2567	1888	616
Down-regulated	925	2710	2783	2771
p.val < 0.05	771	5106	3622	1951
adj.p.val < 0.05	0	1532	246	2
|FC| and p.val	411	3506	2553	1178
|FC| and adj.p.val	0	1390	233	2

Figure 2 also shows DEG in common between different time points. In total, 27 DEG were in common in 3 out of 4 time points. To visualise the expression of these DEG, a heatmap was created (see Supplementary Fig. 1 online). Among the 27 DEG common in 3 out of 4 time points, 8 had an unknown function. The other 19 DEG were separated according to their function in 3 clusters: cellular processes (7 DEG), gene involved in cancer (6 DEG) and genes coding for olfactory/G-protein-coupled receptors (GPCR)

receptors (6 DEG). The DEG common to all time points was in the olfactory/GPCR receptors cluster in the heatmap: olfactory gene 975. It was up-regulated at 2, 14 and 21 days and down-regulated after 7 days of exposure.
Three DEG were also statistically significant after FDR correction: Npc1 in cellular processes and Ifitm10 and Sox17 in genes involved in cancer. These DEG were shown with a black square around them in the heat map.

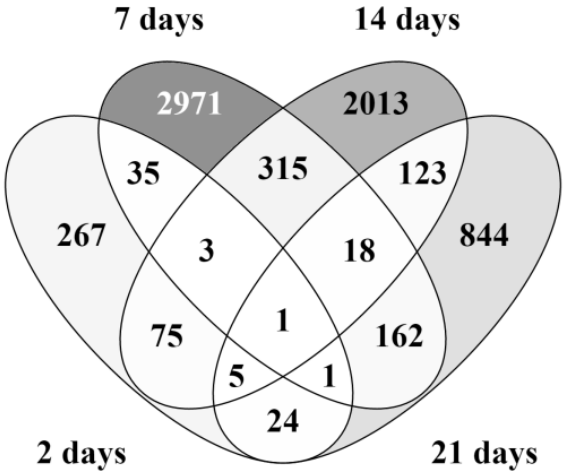

Figure 2: Venn diagram of the overlap (not based on directionality of expression) of DEGs (p<0.05 and Log2 FC>1.5) at different time points (2, 7, 14, and 21 days) after exposure to E171 in colon of mice. Each colour represents a different day

III-2- Pathway analysis per time point

With regard to the pathway analyses applied in the previous study (16), the affected biological mechanisms per time point were studied using the Consensus Pathway Database (CPDB) database for 2 different pathway analyses: over-representation gene set analysis (ORA) and a gene-set enrichment analysis (GSEA). The ORA resulted in 4 pathways after 2 days, the number of pathways increased at day 7 up to a total of 67 pathways and decreased after 14 and 21 days with 40 and 12 pathways respectively (Table 2). In addition, the GSEA resulted in 1 pathway at 2 days, 37 at day 7, 17 at day 14, and 107 at day 21 (see Supplementary Table 5 online). More details about the genes and their direction of expression can be found in Supplementary Tables 1, 2, 3 and 4 online.

Because we raised the hypothesis that ingestion of E171 induces gene expression changes in colon which could be related to inflammation, cancer-related genes and impair of the immune system before the tumours are detectable, the focus of the result section will be on inflammation, immune response, and cancer related pathways.

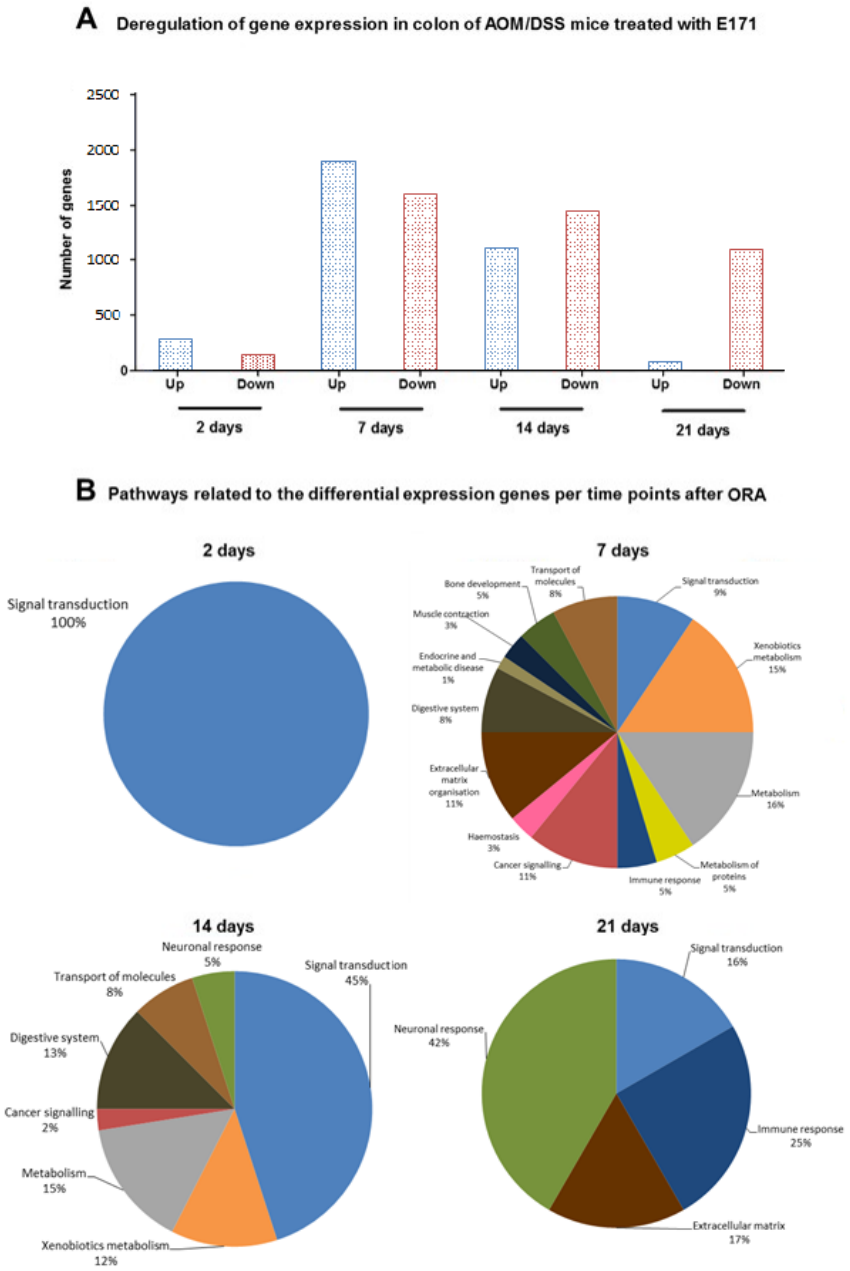

Figure 3: Visualisation of genes and pathways affected after E171 exposure

A) Up and down regulation of expression of genes; B) percent of group of pathways derived from the over-representation analysis (ORA) from colon tissue of mice treated with AOM/DSS and exposed to E171 during 2, 7, 14 and 21 days.

Table 2: Summary table with pathways, number of genes and their direction

Pathways related to the DEG after ORA with ConsensusPathDB. The pathways were grouped per biological function. The q-value is obtained after correction of the p-values for multiple testing using the false discovery rate method.

Days of exposure	Group of pathways	Name of pathway	q-value	Pathway source	Down	Up	Total
2 days	Signal transduction	- Olfactory transduction	5.10E-12	KEGG	5	26	31
		- Olfactory signalling Pathway	4.61E-05	Reactome	5	10	15
		- GPCR downstream signalling	0.0183	Reactome	8	13	21
		- Signalling by GPCR	0.0347	Reactome	8	14	22
7 days	Signal transduction	- Class A/1 (Rhodopsin-like receptors)	2.42E-03	Reactome	45	21	66
		- GPCR ligand binding	3.86E-03	Reactome	56	23	79
		- Peptide ligand-binding receptors	1.56E-02	Reactome	28	14	42
		- G alpha (s) signalling events	1.63E-02	Reactome	18	9	27
		- Non-odorant GPCRs	3.06E-02	Wikipathways	36	19	55
		- Antagonism of Activin by Follistatin	2.42E-02	Reactome	4	0	4
	Xenobiotics metabolism	- Phase 1 - Functionalization of compounds	6.41E-04	Reactome	6	24	30
		- Biological oxidations	8.93E-05	Reactome	8	39	47
		- Xenobiotics	7.40E-04	Reactome	1	15	16
		- Cytochrome P450 - arranged by substrate type	5.75E-03	Reactome	3	20	23
		- bupropion degradation	5.75E-03	MouseCyc	1	13	14
		- nicotine degradation III	7.23E-03	MouseCyc	1	14	15
		- Metabolism of xenobiotics by cytochrome P450	7.54E-03	KEGG	3	23	26
		- Drug metabolism - cytochrome P450	8.75E-03	KEGG	2	23	25
		- nicotine degradation II	9.60E-03	MouseCyc	2	14	16

	-	Drug metabolism - other enzymes	2.31E-02	KEGG	1	16	17
Metabolism	-	Nuclear receptors in lipid metabolism and toxicity	1.04E-02	Wikipathways	4	9	13
	-	Prostaglandin Synthesis and Regulation	2.42E-02	Wikipathways	10	3	13
	-	Synthesis of epoxy (EET) and dihydroxyeicosatrienoic acids (DHET)	8.37E-03	Reactome	0	10	10
	-	Synthesis of (16-20)-hydroxyeicosatetraenoic acids (HETE)	3.67E-02	Reactome	0	10	10
	-	Ascorbate and aldarate metabolism	2.53E-02	KEGG	0	9	9
	-	Linoleic acid metabolism	2.24E-02	KEGG	2	14	16
	-	Arachidonic acid metabolism	6.41E-04	Reactome	18	23	41
	-	Synthesis of Prostaglandins (PG) and Thromboxanes (TX)	1.83E-02	Reactome	5	5	10
	-	Propanoate metabolism	4.98E-02	KEGG	1	11	12
	-	UDP-N-acetyl-D-glucosamine biosynthesis II	2.33E-02	MouseCyc	1	4	5
Metabolism of proteins	-	Regulation of Insulin-like Growth Factor (IGF) Transport and Uptake by Insulin-like Growth Factor Binding Proteins (IGFBPs)	3.86E-03	Reactome	5	9	14
	-	O-linked glycosylation of mucins	9.60E-03	Reactome	3	13	16
	-	Mucin type O-Glycan biosynthesis	1.63E-03	KEGG	4	10	14
Immune response	-	Cytokine-cytokine receptor interaction	5.56E-04	KEGG	54	13	67
	-	Complement and coagulation cascades	9.60E-03	KEGG	18	3	21
	-	Staphylococcus aureus infection	4.98E-02	KEGG	17	0	17
Cancer signalling	-	Chemical carcinogenesis	9.60E-03	KEGG	3	22	25
	-	FGFR3c ligand binding and activation	4.98E-02	Reactome	2	3	5
	-	FGFR3 ligand binding and activation	4.98E-02	Reactome	2	3	5

	-	Signalling by activated point mutants of FGFR3	4.98E-02	Reactome	2	3	5
	-	Signalling by FGFR3 mutants	4.98E-02	Reactome	2	3	5
	-	FGFR1c ligand binding and activation	4.98E-02	Reactome	2	3	5
	-	Signalling by activated point mutants of FGFR1	4.98E-02	Reactome	2	3	5
Haemostasis	-	Common Pathway of Fibrin Clot Formation	4.13E-02	Reactome	6	1	7
	-	Cell surface interactions at the vascular wall	2.26E-02	Reactome	18	8	26
Extracellular matrix organisation	-	Extracellular matrix organization	1.84E-07	Reactome	67	8	75
	-	Degradation of the extracellular matrix	3.98E-05	Reactome	26	5	31
	-	Activation of Matrix Metalloproteinases	8.93E-05	Reactome	17	0	17
	-	Matrix Metalloproteinases	3.86E-03	Wikipathways	12	1	13
	-	Elastic fibre formation	2.42E-02	Reactome	12	1	13
	-	Collagen formation	3.69E-02	Reactome	21	1	22
	-	Assembly of collagen fibrils and other multimeric structures	3.83E-02	Reactome	11	1	12
Digestive system	-	Bile secretion	1.36E-03	KEGG	6	20	26
	-	Pancreatic secretion	8.76E-03	KEGG	15	16	31
	-	Amino sugar and nucleotide sugar metabolism	1.03E-02	KEGG	3	16	19
	-	Protein digestion and absorption	9.60E-03	KEGG	16	12	28
	-	Mineral absorption	6.41E-04	KEGG	8	13	21
Endocrine and metabolic disease	-	Maturity onset diabetes of the young	3.86E-03	KEGG	0	13	13
Muscle contraction	-	Striated Muscle Contraction	4.07E-04	Reactome	15	1	16
	-	Muscle contraction	4.29E-02	Reactome	15	2	17

	Bone development	-	Endochondral Ossification	9.68E-04	Wikipathways	20	5	25
		-	Endocrine and other factor-regulated calcium reabsorption	2.17E-02	KEGG	5	14	19
		-	Calcium signalling pathway	2.33E-02	KEGG	26	20	46
	Transport of molecules	-	Transport of glucose and other sugars, bile salts and organic acids, metal ions and amine compounds	8.76E-03	Reactome	12	17	29
		-	Ion channel transport	2.11E-02	Reactome	12	23	35
		-	Ion transport by P-type ATPases	2.26E-02	Reactome	7	7	14
		-	Organic cation transport	4.98E-02	Reactome	1	4	5
		-	Transmembrane transport of small molecules	7.00E-03	Reactome	41	69	110
14 days	Signal transduction	-	Olfactory transduction	1.57E-44	KEGG	77	72	149
		-	GPCR downstream signalling	5.28E-26	Reactome	97	60	157
		-	Signalling by GPCR	8.59E-25	Reactome	106	63	169
		-	Olfactory signalling Pathway	6.18E-24	Reactome	43	36	79
		-	Signal Transduction	2.50E-10	Reactome	143	82	225
		-	Odorant GPCRs	2.51E-09	Wikipathways	24	19	43
		-	GPCR ligand binding	5.85E-07	Reactome	44	23	67
		-	GPCRs, Class A Rhodopsin-like	1.51E-06	Wikipathways	23	19	42
		-	GPCRs, Other	1.80E-06	Wikipathways	18	12	30
		-	Non-odorant GPCRs	3.08E-06	Wikipathways	34	17	51
		-	Class A/1 (Rhodopsin-like receptors)	4.40E-04	Reactome	32	16	48
		-	G alpha (i) signalling events	4.05E-03	Reactome	24	11	35
		-	Taste transduction	9.95E-03	KEGG	8	4	12
		-	Monoamine GPCRs	2.96E-02	Wikipathways	4	5	9
		-	G alpha (s) signalling events	3.12E-02	Reactome	13	6	19
		-	G alpha (q) signalling events	4.20E-02	Reactome	18	9	27

	-	Class C/3 (Metabotropic glutamate/pheromone receptors)	4.05E-03	Reactome	5	4	9
	-	Amine ligand-binding receptors	3.45E-02	Reactome	5	3	8
Xenobiotics metabolism	-	Phase 1 - Functionalization of compounds	1.60E-02	Reactome	3	16	19
	-	Biological oxidations	6.38E-03	Reactome	4	25	29
	-	Drug metabolism - other enzymes	2.43E-02	KEGG	2	11	13
	-	Drug metabolism - cytochrome P450	3.12E-02	KEGG	3	14	17
	-	Cytochrome P450 - arranged by substrate type	3.82E-02	Reactome	1	14	15
Metabolism	-	Steroid hormone biosynthesis	6.38E-03	KEGG	4	4	8
	-	Steroid hormones	2.73E-02	Reactome	3	10	13
	-	Retinol metabolism	1.08E-04	KEGG	2	18	20
	-	Ascorbate and aldarate metabolism	1.72E-03	KEGG	2	7	9
	-	Vitamin D (calciferol) metabolism	6.67E-03	Reactome	1	3	4
	-	Metabolism of steroid hormones and vitamin D	2.73E-02	Reactome	4	4	8
Cancer signalling	-	Chemical carcinogenesis	1.78E-02	KEGG	4	14	18
Digestive system	-	Recycling of bile acids and salts	4.98E-03	Reactome	2	5	7
	-	Fatty acid degradation	1.98E-02	KEGG	1	12	13
	-	Linoleic acid metabolism	2.96E-02	KEGG	3	9	11
	-	Bile secretion	3.45E-02	KEGG	3	13	16
	-	Fatty acids	3.86E-02	Reactome	0	6	6
Transport of molecules	-	Transmembrane transport of small molecules	4.20E-03	Reactome	35	41	76
	-	SLC-mediated transmembrane transport	3.12E-02	Reactome	15	26	41
	-	Transport of vitamins, nucleosides, and related molecules	3.45E-02	Reactome	4	6	10
Neuronal response	-	Neuroactive ligand-receptor interaction	4.55E-06	KEGG	28	24	52
	-	Serotonin receptors	4.37E-02	Reactome	3	1	4

21 days	Signal transduction	-	Olfactory transduction	3.02E-02	KEGG	29	5	34
		-	G Protein signalling Pathways	4.31E-02	Wikipathways	13	0	13
	Immune response	-	Cell adhesion molecules (CAMs)	8.19E-04	KEGG	22	0	22
		-	Innate Immune System	4.75E-03	Reactome	41	0	41
		-	Immune System	5.76E-03	Reactome	63	0	63
	Extracellular matrix	-	Extracellular matrix organization	1.51E-02	Reactome	23	0	23
		-	Regulation of actin cytoskeleton	3.53E-02	KEGG	21	0	21
	Neuronal response	-	Neuronal System	5.76E-03	Reactome	24	1	25
		-	Transmission across Chemical Synapses	1.50E-02	Reactome	18	1	19
		-	Serotonin and anxiety-related events	2.73E-02	Wikipathways	4	0	4
		-	Neurotransmitter Receptor Binding And Downstream Transmission In The Postsynaptic Cell	4.31E-02	Reactome	14	0	14
		-	HCN channels	3.02E-02	Reactome	3	0	3

III-2-1- 2 days of exposure

ORA and GSEA showed that all DEG expressed after 2 days were related to only one biological function, olfactory/GPCR signalling. ORA resulted in pathways such as olfactory signalling and GPCR signalling pathways (Table 2; Figure 3) whereas the GSEA resulted only in the olfactory transduction pathway (see Supplementary Table 5 online). In all pathways, 66% of the genes were up-regulated. In these pathways 6 genes were related to cancer like pancreas cancer (Ramp1 and Cckbr) (16,30,31), melanoma (Plcb4) (32), cervical and ovarian (Adcyap1 and Trpc3) (33,34), and colorectal cancer (Ptger3) (35). No pathways related to the immune system were found but at the gene level 20 DEG were found to be related to the immune system including the innate immune system (10 DEG), the adaptive immune system (3 DEG), and cytokine signalling (12 DEG).

III-2-2- 7 days of exposure

At day 7 of exposure, the results after ORA showed that more pathways were modulated as compared to 2 days (Table 2; Figure 3). Based on the Reactome classification, the 64 pathways were organised according to their biological functions. The number of DEG related to the transport of molecules was the highest (110 DEG), followed by metabolism (109 DEG), signalling (79 DEG), extracellular matrix (75 DEG), and immune response (67 DEG) (see Supplementary Table 2 online).
Table 2 and Figure 3 show that gene expression changes were observed in 13 different biological functions: signal transduction, immune system, metabolism, xenobiotics metabolism, muscle contraction, cancer signalling, metabolism of protein, transport of small molecules, extracellular matrix organisation, endocrine and metabolic disease, bone development, haemostasis, and digestive system. After ORA, eight of these biological functions were also observed related to the DEG significant after FDR correction: signal transduction, immune system, metabolism, xenobiotics metabolism, cancer, transport of small molecules, bone development, and digestive system.

Almost 80 DEG were related to signal transduction and clustered in 6 different pathways. A majority of these genes were down-regulated. Some of these genes were known to be related to development of cancer such as neuroblastoma (Ptdgr2) (36), diverse types of cancer (Kiss1, Ace) (37,38), breast cancer (Esr1), and colon cancer (Edn2: also significant after FDR correction) (39).

With 109 DEG, another biological function was identified after ORA: metabolism. The number of metabolism pathways was high therefore a separation was made between metabolism (51 DEG) and biotransformation of xenobiotics (58 DEG) (Table 2; Figure 3). These 2 groups of pathways contained an important part of all the DEG associated in pathways after 7 days of exposure. Supplementary Figure 2 online shows the 2 different phases of biotransformation of compounds including up- or down-regulated related DEG for all time points. Phase I reactions exists of oxidation, reduction, and hydrolysis. Oxidation of xenobiotics is performed by several mechanisms: CYP450 monooxygenase system, flavin-containing monooxygenase system, alcohol dehydrogenase, monoamine oxidase, co-oxidation by peroxidase (40). After 7 days, DEG were involved in various biotransformation pathways in Phase 1 and Phase 2. Furthermore, different classes of Cyp450 genes were activated such as Cyp2, Cyp3, Cyp4 and Cyp7. Of all the Cyp450 genes modulated after 7 days of exposure, 18 were also significant after FDR correction. These are shown with top left back square on Supplementary Figure 2. Other DEG in biotransformation of xenobiotics were at around 80% up-regulated, for instance the glutathione genes Gstt2 and Gstt3 (Also significant after FDR correction).
In the metabolism group, genes in various pathways were modulated such as synthesis of prostaglandins and synthesis of epoxy acids. Synthesis of epoxy acids was also a pathway observed from the DEG with after FDR correction. As shown in Figure 3, most of these genes were significantly up-regulated.

Another biological function group, i.e. extracellular matrix organisation, was identified after 7 days of E171 administration. It contained pathways involved in collagen formation, activation of the matrix metalloproteinases, and elastic fibre formation. Ninety percent of the genes were down-regulated in this group such as integrin β1 and α2. Twenty-six genes significant after FDR correction were associated with the extracellular matrix organisation.

The immune response function group contained 3 pathways with 41 DEG mostly related to the innate immune response. The majority of the genes were down-regulated like genes involved in the complement activation (C1, C3, C4 and C5), Fc receptor, and interleukins. After FDR correction, 1 C5 gene, 1 C1 gene, 4 Fc receptor genes, and 10 interleukin genes were observed.

Genes involved in cancer and cancer signalling were clustered in 7 pathways. In these pathways 31 DEG were up-regulated (fibroblast growth factors genes, Apc, Nat genes, Ptgs2, Ugt genes, and Mgst genes). After FDR correction, 6 genes involved in fibroblast growth factor, Apc, 1 Nat gene, 1 Ugt gene, and 1 Mgst gene were observed.

Genes related to muscle contraction (Tnnt3, Tnni2, and Mybpc1), transport of molecules (solute carriers, also observed after FDR correction), and haemostasis (Atp1a3, Thbd, and Plau) were also modulated.

Thirty-seven pathways were identified by GSEA (see Supplementary Table 5 online). Among these pathways, 23 were in common with the ORA and were relevant in the context of the biological functions extracellular matrix organisation, immune response, transport of molecules, metabolism, haemostasis, signalling, and xenobiotics metabolism. One additional biological function group present after GSEA was the neuronal response with the serotonergic synapse pathway containing genes such as Kcnj6, Htr4 and Itpr3.

To conclude, after 7 days of exposure, the molecular response at the gene expression and pathway levels was larger than 2 days after E171 ingestion in combination of AOM/DSS. The biological response after 7 days of exposure leads towards a deregulation of gene expression levels in the transport of molecules, metabolism, signalling, metabolism of xenobiotics, extracellular matrix, and immune response.

III-2-3- 14 days of exposure

After 14 days of exposure to E171, ORA showed significant changes associated with 40 different pathways in 8 biological functions (Table 2; Figure 3; Supplementary Table 3 online): signal transduction, xenobiotics metabolism, metabolism, cancer signalling, digestive system, transport of molecules, and neuronal response. After ORA, 3 of these biological functions were also observed related to the DEG significant after FDR correction: signal transduction, metabolism, and neuronal system.

Genes related to signal transduction were affected after 14 days of exposure and associated to 16 pathways. The DEG in these pathways were 60 to 70% down-regulated (Table 2; Figure 3). Among these DEG, some of them are related to development of cancer like B cell lymphoma (Ptger4) (41) and colorectal cancer (Pyy and Pthlh) (42,43).

In addition, DEG were affected in 2 other biological functions: xenobiotics metabolism and metabolism. In xenobiotics metabolism, several classes of Cyp450 genes were up-regulated :Cyp2 (with one Cyp2 gene observed after FDR correction), Cyp3, and Cyp5 (see Supplementary Figure 2 online). In the metabolism biological function, genes were up-regulated in pathways such as vitamin D metabolism and retinol metabolism. Both pathways are related to inflammation. In both biological functions, most of the genes (90%) were up-regulated (Table 2; Figure 3).

Genes involved in cancer and cancer signalling were also modulated after 14 days of exposure to E171. In the pathway chemical carcinogenesis, DEG were mostly up-regulated like Gsto genes (Gsto1 was significant after FDR correction), Ugt genes, and Adh genes.

The outcome of GSEA showed fewer pathways than after ORA, a total of 17 pathways were expressed after 14 days of exposure (see Supplementary Table 5 online). Among these 17 pathways, the majority (9 pathways) were common to the ORA and associated in several biological functions: signalling, metabolism of protein, metabolism of xenobiotics, and digestive system. Five other pathways were classified in already mentioned biological functions: extracellular matrix organisation, immune system, and haemostasis. The extracellular matrix organisation pathway contained 23 DEG in which 2 were up-regulated, the other genes like matrix metallopeptidase genes, integrin genes, fibulin and fibronectin genes were down-regulated. Within the immune system biological function, the 61 DEG were separated in 3 different pathways related mostly to the innate immune system. A majority of the DEG in these pathways were down-regulated like genes involved in complement, interferons, activation of natural killers genes, whereas the Fas gene was up-regulated. One gene involved in complement was also significant after FDR correction.

To conclude about 14 days of exposure, similar to day 2 and 7, genes were modulated in signalling, cancer signalling, inflammation, immune system, and extracellular matrix organisation.

III-2-4- 21 days of exposure

After a longer exposure, 21 days, 12 pathways were identified by CPDB after ORA. All details about genes and pathways can be found in Supplementary Table 4 online. Genes in these pathways were relevant in the context of the signal transduction, immune response, extracellular matrix organisation, and neuronal response.

Forty-eight DEG were related to signal transduction. Ninety percent of these genes were down-regulated (Table 2; Figure 3). Some of these genes were also related to development of cancer such as colorectal cancer (Camk2g)(44), melanoma (Gna11)(45), breast cancer (Esr1)(46), and prostate cancer (Akap12)(47).

The 77 immune system related DEG were down-regulated. These genes were involved in the complement activation, MHC class I and class II presentation, Tlr genes, and cell adhesion molecules genes.

The 23 DEG involved in extracellular matrix organisation were all down-regulated and played a role in integrins, elastase, intercellular adhesion, collagen and actinin.

After GSEA, the number of pathways was higher than after the ORA, 107 pathways classified in already mentioned biological functions (see Supplementary Table 5 online). Ten out of twelve pathways of the ORA were present in the GSEA and were classified in immune system, neuronal system, extracellular matrix organisation, and signal transduction.

To conclude on 21 days of exposure, both pathway analyses showed an effect of E171 on the immune response, neuronal response, signalling, and extracellular matrix organisation. In addition, the GSEA indicated modulation in cancer signalling pathways, cellular processes, haemostasis, and metabolism of protein. Furthermore, the reaction of the immune system was larger (33 pathways) in the GSEA.

III-3- Comparison of all time points

Some of the effects of E171 on gene expression were in common between the different time points. At all time points, E171 affected mRNA levels related to signalling (olfactory, GPCR, cytokine, cancer signalling) and immune system (innate and adaptive). From 7 to 21 days of exposure genes involved in the extracellular matrix organisation and neuronal system were modulated. After 7 and 14 days of exposure, genes expression levels were significantly different in metabolism, metabolism of xenobiotics, haemostasis, digestive system, and transport of molecules. After FDR correction, genes after 7 and 14 days were commonly involved in signalling, metabolism, neuronal system, and xenobiotics metabolism.

Figure 4, a STEM analysis, shows the directionality of all the genes including the non-differentially expressed ones over time. This analysis indicates, as observed in Table 1 and Figure 3, that the effects of E171 in a CRC mouse model is driven by the time points 7 and 14 days. Within the significant expression profiles, several profiles had a very specific biological process linked to the genes which confirms the effects observed over time. The first profile with a very specific biological response is profile 21, it contains a majority of genes involved in signal transduction pathways (>90%) which is also observed with profile 34. Another profile, profile 15, was specific to immune response genes with over 75% of pathways related to the immune system. The profile is in line with the results observed with the DEG where all the genes were down-regulated after 21d of exposure. The genes involved in cancer were in majority present in profile 40 in which 45% of the related pathways were involved in cancer. All the other significant profiles had several different biological processes involved.

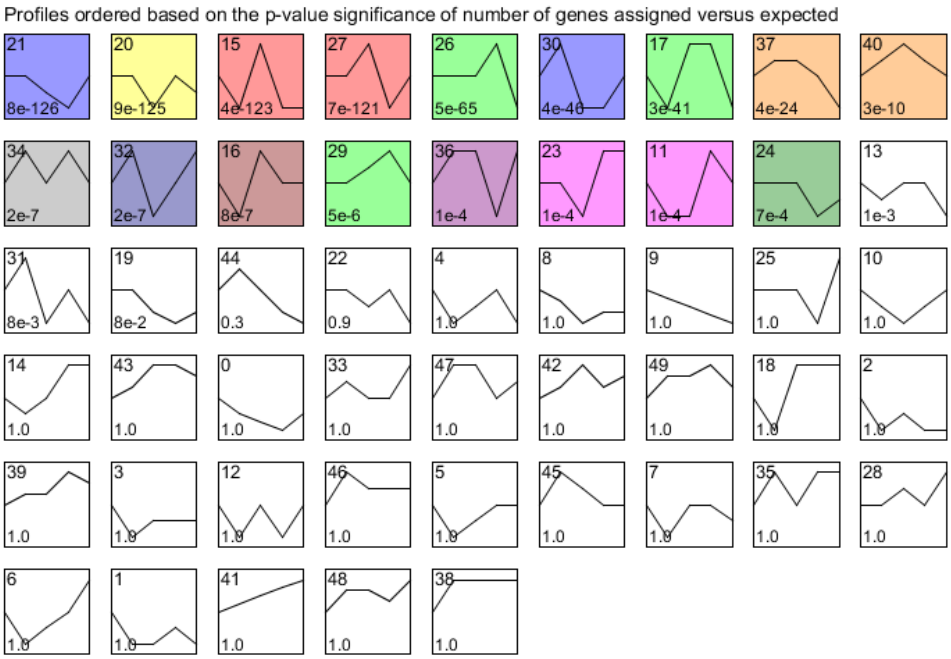

Figure 4: Results of STEM analysis

Analysis performed with all the genes passing the pre-processing. Directionality changes when the maximum unit change in model profiles is between time points is higher than 2. Significant profiles are represented in colour. Similar colours represent the same type of expression profile. The number on the top left corner corresponds to the number of profile. The number at the bottom left corresponds to the associated p-value.

III-4- Time course network analysis

In order to visualise the effects of E171 *in vivo* and compare it to a previous study in which E171 was ingested in BALB/c mice without AOM/DSS treatment (16), a network was made based on the pathway analyses as well as relevant DEG over time in Figure 5. This network was created with the groups of pathways and relevant sub-categories (in red). The results were compared to the similar study performed in the same mouse strain exposed only to E171 (in blue) and the common effects observed were shown in blue and red. After exposure to E171 in the colon of mice in the absence or the presence of AOM/DSS, modulation of genes related to inflammation, oxidative stress, immune reaction, metabolism of protein, and signalling was observed. In addition to the gene expression seen in both models, other effects have been only observed with the combined exposure to E171 and AOM/DSS. Those effects show modifications related to transcription factors, xenobiotics metabolism, extracellular matrix organisation, transport of molecules, and haemostasis.

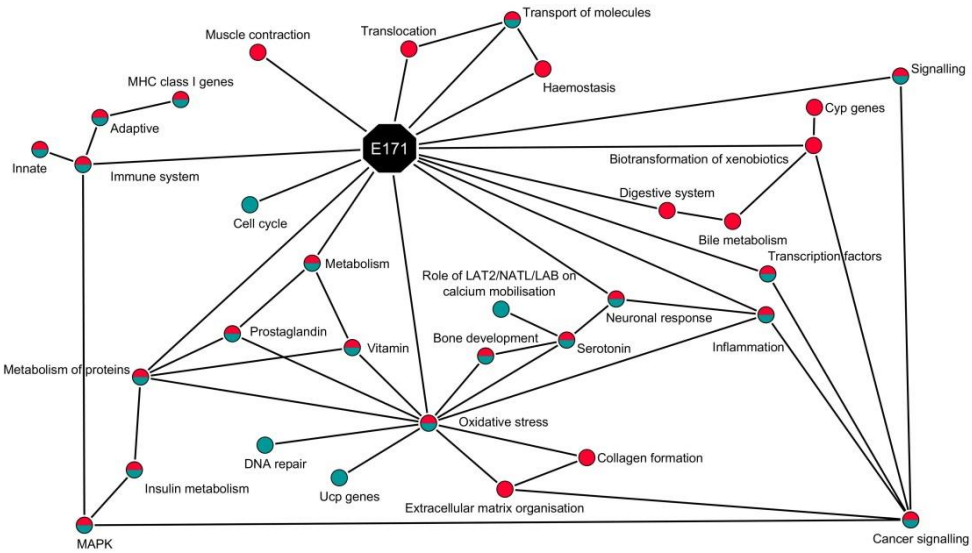

Figure 5: Visualization the interaction between the different biological processes (circles) regulated after exposure to E171 (octagon) for 2, 7, 14 and 21 days.

Network created with Cytoscape. The biological processes only seen in the CRC mouse model in combination with E171 are in red, the ones only seen in the mice solely exposed to E171 are in blue (16), and the ones in common between the previous 2 exposures are in blue and red.

IV- Discussion

In this study, we aim to establish the influence of E171 on gene expression patterns in the colon of a colorectal mouse model after exposure to 5 mg/kg_{bw}/day of E171 for 2, 7, 14, and 21 days. These alterations could lay the basis for the development of tumours in colon that we found in a previous study after 4 weeks of exposure (15). Specifically, the up-regulation of genes involved in inflammation, biotransformation of xenobiotics, genes related to cancer, and impairment of the immune system. Even though the majority of the DEG were not common between time points, their transient nature does not imply that the biological response to E171 is transient as well. Interpretation of the biological functions of the genes using e.g. GSEA and ORA identified biological processes like immune response, signal transduction and cancer signalling to be modulated after day 2, 7, 14, and 21. Therefore, the sequence of effects observed may be well in line with the different consecutive mechanisms that attribute to the development of cancer. The mechanisms identified on the DEG and pathways are further elaborated below.

The current study shows that E171 induces molecular changes in translocation, transport of molecules, and muscle contraction. At day 7, genes involved in the muscle contraction pathway were mostly down-regulated. Among these genes, downregulation of Tnnt3, Tnni2, and Mybpc1 is associated with impaired muscle function (48,49). Presence of E171 may cause a decrease of frequency or strength of muscle contraction in the gut, which would eventually increase absorption and metabolism (50). Absorption of E171 in the colon of rats has been already observed by Bettini et al. (17). They suggest that accumulation of E171 in the colon is due to the slow transit time and favours local absorption by epithelial cells. Also other groups observed a translocation of TiO_2 from the gut to other part of the body (51,52). In addition, changes in haemostasis can influence the absorption of TiO_2 particles as shown previously (17,51-53). In our study, a gene related to haemostasis, Atp1a3, was differentially expressed over time (see Supplementary Fig. 1 online) and codes for an integral membrane protein responsible of establishing and maintaining the electrochemical gradients of Na and K ions across the plasma membrane (54). In addition, other haemostasis genes were affected after exposure to E171 such as thrombomodulin (Thbd) and plasminogen activator, urokinase (Plau) which are involved in blood coagulation (55,56).

The ingestion of E171 in the colon also impacts the expression of genes involved in signalling which was a consistent effect across all the different time points (Table 2; Figure 3). The GPCR gene family is the largest in the genome and the olfactory receptor gene family is one of its member (57). These receptors are essential for the signal transduction in cells and are only activated when a compound or element such as a hormone, neurotransmitter, ion, or photon is presented and recognised by the receptors (58,59). Signal transduction genes were modulated by the exposure to E171 in the colon of mice in presence and also in absence of AOM/DSS (16). In line with these findings, activation of GPCR/olfactory genes was previously observed after TiO_2 NPs inhalation in the lung of mice (60). Repercussions on other gene expression of immune or cancer signalling genes in the cells were observed from 2 to 21 days of exposure. Indeed, increasing evidence linking GPCR/olfactory signalling genes to development of cancer (61,62) and modulation of the immune system (63,64) has emerged. In our study, over time, a total of 22 GPCR DEG (in italic in Supplementary tables 2, 3, and 4 online) have been identified to be involved in the development of cancer of which 7 genes coding for Wnt signalling, frizzleds and receptors of endothelins, prostaglandins, and thrombin were related to growth, metastasis, survival, angiogenesis, and migration of colorectal cancer (61,62). Of these 22 genes, 9 were also significant after FDR correction like Wnt2, Fzd4, Apc, Fgf2, Ccl2, and Erbb2. In addition, enhanced expression of 2 genes was also found in the previous study (16): Esr1 and Ace. Esr1 gene, involved in breast cancer (61,62), was also down-regulated in both models at day 7 and 14 when exposed to E171 only and at day 7 and 21 in this study. Ace gene was modulated in the opposite directions in both *in vivo* mouse models exposed to E171: up-regulated at day 14 and 21 when exposed to E171 only and down-regulated at day 7 in this study and is involved in the regulation of cell proliferation and angiogenesis (38).

In our study, an effect on the immune system was observed from 2 to 21 days of exposure with genes involved in the immune response. We noted that these genes were mostly down-regulated after 2 days of exposure and exclusively down-regulated after 21 days (see Supplementary tables 1-4 online). This expression profile was also observed over time with the STEM analysis (Figure 4). These down-regulated genes are involved in the regulation of the innate and adaptive immune system, MHC class I presentation, production of cytokines, natural killer cytotoxicity, and cell adhesion molecules. In order to escape from the innate or the adaptive immune system, tumour cells have the capacity to stop the expression of MHC class I at the surface of the cell and/or activate type 2 macrophages that would express IL-10^{HIGH}, IL-12^{LOW} and IL-23^{LOW} an anti-inflammatory phenotype which stimulates cancer proliferation (65-67). The results of our study showed

that E171 has a stronger effect on the innate than the adaptive immune system. However, the effect observed on the genes not significant after FDR correction involved in the innate and adaptive immune system might facilitate tumour formation. These data are in line with results of other publications on the evasion of tumours, even early tumours to the immune system (65-67). Furthermore, the downregulation of genes involved in the MHC class I presentation as well as genes of the complement system was also observed in the similar transcriptomics study performed by our group (16). In addition, Bettini et al. also showed that the intragastric exposure to E171 in rats at low doses impairs intestinal immune homeostasis after 1 week of treatment (17).

As oxidative stress is a factor of development of cancer, a particular focus was on gene directly involved in oxidative stress and genes related to this. Oxidative stress genes were not differentially expressed but some genes indirectly related to oxidative stress like genes involved in antioxidant production were observed. After 7 and 14 days of exposure to E171, metabolism of prostaglandin and vitamin D pathways were affected. After FDR correction, half of the DEG involved in prostaglandin pathways were also differentially expressed. This can be regarded as a potential indication of the presence of oxidative stress. Basu et al. showed that a pro-inflammatory environment induced in macrophages, epithelial cells and fibroblasts the production of cyclooxygenase-2 leads to the release of prostaglandins in bone marrow (68). Activation of vitamin metabolism genes but also oxidative stress genes was also observed after 14 and 21 days of exposure in our previous mouse model exposed to E171 (16).

In addition, several groups observed that the presence of oxidative stress damages the extracellular matrix organisation, decreases the fibrillar collagen synthesis genes, and induces changes in the collagen formation (69-71). From 7 days, genes involved in the extracellular matrix and collagen were modulated also after FDR correction (Table 2; Figure 3, Supplementary Fig. 1 online). Extracellular matrix genes are also linked to induction of apoptosis in CRC and in gastric cell lines (71,72). Gencer et al. suggest that the activation of Mmp-15 in gastric cancer cell lines is a direct link to oxidative stress. We observed the activation of Mmp-15 after 7 days of exposure to E171 (see Supplementary Table 2 online). This group also hypothesises that the perturbation of cell matrix adhesion may be a novel mechanism by which a compound can induce apoptosis in colorectal cancer cells. Oxidative stress also leads to the modulation of serotonin genes (73). In our study with AOM and DSS, the addition of E171 had also an influence of the mRNA levels of serotonin related genes. Two serotonin genes, Htr7 and Htr1b, were in common between the chemically-induced colorectal cancer mouse model and the previous mouse model

exposed to E171 only. They are both serotonin receptor genes and were down-regulated in both models. In this study, other genes in neuronal and serotonin pathways were affected by exposure to E171 at 14 and 21 days (Table 2; Figure 3). Alterations in serotonin signalling have been associated with tumour progression in prostate as well as breast cancer (74), although this has not been shown for colon cancer so far. By inducing oxidative stress in the colon cells, E171 exposure may results in the production of antioxidants, serotonin, and degradation of extracellular matrix. Indeed, TiO_2 was previously shown to induce DNA damage and genotoxicity via inflammation and/or oxidative stress in mice as well as *in vitro* in colon cell lines (Caco-2 and HCT116), human epidermal (A431), and HepG2 cells lines (7,16,75-77). Inflammation by oxidative stress as well as suppressing the immune system can ultimately lead to development of cancer (78).

The effect of E171 on expression of genes involved in cancer can also be observed from 2 to 14 days of exposure. This expression profile was also observed over time with the STEM analysis (Figure 4). After 2 days, 6 DEG were related to cancer such as Adcyap1, Ramp1, and Trpc3 which were down-regulated. Adcyap1 methylation is associated with ovarian cancer (33). In our study, this gene is down-regulated which is in line with the Adcyap1 methylation shown by Jung et al. Furthermore, Trpc3 and Ramp1 are associated with ovarian and pancreatic cancer respectively (30,31). At day 7 and 14, E171 up-regulates genes in cancer signalling pathways such as chemical carcinogenesis and FGFR1/1c/3 and 3c ligand binding. At day 7, these pathways were also observed after ORA on the FDR corrected DEG. In addition, over time, 5 genes were modulated, all significant from 7 days of exposure and all related to development of cancer (see Supplementary Fig. 1 online). Some DEG were involved specifically in CRC like Itga5, involved in tumour invasion (79) and Ifitm10 and Sox17, potential markers of CRC (80,81). Sox17 and Ifitm10 were significantly expressed after FDR correction at day 7 and 14 respectively. The exposure to E171 leads to a modulation of cancer related genes which is in line with our previous study in which mice were exposed to only E171 (16).

Changes in gene expression in the metabolism of xenobiotics is observed from 2 to 21 days and may also contribute to the development of cancer by influencing the metabolism of potential carcinogenic compounds and intermediates. Secondary organs, like intestines, are also a site for biotransformation of compounds (82-84). In Supplementary Figure 2, the modulation of the expression of Cyp450 genes over time is shown to be a consistent effect with a modulation of a total of 43 genes, most of them being differentially expressed at day 7 and 14 (see Supplementary Fig. 2 online). Of these 43 genes, 21 were also significant after FDR correction. These results are in line with a

previous *in vitro* study in which shows that NPs have an impact on with Cyp450 enzymes (85). Substrates identified for the oxidation in the biotransformation of xenobiotics include saturated and unsaturated fatty acids, sterols, steroids, bile acids, vitamin D3 derivatives and retinoids (86). After 14 days of exposure, pathways such as vitamin D metabolism, fatty acids, steroid hormones, bile acids (also at day 7), and retinol metabolism were observed (Table 2; Figure 3, Supplementary Table 5 online). The effect of TiO_2 on steroid hormones was also observed in a previous study. Gao et al. showed that after ingestion in mice, TiO_2 crossed the blood-testis barrier, accumulated in the testes, and affected steroid hormones in serum (51). After 7 and 14 days of exposure to E171, glutathione (GSH) genes were up- and down-regulated. Two GSH genes, one at day 7 and one at day 14, were also significant after FDR correction. GSH have also been implicated with the potential of forming reactive intermediates resulting in toxic effects (40). The effects of E171 on the GSH genes is in line with a previous study by Shlukla et al. in which they observed that oxidative stress induced by TiO_2 NPs resulted in a modulation of GSH content in epidermal cells (76). The up- and down-regulation of genes involved in the biotransformation of compounds showed a contribution of E171 to the metabolism of various exogenous compounds including drugs, environmental chemicals, pollutants, and natural plant products. The metabolism of xenobiotics frequently results in successful detoxification of an irritant, but the actions of P450 enzymes may also generate toxic metabolites that contribute to increased risk of cancer, and other toxic effects (40).

Biotransformation of compounds pathways were not the only type of metabolism pathways affected by E171. At day 7, pathways involved in the metabolism of glucose contained mostly up-regulated genes. After FDR correction, 10 genes were also significant and related to insulin events. These results are in line with previous findings which reported an increase of plasma glucose in mice after exposure to TiO_2 via the production of ROS that activate the MAPK pathway (52). In our study, some MAPK genes were also differentially expressed from 7 to 21 days (see Supplementary Table 2, 3 and 4 online). The activation of the MAPK genes and the metabolism of glucose were also observed after 7 days of exposure when mice were exposed to only E171 (16). Activation of signalling MAPK pathway is important in intestinal epithelial differentiation. Its cascade is involved in control of growth signal, cell survival and invasion in cancer (87).

Modulations of mRNA levels of transcription factor genes were observed at all time points after E171 exposure. Initiation and regulation of mRNA levels are performed by transcription factors such as Ngfi-A binding protein 2 (Nab2) and cytoplasmic FMR1 interacting protein 1 (Cyfip1). These transcription factors genes were differently expressed

from 7 to 21 days. Napoli et al. described that Cyfip1 protein binds to the translation initiation factor eIF4E and mediates translational repression in mammalian cells (88). Cyfip1 upregulation affects general mRNA translation (89). Cyfip1 was also observed as the only common DEG up-regulated at all time points in a similar study in which mice were exposed to only 5 mg/kg_{bw}/day of E171 for 2, 7, 14 and 21 days(16). Deregulation of transcription factors leads to deregulation of mRNA levels which can also lead to development of cancer with transcription factors genes like Cyfip1 (90) and Nab2 (91).

In summary, in this study we demonstrated that gene expression in the colon of mice is affected by exposure to E171 in combination with AOM/DSS. Over time, GPCR/olfactory signalling genes were modulated including genes involved in cancer and particularly colorectal cancer. Furthermore, the modulation of gene expression levels after E171 exposure on the biotransformation of xenobiotics shows a detoxification which increases the metabolism of potential carcinogenic compounds and intermediates. In addition, E171 modulated gene expression of immune related genes with a majority of the innate and adaptive immune system genes down-regulated. These results suggest an impairment of the immune system which can ultimately facilitate the development of cancer. E171 ingestion also induced changes at the mRNA levels of vitamin and prostaglandin genes as well as extracellular matrix organisation, collagen formation, and activation of MAPK genes which suggest the presence of oxidative stress responses. With a lower number of genes, these effects were also observed after FDR correction at day 7 and 14. Presence of oxidative stress, impairment of immune system, and modulation of cancer related genes are effects in line with the tumour formation observed previously by our group (15) and in line with the transcriptomics study after exposure to E171 only (16). The presence of AOM/DSS compared to the absence of these compounds in our previous study shows that AOM/DSS enhanced all observed biological reactions affected by the exposure to E171. Altogether, the results of our animal studies and those of others warrant further investigation of the potential adverse effects of consumption of food additive E171 in human.

Supplementary materials

Supplementary Figure 1: Heat map of DEG (p<0.05 and Log2FC>1.5) common in 3 out of 4 time points or in all time points after exposure to E171 in colon of mice for 2, 7, 14 and 21 days.

ftp://web.tgx.unimaas.nl/hproquin/Chapter_3/Supplementary_figure_1.tif

Supplementary Figure 2: Metapathway of biotransformation Phase I and II with DEGs after exposure to E171 for 2, 7, 14 and 21 days in the colon of mice.

ftp://web.tgx.unimaas.nl/hproquin/Chapter_3/Supplementary_Figure_2.png

Supplementary Table 1: Details results of ORA after 2 days of exposure of E171 in BALB/c mice in combination with AOM/DSS. Numbers in bold correspond to upregulated genes. Log2FC= Log2 fold change obtained with LIMMA script with correction for its own time-matched control.

ftp://web.tgx.unimaas.nl/hproquin/Chapter_3/Supplementary_table_1.docx

Supplementary Table 2: Details results of ORA after 7 days of exposure of E171 in BALB/c mice in combination with AOM/DSS. Numbers in bold correspond to upregulated genes. Log2FC= Log2 fold change obtained with LIMMA script with correction for its own time-matched control.

ftp://web.tgx.unimaas.nl/hproquin/Chapter_3/Supplementary_table_2.docx

Supplementary Table 3: Details results of ORA after 14 days of exposure of E171 in BALB/c mice in combination with AOM/DSS. Numbers in bold correspond to upregulated genes. Log2FC= Log2 fold change obtained with LIMMA script with correction for its own time-matched control.

ftp://web.tgx.unimaas.nl/hproquin/Chapter_3/Supplementary_table_3.docx

Supplementary Table 4: Details results of ORA after 21 days of exposure of E171 in BALB/c mice in combination with AOM/DSS. Numbers in bold correspond to upregulated genes. Log2FC= Log2 fold change obtained with LIMMA script with correction for its own time-matched control.

ftp://web.tgx.unimaas.nl/hproquin/Chapter_3/Supplementary_table_4.docx

Supplementary Table 5: Result of the GSEA of the DEG after exposure to E171 in combination with AOM/DSS in the distal colon of BALB/c mice.

ftp://web.tgx.unimaas.nl/hproquin/Chapter_3/Supplementary_table_5.docx

References

1. Jovanovic, B. (2015) Critical review of public health regulations of titanium dioxide, a human food additive. *Integr Environ Assess Manag*, **11**, 10-20.
2. Peters, R.J., van Bemmel, G., Herrera-Rivera, Z., Helsper, H.P., Marvin, H.J., Weigel, S., Tromp, P.C., Oomen, A.G., Rietveld, A.G., and Bouwmeester, H. (2014) Characterization of titanium dioxide nanoparticles in food products: analytical methods to define nanoparticles. *J Agric Food Chem*, **62**, 6285-6293.
3. Weir, A., Westerhoff, P., Fabricius, L., Hristovski, K., and von Goetz, N. (2012) Titanium dioxide nanoparticles in food and personal care products. *Environmental science & technology*, **46**, 2242-2250.
4. EU (2012) Regulation No 231-2012 on food additives. *Official Journal of the European Union*, **83**, 1-295.
5. USFDA (2016) US Food and Drug Administration regulation on Titanium dioxide. *Code of Federal Regulations*, **Title 21, Section 73.575.**
6. Proquin, H., Rodriguez-Ibarra, C., Moonen, C.G., Urrutia Ortega, I.M., Briede, J.J., de Kok, T.M., van Loveren, H., and Chirino, Y.I. (2017) Titanium dioxide food additive (E171) induces ROS formation and genotoxicity: contribution of micro and nano-sized fractions. *Mutagenesis*, **32**, 139-149.
7. Dorier, M., Beal, D., Marie-Desvergne, C., Dubosson, M., Barreau, F., Houdeau, E., Herlin-Boime, N., and Carriere, M. (2017) Continuous in vitro exposure of intestinal epithelial cells to E171 food additive causes oxidative stress, inducing oxidation of DNA bases but no endoplasmic reticulum stress. *Nanotoxicology*, 1-54.
8. IARC (2010) IARC MONOGRAPHS ON THE EVALUATION OF CARCINOGENIC RISKS TO HUMANS: Carbon Black, Titanium dioxide and Talc. **Volume 93**.
9. Tan, C., Zhao, B., Zhang, Z., and He, L. (2017) Rapid detection of TiO2 (E171) in table sugar using Raman spectroscopy. *Food Addit Contam Part A Chem Anal Control Expo Risk Assess*, **34**, 183-191.
10. Faust, J.J., Doudrick, K., Yang, Y., Capco, D.G., and Westerhoff, P. (2016) A Facile Method for Separating and Enriching Nano and Submicron Particles from Titanium Dioxide Found in Food and Pharmaceutical Products. *PLoS One*, **11**, e0164712.
11. Rompelberg, C., Heringa, M.B., van Donkersgoed, G., Drijvers, J., Roos, A., Westenbrink, S., Peters, R., van Bemmel, G., Brand, W., and Oomen, A.G. (2016) Oral intake of added titanium dioxide and its nanofraction from food products, food supplements and toothpaste by the Dutch population. *Nanotoxicology*, **10**, 1404-1414.
12. Zijno, A., De Angelis, I., De Berardis, B., Andreoli, C., Russo, M.T., Pietraforte, D., Scorza, G., Degan, P., Ponti, J., Rossi, F., and Barone, F. (2015) Different mechanisms are involved in oxidative DNA damage and genotoxicity induction by ZnO and TiO nanoparticles in human colon carcinoma cells. *Toxicol In Vitro*, **29**, 1503-1512.
13. Cui, Y., Gong, X., Duan, Y., Li, N., Hu, R., Liu, H., Hong, M., Zhou, M., Wang, L., Wang, H., and Hong, F. (2010) Hepatocyte apoptosis and its molecular mechanisms in mice caused by titanium dioxide nanoparticles. *J Hazard Mater*, **183**, 874-880.
14. Cui, Y., Liu, H., Ze, Y., Zhang, Z., Hu, Y., Cheng, Z., Cheng, J., Hu, R., Gao, G., Wang, L., Tang, M., and Hong, F. (2015) Corrigendum: Gene Expression in Liver Injury Caused by Long-Term Exposure to Titanium Dioxide Nanoparticles in Mice. *Toxicol Sci*, **146**, 202.
15. Urrutia-Ortega, I.M., Garduno-Balderas, L.G., Delgado-Buenrostro, N.L., Freyre-Fonseca, V., Flores-Flores, J.O., Gonzalez-Robles, A., Pedraza-Chaverri, J., Hernandez-Pando, R., Rodriguez-Sosa, M., Leon-Cabrera, S., Terrazas, L.I., van Loveren, H., and Chirino, Y.I. (2016) Food-grade

titanium dioxide exposure exacerbates tumor formation in colitis associated cancer model. *Food Chem Toxicol*, **93**, 20-31.
16. Proquin, H., Jetten, M.J., Jonkhout, M.C.M., Garduno-Balderas, L.G., Briede, J.J., de Kok, T.M., Chirino, Y.I., and van Loveren, H. (2018) Gene expression profiling in colon of mice exposed to food additive titanium dioxide (E171). *Food Chem Toxicol*, **111**, 153-165.
17. Bettini, S., Boutet-Robinet, E., Cartier, C., Comera, C., Gaultier, E., Dupuy, J., Naud, N., Tache, S., Grysan, P., Reguer, S., Thieriet, N., Refregiers, M., Thiaudiere, D., Cravedi, J.P., Carriere, M., Audinot, J.N., Pierre, F.H., Guzylack-Piriou, L., and Houdeau, E. (2017) Food-grade TiO2 impairs intestinal and systemic immune homeostasis, initiates preneoplastic lesions and promotes aberrant crypt development in the rat colon. *Sci Rep*, **7**, 40373.
18. Tanaka, T., Kohno, H., Suzuki, R., Yamada, Y., Sugie, S., and Mori, H. (2003) A novel inflammation-related mouse colon carcinogenesis model induced by azoxymethane and dextran sodium sulfate. *Cancer science*, **94**, 965-973.
19. Qiagen (2012) RNeasy Mini Handbook. *https://www.qiagen.com/us/resources/resourcedetail?id=14e7cf6e-521a-4cf7-8cbc-bf9f6fa33e24&lang=en*.
20. Agilent (2015) One-Color Microarray-Based Gene Expression Analysis. *http://www.agilent.com/cs/library/usermanuals/Public/G4140-90040_GeneExpression_OneColor_6.9.pdf*.
21. Reich, M., Liefeld, T., Gould, J., Lerner, J., Tamayo, P., and Mesirov, J.P. (2006) GenePattern 2.0. *Nature genetics*, **38**, 500-501.
22. Alonso, R., Salavert, F., Garcia-Garcia, F., Carbonell-Caballero, J., Bleda, M., Garcia-Alonso, L., Sanchis-Juan, A., Perez-Gil, D., Marin-Garcia, P., Sanchez, R., Cubuk, C., Hidalgo, M.R., Amadoz, A., Hernansaiz-Ballesteros, R.D., Aleman, A., Tarraga, J., Montaner, D., Medina, I., and Dopazo, J. (2015) Babelomics 5.0: functional interpretation for new generations of genomic data. *Nucleic Acids Res*, **43**, W117-121.
23. Smyth, G.K. (2005) Limma: linear models for microarray data. *Bioinformatics and computational biology solutions using R and Bioconductor*. Springer, pp. 397-420.
24. Kamburov, A., Stelzl, U., Lehrach, H., and Herwig, R. (2013) The ConsensusPathDB interaction database: 2013 update. *Nucleic Acids Res*, **41**, D793-800.
25. Herwig, R., Hardt, C., Lienhard, M., and Kamburov, A. (2016) Analyzing and interpreting genome data at the network level with ConsensusPathDB. *Nat Protoc*, **11**, 1889-1907.
26. Jennen, D.G., Gaj, S., Giesbertz, P.J., van Delft, J.H., Evelo, C.T., and Kleinjans, J.C. (2010) Biotransformation pathway maps in WikiPathways enable direct visualization of drug metabolism related expression changes. *Drug Discov Today*, **15**, 851-858.
27. Kutmon, M., van Iersel, M.P., Bohler, A., Kelder, T., Nunes, N., Pico, A.R., and Evelo, C.T. (2015) PathVisio 3: an extendable pathway analysis toolbox. *PLoS Comput Biol*, **11**, e1004085.
28. Shannon, P., Markiel, A., Ozier, O., Baliga, N.S., Wang, J.T., Ramage, D., Amin, N., Schwikowski, B., and Ideker, T. (2003) Cytoscape: a software environment for integrated models of biomolecular interaction networks. *Genome Res*, **13**, 2498-2504.
29. Ernst, J., and Bar-Joseph, Z. (2006) STEM: a tool for the analysis of short time series gene expression data. *Bmc Bioinformatics*, **7**, 191.
30. Pigozzi, D., Ducret, T., Tajeddine, N., Gala, J.L., Tombal, B., and Gailly, P. (2006) Calcium store contents control the expression of TRPC1, TRPC3 and TRPV6 proteins in LNCaP prostate cancer cell line. *Cell Calcium*, **39**, 401-415.
31. Keleg, S., Kayed, H., Jiang, X.H., Penzel, R., Giese, T., Buchler, M.W., Friess, H., and Kleeff, J. (2007) Adrenomedullin is induced by hypoxia and enhances pancreatic cancer cell invasion. *International Journal of Cancer*, **121**, 21-32.
32. Johansson, P., Aoude, L.G., Wadt, K., Glasson, W.J., Warrier, S.K., Hewitt, A.W., Kiilgaard, J.F., Heegaard, S., Isaacs, T., Franchina, M., Ingvar, C., Vermeulen, T., Whitehead, K.J., Schmidt,

C.W., Palmer, J.M., Symmons, J., Gerdes, A.M., Jonsson, G., and Hayward, N.K. (2016) Deep sequencing of uveal melanoma identifies a recurrent mutation in PLCB4. *Oncotarget*, **7**, 4624-4631.

33. Jung, S., Yi, L., Jeong, D., Kim, J., An, S., Oh, T.J., Kim, C.H., Kim, C.J., Yang, Y., Il Kim, K., Lim, J.S., and Lee, M.S. (2011) The role of ADCYAP1, adenylate cyclase activating polypeptide 1, as a methylation biomarker for the early detection of cervical cancer. *Oncol Rep*, **25**, 245-252.
34. Yang, S.L., Cao, Q., Zhou, K.C., Feng, Y.J., and Wang, Y.Z. (2009) Transient receptor potential channel C3 contributes to the progression of human ovarian cancer. *Oncogene*, **28**, 1320-1328.
35. Colucci, R., Blandizzi, C., Tanini, M., Vassalle, C., Breschi, M.C., and Del Tacca, M. (2005) Gastrin promotes human colon cancer cell growth via CCK-2 receptor-mediated cyclooxygenase-2 induction and prostaglandin E2 production. *Br J Pharmacol*, **144**, 338-348.
36. Sugino, Y., Misawa, A., Inoue, J., Kitagawa, M., Hosoi, H., Sugimoto, T., Imoto, I., and Inazawa, J. (2007) Epigenetic silencing of prostaglandin E receptor 2 (PTGER2) is associated with progression of neuroblastomas. *Oncogene*, **26**, 7401-7413.
37. Stafford, L.J., Xia, C.Z., Ma, W.B., Cai, Y., and Liu, M.Y. (2002) Identification and characterization of mouse metastasis-suppressor KiSS1 and its G-protein-coupled receptor. *Cancer research*, **62**, 5399-5404.
38. Deshayes, F., and Nahmias, C. (2005) Angiotensin receptors: a new role in cancer? *Trends Endocrinol Metab*, **16**, 293-299.
39. Wang, R., Lohr, C.V., Fischer, K., Dashwood, W.M., Greenwood, J.A., Ho, E., Williams, D.E., Ashktorab, H., Dashwood, M.R., and Dashwood, R.H. (2013) Epigenetic inactivation of endothelin-2 and endothelin-3 in colon cancer. *International Journal of Cancer*, **132**, 1004-1012.
40. Xu, C., Li, C.Y., and Kong, A.N. (2005) Induction of phase I, II and III drug metabolism/transport by xenobiotics. *Arch Pharm Res*, **28**, 249-268.
41. Murn, J., Alibert, O., Wu, N., Tendil, S., and Gidrol, X. (2008) Prostaglandin E2 regulates B cell proliferation through a candidate tumor suppressor, Ptger4. *J Exp Med*, **205**, 3091-3103.
42. Tseng, W.W., and Liu, C.D. (2002) Peptide YY and cancer: current findings and potential clinical applications. *Peptides*, **23**, 389-395.
43. Urosevic, J., Garcia-Albeniz, X., Planet, E., Real, S., Cespedes, M.V., Guiu, M., Fernandez, E., Bellmunt, A., Gawrzak, S., Pavlovic, M., Mangues, R., Dolado, I., Barriga, F.M., Nadal, C., Kemeny, N., Batlle, E., Nebreda, A.R., and Gomis, R.R. (2014) Colon cancer cells colonize the lung from established liver metastases through p38 MAPK signalling and PTHLH. *Nature Cell Biology*, **16**, 685-+.
44. Ma, X., Meng, Z., Jin, L., Xiao, Z., Wang, X., Tsark, W.M., Ding, L., Gu, Y., Zhang, J., Kim, B., He, M., Gan, X., Shively, J.E., Yu, H., Xu, R., and Huang, W. (2017) CAMK2 gamma in intestinal epithelial cells modulates colitis-associated colorectal carcinogenesis via enhancing STAT3 activation. *Oncogene*, **36**, 4060-4071.
45. Van Raamsdonk, C.D., Griewank, K.G., Crosby, M.B., Garrido, M.C., Vemula, S., Wiesner, T., Obenauf, A.C., Wackernagel, W., Green, G., Bouvier, N., Sozen, M.M., Baimukanova, G., Roy, R., Heguy, A., Dolgalev, I., Khanin, R., Busam, K., Speicher, M.R., O'Brien, J., and Bastian, B.C. (2010) Mutations in GNA11 in Uveal Melanoma. *New Engl J Med*, **363**, 2191-2199.
46. Widschwendter, M., Siegmund, K.D., Muller, H.M., Fiegl, H., Marth, C., Muller-Holzner, E., Jones, P.A., and Laird, P.W. (2004) Association of breast cancer DNA methylation profiles with hormone receptor status and response to tamoxifen. *Cancer research*, **64**, 3807-3813.
47. Gelman, I.H. (2012) Suppression of tumor and metastasis progression through the scaffolding functions of SSeCKS/Gravin/AKAP12. *Cancer Metast Rev*, **31**, 493-500.
48. Sancisi, V., Germinario, E., Esposito, A., Morini, E., Peron, S., Moggio, M., Tomelleri, G., Danieli-Betto, D., and Tupler, R. (2014) Altered Tnnt3 characterizes selective weakness of fast fibers in

mice overexpressing FSHD region gene 1 (FRG1). *Am J Physiol Regul Integr Comp Physiol*, **306**, R124-137.
49. Ha, K., Buchan, J.G., Alvarado, D.M., McCall, K., Vydyanath, A., Luther, P.K., Goldsmith, M.I., Dobbs, M.B., and Gurnett, C.A. (2013) MYBPC1 mutations impair skeletal muscle function in zebrafish models of arthrogryposis. *Hum Mol Genet*, **22**, 4967-4977.
50. Steadman, C.J., Phillips, S.F., Camilleri, M., Talley, N.J., Haddad, A., and Hanson, R. (1992) Control of muscle tone in the human colon. *Gut*, **33**, 541-546.
51. Gao, G., Ze, Y., Zhao, X., Sang, X., Zheng, L., Ze, X., Gui, S., Sheng, L., Sun, Q., Hong, J., Yu, X., Wang, L., Hong, F., and Zhang, X. (2013) Titanium dioxide nanoparticle-induced testicular damage, spermatogenesis suppression, and gene expression alterations in male mice. *J Hazard Mater*, **258-259**, 133-143.
52. Hu, H., Li, L., Guo, Q., Jin, S., Zhou, Y., Oh, Y., Feng, Y., Wu, Q., and Gu, N. (2016) A mechanistic study to increase understanding of titanium dioxide nanoparticles-increased plasma glucose in mice. *Food Chem Toxicol*, **95**, 175-187.
53. Guo, Z., Martucci, N.J., Moreno-Olivas, F., Tako, E., and Mahler, G.J. (2017) Titanium Dioxide Nanoparticle Ingestion Alters Nutrient Absorption in an In Vitro Model of the Small Intestine. *NanoImpact*, **5**, 70-82.
54. Kinoshita, P.F., Leite, J.A., Orellana, A.M.M., Vasconcelos, A.R., Quintas, L.E.M., Kawamoto, E.M., and Scavone, C. (2016) The Influence of Na+, K+-ATPase on Glutamate Signaling in Neurodegenerative Diseases and Senescence. *Front Physiol*, **7**.
55. Morange, P.E., Suchon, P., and Tregouet, D.A. (2015) Genetics of Venous Thrombosis: update in 2015. *Thromb Haemostasis*, **114**, 910-919.
56. Rodriguez-Yanez, Y., Bahena-Uribe, D., Chavez-Munguia, B., Lopez-Marure, R., Gonzalez-Monroy, S., Cisneros, B., and Albores, A. (2015) Commercial single-walled carbon nanotubes effects in fibrinolysis of human umbilical vein endothelial cells. *Toxicology in Vitro*, **29**, 1201-1214.
57. Zhang, X., and Firestein, S. (2002) The olfactory receptor gene superfamily of the mouse. *Nat Neurosci*, **5**, 124-133.
58. Kroeze, W.K., Sheffler, D.J., and Roth, B.L. (2003) G-protein-coupled receptors at a glance. *J Cell Sci*, **116**, 4867-4869.
59. Rosenbaum, D.M., Rasmussen, S.G., and Kobilka, B.K. (2009) The structure and function of G-protein-coupled receptors. *Nature*, **459**, 356-363.
60. Chen, H.W., Su, S.F., Chien, C.T., Lin, W.H., Yu, S.L., Chou, C.C., Chen, J.J., and Yang, P.C. (2006) Titanium dioxide nanoparticles induce emphysema-like lung injury in mice. *FASEB J*, **20**, 2393-2395.
61. Dorsam, R.T., and Gutkind, J.S. (2007) G-protein-coupled receptors and cancer. *Nat Rev Cancer*, **7**, 79-94.
62. Lappano, R., and Maggiolini, M. (2012) GPCRs and cancer. *Acta Pharmacol Sin*, **33**, 351-362.
63. Lombardi, M.S., Kavelaars, A., and Heijnen, C.J. (2002) Role and modulation of G protein-coupled receptor signaling in inflammatory processes. *Crit Rev Immunol*, **22**, 141-163.
64. Cho, H., and Kehrl, J.H. (2009) Regulation of immune function by G protein-coupled receptors, trimeric G proteins, and RGS proteins. *Prog Mol Biol Transl Sci*, **86**, 249-298.
65. Fehlker, M., Huska, M.R., Jons, T., Andrade-Navarro, M.A., and Kemmner, W. (2014) Concerted down-regulation of immune-system related genes predicts metastasis in colorectal carcinoma. *BMC Cancer*, **14**, 64.
66. Garziera, M., and Toffoli, G. (2014) Inhibition of host immune response in colorectal cancer: Human leukocyte antigen-G and beyond. *World J Gastroentero*, **20**, 3778-3794.
67. Pernot, S., Terme, M., Voron, T., Colussi, O., Marcheteau, E., Tartour, E., and Taieb, J. (2014) Colorectal cancer and immunity: what we know and perspectives. *World J Gastroentero*, **20**, 3738-3750.

68. Basu, S., Michaelsson, K., Olofsson, H., Johansson, S., and Melhus, H. (2001) Association between oxidative stress and bone mineral density. *Biochem Bioph Res Co*, **288**, 275-279.
69. Siwik, D.A., Pagano, P.J., and Colucci, W.S. (2001) Oxidative stress regulates collagen synthesis and matrix metalloproteinase activity in cardiac fibroblasts. *Am J Physiol Cell Physiol*, **280**, C53-60.
70. Wang, P., Zhou, S., Xu, L., Lu, Y., Yuan, X., Zhang, H., Li, R., Fang, J., and Liu, P. (2013) Hydrogen peroxide-mediated oxidative stress and collagen synthesis in cardiac fibroblasts: blockade by tanshinone IIA. *J Ethnopharmacol*, **145**, 152-161.
71. Gencer, S., Cebeci, A., and Irmak-Yazicioglu, M.B. (2013) Matrix metalloproteinase gene expressions might be oxidative stress targets in gastric cancer cell lines. *Chinese J Cancer Res*, **25**, 322-333.
72. Buda, A., Qualtrough, D., Jepson, M.A., Martines, D., Paraskeva, C., and Pignatelli, M. (2003) Butyrate downregulates alpha2beta1 integrin: a possible role in the induction of apoptosis in colorectal cancer cell lines. *Gut*, **52**, 729-734.
73. Gershon, M.D., and Tack, J. (2007) The serotonin signaling system: from basic understanding to drug development for functional GI disorders. *Gastroenterology*, **132**, 397-414.
74. Dizeyi, N., Bjartell, A., Nilsson, E., Hansson, J., Gadaleanu, V., Cross, N., and Abrahamsson, P.A. (2004) Expression of serotonin receptors and role of serotonin in human prostate cancer tissue and cell lines. *Prostate*, **59**, 328-336.
75. Trouiller, B., Reliene, R., Westbrook, A., Solaimani, P., and Schiestl, R.H. (2009) Titanium dioxide nanoparticles induce DNA damage and genetic instability in vivo in mice. *Cancer research*, **69**, 8784-8789.
76. Shukla, R.K., Sharma, V., Pandey, A.K., Singh, S., Sultana, S., and Dhawan, A. (2011) ROS-mediated genotoxicity induced by titanium dioxide nanoparticles in human epidermal cells. *Toxicol In Vitro*, **25**, 231-241.
77. Shi, Z.Q., Niu, Y.J., Wang, Q., Shi, L., Guo, H.C., Liu, Y., Zhu, Y., Liu, S.F., Liu, C., Chen, X., and Zhang, R. (2015) Reduction of DNA damage induced by titanium dioxide nanoparticles through Nrf2 in vitro and in vivo. *Journal of Hazardous Materials*, **298**, 310-319.
78. Waldner, M.J., and Neurath, M.F. (2009) Colitis-associated cancer: the role of T cells in tumor development. *Semin Immunopathol*, **31**, 249-256.
79. Viana, L.D., Affonso, R.J., Silva, S.R.M., Denadai, M.V.A., Matos, D., de Souza, C.S., and Waisberg, J. (2013) Relationship between the Expression of the Extracellular Matrix Genes SPARC, SPP1, FN1, ITGA5 and ITGAV and Clinicopathological Parameters of Tumor Progression and Colorectal Cancer Dissemination. *Oncology-Basel*, **84**, 81-91.
80. Andreu, P., Colnot, S., Godard, C., Laurent-Puig, P., Lamarque, D., Kahn, A., Perret, C., and Romagnolo, B. (2006) Identification of the IFITM family as a new molecular marker in human colorectal tumors. *Cancer research*, **66**, 1949-1955.
81. Oishi, Y., Watanabe, Y., Yoshida, Y., Sato, Y., Hiraishi, T., Oikawa, R., Maehata, T., Suzuki, H., Toyota, M., Niwa, H., Suzuki, M., and Itoh, F. (2012) Hypermethylation of Sox17 gene is useful as a molecular diagnostic application in early gastric cancer. *Tumour Biol*, **33**, 383-393.
82. Hoensch, H.P., Hutt, R., and Hartmann, F. (1979) Biotransformation of xenobiotics in human intestinal mucosa. *Environmental health perspectives*, **33**, 71-78.
83. Kaminsky, L.S., and Zhang, Q.Y. (2003) The small intestine as a xenobiotic-metabolizing organ. *Drug Metab Dispos*, **31**, 1520-1525.
84. Paine, M.F., Hart, H.L., Ludington, S.S., Haining, R.L., Rettie, A.E., and Zeldin, D.C. (2006) The human intestinal cytochrome P450 "pie". *Drug Metab Dispos*, **34**, 880-886.
85. Frohlich, E., Kueznik, T., Samberger, C., Roblegg, E., Wrighton, C., and Pieber, T.R. (2010) Size-dependent effects of nanoparticles on the activity of cytochrome P450 isoenzymes. *Toxicol Appl Pharm*, **242**, 326-332.

86. Nebert, D.W., and Russell, D.W. (2002) Clinical importance of the cytochromes P450. *Lancet*, **360**, 1155-1162.
87. Fang, J.Y., and Richardson, B.C. (2005) The MAPK signalling pathways and colorectal cancer. *Lancet Oncol*, **6**, 322-327.
88. Napoli, I., Mercaldo, V., Boyl, P.P., Eleuteri, B., Zalfa, F., De Rubeis, S., Di Marino, D., Mohr, E., Massimi, M., Falconi, M., Witke, W., Costa-Mattioli, M., Sonenberg, N., Achsel, T., and Bagni, C. (2008) The fragile X syndrome protein represses activity-dependent translation through CYFIP1, a new 4E-BP. *Cell*, **134**, 1042-1054.
89. De Rubeis, S., Pasciuto, E., Li, K.W., Fernandez, E., Di Marino, D., Buzzi, A., Ostroff, L.E., Klann, E., Zwartkruis, F.J., Komiyama, N.H., Grant, S.G., Poujol, C., Choquet, D., Achsel, T., Posthuma, D., Smit, A.B., and Bagni, C. (2013) CYFIP1 coordinates mRNA translation and cytoskeleton remodeling to ensure proper dendritic spine formation. *Neuron*, **79**, 1169-1182.
90. Silva, J.M., Ezhkova, E., Silva, J., Heart, S., Castillo, M., Campos, Y., Castro, V., Bonilla, F., Cordon-Cardo, C., Muthuswamy, S.K., Powers, S., Fuchs, E., and Hannon, G.J. (2009) Cyfip1 Is a Putative Invasion Suppressor in Epithelial Cancers. *Cell*, **137**, 1047-1061.
91. Gitenay, D., and Baron, V.T. (2009) Is EGR1 a potential target for prostate cancer therapy? *Future Oncol*, **5**, 993-1003.

Chapter 4

The titanium dioxide food additive E171 increases tumour formation and affects gene expression in a transgenic mouse model of colon cancer

In preparation

Héloïse Proquin

Marlon J. Jetten

Yannick Schrooders

Marloes C.M. Jonkhout

Jacob J. Briedé

Yolanda I. Chirino

Henk van Loveren

Theo M. de Kok

Abstract

Diet and life style of Western countries are suspected to cause an increase in the incidence of colorectal cancer (CRC). In the diet, the titanium dioxide (TiO_2) food additive E171 is now being scrutinised because of its potential adverse effects. Previous research in mice showed that oral exposure to E171 enhances the number of colorectal tumours in a chemically induced CRC model. Additionally, gene expression changes after short exposure to E171 in normal BALB/c and in the CRC mouse model showed responses towards inflammation, dysregulation of the immune system, modulation of olfactory/GPCR signalling genes, and cancer-related genes in the colon. In order to reproduce these findings, a transgenic mouse model based on the Cre-LoxP system that provides a colon specific knockout model which spontaneously develops colorectal tumours was used. First, tumour development was studied during 9 weeks of oral exposure to 5 mg/kg_{bw}/day of E171. This study showed that E171 enhanced the number of mice with tumours as well as the average number of tumours in these mice. In addition, gene expression changes in the colon were established after oral exposure to 1, 2, and 5 mg/kg_{bw}/day of E171 for 2, 7, 14, and 21 days. Whole-genome mRNA analysis revealed modulation of genes involved in oxidative stress responses, in DNA damage and DNA repair, in innate immune responses, in olfactory/GPCR signalling pathways, and of cancer related genes. The processes associated with these genes may be involved in the enhanced tumour formation induced by E171.

I- Introduction

Colorectal cancer (CRC) is a complex disease with a morbidity and mortality that are significantly higher in developed countries as compared to developing countries (1). One of the suspected exacerbating factors to develop CRC is the diet. Especially, there is concern that small sized particles like nanoparticles (NPs) (<100nm) in food may induce adverse effects. Titanium dioxide (TiO_2) based food additive, approved in food products since 1969 by the European Union under the name of E171, consists of 25 to 40% of NPs and 60 to 75% of microparticles (MPs) (>100nm) (2-5). It is used for its very bright white colour, high refraction index, and resistance to UV which makes it a very stable pigment over time. Consequently, E171 is used in a high variety of food products such as dairy, sweets, cookies, and many sauces (5-9).

Adverse effects of TiO_2 were first studied after inhalation. Based on new epidemiological studies in human and rodents showing the development of lung tumours after TiO_2 inhalation, the International Agency for Research in Cancer (IARC) classified TiO_2 as a possible carcinogen to humans (Group 2B) (10). Findings in inhalation studies as well as the change of classification to group 2B raised concern about other routes of exposure such as ingestion. Therefore, the potential carcinogenicity of E171 after ingestion as well as studies to discern mechanisms of action have been performed. In a chemically induced CRC model with azoxymethane (AOM) and dextran sodium sulphate (DSS), BALB/c mice were exposed orally to 5 mg/kgbw/day of E171 for 10 weeks (11). The number of tumours in the colon was significantly increased after intragastric exposure to E171 as compared to the control (AOM/DSS). Furthermore, expression of markers of tumour progression i.e. COX2, Ki67, and β-catenin were increased. In the same study, no development of tumours was observed after exposure to only E171, although, a decrease in goblet cells and the induction of dysplastic changes in the colonic epithelium were detected. Another study in a chemically induced CRC rat model showed, after exposure to 10 mg/kgbw/day of E171 for 100 days, the growth of aberrant crypt foci in the colon (12). In that study, preneoplastic lesions were also observed after oral exposure to 10 mg/kgbw/day of only E171 for 100 days in normal rats. The underlying mechanisms affected after oral exposure of E171 were studied in normal BALB/c mice, chemically induced CRC mice (AOM/DSS) (CI), and in rats. Gene expression changes after exposure to 5 mg/kgbw/day of E171 for 2, 7, 14, and 21 days in normal BALB/c mice showed changes in olfactory/GPCR signalling genes, immune system, oxidative stress, and cancer-related genes in the colon (13). Similar results were observed in the CI mouse model with the same experimental design. Gene expression changes in colon indicated modulation of immune related genes,

olfactory/GPCR signalling genes, oxidative stress, and biotransformation of xenobiotics (14). In rats, intragastric exposure to 10 mg/kgbw/day of E171 for 1 week showed a shift in the Th1/Th17 balance in the immune system as well as an impairment of the intestinal homeostasis (12).

These aforementioned studies investigated the tumour progression and potential adverse mechanisms in the colon after E171 ingestion. In the current study, we intended to use a transgenic (Tg) mouse model which does not require chemical induction, but is based on the Cre-LoxP system for generating a tissue specific knockout mouse model. A knockout of a floxed Apc gene in the colon by the Cre-recombinase with a Car1 promotor allows 26% of the mice to spontaneously develop colorectal tumours (15). The model is representative for the human situation as, in humans, the loss of function of the APC gene triggers the "adenoma-carcinoma" sequence which is a gradual series of histological changes accompanied by genetic alteration in a specific oncogene or tumour suppressor gene. The APC mutation is the primary cause of CRC, it is found in around 80% of all human colon tumours (16). The normal epithelium becomes an early adenoma/dysplastic crypt and an accumulation of β-catenin which may also be related to the stimulation of cellular growth and proliferation can be observed. We investigated effects of oral exposure to E171 in this Tg mouse model, by monitoring tumour formation and by gene expression profiling in the distal colon. In order to compare results with earlier studies from our group in mice, the exposure schedule was similar as previously: 2, 7, 14, and 21 days (13,14). Our hypothesis is that E171 induces gene expression changes that may lead to altered signal transduction, oxidative stress, inflammation, impairment of the immune system, and activation of cancer-related genes, which all may have a role in the exacerbation of tumour formation.

II- Materials and Methods

II-1- E171 characterization

E171 was kindly donated by the Sensient Technologies Company in Mexico. Characterization of E171 by electron microscopy with Scios DualBeam FIB/SEM (SEM, 20 KV, Holland) at 150,000x magnification showed that E171 comprises 39% of NPs and 61% of MPs and particles are slightly to fully rounded (17).

II-2- Animals

All animal experiments were reviewed and approved by the Animal Experimental Committee which includes an ethical testing framework of Maastricht University, The Netherlands. The tumour formation study was approved under number 2014-080 and the gene expression study was approved under number 2014-079. All mice were housed in polycarbonate cages and kept in a housing room (21°C, 50-60% relative humidity, 12 h light/dark cycles, air filtered until 5 µm particles and was exchanged 18 times/h). Mice were given a standard chow diet and water *ad libitum*. Cardboard was removed from the cages as this is suspected to contain TiO_2 (18).

$CAC5^{Tg/Tg}$ mice (C57BL/6-Tg(Car1-cre)5Flt/J) originated from Jackson Laboratory. These express Cre-recombinase under the control of the mouse Car1 promoter. APC^{580S} mice were originated from the Mouse Model of Human Cancers Consortium (National Cancer Institute - Frederick) and carrying an adenomatosis polyposis coli (Apc) gene allele with LoxP sites flanking exon 14 ($APC^{580S/580S}$).

The $CAC5^{Tg/Tg}$ and $APC^{580S/+}$ were crossed to obtain $CAC^{Tg/Tg}$;$APC^{580S/+}$ mice based on the model created by Xue et al. (15). The combination of the LoxP and Cre recombinase expressed in the colon induce, in 26% of the mice, a spontaneous development of colon carcinomas in the first 10 weeks of age (15). No additional tumours were observed after 10 weeks of age.

In order to confirm the heterozygosis of the APC genes and the homozygosis of the Cre-recombinase gene with the Car-1 promotor, DNA was extracted from the tip of the tails of the mice and a PCR was performed before the start of each experiment. Samples were extracted and analysed by Charles River.

II-3- Experimental design to assess the effect of E171

Tumour formation study

A number of 80 $CAC^{Tg/Tg}$;$APC^{580S/+}$ mice were generated by crossing $CAC^{Tg/Tg}$ mice with $APC^{580S/+}$ mice. $CAC^{Tg/Tg}$;$APC^{580S/+}$ pups were weaned at 3 weeks of age. Mice were randomly divided in 2 groups: the E171 exposure group and the control group. From 5 weeks of age, $CAC^{Tg/Tg}$;$APC^{580S/+}$ mice were treated either with 5 mg/kg_{bw}/day of E171 (n=40) or sterile water (Life Sciences, The Netherlands) as control (n=40) for a maximum of 9 weeks. E171 was dispersed in a bath sonicator (Branson 2200) at 40 kHz for 30 min in sterile water for an administrated concentration of 5 mg/kg_{bw}. Control sterile water was also put in the bath sonicator. Mice were given 250 µL of E171 or sterile water by intragastric administration. Exposure was performed 5 days a week. Weight gain or loss was monitored weekly. Sixteen mice (8 from the E171 group and 8 from control group), 4 males and 4 females in each group, were euthanized after 1, 3, 5, 7 and 9 weeks of exposure. Euthanasia was performed under light anaesthesia (4% Isoflorane) followed by cervical dislocation.

At week 4, one mouse in the E171 group (group of 9 weeks exposure) was euthanized ahead of schedule due to severe rectal prolapse. At week 7, one mouse in the control group had tumours all over the colon from the caecum to the distal colon, something that is not normally observed in this model (15). Therefore this mouse was considered as an outlier. Colon, liver, and spleen were removed and weighed. Colons were also checked for the presence of tumours, and the number of visible tumours was registered.

Gene expression study

For the gene expression study, a number of 140 $CAC^{Tg/Tg}$;$APC^{580S/+}$ mice were randomly divided in 4 groups: 3 exposure groups with 3 different concentrations of E171 (1, 2, and 5 mg/kg_{bw}/day) and one control group with sterile water. Mice were exposed 5 days/week to the different concentrations of E171 or sterile water. Preparation of E171 and sterile water was performed the same way as for the tumour formation study. After 2, 7, 14, and 21 days, 35 mice were euthanized: 7 mice per group, 3 females and 4 males in each group. Euthanasia was performed under light anaesthesia followed by cervical dislocation. Three mice were euthanized ahead of schedule due to severe rectal prolapse and were not used for further analysis: one mouse in the E171 1 mg/kg_{bw}/day group 21 days and 2 mice in the control group; one of group 14 days and one of group 21 days. Colon, liver, and spleen was sampled from every mouse. The presence of tumours in the colon was registered.

II-4- mRNA extraction from colonic tissues

As tumour formation in this mouse model is mainly found in the distal colon (15), mRNA was extracted from this part of the colon as also reported earlier (13,14). Briefly, before RNA isolation, the distal colon was disrupted and homogenized by submerging them in Qiazol (Qiagen, The Netherlands) and subsequently using a Mini Bead Beater (BioSpec Products, The Netherlands) on a speed of 48 beats per second for 30 seconds. Isolation of mRNA followed the manufacturer's protocol for "Animal Cells and Animal Tissues" (19) in the mRNeasy Mini Kit (Qiagen, The Netherlands) with DNase treatment (Qiagen, The Netherlands). Quality and yield of the mRNA was verified on a Nanodrop® ND-1000 spectrophotometer (Thermo Fischer, The Netherlands). Samples passing the quality with a 260/230 ratio between 1.8 and 2.0 and a 260/280 ratio between 1.9 and 2.1 were checked for RNA integrity on a 2100 Bioanalyzer using manufacturer's protocol (Agilent Technologies, The Netherlands). All samples with a RNA integrity number (RIN) above 6 were used for microarray analysis. The average RIN value of the samples used, 125 in total, was 7.8 ± 0.8.

II-5- cRNA synthesis, labelling and hybridization

Samples were prepared for microarray analysis by synthetizing the mRNA into cRNA, labelling with Cy3, amplifying, and purify it using the RNeasy Mini Kit (Qiagen, The Netherlands) according to the One-Color Microarray-Based Gene Expression Analysis protocol version 6.6 (20). Furthermore, quantification of Cy3 labelled to the cRNA was performed using a Nanodrop® ND-1000 spectrophotometer with a Microarray Measurement. For hybridization, 600 ng of labelled cRNA was used on a SurePrint G3 mouse Gene exp 60kv2 microarrays slides (Agilent Technologies, The Netherlands). Moreover, microarray slides were scanned using an Agilent DNA Microarray Scanner with Surescan High-resolution Technology (Agilent Technologies, The Netherlands) with scanner settings to Dye Channel: G, Profile: AgilentG3_GX_1Color, Scan region: Agilent HD (61 x 21.3 mm), Scan resolution 3 µm, Tiff file dynamic range: 20 bit, Red PMT gain: 100%, Green PMT gain: 100%.

II-6- Pre-processing and data analysis of microarrays

The pre-processing methods used on the microarrays raw data were the same as previously described (13). In brief, after quality verification by the quality control pipeline provided by Agilent (Feature extraction software (FES) version 10.7.3.1), all samples were checked for quality and normalised with an in-house quality check pipeline previously published (github.com/BiGCAT-UM/arrayQC_Module). The in-house quality pipeline is based on local background correction, flagging of bad spots, controls and spots with too low intensity, log2 transformation and quantile normalization. The bad spots identified by the quality control were removed from the raw data. Sixteen groups were defined based on exposure and time points: 4 different exposure groups and 4 different time points. Spot identifiers were deleted when more than 40% of samples in each group had a missing value. Spot identifiers were also deleted when the average expression was less than 4 in all groups. Missing values were imputed by the k-nearest neighbours using the standard settings of the GenePattern ImputeMissingValues.KNN module v13 (21). Repeated identifiers were merged with Babelomics 5 (22). Differentially expressed genes (DEG) were identified by using LIMMA (version 1.0) which corrected the exposure samples with their time-matched controls. The standard cut-off values of a fold-change (FC)>1.5 and a p-value<0.05 were used (23). In addition, the false discovery rate (FDR) was calculated according to the Benjamini-Hochberg method with a threshold q-value<0.05.

II-7- Pathway analysis

In order to identify the biological processes associated with the DEG, an over-representation analysis (ORA) was performed in CPDB with the DEG of each time point (24). The p-value was calculated for each annotation set and, within each set, a correction for multiple testing was performed (q-value) (24,25). Cut-offs for the ORA were with a minimum overlap of the genes with the input list of 2 and a p-value<0.01 for each pathway. All the databases from CPDB were used.

III- Results

III-1- Tumour formation study

The $CAC^{Tg/Tg}$;$APC^{580S/+}$ Tg mouse model was used to study tumour formation in colon after exposure to 5 mg/kg_{bw}/day of E171 by intragastic administration for 9 weeks. These results were also used to confirm the capacity of E171 to enhance tumour formation as observed in the CI model that our group has published before (11).

Average weight of mice and organs

As shown in Figure 1, the mice body weight was monitored every week and organs i.e. colon, liver, and spleen were weight when sampled. Figure 1A shows that the body weight was not affected by E171 exposure during the experiment. After being sacrificed, the colons of the mice were weighed and no difference between the exposure group and the control group was found (Figure 1B). The same observation was made for the liver and the spleen (Figure 1C an 1D).

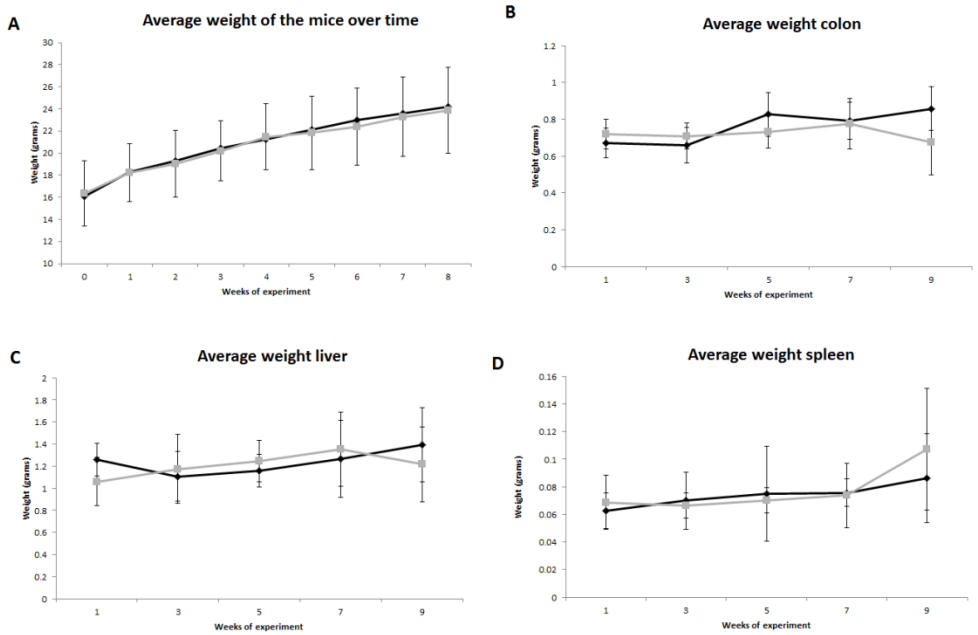

Figure 1: Average weight of the mice and organs after exposure to 5 mg/kg_{bw}/day of E171 over time.

(A) Measurement of body weight of the mice. After euthanasia colon (B), liver (C), and spleen (D) were weighted (n=137). Mice euthanized ahead of schedule were not included in the graphs. The black lines correspond to the control mice exposed to sterile water. The grey lines correspond to the

mice exposed to 5 mg/kg_{bw}/day of E171. Data are presented as mean ± standard deviation of each group.

Number of tumours in colon after E171 exposure

Figure 2 shows that the number of mice with tumours was increased after E171 exposure as compared to controls with a factor of 4 after 7 weeks and a factor of 1.25 after 9 weeks (Figure 2A). Similar increase was observed with the average number of tumours per mouse with a 4.4 times increase after 7 weeks of exposure and 1.7 times after 9 weeks of exposure (Figure 2B).

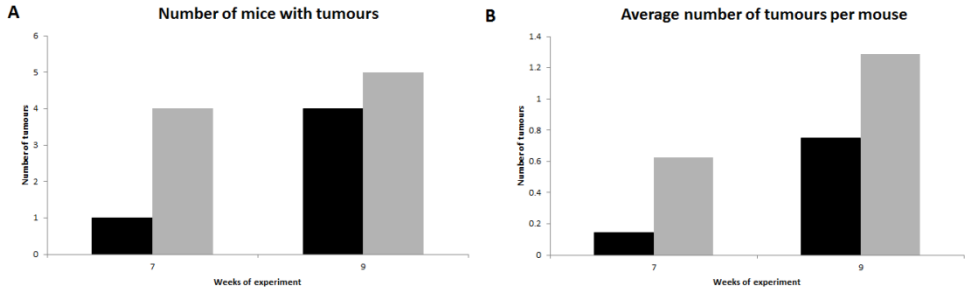

Figure 2: Tumour formation in colon of mice exposed to 5 mg/kg_{bw}/day of E171.
(A) Number of mice which were developing tumours and (B) the average of these tumours per total number of mice in each group. The black bars correspond to the control mice exposed to sterile water. The grey bars correspond to the mice exposed to 5 mg/kg_{bw}/day of E171. Data are presented as mean of each group (n=8 for each group except for the group exposed to E171 for 9 weeks, n=7).

III-2- Gene expression study

Gene expression analysis

DEG were identified after LIMMA with cut-offs of a fold change (FC)>1.5 and a p-value<0.05. After correction for multiple testing with the FDR method, the DEG were identified with an FC>1.5 and a q-value<0.05. No dose response was observed over time while analysing the number of DEG (Figure 3). At all concentrations, the number of DEG at the end of the experiment was always higher than at the start. A higher number of DEG was observed after exposure to 1 mg/kg_{bw}/day compared to 2 and 5 mg/kg_{bw}/day. For all time points, the lowest number of DEG was detected after exposure to 2 mg/kg_{bw}/day. A stable increase of the number of DEG over time was observed after exposure to 2 mg/kg_{bw}/day. This stable increase was not observed after exposure to 5 and 1 mg/kg_{bw}/day where the number of DEG at day 14 was lower than day 7.

After FDR correction, 2 DEG were detected after exposure to 2 mg/kg_{bw}/day: one at day 14 and one at day 21. After exposure to 5 mg/kg_{bw}/day, 13 DEG were observed: 10

at day 14 and 3 at day 21. The exposure to 1 mg/kg_{bw}/day showed a total of 388 DEG over all time points: 106 at day 2, 73 at day 7, 41 at day 14, and 168 at day 21. The total number of genes and the number of genes after FDR correction indicate that exposure to 1 mg/kg_{bw}/day showed the highest response. The absence of a linear dose response curve may be the consequence of aggregation and agglomeration of particles at higher concentrations, as observed by us previously after dispersion of E171 in different media and HBSS by dynamic light scattering (DLS) (17). In addition, after exposure to 1 mg/kg_{bw} for 21 days, one tumour was found in the colon of one mouse (data not shown). All other concentrations as well as control did not show any tumours. For these reasons we decided to use only the DEG after 1 mg/kg_{bw}/day for further analysis and interpretation, including pathway and gene analyses.

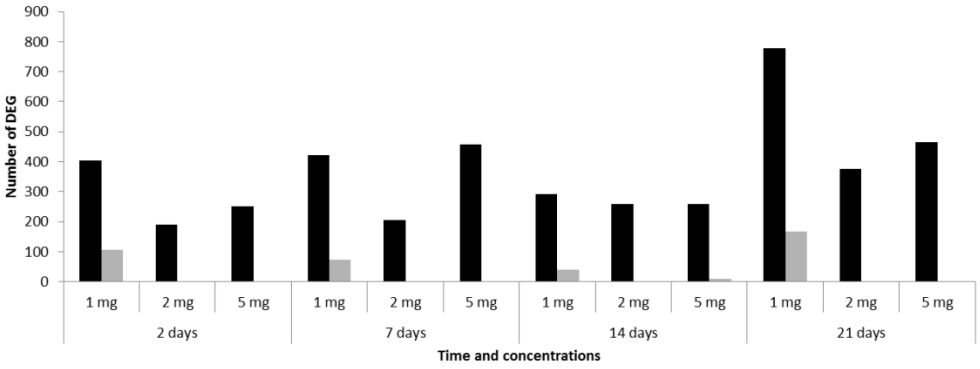

Figure 3: Number of DEG after exposure to different doses over time in the colon of mice.
Black bars correspond to a fold change (FC)>1.5 and a p-value<0.05. Grey bars correspond to a FC>1.5 and a q-value<0.05 (n=125).

Pathway and gene analyses

The pathway analysis performed with CPDB shows the association between the DEG and the biological mechanisms after exposure to 1 mg/kg_{bw}/day of E171 (Table 1). The suggested adverse mechanisms after E171 oral exposure were an induction of gene expression changes that may lead to altered signal transduction, oxidative stress, inflammation, impairment of the immune system, and activation of cancer-related genes, which all may have a role in the exacerbation of tumour formation. Consequently the focus of the result section will be on these mechanisms.

Pathways related to inflammation or as a response to inflammation were observed over time. After 2 and 21 days of exposure, prostaglandin pathway and metabolism of vitamin D pathway were observed respectively. Both pathways are

involved in response to oxidative stress. At the gene level, Nos2 gene which encodes for an enzyme normally present in macrophages called nitric oxide synthase was also observed after 2 and 21 days of exposure. This enzyme transforms the substrate L-arginine into L-citrulline and NO, the latter is a free radical which is involved in inflammation. NO enhances the synthesis of pro-inflammatory interleukins such as IL-6 and IL-8 (26). The genes encoding for these interleukins were differentially expressed at day 2 and 21 (also after FDR correction). Other genes associated with inflammation have been identified at day 2 and 21 like Mapk genes including 2 Mapk genes significant after FDR correction: one at day 2 and one at day 21.

No pathways related to DNA damage or DNA repair were observed, although several individual genes involved in DNA damage and DNA repair were differentially expressed over time from 2 to 21 days of exposure. After 2 days, 5 genes including 2 histone genes were differentially expressed (one histone gene significant after FDR correction). After 7 days of exposure, DNA repair genes like Cdk2, Ccna1 (significant after FDR correction), Ccna2, and histone genes were also identified. After 14 days of exposure, 3 DEG including one histone gene were observed. In addition, 10 genes including 5 histone genes and Ccna1 (significant after FDR correction) were differentially expressed after 21 days of exposure.

As seen in Table 1, pathways involved in the immune system were observed after 21 days of exposure: 6 pathways were observed with a total of 45 DEG, 4 in the innate immune system (defensins, α-defensins, TCF signalling, and complement), 1 in the adaptive immune system (cell adhesion molecules (CAMs)), and 1 in the cytokine signalling (cytokine-cytokine receptor interaction). The CAMs pathway was also observed in the pathway analysis performed with the FDR corrected genes (Table 2). At the gene level, DEG involved in the immune system were observed at all time points. After 2 days of exposure, 39 DEG involved in the complement system of the immune system were observed including TLR, Fc fragment, ROS in phagocytes, neutrophils degranulation, and MHC class I presentation. These biological responses (except Fc fragment) were also observed after 7 days of exposure with 31 DEG. In addition to these effects, genes involved in MHC class II presentation and TCR signalling were observed at day 7. Fewer genes influenced by the exposure to E171 were observed after 14 days of exposure; a total of 19 DEG were involved in TLR, neutrophils degranulation, and MHC class I and class II presentation.

Table 1: Pathway over-representation analysis (ORA) of the DEG after exposure to 1 mg/kg$_{bw}$/day of E171

Pathways related to the DEG after ORA with ConsensusPathDB. The pathways were grouped per time points and per biological function.

Time of exposure	Biological function	Name of pathway	p-value	Source
2 days	Signal transduction	- Peptide GPCRs	0.00164	Wikipathways
		- GPCRs, Class A Rhodopsin-like	0.00857	Wikipathways
	Cancers	- Small cell lung cancer	0.00394	KEGG
		- Pathways in cancer	0.00822	KEGG
	Cell Cycle	- S Phase	5.97E-05	Reactome
		- Mitotic G1-G1/S phases	0.000312	Reactome
		- G1/S Transition	0.000323	Reactome
		- Cyclin D associated events in G1	0.00161	Reactome
		- G1 Phase	0.00161	Reactome
		- DNA strand elongation	0.0021	Reactome
		- Telomere C-strand synthesis initiation	0.00326	Reactome
		- G1 to S cell cycle control	0.00449	Wikipathways
		- Inhibition of replication initiation of damaged DNA by RB1/E2F1	0.00483	Reactome
		- Telomere C-strand (Lagging Strand) Synthesis	0.00641	Reactome
		- Extension of Telomeres	0.00831	Reactome
		- Synthesis of DNA	0.000323	Reactome
		- DNA replication initiation	0.00326	Reactome
	Circadian Clock	- Circadian rhythm	3.43E-08	KEGG
		- Circadian Clock	6.98E-05	Reactome
		- Circadian Clock	6.98E-05	Reactome
		- Circadian clock tutorial CGrove	0.000118	Wikipathways
		- Exercise-induced Circadian Regulation	0.00198	Wikipathways
	DNA Replication	- DNA Replication	0.00049	Reactome
		- DNA replication	0.00373	KEGG
		- Synthesis of DNA	0.000323	Reactome
		- DNA replication initiation	0.00326	Reactome

	Metabolism	-	Phase 1 - Functionalization of compounds	0.0013	Reactome
		-	Prostaglandin Synthesis and Regulation	0.00184	Wikipathways
		-	Cytochrome P450 - arranged by substrate type	0.00237	Reactome
		-	biosynthesis of corticosteroids	0.00483	MouseCyc
	Metabolism of RNA	-	Destabilization of mRNA by AUF1 (hnRNP D0)	0.00668	Reactome
	Muscle contraction	-	Hypertrophy Model	0.00289	Wikipathways
7 days	Signal transduction	-	Olfactory transduction	0.00175	KEGG
		-	Chemokine receptors bind chemokines	0.00902	Reactome
	Cell cycle	-	Resolution of Sister Chromatid Cohesion	1.09E-11	Reactome
		-	Mitotic Prometaphase	4.04E-11	Reactome
		-	Cell Cycle, Mitotic	9.99E-11	Reactome
		-	M Phase	2.12E-10	Reactome
		-	Cyclin A/B1 associated events during G2/M transition	2.19E-10	Reactome
		-	Mitotic M-M/G1 phases	5.72E-10	Reactome
		-	Separation of Sister Chromatids	1.21E-09	Reactome
		-	Mitotic Anaphase	2.61E-09	Reactome
		-	Mitotic Metaphase and Anaphase	2.95E-09	Reactome
		-	APC/C-mediated degradation of cell cycle proteins	3.12E-09	Reactome
		-	Regulation of mitotic cell cycle	3.12E-09	Reactome
		-	Cell Cycle	4.01E-09	Reactome
		-	Cell cycle	1.02E-08	Wikipathways
		-	Regulation of APC/C activators between G1/S and early anaphase	1.87E-08	Reactome
		-	Cell cycle	1.36E-07	KEGG
		-	Oocyte meiosis	4.51E-07	KEGG
		-	Activation of NIMA Kinases NEK9, NEK6, NEK7	2.56E-06	Reactome
		-	Phosphorylation of Emi1	2.56E-06	Reactome
		-	G2/M Transition	6.74E-06	Reactome
		-	Cdc20:Phospho-APC/C mediated degradation of Cyclin A	7.05E-06	Reactome
		-	Mitotic G2-G2/M phases	8.16E-06	Reactome

-	Activation of APC/C and APC/C:Cdc20 mediated degradation of mitotic proteins	9.12E-06	Reactome
-	G2 Phase	8.42E-05	Reactome
-	Cyclin B2 mediated events	8.42E-05	Reactome
-	Chk1/Chk2(Cds1) mediated inactivation of Cyclin B:Cdk1 complex	8.42E-05	Reactome
-	Polo-like kinase mediated events	8.42E-05	Reactome
-	G2/M DNA replication checkpoint	8.42E-05	Reactome
-	Golgi Cisternae Pericentriolar Stack Reorganization	0.000109	Reactome
-	Cell Cycle Checkpoints	0.00011	Reactome
-	APC/C:Cdc20 mediated degradation of mitotic proteins	0.00011	Reactome
-	Phosphorylation of the APC/C	0.000264	Reactome
-	APC/C:Cdc20 mediated degradation of Cyclin B	0.000659	Reactome
-	G2/M DNA damage checkpoint	0.000665	Reactome
-	APC-Cdc20 mediated degradation of Nek2A	0.000963	Reactome
-	APC/C:Cdh1 mediated degradation of Cdc20 and other APC/C:Cdh1 targeted proteins in late mitosis/early G1	0.00115	Reactome
-	Condensation of Prometaphase Chromosomes	0.00127	Reactome
-	G2/M Checkpoints	0.00201	Reactome
-	SCF(Skp2)-mediated degradation of p27/p21	0.00213	Reactome
-	Mitotic G1-G1/S phases	0.00337	Reactome
-	G1/S Transition	0.00387	Reactome
-	G0 and Early G1	0.00477	Reactome
-	Inactivation of APC/C via direct inhibition of the APC/C complex	0.00477	Reactome
-	Inhibition of the proteolytic activity of APC/C required for the onset of anaphase by mitotic spindle checkpoint components	0.00477	Reactome
-	Regulation of PLK1 Activity at G2/M Transition	0.00504	Reactome
-	Mitotic Spindle Checkpoint	0.00563	Reactome
-	Nuclear Envelope Breakdown	0.00684	Reactome

	-	Cyclin E associated events during G1/S transition	0.00764	Reactome
	-	Cyclin A:Cdk2-associated events at S phase entry	0.00764	Reactome
Cellular responses to external stimuli	-	DNA Damage/Telomere Stress Induced Senescence	0.00329	Reactome
Circadian Clock	-	Circadian rhythm	0.000282	KEGG
	-	Circadian Clock	0.00213	Reactome
	-	Circadian Clock	0.00213	Reactome
	-	Exercise-induced Circadian Regulation	0.00325	Wikipathways
	-	Circadian clock tutorial CGrove	0.00603	Wikipathways
Digestion and absorption	-	Lipid digestion, mobilization, and transport	0.00103	Reactome
DNA repair	-	miRNA regulation of DNA Damage Response	0.00183	Wikipathways
Endocrine system	-	Progesterone-mediated oocyte maturation	6.46E-07	KEGG
Haemostasis	-	Kinesins	5.53E-05	Reactome
	-	Formation of Fibrin Clot (Clotting Cascade)	0.00764	Reactome
Membrane transport	-	ABC transporters	0.00902	KEGG
Metabolism	-	Cholesterol biosynthesis	1.87E-07	Reactome
	-	Cholesterol Biosynthesis	3.06E-07	Wikipathways
	-	superpathway of cholesterol biosynthesis	3.66E-07	MouseCyc
	-	mevalonate pathway I	3.36E-05	MouseCyc
	-	Trafficking of dietary sterols	0.000425	Reactome
	-	cholesterol biosynthesis II (via 24,25-dihydrolanosterol)	0.00045	MouseCyc
	-	Terpenoid backbone biosynthesis	0.000659	KEGG
	-	cholesterol biosynthesis III (via desmosterol)	0.00127	MouseCyc
	-	cholesterol biosynthesis I	0.00166	MouseCyc
	-	SREBF and miR33 in cholesterol and lipid homeostasis	0.00166	Wikipathways
	-	Drug metabolism - other enzymes	0.00984	KEGG
Neuronal System	-	GABA A receptor activation	0.00833	Reactome

	Transport of small molecules	-	ABCA transporters in lipid homeostasis	0.00127	Reactome
14 days	Signal Transduction	-	FGFR3c ligand binding and activation	0.00389	Reactome
		-	FGFR3 ligand binding and activation	0.00389	Reactome
		-	Peptide ligand-binding receptors	0.00418	Reactome
		-	FGFR4 ligand binding and activation	0.00496	Reactome
		-	FGFR2c ligand binding and activation	0.00496	Reactome
		-	Nuclear Receptors	0.00855	Wikipathways
		-	FGFR2 ligand binding and activation	0.00888	Reactome
		-	Activated point mutants of FGFR2	0.00888	Reactome
	Cancers	-	Melanoma	0.00663	KEGG
	Circadian Clock	-	Circadian rhythm	2.23E-05	KEGG
		-	Circadian Clock	0.000453	Reactome
		-	Circadian Clock	0.000453	Reactome
		-	Circadian clock tutorial CGrove	0.00212	Wikipathways
		-	Exercise-induced Circadian Regulation	0.00284	Wikipathways
	Digestive system	-	Bile secretion	0.00556	KEGG
	Disease	-	Signalling by activated point mutants of FGFR3	0.00389	Reactome
		-	Signalling by FGFR3 mutants	0.00389	Reactome
		-	Signalling by FGFR2 mutants	0.00888	Reactome
	Gene expression (Transcription)	-	Nuclear Receptor transcription pathway	0.00191	Reactome
	Neuronal System	-	Neuroactive ligand-receptor interaction	0.00148	KEGG
		-	Nicotine addiction	0.00291	KEGG
		-	GABA A receptor activation	0.00294	Reactome
	Transport of small molecules	-	Transmembrane transport of small molecules	0.00177	Reactome
		-	Ion channel transport	0.000399	Reactome
		-	Ligand-gated ion channel transport	0.00615	Reactome

	Vesicle-mediated transport	-	Scavenging of Heme from Plasma	0.00746	Reactome
21 days	Signal Transduction	-	Antagonism of Activin by Follistatin	0.000199	Reactome
		-	Hippo signalling pathway	0.000248	KEGG
		-	Olfactory transduction	0.000453	KEGG
		-	Olfactory Signalling Pathway	0.00128	Reactome
		-	Peptide ligand-binding receptors	0.0025	Reactome
		-	Signalling by GPCR	0.0043	Reactome
		-	Wnt Signalling Pathway and Pluripotency	0.0066	Wikipathways
		-	Class A/1 (Rhodopsin-like receptors)	0.007	Reactome
		-	GPCR downstream signalling	0.00795	Reactome
		-	Wnt signalling pathway	0.00808	KEGG
	Cancers	-	Basal cell carcinoma	6.77E-05	KEGG
	Circadian clock	-	Circadian clock	0.000585	KEGG
	Digestion and absorption	-	Fat digestion and absorption	0.00699	KEGG
	Endocrine system	-	Melanogenesis	0.0053	KEGG
	Extracellular matrix organization	-	Activation of Matrix Metalloproteinases	0.002	Reactome
		-	Degradation of the extracellular matrix	0.00861	Reactome
		-	Matrix Metalloproteinases	0.00955	Wikipathways
	Gene expression (Transcription)	-	Nuclear Receptor transcription pathway	0.00544	Reactome
	Haemostasis	-	Blood Clotting Cascade	0.00877	Wikipathways
		-	Complement and Coagulation Cascades	0.00924	Wikipathways
	Immune system	-	Alpha-defensins	0.000332	Reactome
		-	Defensins	0.00103	Reactome
		-	TGF Beta Signalling Pathway	0.00208	Wikipathways
		-	Cytokine-cytokine receptor interaction	0.00319	KEGG
		-	Cell adhesion molecules (CAMs)	0.00416	KEGG
	Metabolism	-	Mineralocorticoid biosynthesis	9.17E-06	Reactome
		-	Metabolism of steroid hormones	3.23E-05	Reactome

		and vitamin D		
	-	Steroid hormones	3.23E-05	Reactome
	-	Androgen biosynthesis	0.000205	Reactome
	-	Biogenic Amine Synthesis	0.00103	Wikipathways
	-	Glucocorticoid biosynthesis	0.0016	Reactome
	-	Steroid Biosynthesis	0.00249	Wikipathways
	-	Glucocorticoid & Mineralcorticoid Metabolism	0.00364	Wikipathways
	-	Vitamin D (calciferol) metabolism	0.0079	Reactome
Metabolism of proteins	-	Glycoprotein hormones	0.000484	Reactome
	-	Peptide hormone biosynthesis	0.0016	Reactome
Neuronal System	-	GABA synthesis, release, reuptake and degradation	0.000297	Reactome
	-	GABA synthesis	0.00138	Reactome
	-	Neurotransmitter Release Cycle	0.00337	Reactome
	-	Reuptake of GABA	0.0079	Reactome
	-	glutamate degradation IV	0.0079	MouseCyc
	-	glutamate degradation III (via 4-aminobutyrate)	0.0079	MouseCyc

Table 1 shows that after exposure to 1 mg/kg_{bw}/day of E171, cancer and cancer related pathways were identified at all time points. These pathways were classified in the biological processes “disease” by Reactome and “cancer” by KEGG. After 2 days of exposure, 2 pathways were related to cancer (small lung cancer and pathways in cancer), 13 pathways to cell cycle, 1 to metabolism of RNA, and 2 pathways to signal transduction. After 7 days of exposure, 48 pathways related to cell cycle were observed as well as 2 pathways related to signal transduction and 3 pathways to gene expression (transcription). After 14 days of exposure, 1 pathway was found to be related to cancer (melanoma), 3 pathways to disease, 1 pathway to gene expression (transcription), and 8 pathways to signal transduction. After 21 days of exposure, another pathway was related to cancer (basal cell carcinoma) and 10 pathways were related to signal transduction including 2 pathways involved in Wnt signalling.

Cancer and cancer related pathways were also associated with the DEG significant after FDR correction. After 2 days of exposure, 1 pathway related to cancer (pathways in cancer), 3 pathways to cell cycle, and one pathway to gene expression (transcription) (nuclear Receptor transcription pathway) were observed. The latter was also observed at day 14 and 21. After 7 days, 2 pathways in cell cycle and 2 in gene expression (transcription) were observed. After 14 days, 3 pathways in the gene expression (transcription) biological process were observed. Same biological process was observed after 21 days with 2 pathways.

Table 2: Pathway over-representation analysis (ORA) of the FDR corrected DEG after exposure to 1 mg/kg$_{bw}$/day of E171

Pathways related to the DEG after ORA with ConsensusPathDB. The pathways were grouped per time points and per biological function.

Time of exposure	Biological function	Name of pathway	p-value	Source
2 days	Bone development	- Endochondral Ossification	0.00433	Wikipathways
	Cancer	- Pathways in cancer	0.00686	KEGG
	Cell cycle	- Mitotic G1-G1/S phases	0.000735	Reactome
		- G1/S Transition	0.00316	Reactome
		- S Phase	0.00896	Reactome
	Circadian Clock	- Circadian rhythm	1.20E-08	KEGG
		- Circadian Clock	5.07E-05	Reactome
		- Exercise-induced Circadian Regulation	0.000176	Wikipathways
		- Circadian clock tutorial CGrove	0.00049	Wikipathways
		- Diurnally Regulated Genes with Circadian Orthologues	0.00266	Wikipathways
	Gene expression (Transcription)	- Nuclear Receptor transcription pathway	0.00207	Reactome
	Metabolism	- Retinol metabolism	0.000891	Wikipathways
7 days	Cell cycle	- Cyclin A/B1 associated events during G2/M transition	0.00399	Reactome
		- Resolution of Sister Chromatid Cohesion	0.00855	Reactome
	Circadian Clock	- Circadian rhythm	1.25E-07	KEGG
		- Circadian Clock	2.07E-05	Reactome
		- Exercise-induced Circadian Regulation	5.45E-05	Wikipathways
		- Circadian clock tutorial CGrove	0.000271	Wikipathways
		- Diurnally Regulated Genes with Circadian Orthologues	0.00113	Wikipathways
	Digestive system	- SREBF and miR33 in cholesterol and lipid homeostasis	1.60E-05	Wikipathways
		- Lipid digestion, mobilization, and transport	1.96E-05	Reactome
		- Bile secretion	0.000113	KEGG
		- Statin Pathway	0.00185	Wikipathways
		- Fat digestion and absorption	0.00885	KEGG

	Gene expression (Transcription)	-	Nuclear Receptor transcription pathway	0.000874	Reactome
		-	Nuclear receptors in lipid metabolism and toxicity	0.00436	Wikipathways
		-	Nuclear Receptors	0.00992	Wikipathways
	Metabolism	-	Trafficking of dietary sterols	1.82E-05	Reactome
		-	mevalonate pathway I	0.000803	MouseCyc
		-	Cholesterol Biosynthesis	0.00185	Wikipathways
		-	Terpenoid backbone biosynthesis	0.0033	KEGG
		-	Cholesterol biosynthesis	0.00399	Reactome
		-	Lipoprotein metabolism	0.00436	Reactome
		-	superpathway of cholesterol biosynthesis	0.00474	MouseCyc
		-	Retinol metabolism	0.00885	Wikipathways
	Transport of small molecules	-	Transmembrane transport of small molecules	0.00905	Reactome
		-	ABCA transporters in lipid homeostasis	1.20E-05	Reactome
		-	ABC-family proteins mediated transport	0.000227	Reactome
		-	ABC transporters	0.000659	KEGG
14 days	Circadian Clock	-	Circadian rhythm	5.00E-07	KEGG
		-	Exercise-induced Circadian Regulation	4.33E-06	Wikipathways
		-	Circadian clock tutorial CGrove	7.82E-05	Wikipathways
		-	Diurnally Regulated Genes with Circadian Orthologues	0.000178	Wikipathways
		-	Circadian Clock	0.000402	Reactome
	Gene expression (Transcription)	-	Nuclear Receptor transcription pathway	0.000137	Reactome
		-	Generic Transcription Pathway	0.00231	Reactome
		-	Nuclear Receptors	0.00298	Wikipathways
21 days	Circadian clock	-	Exercise-induced Circadian Regulation	0.000956	Wikipathways
		-	Circadian clock	0.00218	KEGG
		-	The canonical retinoid cycle in rods (twilight vision)	0.0042	Reactome
		-	Diurnally Regulated Genes with Circadian Orthologues	0.00915	Wikipathways

Gene expression	-	Nuclear Receptor transcription pathway	0.000634	Reactome
(Transcription)	-	Nuclear Receptors	0.00376	Wikipathways
Immune system	-	Cell adhesion molecules (CAMs)	0.0071	KEGG

IV- Discussion

The present study showed the capacity of E171 to contribute to CRC development in a Tg $CAC^{Tg/Tg}$;$APC^{580S/+}$ mouse model. The Tg model is more similar to the human situation due to the loss of Apc gene. Both the numbers of mice bearing tumours as well as the average number of these tumours in the colon were increased as compared to controls. These results are in line with a previous study in a chemically induced CRC murine model with AOM/DSS (11). The effects of E171 in the Tg mice on tumour formation are less pronounced compared to the effects of E171 in the AOM/DSS model (11) but confirm the capacity of E171 to increase incidence and number of tumours in colon. This Tg model is therefore suitable to further explore the effects of E171 on CRC development and the molecular mechanisms involved.

The hypothesis regarding the mechanisms of enhancement of CRC development after E171, that we based on our previous studies (13,14), states that modulation of gene expression causes changes in signal transduction and oxidative stress, that may be associated with inflammation and DNA damage, impairment of the immune system, and eventually enhance the risk of CRC. Gene and pathway analyses showed that the gene expression changes confirmed our hypothesis (Table 1). At day 2, 7, 14, and 21, genes and pathways related to signal transduction were identified. Increasing evidence of the functionality of GPCR genes in the development of cancer; their overexpression contributes to cancer proliferation, metastasis, survival, migration, and angiogenesis by being activated by circulating or locally produced ligands (27,28) has emerged. Additionally, the modulation of the immune system by GPCR have been observed in several studies and show an interconnection between GPCR and TLR, cytokine receptors, integrins, and lymphocytes trafficking and motility (29,30). Signalling genes were also modulated in the colon of normal BALB/c and CI mouse models, after exposure to 5 mg/kg_{bw}/day E171 for 2, 7, 14, and 21 days (13,14), including the modulation of 5 identical genes involved in gastric cancer (Bcl6b) (31), breast cancer (Esr1; also present after FDR correction in Tg model) (32), and colorectal cancer (Sox9, Cdkn1a and Hes1; also present after FDR correction in Tg model) (33-35). Moreover, 2 cancer related genes with significant changes in mRNA levels were identified between the CI and the Tg mouse models with Edn2 (also significant after FDR correction in CI model) and Ptgs2 involved in CRC (36) and a potent gene involved in CRC (37) respectively. In common between the exposure in the normal BALB/c and the Tg mouse models, other identical genes involved in cancer, cell cycle, gene expression (transcription), and encoding for transcription factors were modulated. The common genes related to cancer process were 1 frizzeld and 1

histone genes. In addition, one poly(a) polymerase γ gene was upregulated in both models and involved in transcription factors. Furthermore, in the current study, cancer pathways were observed at day 2, 14, and 21 with 12, 6, and 9 DEG respectively. In addition to cancer pathways, cell cycle and disease pathways were observed. The modulation of genes involved in cancer (including CRC), cell cycle, and disease indicate one of the mechanisms by which E171 exposure may increase CRC risk.

The expression of genes involved in the immune system was also modulated after E171 exposure. From 2 to 21 days, gene expression changes were identified in the innate immune system with genes involved in complement, TLR, Fc fragment, and MHC class I presentation. The gene expression in the adaptive immune system was mostly affected in CAMs genes after 21 days of exposure. Additionally, gene expression changes related to the adaptive immune system were also found related to MHC class II presentation, TCR signalling and co-stimulation by the CD28 gene family. The cytokine signalling gene expression was also modulated from 2 to 21 days with a large majority of the DEG being up-regulated. Other markers of modulation of the immune system and inflammation were observed with a down-regulation of interleukin genes and tumour necrosis factors after 2, 7, and 14 days and up-regulation after 21 days. A few of these genes were also present after FDR correction. These results are in line with previous findings where E171 was shown to induce a shift in the Th1/Th17 balance in the immune system as well as an impairment of the intestinal homeostasis after oral exposure in rats of 10 mg/kg_{bw}/day of E171 for 1 week (12). In addition, gene expression changes in the immune system were also observed in normal BALB/c and CI mouse models, after exposure to 5 mg/kg_{bw}/day E171 for 2, 7, 14, and 21 days (13,14). In line with this study, 3 genes in the complement system were commonly down-regulated and one was up-regulated only in the Tg model and down-regulated in the normal BALB/c and CI models. In addition, genes involved in TLR cascade and leucine rich domain receptors were also commonly modulated. We hypothesise that oral exposure to E171 induces gene expression changes indicating a dysregulation of the innate and adaptive immune system as well as cytokine signalling. This dysregulation includes a down-regulation of HLA genes, which eventually would allow tumour cells to evade the immune system and develop further.

Inflammation might be a consequence of the modulation of the immune system and oxidative stress. The latter may also lead to DNA damage. From 2 days of exposure, genes and pathways related to oxidative stress response were modulated like Tnfaip6, encoding for a Tnf-α protein, Mapk genes, and Vitamin D metabolism. Comparable observations were made after 21 days of exposure. One marker of inflammation, Tnfaip6,

was also modulated in normal BALB/c and CI mouse models, after exposure to 5 mg/kg_{bw}/day E171 for 2, 7, 14, and 21 days (13,14). In all experiments, this gene was down-regulated which is also in line with a previous CRC mouse experiment in which reduction of Tnf-α protein was observed after oral exposure of 5 mg/kg_{bw}/day of E171 in combination with AOM/DSS (11). Other markers of inflammation were commonly modulated like Il-33 or Aif1l as well as vitamin D metabolism. In addition, oxidative stress related genes were also commonly modulated in CI and Tg models with prostaglandin genes, vitamin D genes, and Mapk genes. Modulation of Mapk genes after exposure to TiO_2 NPs in mice was already observed and suggested to be a consequence of oxidative stress which would result in an increase of plasma glucose (38). One gene (Igf2bp1) related to insulin events was also up-regulated in the CI and Tg models. DNA damage and DNA repair related changes were identified from 2 to 21 days of exposure, also after FDR correction. A majority of these genes were up-regulated indicating that the mechanism of DNA repair has been activated. These results are in line with previous studies on TiO_2 NPs exposure where DNA damage was found in other tissue types such as liver, red blood cells, bone marrow, and kidney after oral exposure from 40 to 2000 mg/kg_{bw}/day for 5 to 7 days (39-41).

A summary of the biological processes associated with affected genes after oral exposure to E171 in normal BALB/c mice (13), in the CI mouse model (14) and in the Tg mouse models described herein is presented in Figure 4. Twenty biological processes were in common in all 3 different experimental conditions: DNA repair, metabolism, immune system (including the adaptive, the innate immune system, and MHC class I genes), signalling, cancer signalling, metabolism of proteins, oxidative stress, transport of molecules, bone development, neuronal response, vitamin, Cyp genes, transcription factors, insulin metabolism, MAPK, prostaglandin, inflammation, and disease. In addition, 3 biological processes were in common between the normal BALB/c and the Tg mouse models (gene expression (transcription), metabolism of RNA, and cell cycle) and 7 were in common between the CI and the Tg mouse models (digestive system, bile metabolism, translocation, haemostasis, extracellular matrix organisation, biotransformation of compounds, and muscle contraction). Specific effects only observed in the Tg model were circadian clock and endocrine system. Specific effects only observed in the normal BALB/c mice were Ucp genes and calcium mobilisation. One specific biological process was observed only in the CI model: collagen formation.

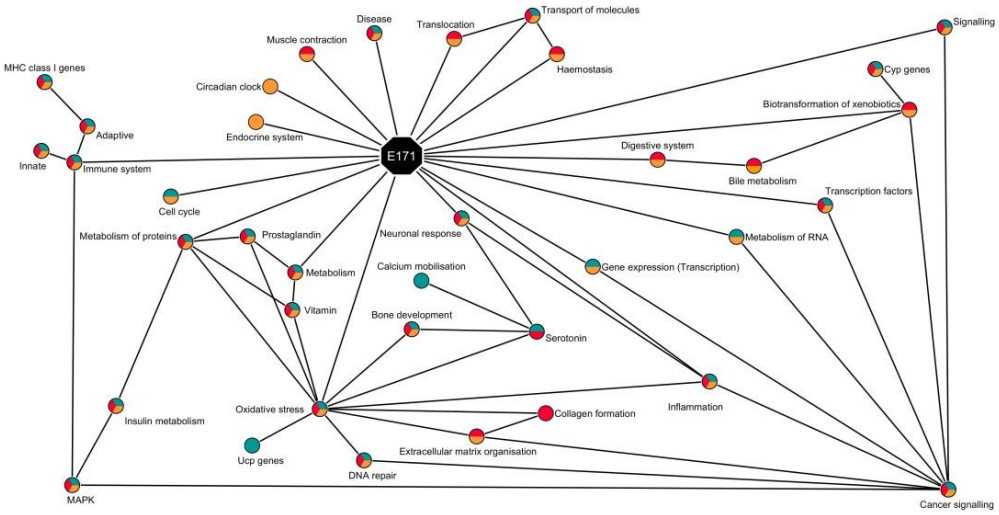

Figure 4: Network summarizing the different biological processes affected after exposure of E171 in normal BALB/c mice, CI and Tg mouse models.
Each colour represents a mouse model. Blue is the for the normal BALB/c mice, red is for the CI mouse model, and orange is for the Tg mouse model.

In summary, the gene expression profiles indicate which biological processes are affected by E171 observed in this study confirm previous findings, and suggest that E171 contributes to development of cancer by modulating genes involved in oxidative stress as well as genes involved in DNA damage and DNA repair implying the presence of DNA damage. In addition, parallel or as a consequence, the immune system appears to be impaired as indicated by modulation of genes related to the innate immune system, up-regulation of cytokine genes, and down-regulation of HLA genes. Dysregulation of the immune system may allow tumour cells to evade the immune system. In addition, cancer related genes were modulated. Recent studies have shown that genes involved in signal transduction, like GPCR genes, have a functional role in cancer development e.g. CRC, breast, head and neck, pancreatic, and prostate cancers and in modulation of the immune system. The combination of these effects may lead to the enhancement of tumour development as seen in the current tumour development study as well as in the previous study performed by our group (11).

References

1. Globocan (2012) CANCER FACT SHEETS: COLORECTAL CANCER.
2. Dorier, M., Beal, D., Marie-Desvergne, C., Dubosson, M., Barreau, F., Houdeau, E., Herlin-Boime, N., and Carriere, M. (2017) Continuous in vitro exposure of intestinal epithelial cells to E171 food additive causes oxidative stress, inducing oxidation of DNA bases but no endoplasmic reticulum stress. *Nanotoxicology*, 1-54.
3. Dudefoi, W., Moniz, K., Allen-Vercoe, E., Ropers, M.H., and Walker, V.K. (2017) Impact of food grade and nano-TiO2 particles on a human intestinal community. *Food Chem Toxicol*, **106**, 242-249.
4. Yang, Y., Doudrick, K., Bi, X.Y., Hristovski, K., Herckes, P., Westerhoff, P., and Kaegi, R. (2014) Characterization of Food-Grade Titanium Dioxide: The Presence of Nanosized Particles. *Environmental science & technology*, **48**, 6391-6400.
5. Weir, A., Westerhoff, P., Fabricius, L., Hristovski, K., and von Goetz, N. (2012) Titanium dioxide nanoparticles in food and personal care products. *Environmental science & technology*, **46**, 2242-2250.
6. Lomer, M.C.E., Thompson, R.P.H., Commisso, J., Keen, C.L., and Powell, J.J. (2000) Determination of titanium dioxide in foods using inductively coupled plasma optical emission spectrometry. *Analyst*, **125**, 2339-2343.
7. Peters, R.J., van Bemmel, G., Herrera-Rivera, Z., Helsper, H.P., Marvin, H.J., Weigel, S., Tromp, P.C., Oomen, A.G., Rietveld, A.G., and Bouwmeester, H. (2014) Characterization of titanium dioxide nanoparticles in food products: analytical methods to define nanoparticles. *J Agric Food Chem*, **62**, 6285-6293.
8. Shi, H., Magaye, R., Castranova, V., and Zhao, J. (2013) Titanium dioxide nanoparticles: a review of current toxicological data. *Particle and fibre toxicology*, **10**, 15.
9. Venator (2018) Venator Materials PLC website.
10. IARC (2010) IARC MONOGRAPHS ON THE EVALUATION OF CARCINOGENIC RISKS TO HUMANS: Carbon Black, Titanium dioxide and Talc. **Volume 93**.
11. Urrutia-Ortega, I.M., Garduno-Balderas, L.G., Delgado-Buenrostro, N.L., Freyre-Fonseca, V., Flores-Flores, J.O., Gonzalez-Robles, A., Pedraza-Chaverri, J., Hernandez-Pando, R., Rodriguez-Sosa, M., Leon-Cabrera, S., Terrazas, L.I., van Loveren, H., and Chirino, Y.I. (2016) Food-grade titanium dioxide exposure exacerbates tumor formation in colitis associated cancer model. *Food Chem Toxicol*, **93**, 20-31.
12. Bettini, S., Boutet-Robinet, E., Cartier, C., Comera, C., Gaultier, E., Dupuy, J., Naud, N., Tache, S., Grysan, P., Reguer, S., Thieriet, N., Refregiers, M., Thiaudiere, D., Cravedi, J.P., Carriere, M., Audinot, J.N., Pierre, F.H., Guzylack-Piriou, L., and Houdeau, E. (2017) Food-grade TiO2 impairs intestinal and systemic immune homeostasis, initiates preneoplastic lesions and promotes aberrant crypt development in the rat colon. *Sci Rep*, **7**, 40373.
13. Proquin, H., Jetten, M.J., Jonkhout, M.C.M., Garduno-Balderas, L.G., Briede, J.J., de Kok, T.M., Chirino, Y.I., and van Loveren, H. (2018) Gene expression profiling in colon of mice exposed to food additive titanium dioxide (E171). *Food Chem Toxicol*, **111**, 153-165.
14. Proquin, H., Jetten, M.J., Jonkhout, M.C.M., Garduno-Balderas, L.G., Briede, J.J., de Kok, T.M., van Loveren, H., and Chirino, Y.I. (2018) Transcriptomics analysis reveals new insights in E171-induced molecular alterations in a mouse model of colon cancer. *Submitted*.
15. Xue, Y., Johnson, R., Desmet, M., Snyder, P.W., and Fleet, J.C. (2010) Generation of a transgenic mouse for colorectal cancer research with intestinal cre expression limited to the large intestine. *Molecular cancer research : MCR*, **8**, 1095-1104.
16. Terzic, J., Grivennikov, S., Karin, E., and Karin, M. (2010) Inflammation and colon cancer. *Gastroenterology*, **138**, 2101-2114 e2105.

17. Proquin, H., Rodriguez-Ibarra, C., Moonen, C.G., Urrutia Ortega, I.M., Briede, J.J., de Kok, T.M., van Loveren, H., and Chirino, Y.I. (2017) Titanium dioxide food additive (E171) induces ROS formation and genotoxicity: contribution of micro and nano-sized fractions. *Mutagenesis*, **32**, 139-149.
18. MacNicoll, A., Kelly, M., Aksoy, H., Kramer, E., Bouwmeester, H., and Chaudhry, Q. (2015) A study of the uptake and biodistribution of nano-titanium dioxide using in vitro and in vivo models of oral intake. *J Nanopart Res*, **17**.
19. Qiagen (2012) RNeasy Mini Handbook. *https://www.qiagen.com/us/resources/resourcedetail?id=14e7cf6e-521a-4cf7-8cbc-bf9f6fa33e24&lang=en*.
20. Agilent (2015) One-Color Microarray-Based Gene Expression Analysis. *http://www.agilent.com/cs/library/usermanuals/Public/G4140-90040_GeneExpression_OneColor_6.9.pdf*.
21. Reich, M., Liefeld, T., Gould, J., Lerner, J., Tamayo, P., and Mesirov, J.P. (2006) GenePattern 2.0. *Nature genetics*, **38**, 500-501.
22. Alonso, R., Salavert, F., Garcia-Garcia, F., Carbonell-Caballero, J., Bleda, M., Garcia-Alonso, L., Sanchis-Juan, A., Perez-Gil, D., Marin-Garcia, P., Sanchez, R., Cubuk, C., Hidalgo, M.R., Amadoz, A., Hernansaiz-Ballesteros, R.D., Aleman, A., Tarraga, J., Montaner, D., Medina, I., and Dopazo, J. (2015) Babelomics 5.0: functional interpretation for new generations of genomic data. *Nucleic Acids Res*, **43**, W117-121.
23. Smyth, G.K. (2005) Limma: linear models for microarray data. *Bioinformatics and computational biology solutions using R and Bioconductor*. Springer, pp. 397-420.
24. Kamburov, A., Stelzl, U., Lehrach, H., and Herwig, R. (2013) The ConsensusPathDB interaction database: 2013 update. *Nucleic Acids Res*, **41**, D793-800.
25. Herwig, R., Hardt, C., Lienhard, M., and Kamburov, A. (2016) Analyzing and interpreting genome data at the network level with ConsensusPathDB. *Nat Protoc*, **11**, 1889-1907.
26. Vuolteenaho, K., Koskinen, A., Kukkonen, M., Nieminen, R., Paivarinta, U., Moilanen, T., and Moilanen, E. (2009) Leptin enhances synthesis of proinflammatory mediators in human osteoarthritic cartilage--mediator role of NO in leptin-induced PGE2, IL-6, and IL-8 production. *Mediators Inflamm*, **2009**, 345838.
27. Dorsam, R.T., and Gutkind, J.S. (2007) G-protein-coupled receptors and cancer. *Nat Rev Cancer*, **7**, 79-94.
28. Lappano, R., and Maggiolini, M. (2012) GPCRs and cancer. *Acta Pharmacol Sin*, **33**, 351-362.
29. Lombardi, M.S., Kavelaars, A., and Heijnen, C.J. (2002) Role and modulation of G protein-coupled receptor signaling in inflammatory processes. *Crit Rev Immunol*, **22**, 141-163.
30. Cho, H., and Kehrl, J.H. (2009) Regulation of immune function by G protein-coupled receptors, trimeric G proteins, and RGS proteins. *Prog Mol Biol Transl Sci*, **86**, 249-298.
31. Xu, L.X., Li, X.X., Chu, E.S.H., Zhao, G.J., Go, M.N.Y.Y., Tao, Q., Jin, H.C., Zeng, Z.R., Sung, J.J.Y., and Yu, J. (2012) Epigenetic inactivation of BCL6B, a novel functional tumour suppressor for gastric cancer, is associated with poor survival. *Gut*, **61**, 977-985.
32. Widschwendter, M., Siegmund, K.D., Muller, H.M., Fiegl, H., Marth, C., Muller-Holzner, E., Jones, P.A., and Laird, P.W. (2004) Association of breast cancer DNA methylation profiles with hormone receptor status and response to tamoxifen. *Cancer research*, **64**, 3807-3813.
33. Abbas, T., and Dutta, A. (2009) p21 in cancer: intricate networks and multiple activities. *Nat Rev Cancer*, **9**, 400-414.
34. Lu, B.J., Fang, Y.H., Xu, J., Wang, L.P., Xu, F.Y., Xu, E.P., Huang, Q., and Lai, M.D. (2008) Analysis of SOX9 Expression in Colorectal Cancer. *Am J Clin Pathol*, **130**, 897-904.
35. Gao, F., Zhang, Y.Q., Wang, S.C., Liu, Y.Q., Zheng, L., Yang, J.Q., Huang, W., Ye, Y.F., Luo, W.R., and Xiao, D. (2014) Hes1 is involved in the self-renewal and tumourigenicity of stem-like cancer cells in colon cancer. *Sci Rep-Uk*, **4**.

36. Wang, R., Lohr, C.V., Fischer, K., Dashwood, W.M., Greenwood, J.A., Ho, E., Williams, D.E., Ashktorab, H., Dashwood, M.R., and Dashwood, R.H. (2013) Epigenetic inactivation of endothelin-2 and endothelin-3 in colon cancer. *International Journal of Cancer*, **132**, 1004-1012.
37. Cox, D.G., Pontes, C., Guino, E., Navarro, M., Osorio, A., Canzian, F., Moreno, V., and Bellvitge Colorectal Cancer Study, G. (2004) Polymorphisms in prostaglandin synthase 2/cyclooxygenase 2 (PTGS2/COX2) and risk of colorectal cancer. *Br J Cancer*, **91**, 339-343.
38. Hu, H., Li, L., Guo, Q., Jin, S., Zhou, Y., Oh, Y., Feng, Y., Wu, Q., and Gu, N. (2016) A mechanistic study to increase understanding of titanium dioxide nanoparticles-increased plasma glucose in mice. *Food Chem Toxicol*, **95**, 175-187.
39. Trouiller, B., Reliene, R., Westbrook, A., Solaimani, P., and Schiestl, R.H. (2009) Titanium dioxide nanoparticles induce DNA damage and genetic instability in vivo in mice. *Cancer research*, **69**, 8784-8789.
40. Shi, Z.Q., Niu, Y.J., Wang, Q., Shi, L., Guo, H.C., Liu, Y., Zhu, Y., Liu, S.F., Liu, C., Chen, X., and Zhang, R. (2015) Reduction of DNA damage induced by titanium dioxide nanoparticles through Nrf2 in vitro and in vivo. *Journal of Hazardous Materials*, **298**, 310-319.
41. Sycheva, L.P., Zhurkov, V.S., Iurchenko, V.V., Daugel-Dauge, N.O., Kovalenko, M.A., Krivtsova, E.K., and Durnev, A.D. (2011) Investigation of genotoxic and cytotoxic effects of micro- and nanosized titanium dioxide in six organs of mice in vivo. *Mutation research*, **726**, 8-14.

Chapter 5

Titanium dioxide food additive (E171) induces ROS formation and genotoxicity: contribution of micro and nano-sized fractions

Mutagenesis, October 2016, Volume 32, Issue 1, Pages 139-149
Corrigendum, Mutagenesis, August 2018, gey011

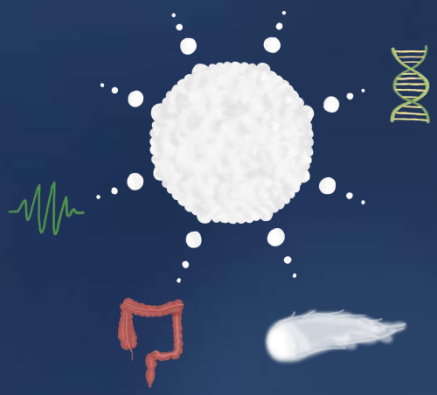

Héloïse Proquin,
Carolina Rodríguez-Ibarra,
Carolyn G.J. Moonen,
Ismael M. Urrutia Ortega,
Jacob J. Briedé,
Theo M. de Kok,
Henk van Loveren,
Yolanda I. Chirino

Abstract

Since 1969, the European Union approves food grade titanium dioxide (TiO_2), also known as E171 colouring food additive. E171 is a mixture of micro (MPs) and nano-sized particles (NPs). Previous studies have indicated adverse effects of oral exposure to E171, i.e. facilitation of colon tumour growth. This could potentially be partially mediated by the capacity to induce reactive oxygen species (ROS). The aim of the present study is to determine whether E171 exposure induces ROS formation and DNA damage in an *in vitro* model using human Caco-2 and HCT116 cells, and to investigate the contribution of the separate MPs and NPs TiO_2 fractions to these effects. After suspension of the particles in HBSS buffer and cell culture medium with either bovine serum albumin (BSA) or foetal bovine serum (FBS), characterization of the particles was performed by Dynamic Light Scattering (DLS), ROS formation was determined by electron spin/paramagnetic resonance (ESR/EPR) spectroscopy and DNA damage was determined by the comet and micronucleus assays. The results showed that E171, MPs and NPs are stable in cell culture medium with 0.05% BSA. The capacity for ROS generation in a cell-free environment was highest for E171 followed by NPs and MPs. Only MPs were capable to induce ROS formation in exposed Caco-2 cells. E171, MPs and NPs all induced single-strand DNA breaks. Chromosome damage was shown to be induced by E171, as tested with the micronucleus assay in HCT116 cells. In conclusion, E171 has the capability to induce ROS formation in a cell-free environment and E171, MPs and NPs have genotoxic potential. The capacity of E171 to induce ROS formation and DNA damage raises concerns about potential adverse effects associated with E171 and TiO_2 in food.

I- Introduction

Since 1969, the European Union approved the use of food grade titanium dioxide (TiO_2) known as E171 colouring food additive. Titanium dioxide (TiO_2) is a white pigment used as colouring agent in many products such as food and personal care products (1-4). E171 is used in food such as in salad dressing, gum, icing, cookies, and candies (5) and even though TiO_2 is sourced from rutile, anatase and brookite, the European Union allows E171 in the food only as anatase form (5). According to the European Union, E171 belongs to the group II: food colours authorised at *quantum satis* which means "no maximum level is specified and that it should be used at levels not higher than deemed necessary for the product" (5). In the U.S., the Food and Drug Administration (FDA) allows the food additive E171 as long as it does not exceed 1% by total weight of the product (6).

Inhalation studies with TiO_2 exposure have demonstrated adverse effects, including 8-OHdG DNA adduct formation and genotoxicity (7-11). In 2010, the International Agency for Research in Cancer (IARC) classified TiO_2 as possible carcinogen to humans (Group 2B) (12). For these reasons, concern about oral consumption of E171 has been raised (13-17).

E171 is a mixture of micro (MPs), 64%, and nano-sized particles (NPs), 36% (4) and the NPs proportion is expected to increase in the decades to come (18). NPs have a higher surface area than MPs allowing them to have more interaction with the cells, which in turn can induce reactive oxygen species (ROS) formation after internalization. The exposure of cells to particles can lead to oxidative stress as has been shown for other particles (19,20). Cellular oxidative stress induced by exposure to TiO_2 NPs could lead to potential non-selective DNA damage though the generation of the superoxide anion (21), the precursor of the highly reactive hydroxyl radical, which is a well-known potent mutagen that attacks DNA (22-24). MPs of TiO_2, can accumulate in lymphoid tissue after oral ingestion (25) and also in macrophages of human gut-associated lymphoid tissue (26). The nano-sized fraction is able to cause anaemia and genotoxicity by intragastric administration in a rat experimental model (27). In addition, we previously found that intragastric E171 administration enhanced the tumour formation, induced chemically by azoxymethane/dextran sodium sulphate (AOM/DSS), in colon of exposed mice (28). The cellular mechanism of damage after internalization of E171, MPs and NPs has not been established yet but ROS formation could contribute to the induction of cell damage. Therefore, we hypothesize that nano-sized and micro-sized fractions of E171 could have a different contribution in ROS formation and induction of DNA damage. To test our

hypothesis, we measured ROS formation induced by E171, TiO_2 MPs and NPs in cell-free conditions using electron spin/paramagnetic resonance (ESR/EPR) spectroscopy recognized as a 'gold standard' and state-of the art tool for detection and quantification of ROS and free radicals (29,30). This technique is particularly preferred in studying effect of E171 as photocatalytic properties of TiO_2 cause interference in fluorescent or chemiluminescent assays (31,32). Furthermore, we determined the DNA damage induced by these different types of particles by the comet and micronuclei frequency (MN) assays in colon-derived cell lines exposed to non-cytotoxic E171, TiO_2 MPs and NPs concentrations.

II- Materials and methods

II-1- TiO_2 particles properties

E171 was kindly donated by the Sensient Technologies Company in Mexico. TiO_2 microparticles (MPs) were customarily made by PlasmaChem with an average size of 535 nm characterized by TEM. TiO_2 nanoparticles (NPs) were purchased at Io-Li-Tec (Germany) and are 99.5% anatase with particles size of 10-25 nm with a specific surface area of 50-150 m^2/g according to manufacturer's information. All particles were sterilised at 121°C for 20 min prior use.

II-2- Dispersion of TiO_2 particles

TiO_2 particles (E171, NPs or MPs) were weighed into glass tubes and dispersed in 0.05% bovine serum albumin (BSA) Dulbecco's Modified Eagle's Medium (DMEM) (Sigma Aldrich), Hank's Balanced Salt Solution (HBSS) supplemented with Mg^{2+} and Ca^{2+} (Life Technologies, The Netherlands) or PBS at a concentration of 1 mg/mL. Particles stock suspensions were sonicated in a bath sonicator (Branson 2200, 40 KHz) for 30 minutes and further used to prepare the dilutions needed for exposure.

For the MN assay, one milligram of E171 particles was dispersed in medium with 10% fetal bovine serum (FBS) since 10% FBS is recommended for MN assays in order to avoid false positive results in cell cultures (33).

II-3- Characterization of TiO_2 particles with electron microscopy and Dynamic Light Scattering (DLS)

Scios DualBeam FIB/SEM (SEM, 20 KV, Holland) was used at different magnification from 50,000x for the MPs to 150,000x for E171 and NPs to evaluate the size and morphology of E171, MPs and NPs. All samples were spread on carbon tape and sputter-coated with gold before SEM analysis. The size of the particles was measured on several pictures by the software Image J, more than 100 particles were measured for each sample.

To characterize the hydrodynamic size distribution and the zeta potential of the TiO_2 particles (E171, NPs and MPs), a Malvern Nano ZS (Malvern Instruments, UK) dynamic light scattering (DLS) instrument equipped with a 633 nm He-Ne laser was used. Two representative dispersions 0.001 and 1 mg/mL (corresponding to 0.143 and 143 µg/cm², respectively) dispersed in 0.05% bovine serum albumin (BSA) Dulbecco's Modified Eagle's

Medium (DMEM) or Hank's Balanced Salt Solution (HBSS) supplemented with Mg^{2+} and Ca^{2+} or Mc. Coy +10% FBS were prepared in duplicate and transferred in a disposable folded capillary (DTS 1060, Malvern Instruments). Measurements were performed in triplicate at 25°C, with equilibration time set at 0 seconds, a viscosity at 0.8872cP and a refracting index of 1.330. The zeta potential indicates the potential stability of the colloidal system which is in our study solid particles dispersed in liquid (0.05% BSA medium, 10% FBS medium or buffer). When the zeta potential have large negative or positive potential (±30 mV), they will tend to repel each other where there is no tendency to agglomerate. In contrast, if the particles have low zeta potential values, there is no force to prevent the particles attaching to each other and agglomerating.

II-4- Cell culture of colon Caco-2 cells

The human colon carcinoma cell line Caco-2 was obtained from the American Type Culture Collection (ATCC® HTB-37™) and cultured in DMEM supplemented with glutamine, glucose, sodium pyruvate, penicillin/streptomycin and 10% heat-inactivated FBS. Cells were grown and maintained at 37°C in a humidified incubator containing 5% CO_2. For experiments, Caco-2 cells were seeded in 21 cm^2 culture dishes and grown for three days to reach 80-100% confluency in 10% FBS medium in order to obtain ± 3.10^6 cells/dish.

II-5- Cell culture of colon HCT116 cells

Due to the heterogeneity and genetic instability of the Caco-2 cells, we used the recommended HCT116 cell line for MN assays, which has genomic stability (34). The human colon adenocarcinoma (HCT116) cell line was obtained from the American Type Culture Collection (ATCC® CCL-247™). HCT116 cells were incubated in a 37°C and 5% CO_2 atmosphere and maintained in McCoy 5a modified medium with 1.5 mM L-Glutamin and 2.2 mg/ml sodium bicarbonate (In vitro, no. cat. ME-042) supplemented with 10% FBS (Biowest, no. cat. US1520).

II-6- Cytotoxicity of TiO_2 particles to Caco-2 cells

Prior to exposure, colon Caco-2 cells were cultured for 3 days in 10% FBS medium and thereafter washed twice with HBSS. Then, cells were exposed to a range of concentrations E171, MPs or NPs (0.143 – 143 µg/cm² which equivalents to 0.001 – 1 mg/mL) dispersed in 0.05% bovine serum albumin (BSA)-medium for 24 hours. Three different viability/cytotoxicity tests were performed: lactate dehydrogenase (LDH), Thiazolyl blue tetrazolium bromide (MTT) and Trypan Blue assays, 2 of them showed interaction between the test and the particles. Then, the viability of the cells was assessed

with Trypan blue assay. After 24 hours, cells were washed twice with HBSS followed by trypsinization of the cells and counted with an automatic cell-counter (Logos Biosystems) where Trypan blue stain (0.4%) was added to the cell suspension (1:1). Non-cytotoxic concentrations of E171, TiO_2 NPs or MPs were selected based on viability (>80%) of the cells. Triton-X-100 (Sigma-Aldrich) (1%) was added to the cells as positive control.

II-7- Cytotoxicity of E171 to HCT116 cells

For HCT116 cells, the viability was assessed by Trypan blue assay. After 24 hours of exposure to 0, 5, 10, 50 and 100 µg/cm^2 (0, 50, 100, 500 and 1,000 µg/mL, respectively) of E171, cells were washed twice with HBSS followed by trypsinization and cells were counted with a Neubauer chamber. Living cells were identified by adding Trypan blue stain (0.4%) to 10 µl of cell suspension (1:2).

II-8- ROS formation assessed by electron spin resonance (ESR) spectroscopy

ROS quantification in acellular conditions

Particles were dispersed and stock suspensions of 1 mg/mL were serially diluted in 0.05% BSA medium, HBSS supplemented with Ca^{2+} and Mg^{2+} or PBS (1x). To assess the capacity of ROS formation by titanium dioxide particles, suspensions were incubated in a CO_2 incubator at 37°C with 50 mM DMPO for 30 minutes. Hydrogen peroxide (1mM) was added to particles suspensions to assess the reactions which could take place in an alkali environment. After incubation, homogenized particles suspension was taken up into a 100 µL glass capillary. Radical formation was measured by ESR spectroscopy.

ROS quantification in exposed cell cultures

The experiment was performed according to the protocol of Nymark et al. (35). In brief, Caco-2 cells (passage 24-32) were cultured as explained previously. Particles were dispersed and stock suspensions of 1 mg/mL were serially diluted in dispersion suspensions to obtain non-cytotoxic concentrations of 0.143 and 1.43 µg/cm^2 (which equivalents to 0.001 and 0.01 mg/mL, respectively). Prior exposure, cells were washed twice with HBSS supplemented with Ca^{2+} and Mg^{2+}. Cells were exposed to non-cytotoxic concentrations of E171, NPs or MPs in a CO_2 incubator at 37°C for several exposure times (30 minutes, 1, 2, 4, 6 and 24 hours, respectively). The maximum signal was seen at 1 hour exposure. In addition, H_2O_2 was added at a non-cytotoxic concentration (20 µM, according to cytotoxicity tests by Briede et al. (36) to cells together with particles suspensions to mimic an inflammatory environment. Thirty minutes before ending the exposure, spin trap DMPO (50 mM) was added to the cells and incubated at 37°C. This incubation time was based and tested for TiO_2 on previous time-course experiments performed by Hebels

et al. where at 30 minutes the highest DMPO-radical adduct concentration generation was found (37). After exposure, cells were harvested by scraping and taken up into a 100 µL glass capillary and radical formation was measured by ESR spectrometry.

The same protocol was used for a co-exposure with AOM was added at a non-cytotoxic concentration (20 µg/mL) to the cells together with particles suspensions. The concentration AOM was confirmed as non-cytotoxic with Trypan blue viability tests (data not shown).

ESR spectroscopy measurements

Radical formation in response to non-cytotoxic concentrations of TiO_2 was measured by ESR spectroscopy. Before use, DMPO was purified according to the protocol of Hebels et al. (37). Stock solutions of DMPO were tested on forehand on •OH formation by H_2O_2 and $FeSO_4$ (0.75 mM) to verify the activity of DMPO (data not shown). After sealing, the capillary was immediately placed in the resonator in the ESR spectrometer. All measurements were performed in the dark. ESR spectra were recorded with the same conditions as Nymark et al. and Hebels et al. (35,37).

II-9- DNA damage assessment in Caco-2 cell cultures by the Comet Assay

Cells were grown for 3 days to reach confluency of 80-90% and were washed twice with HBSS before exposure. Cells were exposed to non-cytotoxic concentrations E171, NPs or MPs in a CO_2 incubator at 37°C for 24 hours with or without 20 µg/mL azoxymethane (AOM) (Sigma Aldrich), a genotoxicant. Each condition was assessed in duplicate. As a positive control, cells were exposed for 30 minutes to 200 µM H_2O_2. The assay was performed as described by Hebels et al (38). Comet appearances were analysed using fluorescence microscope (Zeiss, Germany) at 400x magnification using immersion oil (Supplementary Figure 2). A total of randomly selected 50 cells were analysed per slide per experiment. Comet image analysis software program was used for quantification of DNA damage. Comet tail and intensity were measured by using Comet IV software. The median tail intensity was used as DNA damage indicator. All experiments were made with 4 biological replicates and in duplicate, each duplicate was put on 2 slides (n=16).

II-10- Chromosome damage in HCT116 cells assessed by MN assay

HCT116 cells were seeded 150,000 cells on 6 cm^2 coverslips. Cells were treated with 0, 5, 10, 50 and 100 µg/cm^2 (0, 50, 100, 500 and 1,000 µg/ml respectively) of E171 for 24 hours. MN assay cannot be assessed in cell cultures exposed to 100 µg/cm^2 or more since agglomerates interfere with MN identification. MN assay was carried out as

described by Fenech (39). Briefly, to block the cytokinesis and to obtain binucleated cells, after 24 hours of treatment, the medium with E171 was removed and cells were washed with PBS and treated with 4.5 µg/ml of cytochalasin B (Cyt-B; Sigma-Aldrich, no. cat. C6762) for 24 hours. After treatment with Cyt-B, the cells were fixed with 1 ml of paraformaldehyde 3% for 1 hour and stained with Hoescht 1:200 (Thermo Scientific, no. cat. 62249) at 37°C and constant agitation for 1 hour. The slides were scored using an Axio Vert. A1 Carl Zeiss fluorescence microscope at 1,000x magnification, under oil immersion. To calculate the frequency of binucleated cells with MN and the total number of MN, 1,000 binucleated cells were scored and classified according to their number of micronucleus. The frequency was expressed as the percentage of binucleated cells with micronucleus in 1,000 binucleated cells. All experiments were made per triplicate.

II-11- E171 interaction with kinetochore poles

HCT116 cells were seeded ($1.5x10^5$ cells) on cover slips and a stock of E171 particles were resuspended in cell culture medium supplemented with FBS 10%. Cell cultures were exposed to final concentrations of 5, 10, 50 and 100 µg/cm² for 24 h. After exposure, cells were washed with PBS, fixed with 2% paraformaldehyde and permeabilized with a solution containing 0.1% Na-Citrate and 0.1% Triton. Nonspecific binding sites were blocked by incubating cells with 5% BSA and then the cells were stained with a 1:200 dilution of mouse monoclonal anti-α-tubulin antibody and DAPI (1 µg/ml) followed by a 1:150 dilution of anti-mouse FITC conjugated IgG antibody. Three independent experiments were performed and three random fields were analysed in each slide using an Axio Vert. A1 Carl Zeiss fluorescence microscope at 1,000x magnification, under oil immersion.

II-12- Data analysis

Each (cellular) experiment was performed with three biological replicates with each unique sample in duplicate. Results were expressed as mean ± standard error (SE) except for cytotoxicity results which were expressed as mean ± standard deviation (SD). Differences between groups were evaluated using Analysis of variance (ANOVA) except for cytotoxicity assay results which were evaluated using unpaired two-tailed Student's T-test. For the MN assay, four independent assays were performed and the data were analysed by one-way analysis of variance (ANOVA) and the groups were compared to control by Dunnet's test. Differences were considered significant with a p value <0.05.

III- Results

III-1- Particle characterisation

SEM characterization

The SEM characterisation revealed that the titanium dioxide powder consists of particles of different sizes and that it contains slightly to rounded particles (Figure 1). The characterisation of the primary size of the particle was performed from several pictures of each particle. The manufacturer's information on the NPs was verified, measuring a range from 10 to 30 nm (while the manufacturer indicated 15-25 nm) and on the MPs (measuring above 100 nm as indicated by the manufacturer). Furthermore, the characterization made by Weir et al. on the E171 can be confirmed, because a proportion of 39% NPs and 61% MPs was found while Weir et al. found 36% NPs and 64% MPs (4). To finish, the similarity of the three-dimensional structures of E171, TiO_2 NPs and MPs were confirmed by SEM. Agglomeration and aggregation can be observed on the different images. Agglomerates/aggregates of tens to hundreds of nanometres were formed with surface irregularities which correspond to the single particles.

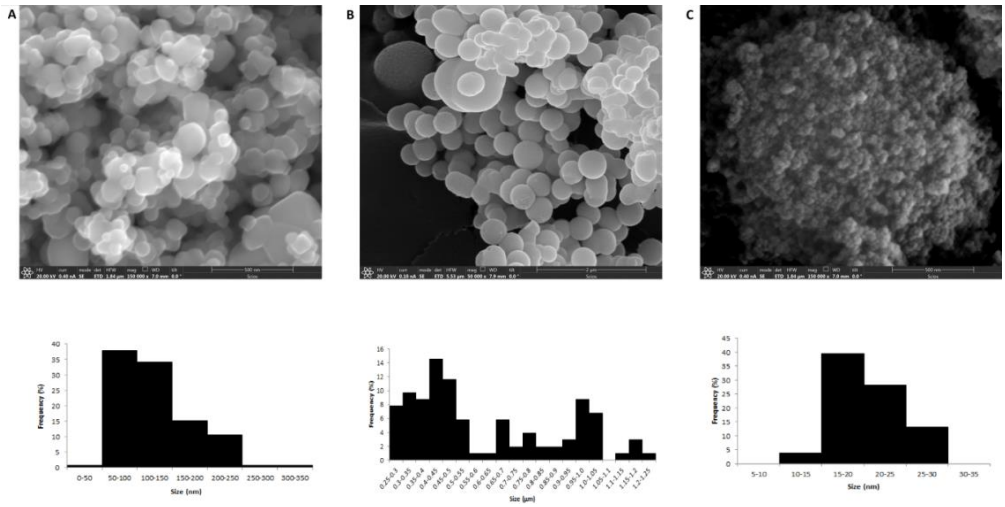

Figure 1: Representative scanning electron microscopy (SEM) of E171 particles.
A: E171, B: TiO_2 MPs, C: TiO_2 NPs.
Under each picture histogram of the characterisation of the particle is shown.

Characterisation by DLS

Hydrodynamic size and zeta potential of E171 were characterised by using a Malvern Nano ZS Dynamic Light Scattering (DLS) instrument. Particles were then dispersed in medium DMEM + 0.05% BSA , in HBSS buffer and in Mc. Coy + 10% FBS at two different concentrations: 0.001 and 1 mg/mL (0.143 and 143 µg/cm² respectively). Even though some samples have a high PI index, the presence of serum reduces the agglomeration of the particles after 30 min of sonication (40 kHz; Table 1). The stock suspension of 1 mg/mL has the lowest hydrodynamic size at 316.8 ± 282.4 dynamic nm (d.nm) with E171 in Mc Coy + 10% FBS and the highest size at 3085.00 ± 187.82 d.nm with E171 in HBSS. This can also be observed for the MPs at a concentration of 1 mg/mL and the NPs at a concentration of 0.001 mg/mL. This shows the importance of serum to improve the dispersion and the stability of the suspension. There is a significant size difference between the presence and the absence of serum at a concentration of 1 mg/mL: without added serum (HBSS), the average hydrodynamic size of the particles is higher than 1000 d.nm for all samples whereas with serum it starts at 669.62 ± 17.40 d.nm. All sizes are in the micro range except in HBSS which has its first size at 5.34 d.nm. The results of the 1.10^{-3} mg/mL show 2 to 3 different sizes depending on the type of particle and suspension. All sizes of MPs and NPs are in the micro range. Surprisingly, E171 has the lowest hydrodynamic size in DMEM (316.8 ± 282.4 d.nm) compared to MPs (1385.83 ± 38.85 d.nm) and NPs the highest size (1942.17 ± 61.12 d.nm).

Zeta potential

The results obtained by the zeta potential are also included in Table 1, there is a significant difference between the dispersion in with medium with serum and buffer (HBSS) except at a concentration of 0.001 mg/mL. As, in total, three different concentrations were tested, this difference between the buffer and the medium can be explained by the addition of serum even at low concentrations (0.05%) leads to more colloidal stability which results in a decrease of aggregation and agglomeration of the particles hence to a slightly more stable suspensions. However, the zeta potential values are between -30 mV and +30 mV which indicate that the suspensions remain unstable (40,41).

Table 1: DLS measurements; size in intensity (d.nm) of the different particles (E171, MPs and NPs) dispersed in DMEM with 0.05% BSA or in HBSS supplemented with Ca^{2+} and Mg^{2+} or FBS and zeta potential results of E171, MPs and NPs with the same conditions as DLS.

Dispersant	Sample	Concen-tration (mg/mL)	Peak 1 (d.nm)	Peak 2 (d.nm)	Peak 3 (d.nm)	Peak 4 (d.nm)	PI	Zeta potential (mV)
HBSS	E171	1	>1000	-	-	-	0.23 ± 0.03	-4.39 ± 0.12
		0.01	978.53 ± 59.59[2]	-	-	-	0.71 ± 0.06	-6.28 ± 1.56[2]
		0.001	5.34[1]	644.40[1]	>1000[1]	-	0.76 ± 0.11	-15.03 ± 1.62
	MPs	1	>1000	-	-	-	0.14 ± 0.02	-5.62 ± 0.09
		0.001	639.43 ± 322.95[2]	>1000	-	-	0.76 ± 0.06	-6.95 ± 0.62
	NPs	1	>1000	-	-	-	0.15 ± 0.05	-6.08 ± 0.09
		0.001	>1000[2]	-	-	-	0.69 ± 0.15	-8.02 ± 0.69
DMEM +0.05% BSA	E171	1	669.62 ± 30.13	-	-	-	0.30 ± 0.02	-12.97 ± 0.29
		0.001	354.48 ± 65.66	1045.13 ± 272.82	>1000	-	0.57 ± 0.03	-12.78 ± 0.52
	MPs	1	1385.83 ± 38.85	-	-	-	0.17 ± 0.04	-14.10 ± 0.56
		0.001	1089.10 ± 158.93[2]	>1000	-	-	0.67 ± 0.09	-13.40 ± 0.44
	NPs	1	>1000	-	-	-	0.12 ± 0.03	-13.12 ± 0.44
		0.001	1212.5 ± 332.5[2]	-	-	-	0.75 ± 0.10	-10.96 ± 0.98
	Control		15.34 ± 2.58[2]	165.4 ± 38.5[2]	680.25 ± 10.55[2]	>1000[2]	0.60 ± 0.09	-6.18 ± 1.35
Mc Coy +10% FBS	E171	1	316.8 ± 282.4	>1000	-	-	0.39 ± 0.07	-12.56 ± 8.3
		0.01	296.3 ± 367.8	226.9 ± 310.3	23.9	3.1	0.79 ± 0.21	-11.9 ± 0.55
		0.001	70.78 ± 0.37	-	-	-	0.26 ± 0.01	-12.56 ± 0.06

[1] One sample PI>0.7 [2] One or more reads PI>0.7

III-2- Cytotoxicity of E171, MPs and NPs

E171 reached its cytotoxic concentration at 14.3 µg/cm² (0.1 mg/mL) after 24h of exposure and the viability of Caco-2 decreased 27%. The exposure to 143 µg/cm² induced a decrease of 73% in cell viability, as shown in Supplementary Figure 1, the cell counter differentiates the alive cells from the dead ones even with this high concentration, interaction of the test with the particles is not responsible of this low cell viability. Exposure to 143 µg/cm² of MPs and NPs induced a decrease of 33% and 48.4% respectively (Figure 2). Further studies with E171 were performed at non-cytotoxic concentrations of 1.43 and 14.3 µg/cm². HCT116 cells did not show signs of cytotoxicity up to the concentration of 100 µg/cm² (Figure 3).

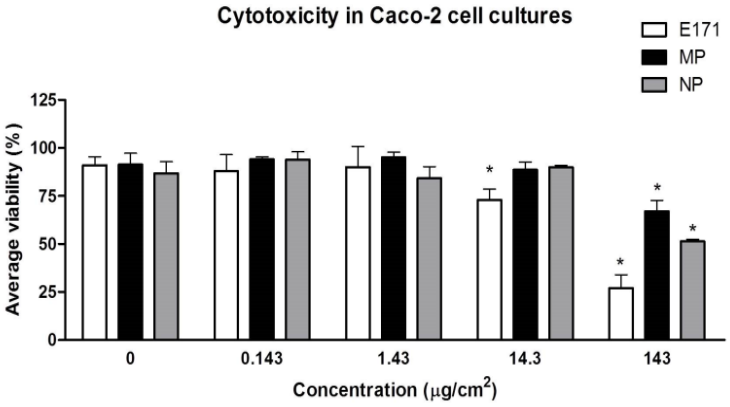

Figure 2: Cytotoxicity in Caco-2 cells after 24 h exposure to E171, MPs and NPs in DMEM plus 0.05% BSA measured by trypan blue viability test. Statistically significant changes and differences are indicated by an asterisk (*p< 0.05, mean ± SD). Three independent experiments were performed.

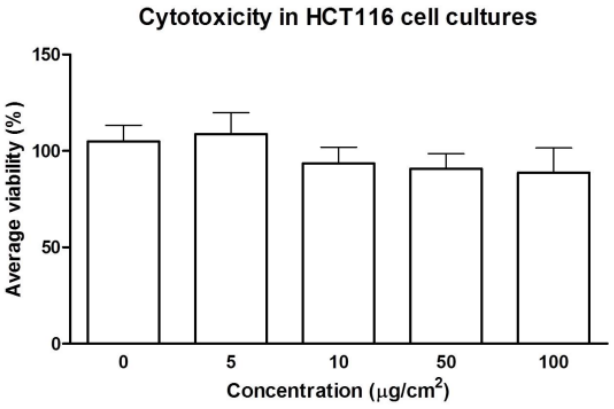

Figure 3: Cytotoxicity in HCT116 cells after 24 h exposure to E171 measured by trypan blue viability test. There are no statistically significant changes and differences. Three independent experiments were performed.

III-3- ROS quantification under cell-free conditions

The capacity of the particles to produce ROS under cell-free conditions was investigated (Figure 4). Suspensions of E171 particles were prepared in HBSS prior to testing. The particles were also tested in medium with 0.05% BSA, which showed no ROS production (data not shown). This can be attributed to the presence of proteins present in BSA, which form a protein corona that scavenges ROS. E171 had the highest capacity to produce ROS in suspensions with the concentration of 143 µg/cm² (Figure 4) followed by NPs in the presence of H_2O_2. At a concentration of 14.3 µg/cm², NPs induce significant amounts of ROS compared to control. However, MPs do not generate ROS (Figure 4). The presence of H_2O_2 does not enhance the formation of ROS by the particles.

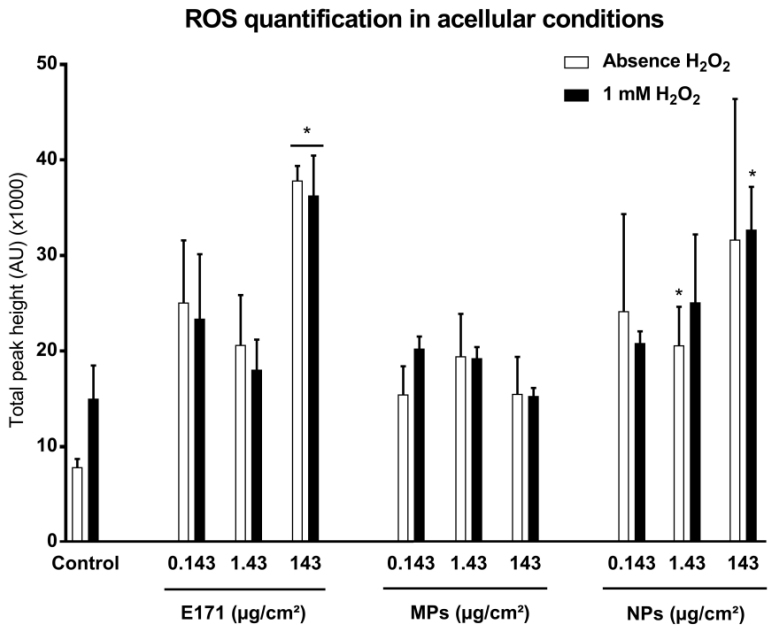

Figure 4: Intensity of cell-free radical formation with various concentrations E171, microparticles (MPs) and nanoparticles (NPs) in HBSS in presence (1 mM) or absence of H_2O_2 shown on x-axis.
Y-axis represents the average total peak height of obtained ESR spectra calculated per sample. Results include background levels. *p<0.05: significant difference compared to the control (mean±SE). No significant difference was found when the presence and absence of H_2O_2 were compared. Three independent experiments were performed.

III-4- ROS quantification in Caco-2 cells exposed to particles

As previously explained, HBSS buffer was chosen as dispersion suspension for the measurement of ROS since no ROS formation was detected when particles were dispersed in 0.05% BSA medium. First, a time course was performed which showed that the best exposure time to observe ROS formation is 1h (data not shown). Figure 5 shows the peak height calculated from the DMPO-OH signal obtained from cellular radical formation. Caco-2 cells exposed to MPs at a concentration of 1.43 µg/cm^2 produce significant amounts of ROS. Indeed these results were the most stable ones with a lower standard deviation. The ESR machine is very sensitive, the standard deviation can differ due to biological differences with the presence of cells. A significant level of ROS formation was also determined when cells were exposed to MPs at the lowest non-cytotoxic concentration (1.43.10^{-1} µg/cm^2) of MPs co-exposed to H_2O_2. Either with or without H_2O_2, no significant ROS formation was found after E171 or NPs exposure as compared to the control. In a cellular environment, only MPs were capable to induce ROS production, whereas E171 and NPs did not induce ROS.

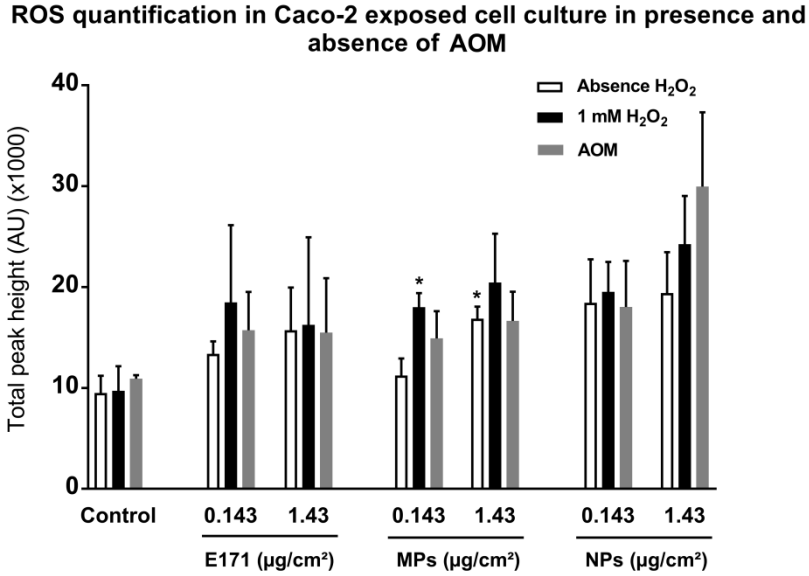

Figure 5: Intensity of cellular radical formation at non-cytotoxic concentrations E171, microparticles (MPs) and nanoparticles (NPs) in HBSS in cellular (Caco-2) co-exposed to 1 mM of H_2O_2 or 20 µg/mL AOM shown on x-axis.

Y-axis represents the average total peak height of obtained ESR spectra calculated per sample. Significant difference compared to the control (*p<0.05, Mean ± SE). Three independent experiments were performed, each of them was performed in duplicate n=12.

We hypothesized that E171 enhances the genotoxic effects of AOM in Caco-2 cells via the production of ROS. Therefore, Caco-2 cells were exposed simultaneously to the genotoxic compound AOM and to E171, MPs and NPs at non-cytotoxic concentrations. Co-exposure of AOM did not lead to significant increased ROS levels as compared to AOM alone. No significant difference was found between TiO_2 exposure and exposure to AOM of Caco-2 cells (Figure 5).

III-5- Single-strand DNA breaks in Caco-2 cell cultures exposed to E171, MP and NPs

The level of single-strand DNA breaks and alkali-labile sites including abasic sites were assessed by the comet assay and the median tail intensity was significantly higher after exposure to H_2O_2 as compared to AOM. Cells were co-exposed with different particles: E171 with or without AOM. The results show that E171, MPs and NPs had a capacity to induce single-strand DNA breaks in Caco-2 cells either with or without the presence of AOM (Figure 6). For the NPs, another non-cytotoxic concentration was tested, no dose-response on these particles is observed.

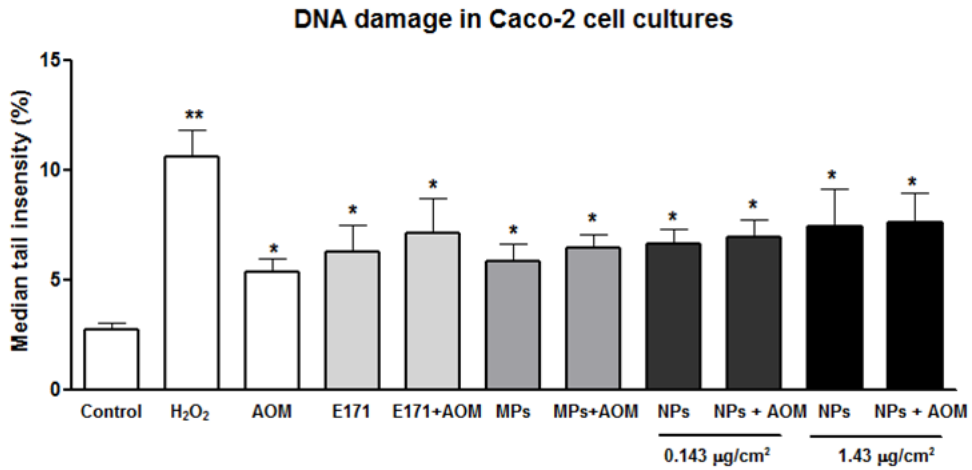

Figure 6: DNA damage in Caco-2 cells after 24h exposure to E171, microparticles (MPs) and nanoparticles (NPs).

All treatments were at a non-cytotoxic concentration of 0.143 µg/cm² with or without co-exposure of AOM. For the NPs a higher non-cytotoxic concentration was added, 1.43 µg/mL with and without AOM. 30 minutes exposure of 200 µM H_2O_2 was used as positive control, AOM; 20 µg/mL AOM. DNA damage is represented by median tail intensity shown at y-axis. All conditions are compared to control (*p< 0.05, **p < 0.001; mean±SE). The average is from 4 independent experiments, each of them was performed in duplicate and every sample was on 2 slides, n=16.

III-6- E171 induced chromosome damage in HCT116 cell cultures

To investigate whether single-strand DNA breaks induced by E171 exposure could cause further chromosome damage, we selected HCT116 as a chromosomally stable cell line to perform a MN assay (42) under non-cytotoxic conditions. First, we exposed HCT116 cell cultures to 5, 10, 50 and 100 µg/cm^2 of E171 and no decrease in cell viability was found measured by Trypan blue assay (Figure 3). We found an increase in MN formation (Figure 7A) of 1.9, 2.4 and 3.6-fold of increase in cell cultures exposed to 5, 10 and 50 µg/cm^2, respectively (Figure 7B). Frequency of binucleated cells with micronucleus in 1,000 binucleated cells after exposure to 5, 10 and 50 µg/cm^2 of E171 was 1.76, 3.3, 4.1 and 6.6% respectively. MN in cells exposed to 100 µg/cm^2 could not be assessed.

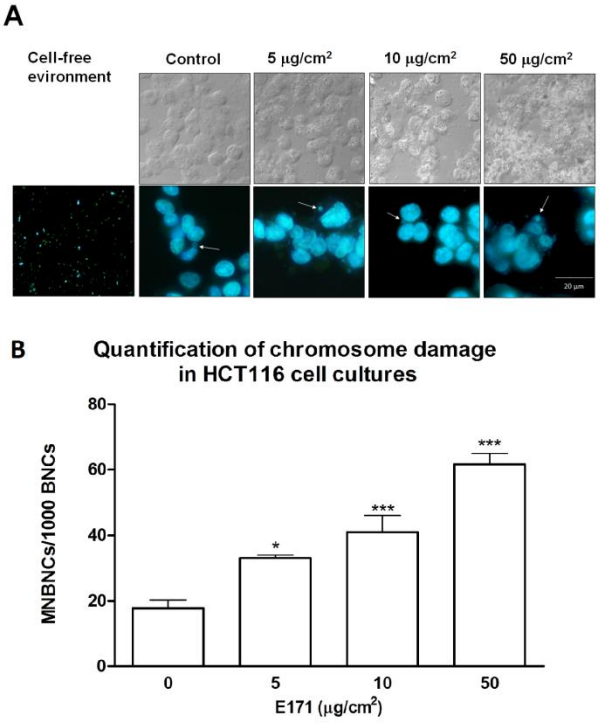

Figure 7: E171 induced chromosome damage in HCT116 cell cultures. A) Representative images of HCT116 micronucleated binucleated cells (MNBNCs) after E171 exposure (5, 10, 50 and 100 µg/cm2) for 24 hours.

Upper panel shows differential interference contrast in which E171 particles is shown as white agglomerates. Lower panel shows DNA stained by Hoesch dye and micronuclei formation is shown by white arrows. Three independent experiments were performed. B) Quantification of chromosome damage in HCT116 cell cultures. Numbers of MNBNCs in 1000 binucleated cells (BNCs) are represented in y-axis. Statistically significant changes and differences are indicated by an asterisk (*p<0.05, **p<0.01, ***p< 0.0001 mean±SD). Three independent experiments were performed.

III-7- E171 interaction with the kinetochore

Since DNA damage could be attributed to E171 interaction during disassembly of nuclear envelope for cell division, we investigated if E171 can interact with kinetochores in exposed HCT116 cell cultures. E171 seems to interact with the centromere region of kinetochore poles during mitosis (Figure 8). The union of particles with the poles of centromeres appears to be a co-localization of E171 with α-tubulin, thus suggesting that E171 particles were attached to DNA of mitotic cells (Figure 8).

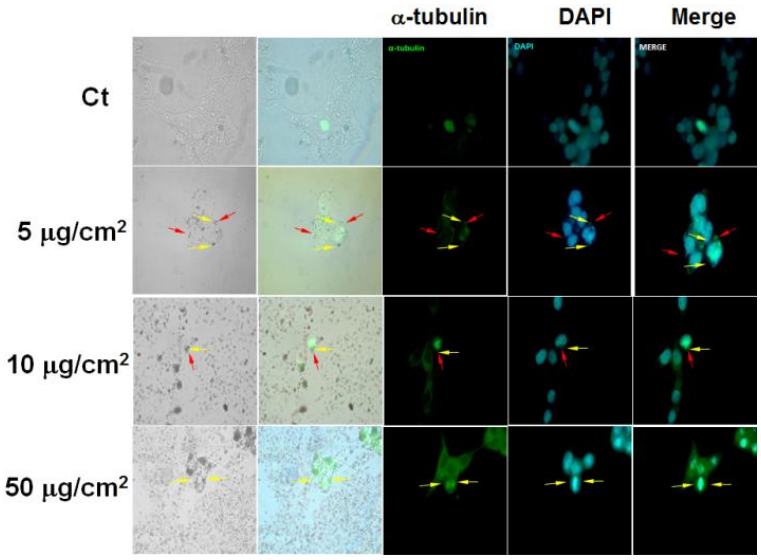

Figure 8: Identification of E171 interaction with kinetochores. HCT117 cell cultures were exposed to E171 particles (5, 10, 50 and 100 µg/cm^2).

A positive E171 interaction with mitotic kinetochore poles is shown by yellow arrows. E171 particles co-localized with mitotic genome and α-tubulin is showed by red arrows. Untreated cell had no presence of particles.

IV- Discussion

We found that TiO_2 particles as they are present in the food additive E171 are able to induce ROS formation and DNA damage in colon-derived Caco-2 and HCT116 cell lines. These effects may in part explain earlier findings of facilitation of colon tumour growth in an animal model after ingestion of relevant quantities of E171 (28). Effects were dependent on the size of the particles; indeed MPs induced ROS formation in cellular environment whereas all particles induced DNA damage. In order to assess the interaction of the particles with the medium and buffer, the particles were characterised and the zeta potential was determined with DLS (Table 1). A dispersing agent such as BSA or FBS is needed to stabilise and disperse E171, TiO_2 NPs and MPs, as already shown for different nanomaterials including TiO_2 (43,44), and has been applied in larger harmonized studies on nanomaterials genotoxicity (45). We observed less aggregation, and noted that E171, NPs or MPs were more stable while their hydrodynamic size was significantly lower in medium with 0.05% BSA or medium with 10% FBS than in HBSS buffer.

To assess the cytotoxicity of the particles a Trypan blue viability assay was performed. Initially, we applied the MTT and LDH assay (data not shown) but we found interference between TiO_2 and viability assays like LDH, MTT and WST-1. Such interference is also reported by others (30,46,47). For this reason we applied the trypan blue assay. The interference with the trypan blue assay was circumvented by checking by eye on the screen of the cell counter whether the cells tagged by Trypan blue correspond to living Caco-2 cells or not. Furthermore, the results of the cell counter were compared with the one done at the microscope directly and these corroborate (Supplementary Figure 1). The results showed that E171 is cytotoxic in Caco-2 cells at a lower concentration than the NPs and MPs. However, E171 has no toxic effects in HCT116 cell cultures at concentrations used in this study (5, 10, 50 and 100 $\mu g/cm^2$) (Figure 2).

As E171 comprises 39% NPs and 61% MPs (Figure 1) which confirms previous findings by Weir et al.(4), we suggest that the combination of NPs and MPs is more cytotoxic to Caco-2 cells than NPs or MPs alone. Other studies (13,48), only focussed on TiO_2 NPs and fewer studies have been performed using TiO_2 food-grade. In line with our data, concentrations up to 0.1 mg/mL TiO_2 NPs (in this study it corresponds to 14.3 $\mu g/cm^2$) were also found to be non-cytotoxic in human lung epithelial cells (49) with the Trypan blue exclusion tests. Furthermore, in other cell lines such as human neural cells and normal fibroblasts, MPs and NPs are equally effective in inducing cell death in human neural cells and normal fibroblasts (50). This implies that some effects are not only due to

the size of the particles. Furthermore, we suggest that particle accumulation is different in Caco-2 and HCT116 cells, because nanoparticle internalization depends on cell type as it has been demonstrated that internalization of gold nanoparticles sized in 50 nm is approximately 2-fold higher in macrophages than in human liver cancer cells after 24 hours of exposure (51).

In addition, even if both types of cells are epithelial cultures derived from colon, the cytotoxicity of E171 particles can be lower in HCT116 cells (Figure 3), firstly, because the modal chromosome number at 45 in this cell line confers higher genomic stability than Caco-2 cells, which have a stemline modal chromosome number of 96 (http://www.atcc.org/products/all/HTB-37.aspx#characteristics). Secondly, HCT116 cell line has a p16 mutation which leads to increased proliferation with evasion of cell cycle arrest (52,53).

Based on these data, we used equal non-cytotoxic concentrations for all three types of particles for further studies on ROS formation in a cell-free environment and in cell cultures and for establishing the induction of DNA damage in Caco-2 cells. HCT116 cells were selected for MN measurements since Caco-2 cells like many other cell lines are chromosomally instable and therefore not suitable for this assay (42).

Numerous studies confirm that TiO_2 particles can induce ROS production (10,54-57). Toxicity mediated by oxidative stress after exposure to TiO_2 NPs and MPs has been previously described in other groups (55,58,59), however, MPs showed lower intensity in ROS generation (60) but TiO_2 NPs exposure is able to cause DNA lesions (10,55-57). In our study, particles in 0.05% BSA show no ROS formation whereas in absence of BSA (HBSS) increased levels of ROS were observed both under cellular and cell-free conditions (Figure 4-5). Therefore, we conclude that BSA scavenges ROS that are formed on the surface of the particles or may prevent ROS formation by inhibiting the contact between particle surface and ROS precursors. In a cell-free environment, E171 and NPs induce significantly higher ROS production as compared to the control (Figure 4). These results are in agreement with the findings of Zijno et al. who have tested TiO_2 NPs with ESR spectroscopy and also observed ROS production in a cell-free environment (14). In contrast to E171 and NPs, MPs do not induce any ROS production when they are dispersed in buffer (Figure 4). In a cellular environment the capacity of E171 and NPs to produce ROS was strongly reduced while only MPs were capable of producing ROS (Figure 5). We suggest that MPs, via ROS production would induce a pro-inflammatory response. This was already observed in a co-culture of intestinal cells and macrophages exposed to TiO_2

MPs in which the team measured an upregulation of pro-inflammatory caspases and cytokines such as caspase-1 and IL-1β and IL-18 (61). Furthermore, another group observed a Th1 mediated inflammatory response in the small bowel in mice (62). We recently found that E171 *in vivo* exposure enhanced the number of tumours in the colon of mice exposed to AOM/DSS (28). The combined exposure to AOM/DSS is commonly used for the chemical induction of colonic tumours in animal experiments where AOM acts as a DNA alkylation reagent initiating the carcinogenic process (63). In order to shed light on the mechanisms behind these *in vivo* results, we co-exposed Caco-2 cells to AOM and TiO_2 particles (E171, NPs and MPs) and performed ESR spectrometry and a comet assay to detect single-strand DNA breaks and alkali-labile sites. To test the effect of AOM on ROS formation, Caco-2 cells were co-exposed to AOM and E171, NPs or MPs. ROS levels were not significantly different between cells that were only exposed to the particles and cells that were co-exposed to AOM (Figure 5). This shows that the increased tumour formation in mice might not be attributed to ROS. More studies *in vitro* and *in vivo* studies such as full genome expression analysis need to be performed to be able to conclude about the mechanisms behind the potential carcinogenic effect of E171. The absence of ROS induction by E171 and NPs in our study could possibly be explained by the fact that after internalization, particles react immediately with cellular structures that block ROS production. Indeed, the NPs partition would enters the cells as shown by Shukla et al. where they illustrate that the NPs of TiO_2 can easily enter the cell and even reach the nucleus of human epidermal cells (32). After entering the cell, the radicals produced by the particles could then decrease the cellular glutathione (GSH) content as shown by Shlukla et al. where they exposed human epidermal cells to TiO_2 NPs and observed a significant reduction of cellular GSH content from 8 µg/mL (32). This would help to re-establish the redox balance. Yet, the ability of E171 and NPs to interact with other biomolecules could lead to cellular alterations, including protein, RNA and DNA modifications.

The results of the comet assay showed that E171 and TiO_2 NPs and MPs are genotoxic by inducing single-strand DNA breaks and no dose-response was found for the NPs, the genotoxicity was the same (Figure 6). In addition, E171 causes chromosome damage in the HCT116 cell line measured by the micronucleus assay (Figure 7). As micronucleus is a fragment of DNA, it is expected to identify it by a blue staining by Hoechst dye. Then, micronucleus can be observed as circular shapes with smooth edges. The basal levels of micronucleus frequency in our results agree with previous literature, which are estimated between 2.5% and 3.2% (64,65). The results from two different cell lines indicate the *in vitro* genotoxicity of E171. DNA damage may be the consequence of

E171 interacting with microtubules, as seem to occur in HCT116 cells, which could take place during the nuclear envelope disassembly which precedes mitosis. The interaction between E171 and microtubules from the kinetochores could lead to chromosome missegregation and the formation of MN (66) (Figure 8). Furthermore, genotoxicity is known to play an important role in the initiation state of carcinogenesis since it can lead to changes in the genetic material resulting in alterations on cellular signalling pathways related to cell proliferation and apoptosis (62). We therefore hypothesize that E171 genotoxicity in colon cells could be participating in carcinogenic processes such as enhancing tumour formation in an azoxymethane-induced colorectal cancer model by intragastric E171 particles administration (28).

The colon is the major site for nutrient uptake but potentially also for hazardous compounds which can be present in the food. The E171 particles, known as food TiO_2 additive is present in many different type of food. It is difficult to correlate between *in vitro* and *in vivo* concentrations in the gut without making a number of assumptions. Nevertheless, we made an estimation of the concentration of TiO_2 in the colon assuming the average exposure of an adult to be 1 mg/kg_{bw}/day (4) an average weight of 70 kg and a quantity of faeces excreted per day between 100 and 250g per day. If we make a conservative estimate, the adult of 70 kg would ingest 70 mg of TiO_2 per day, this person would produce 250g of faeces which would make a concentration of TiO_2 in the faeces of 0.28 mg of TiO_2/g of faeces. Faeces contain 75% of water, so if we consider that the density of faeces is the same as water, the concentration of TiO_2 would be 0.28 mg/mL of faeces. If we assume that only 1% of these is biologically available for exposure, 0.0028 mg/mL of TiO_2 is potentially reaching the colon cells. The non-cytotoxic concentrations of TiO_2 used during the *in vitro* experiments are 0.01 mg/mL and 0.001 mg/mL. Therefore, the concentrations are in the same order of magnitude as the estimated concentration of TiO_2 in the colon. To the best of our knowledge this is the first time that the genotoxicity of E171 and different size fractions were shown in colon-derived cell cultures. The findings of the present *in vitro* study demonstrate that TiO_2 as food additives coded as E171, even at the lowest concentration tested, have DNA damaging potential in human colonic cells, and that the micro-sized particles in E171 might be the most relevant for ROS formation as shown in presence of Caco-2 cells. The capacity to generate ROS and to induce DNA damage raises concerns about the safe use of E171 in numerous food products.

Supplementary materials

Supplementary Figure S1: Trypan blue staining for cytotoxicity testing on Caco-2 cells exposed to 14.3 µg/cm² of E171. A: Caco-2 cells exposed to E171 without staining, B: Trypan blue staining, view from the screen of the cell counter, C: Flagging of the cells counted by the cell counter for the cytotoxicity testing with Trypan blue.

ftp://web.tgx.unimaas.nl/hproquin/Chapter_5/Supplementary_Figure_1.tif

Supplementary Figure S2: Comet assay pictures with Caco-2 cells and E171. A: Control cell, B: Exposure to AOM, C: Exposure to NPs (1.43 µg/cm²) + AOM, D: Exposure to NPs (1.43 µg/cm²), E: Exposure to NPs (1.43x10-1 µg/cm²) + AOM, F: Exposure to NPs (1.43x10-1 µg/cm²).

ftp://web.tgx.unimaas.nl/hproquin/Chapter_5/Supplementary_Figure_2.tif

References

1. Lomer, M.C.E., Thompson, R.P.H., Commisso, J., Keen, C.L., and Powell, J.J. (2000) Determination of titanium dioxide in foods using inductively coupled plasma optical emission spectrometry. *Analyst*, **125**, 2339-2343.
2. Peters, R.J., van Bemmel, G., Herrera-Rivera, Z., Helsper, H.P., Marvin, H.J., Weigel, S., Tromp, P.C., Oomen, A.G., Rietveld, A.G., and Bouwmeester, H. (2014) Characterization of titanium dioxide nanoparticles in food products: analytical methods to define nanoparticles. *J Agric Food Chem*, **62**, 6285-6293.
3. Shi, H., Magaye, R., Castranova, V., and Zhao, J. (2013) Titanium dioxide nanoparticles: a review of current toxicological data. *Particle and fibre toxicology*, **10**, 15.
4. Weir, A., Westerhoff, P., Fabricius, L., Hristovski, K., and von Goetz, N. (2012) Titanium dioxide nanoparticles in food and personal care products. *Environmental science & technology*, **46**, 2242-2250.
5. EU (2012) Regulation No 231-2012 on food additives. *OJL*, 83, 1-295.
6. USFDA (2016) US Food and Drug Administration regulation on Titanium dioxide. *Code of Federal Regulations*, **Title 21, Section 73.575.** US Food and Drug Administration, Silver Springs, MD.
7. Bhattacharya, K., Davoren, M., Boertz, J., Schins, R.P., Hoffmann, E., and Dopp, E. (2009) Titanium dioxide nanoparticles induce oxidative stress and DNA-adduct formation but not DNA-breakage in human lung cells. *Particle and fibre toxicology*, **6**, 17.
8. Falck, G.C., Lindberg, H.K., Suhonen, S., Vippola, M., Vanhala, E., Catalan, J., Savolainen, K., and Norppa, H. (2009) Genotoxic effects of nanosized and fine TiO2. *Hum Exp Toxicol*, **28**, 339-352.
9. Kang, S.J., Kim, B.M., Lee, Y.J., and Chung, H.W. (2008) Titanium dioxide nanoparticles trigger p53-mediated damage response in peripheral blood lymphocytes. *Environ Mol Mutagen*, **49**, 399-405.
10. Wang, J.J., Sanderson, B.J., and Wang, H. (2007) Cyto- and genotoxicity of ultrafine TiO2 particles in cultured human lymphoblastoid cells. *Mutation research*, **628**, 99-106.
11. Armand, L., Tarantini, A., Beal, D., Biola-Clier, M., Bobyk, L., Sorieul, S., Pernet-Gallay, K., Marie-Desvergne, C., Lynch, I., Herlin-Boime, N., and Carriere, M. (2016) Long-term exposure of A549 cells to titanium dioxide nanoparticles induces DNA damage and sensitizes cells towards genotoxic agents. *Nanotoxicology*, 1-11.
12. IARC. (2010) *IARC Monographs on the Evaluation of Carcinogenic Risks to Humans: Carbon Black, Titanium dioxide and Talc,* Vol. 93. International Agency for Research on Cancer, Lyon, France.
13. Gerloff, K., Albrecht, C., Boots, A.W., Forster, I., and Schins, R.P.F. (2009) Cytotoxicity and oxidative DNA damage by nanoparticles in human intestinal Caco-2 cells. *Nanotoxicology*, **3**, 355-364.
14. Zijno, A., De Angelis, I., De Berardis, B., Andreoli, C., Russo, M.T., Pietraforte, D., Scorza, G., Degan, P., Ponti, J., Rossi, F., and Barone, F. (2015) Different mechanisms are involved in oxidative DNA damage and genotoxicity induction by ZnO and TiO nanoparticles in human colon carcinoma cells. *Toxicol In Vitro*, **29**, 1503-1512.
15. Dorier, M., Brun, E., Veronesi, G., Barreau, F., Pernet-Gallay, K., Desvergne, C., Rabilloud, T., Carapito, C., Herlin-Boime, N., and Carriere, M. (2015) Impact of anatase and rutile titanium dioxide nanoparticles on uptake carriers and efflux pumps in Caco-2 gut epithelial cells. *Nanoscale*, **7**, 7352-7360.
16. Song, Z.M., Chen, N., Liu, J.H., Tang, H., Deng, X., Xi, W.S., Han, K., Cao, A., Liu, Y., and Wang, H. (2015) Biological effect of food additive titanium dioxide nanoparticles on intestine: an in vitro study. *J Appl Toxicol*, **35**, 1169-1178.

17. Tarantini, A., Lanceleur, R., Mourot, A., Lavault, M.T., Casterou, G., Jarry, G., Hogeveen, K., and Fessard, V. (2015) Toxicity, genotoxicity and proinflammatory effects of amorphous nanosilica in the human intestinal Caco-2 cell line. *Toxicol In Vitro*, **29**, 398-407.
18. Robichaud, C.O., Uyar, A.E., Darby, M.R., Zucker, L.G., and Wiesner, M.R. (2009) Estimates of upper bounds and trends in nano-TiO2 production as a basis for exposure assessment. *Environmental science & technology*, **43**, 4227-4233.
19. Pan, Y., Leifert, A., Ruau, D., Neuss, S., Bornemann, J., Schmid, G., Brandau, W., Simon, U., and Jahnen-Dechent, W. (2009) Gold nanoparticles of diameter 1.4 nm trigger necrosis by oxidative stress and mitochondrial damage. *Small*, **5**, 2067-2076.
20. Schaeublin, N.M., Braydich-Stolle, L.K., Schrand, A.M., Miller, J.M., Hutchison, J., Schlager, J.J., and Hussain, S.M. (2011) Surface charge of gold nanoparticles mediates mechanism of toxicity. *Nanoscale*, **3**, 410-420.
21. Niska, K., Pyszka, K., Tukaj, C., Wozniak, M., Radomski, M.W., and Inkielewicz-Stepniak, I. (2015) Titanium dioxide nanoparticles enhance production of superoxide anion and alter the antioxidant system in human osteoblast cells. *Int J Nanomed*, **10**, 1095-1107.
22. Cooke, M.S., Evans, M.D., Dizdaroglu, M., and Lunec, J. (2003) Oxidative DNA damage: mechanisms, mutation, and disease. *FASEB J*, **17**, 1195-1214.
23. Inoue, S., and Kawanishi, S. (1987) Hydroxyl radical production and human DNA damage induced by ferric nitrilotriacetate and hydrogen peroxide. *Cancer research*, **47**, 6522-6527.
24. Jackson, J.H., Schraufstatter, I.U., Hyslop, P.A., Vosbeck, K., Sauerheber, R., Weitzman, S.A., and Cochrane, C.G. (1987) Role of oxidants in DNA damage. Hydroxyl radical mediates the synergistic DNA damaging effects of asbestos and cigarette smoke. *J Clin Invest*, **80**, 1090-1095.
25. Powell, J.J., Ainley, C.C., Harvey, R.S., Mason, I.M., Kendall, M.D., Sankey, E.A., Dhillon, A.P., and Thompson, R.P. (1996) Characterisation of inorganic microparticles in pigment cells of human gut associated lymphoid tissue. *Gut*, **38**, 390-395.
26. Lomer, M.C., Thompson, R.P., and Powell, J.J. (2002) Fine and ultrafine particles of the diet: influence on the mucosal immune response and association with Crohn's disease. *The Proceedings of the Nutrition Society*, **61**, 123-130.
27. Grissa, I., Elghoul, J., Ezzi, L., Chakroun, S., Kerkeni, E., Hassine, M., El Mir, L., Mehdi, M., Ben Cheikh, H., and Haouas, Z. (2015) Anemia and genotoxicity induced by sub-chronic intragastric treatment of rats with titanium dioxide nanoparticles. *Mutat Res Genet Toxicol Environ Mutagen*, **794**, 25-31.
28. Urrutia-Ortega, I.M., Garduno-Balderas, L.G., Delgado-Buenrostro, N.L., Freyre-Fonseca, V., Flores-Flores, J.O., Gonzalez-Robles, A., Pedraza-Chaverri, J., Hernandez-Pando, R., Rodriguez-Sosa, M., Leon-Cabrera, S., Terrazas, L.I., van Loveren, H., and Chirino, Y.I. (2016) Food-grade titanium dioxide exposure exacerbates tumor formation in colitis associated cancer model. *Food Chem Toxicol*, **93**, 20-31.
29. Hawkins, C.L., and Davies, M.J. (2014) Detection and characterisation of radicals in biological materials using EPR methodology. *Biochim Biophys Acta*, **1840**, 708-721.
30. Kroll, A., Pillukat, M.H., Hahn, D., and Schnekenburger, J. (2012) Interference of engineered nanoparticles with in vitro toxicity assays. *Arch Toxicol*, **86**, 1123-1136.
31. Jugan, M.L., Barillet, S., Simon-Deckers, A., Herlin-Boime, N., Sauvaigo, S., Douki, T., and Carriere, M. (2012) Titanium dioxide nanoparticles exhibit genotoxicity and impair DNA repair activity in A549 cells. *Nanotoxicology*, **6**, 501-513.
32. Shukla, R.K., Sharma, V., Pandey, A.K., Singh, S., Sultana, S., and Dhawan, A. (2011) ROS-mediated genotoxicity induced by titanium dioxide nanoparticles in human epidermal cells. *Toxicol In Vitro*, **25**, 231-241.
33. Gonzalez, L., Sanderson, B.J., and Kirsch-Volders, M. (2011) Adaptations of the in vitro MN assay for the genotoxicity assessment of nanomaterials. *Mutagenesis*, **26**, 185-191.

34. Masramon, L., Vendrell, E., Tarafa, G., Capella, G., Miro, R., Ribas, M., and Peinado, M.A. (2006) Genetic instability and divergence of clonal populations in colon cancer cells in vitro. *J Cell Sci*, **119**, 1477-1482.
35. Nymark, P., Jensen, K.A., Suhonen, S., Kembouche, Y., Vippola, M., Kleinjans, J., Catalan, J., Norppa, H., van Delft, J., and Briede, J.J. (2014) Free radical scavenging and formation by multi-walled carbon nanotubes in cell free conditions and in human bronchial epithelial cells. *Particle and fibre toxicology*, **11**, 4.
36. Briede, J.J., van Delft, J.M., de Kok, T.M., van Herwijnen, M.H., Maas, L.M., Gottschalk, R.W., and Kleinjans, J.C. (2010) Global gene expression analysis reveals differences in cellular responses to hydroxyl- and superoxide anion radical-induced oxidative stress in caco-2 cells. *Toxicol Sci*, **114**, 193-203.
37. Hebels, D.G., Briede, J.J., Khampang, R., Kleinjans, J.C., and de Kok, T.M. (2010) Radical mechanisms in nitrosamine- and nitrosamide-induced whole-genome gene expression modulations in Caco-2 cells. *Toxicol Sci*, **116**, 194-205.
38. Hebels, D.G., Sveje, K.M., de Kok, M.C., van Herwijnen, M.H., Kuhnle, G.G., Engels, L.G., Vleugels-Simon, C.B., Mares, W.G., Pierik, M., Masclee, A.A., Kleinjans, J.C., and de Kok, T.M. (2011) N-nitroso compound exposure-associated transcriptomic profiles are indicative of an increased risk for colorectal cancer. *Cancer letters*, **309**, 1-10.
39. Fenech, M. (2000) The in vitro micronucleus technique. *Mutation research*, **455**, 81-95.
40. Ismail, M.F., Elmeshad, A.N., and Salem, N.A. (2013) Potential therapeutic effect of nanobased formulation of rivastigmine on rat model of Alzheimer's disease. *Int J Nanomedicine*, **8**, 393-406.
41. Lin, P.C., Lin, S., Wang, P.C., and Sridhar, R. (2014) Techniques for physicochemical characterization of nanomaterials. *Biotechnol Adv*, **32**, 711-726.
42. Thompson, S.L., and Compton, D.A. (2008) Examining the link between chromosomal instability and aneuploidy in human cells. *J Cell Biol*, **180**, 665-672.
43. Bihari, P., Vippola, M., Schultes, S., Praetner, M., Khandoga, A.G., Reichel, C.A., Coester, C., Tuomi, T., Rehberg, M., and Krombach, F. (2008) Optimized dispersion of nanoparticles for biological in vitro and in vivo studies. *Particle and fibre toxicology*, **5**, 14.
44. Vippola, M., Falck, G.C., Lindberg, H.K., Suhonen, S., Vanhala, E., Norppa, H., Savolainen, K., Tossavainen, A., and Tuomi, T. (2009) Preparation of nanoparticle dispersions for in-vitro toxicity testing. *Hum Exp Toxicol*, **28**, 377-385.
45. NANOGENOTOX (2011) Final Protocol for Producing Suitable Manufactured Nanomaterial Exposure Media. *Nancy: Bialec*.
46. Guadagnini, R., Halamoda Kenzaoui, B., Walker, L., Pojana, G., Magdolenova, Z., Bilanicova, D., Saunders, M., Juillerat-Jeanneret, L., Marcomini, A., and Huk, A. (2015) Toxicity screenings of nanomaterials: challenges due to interference with assay processes and components of classic in vitro tests. *Nanotoxicology*, **9**, 13-24.
47. Holder, A.L., Goth-Goldstein, R., Lucas, D., and Koshland, C.P. (2012) Particle-induced artifacts in the MTT and LDH viability assays. *Chem Res Toxicol*, **25**, 1885-1892.
48. Gerloff, K., Fenoglio, I., Carella, E., Kolling, J., Albrecht, C., Boots, A.W., Forster, I., and Schins, R.P. (2012) Distinctive toxicity of TiO2 rutile/anatase mixed phase nanoparticles on Caco-2 cells. *Chem Res Toxicol*, **25**, 646-655.
49. Prasad, R.Y., Wallace, K., Daniel, K.M., Tennant, A.H., Zucker, R.M., Strickland, J., Dreher, K., Kligerman, A.D., Blackman, C.F., and Demarini, D.M. (2013) Effect of treatment media on the agglomeration of titanium dioxide nanoparticles: impact on genotoxicity, cellular interaction, and cell cycle. *ACS Nano*, **7**, 1929-1942.
50. Lai, J.C., Lai, M.B., Jandhyam, S., Dukhande, V.V., Bhushan, A., Daniels, C.K., and Leung, S.W. (2008) Exposure to titanium dioxide and other metallic oxide nanoparticles induces cytotoxicity on human neural cells and fibroblasts. *Int J Nanomedicine*, **3**, 533-545.

51. Cheng, X., Tian, X., Wu, A., Li, J., Tian, J., Chong, Y., Chai, Z., Zhao, Y., Chen, C., and Ge, C. (2015) Protein Corona Influences Cellular Uptake of Gold Nanoparticles by Phagocytic and Nonphagocytic Cells in a Size-Dependent Manner. *ACS Appl Mater Interfaces*, **7**, 20568-20575.
52. Guan, R.J., Fu, Y., Holt, P.R., and Pardee, A.B. (1999) Association of K-ras mutations with p16 methylation in human colon cancer. *Gastroenterology*, **116**, 1063-1071.
53. Hara, E., Smith, R., Parry, D., Tahara, H., Stone, S., and Peters, G. (1996) Regulation of p16CDKN2 expression and its implications for cell immortalization and senescence. *Mol Cell Biol*, **16**, 859-867.
54. Iavicoli, I., Leso, V., and Bergamaschi, A. (2012) Toxicological Effects of Titanium Dioxide Nanoparticles: A Review of In Vivo Studies. *J Nanomater*.
55. Gurr, J.R., Wang, A.S., Chen, C.H., and Jan, K.Y. (2005) Ultrafine titanium dioxide particles in the absence of photoactivation can induce oxidative damage to human bronchial epithelial cells. *Toxicology*, **213**, 66-73.
56. Dunford, R., Salinaro, A., Cai, L., Serpone, N., Horikoshi, S., Hidaka, H., and Knowland, J. (1997) Chemical oxidation and DNA damage catalysed by inorganic sunscreen ingredients. *FEBS Lett*, **418**, 87-90.
57. Rahman, Q., Lohani, M., Dopp, E., Pemsel, H., Jonas, L., Weiss, D.G., and Schiffmann, D. (2002) Evidence that ultrafine titanium dioxide induces micronuclei and apoptosis in Syrian hamster embryo fibroblasts. *Environmental health perspectives*, **110**, 797-800.
58. Ramires, P.A., Romito, A., Cosentino, F., and Milella, E. (2001) The influence of titania/hydroxyapatite composite coatings on in vitro osteoblasts behaviour. *Biomaterials*, **22**, 1467-1474.
59. Hussain, S.M., Hess, K.L., Gearhart, J.M., Geiss, K.T., and Schlager, J.J. (2005) In vitro toxicity of nanoparticles in BRL 3A rat liver cells. *Toxicol In Vitro*, **19**, 975-983.
60. Kang, J.L., Moon, C., Lee, H.S., Lee, H.W., Park, E.M., Kim, H.S., and Castranova, V. (2008) Comparison of the biological activity between ultrafine and fine titanium dioxide particles in RAW 264.7 cells associated with oxidative stress. *J Toxicol Env Heal A*, **71**, 478-485.
61. Becker, H.M., Bertschinger, M.M., and Rogler, G. (2012) Microparticles and their impact on intestinal immunity. *Dig Dis*, **30 Suppl 3**, 47-54.
62. Nogueira, C.M., de Azevedo, W.M., Dagli, M.L., Toma, S.H., Leite, A.Z., Lordello, M.L., Nishitokukado, I., Ortiz-Agostinho, C.L., Duarte, M.I., Ferreira, M.A., and Sipahi, A.M. (2012) Titanium dioxide induced inflammation in the small intestine. *World J Gastroenterol*, **18**, 4729-4735.
63. Tanaka, T., Kohno, H., Suzuki, R., Yamada, Y., Sugie, S., and Mori, H. (2003) A novel inflammation-related mouse colon carcinogenesis model induced by azoxymethane and dextran sodium sulfate. *Cancer science*, **94**, 965-973.
64. Camps, J., Ponsa, I., Ribas, M., Prat, E., Egozcue, J., Peinado, M.A., and Miro, R. (2005) Comprehensive measurement of chromosomal instability in cancer cells: combination of fluorescence in situ hybridization and cytokinesis-block micronucleus assay. *FASEB J*, **19**, 828-830.
65. Bakhoum, S.F., Kabeche, L., Wood, M.D., Laucius, C.D., Qu, D., Laughney, A.M., Reynolds, G.E., Louie, R.J., Phillips, J., Chan, D.A., Zaki, B.I., Murnane, J.P., Petritsch, C., and Compton, D.A. (2015) Numerical chromosomal instability mediates susceptibility to radiation treatment. *Nat Commun*, **6**, 5990.
66. Huang, S., Chueh, P.J., Lin, Y.W., Shih, T.S., and Chuang, S.M. (2009) Disturbed mitotic progression and genome segregation are involved in cell transformation mediated by nano-TiO2 long-term exposure. *Toxicol Appl Pharmacol*, **241**, 182-194.

Chapter 6

Transcriptomic-based identification of gene expression changes after exposure of Caco-2 cells to food-grade titanium dioxide (E171): contribution of the micro and nano-sized fraction

Submitted for publication

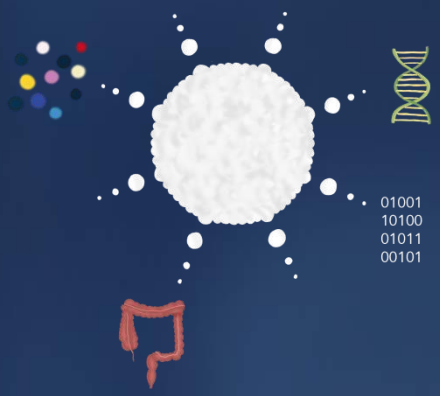

Héloïse Proquin

Marloes C.M. Jonkhout

Marlon J. Jetten

Henk van Loveren

Theo M. de Kok

Jacob J. Briedé

Abstract

The food additive titanium dioxide (TiO_2), also known as E171 gives a white colour to food. Recent studies showed after E171 ingestion a significantly increased number of colorectal tumours in a colorectal cancer mouse model, inflammatory responses in the intestine and dysregulation of the immune system in rats. In mouse colon, E171 induced gene expression changes related to oxidative stress responses, impairment of the immune system, activation of signalling and cancer-related processes. E171 comprises nanoparticles (NPs) and microparticles (MPs). Previous *in vitro* studies showed the capacity of E171, NPs and MPs to induce oxidative stress, DNA damage, and micronuclei. The aim of our study is to investigate the relative contribution of the NPs and MPs fractions to the effects of E171 at the transcriptome level after exposure of Caco-2 cells in combination with genome wide microarray analysis. The results showed that E171, NPs, and MPs induce gene expression changes related to signalling, inflammation, immune system, transport, and cancer. NPs showed similar gene expression changes as E171 resulted in TLR cascade, MHC class I and II presentation, late cornified envelope, potassium channels, and cell cycle. MPs induced similar changes as E171 in gene expression related to Hedgehog family, α-defensins, cadherin and cholinergic receptors. At the pathway level, metabolism of proteins with the insulin processing pathway and haemostasis were specific to E171 exposure. Overall the gene expression changes associated with the immune system and inflammation induced by E171, MPs, and NPs suggest the creation of a favourable environment for colon cancer development.

I- Introduction

Titanium dioxide (TiO_2) is widely used as a food colorant in, among others, sweets, cookies, cake icing, and salad dressings (1-3). TiO_2 has been approved as a food additive in 1969 by the European Union (EU) under the name of E171 (4). This approval was based on a report written by the Joint WHO/FAO expert committee of Food Additives (JECFA) referring to the results of 5 studies published in 1927, 1928, 1950, 1955 and 1963 and one unpublished study in 1962 assessing TiO_2 absorption and toxicity in animals after ingestion (5). Based on the results of these studies, JECFA concluded that TiO_2 was free from toxic effects on account of its insolubility and inertness (6). Therefore the EU classified E171 as a non-active compound and there is no limit of authorised concentration in food products. In the USA, the Food and Drug Administration (FDA) approved the use of TiO_2 as a food additive in 1966 and TiO_2 should not exceed 1% by total weight of the product (7).

E171 is a mixture different particles with sizes in both the nano and the micro range. This size distribution was observed in commercially purchased E171 from different manufacturers and in E171 extracted from food products. All results from Scanning Electron Microscopy (SEM) or Transmission Electron Microscopy (TEM) showed that, in E171, the nanoparticles (NPs) fraction comprised 25 to 40% of all material, the remainder being microparticles (MPs) (1,8-11)

More recently, a limited number of animal studies have been published that provide evidence on the potential adverse effects after ingestion of E171 (2 in mice and 2 in rats). The first described effects of E171 ingestion in a murine colorectal cancer model (12). After 10 weeks of intragastric ingestion of 5 mg/kg_{bw}/day of E171 in combination with the genotoxicant azoxymethane (AOM) and the irritant dextran sodium sulphate (DSS), the number of tumours in the colon was significantly increased as compared to the control (AOM/DSS). The second *in vivo* study aimed to investigate the effects of E171 on the immune system in rats (13). Bettini et al. showed that, after intragastric exposure of 10 mg/kg_{bw}/day of E171 for 7 days, a decrease of regulatory T and Th cells and an increase production of IFN-γ in Peyer's patches were observed which would eventually lead to an impairment of the immune system. A third study applying a long term (100 days) exposure, in a chemically induced carcinogenesis rat model, showed that E171 (10 mg/kg_{bw}/day) promoted colon carcinogenesis by inducing preneoplastic lesions as well as the growth of aberrant crypt foci and mucosal low-grade inflammation (13). The fourth *in vivo* study was performed on a normal BALB/c mouse model in which intragastric

ingestion by oral gavage of 5 mg/kg_{bw}/day of E171 was executed for 2, 7, 14, and 21 days (14). Gene expression changes were observed in the colon which indicated oxidative stress responses, an impairment of the immune system, activation of signalling and cancer-related genes.

More studies have been performed after ingestion of the smallest fraction of TiO_2, the NPs fraction, indicating the translocation of the TiO_2 NPs to the blood stream and other organs. Several groups showed that after intragastric administration of TiO_2 NPs, these particles were found in the brain, blood, liver, spleen, and kidneys (15-20). In the gut, inflammatory response via cytokine production or NLRP3 inflammasome, and dysregulation of the innate and adaptive immune system were identified after ingestion of TiO_2 NPs (13,21,22). Two *in vivo* studies have been performed on MPs to assess translocation and toxicity. After intragastric ingestion, the particles were found in spleen, brain, while an inflammatory response in the small intestine was observed detected by an increased inflammatory cytokine production and T $CD4^+$ cell proliferation (18,22). Few *in vitro* studies show the potential of E171 as well as TiO_2 NPs and MPs to induce oxidative stress in Caco-2, Caco-2/HT29-MTX, human epidermal, and human amnion epithelial (WISH) cells (8,10,23-25). In the exact same cell lines, DNA damage was also observed after exposure to E171, NPs and MPs of TiO_2. In addition, induction of micronuclei was observed in HCT116 cells (10). Another *in vitro* study showed that E171 extracted from gum disrupted the normal arrangement of constituent microvilli of the Caco-2_{BBe1} brush border (26).

The aim of our study was to investigate the relative contribution of the NPs and MPs fractions to the effects of E171 at the transcriptome level. This investigation was performed using *in vitro* exposure of Caco-2 cells to E171 as well as the NPs and MPs fractions of TiO_2 and assessing genome wide gene expression analysis. We assumed that because of its small size and higher surface area, the NPs fraction would show the most pronounced effect on gene expression. Therefore, we first performed a time course study (2, 4, and 24h of exposure) with this fraction to identify the most relevant time point at which the highest number of genes and related biological processes would be influenced. Next, we performed exposure of Caco-2 cells with E171, and the MPs fraction at that optimal duration (24h) to conclude on the relative contribution of each fraction to the various gene expression changes and related biological processes that E171 influences and eventually lead to adverse conditions such as the facilitation of colon cancer development.

II- Materials and methods

II-1- Cell Culture

Human colon carcinoma cell line Caco-2 (American Type Culture Collection ATCC, HTB-37) a frequently used colon cell line for *in vitro* toxicity studies, were cultured in an incubator under standard cell culture conditions (37°C, 5% CO_2) in Dulbecco's Modified Eagles Medium (DMEM) (Sigma-Aldrich, the Netherlands). DMEM was supplemented with 10% FBS, 1% non-essential amino acids, 1% sodium pyruvate and 1% penicillin/streptomycin. Cells were passaged at 80 to 90% confluency.

II-2- Compounds

TiO_2 NPs were purchased at Io-Li-Tec, Germany, with 99.5% anatase particles. The particle size ranged from 10 to 30 nm (10) with a surface area of 50 to 150 m^2/g (information provided by the manufacturer). TiO_2 MPs were customarily manufactured by PlasmaChem (Germany), with a size higher than 100 nm and an average size of 622 nm (10). E171 was kindly donated by Sensient Technologies, Mexico. E171 contains slightly to fully rounded particles with a proportion of 39% NPs and 61% MPs (10). All particles were sterilised at 121°C for 20 minutes prior to use.

II-3- Particle Exposure

Caco-2 cells were used with a passage number ranging from 27 to 37. Each exposure was performed in triplicate and within each experiment, all the samples were in duplicate. Three days before exposure, ± 1.10^6 Caco-2 cells were seeded in 21 cm^2 culture dishes with 3 ml supplemented DMEM (Sigma Aldrich) and grown to reach 80 to 90% confluency.

E171 or TiO_2 NPs or TiO_2 MPs, were dispersed in glass tubes at a concentration of 1 mg/ml in supplemented DMEM where FBS was replaced by 0.05% BSA in order to reduce the antioxidant effect of FBS. The solutions were vortexed and subsequently sonicated for 30 minutes at 40 KHz in a bath sonicator (Branson 2200). After sonication, the particles were further dissolved to 0.01 mg/ml in 0.05% BSA supplemented DMEM. Prior to exposure, cells were washed twice with Hank's Balanced Salt Solution (HBSS) without $Ca^{2+}$and Mg^{2+} (Sigma-Aldrich, The Netherlands). Cells were exposed to 3 ml of 0.01 mg/ml TiO_2 NPs, MPs or E171 for 2, 4 or 24 hours which gives a final concentration of 1.43 µg/cm^2. This concentration was previously shown by our group to be non-cytotoxic (10). After exposure, cells were washed with HBSS (without $Ca^{2+}$and Mg^{2+}) once and lysed

using 1 ml Qiazol Lysis Reagent (Qiagen, The Netherlands). The Qiazol cell solution was stored at -80°C until RNA isolation.

II-4- RNA isolation

Total RNA was isolated from Caco-2 cells exposed to TiO_2 NPs, TiO_2 MPs, and E171 in Qiazol (Qiagen, The Netherlands) using the miRNeasy Mini Kit (Qiagen, The Netherlands) according to the manufacturer's protocols for Animal Cells and Animal Tissues including a DNase treatment (27). Total RNA yield as well as the 260/230 and the 260/280 were measured on a Nanodrop® ND-1000 spectrophotometer (Thermo Fischer, The Netherlands). Samples with a 260/230 ratio between 1.8 and 2.0 and a 260/280 ratio between 1.9 and 2.1 were checked for their integrity. The integrity of total RNA was checked using RNA Nanochips on a 2100 Bioanalyzer (Agilent Technologies, The Netherlands). All samples had on average a RNA integrity number (RIN) of 9.5 ± 0.4, which is above 6, the number at which each sample is approved for microarray analysis.

II-5- cRNA synthesis, labelling and hybridization

Total RNA was converted into cRNA and labelled according to the One-Color Microarray-Based Gene Expression Analysis protocol version 6.6 (Agilent Technologies, The Netherlands) (28) as described previously (29). In brief, 200 ng of total RNA was diluted in Spike Mix. The primer and the template were denaturated by using a thermocycler (Tprofessional, Biometra, Germany) at 65°C for 15 minutes. cDNA was synthetized by incubating each sample with cDNA Master Mix in a thermocycler at 40°C for two hours and 70°C for 15 minutes. Afterwards, cRNA was synthetized and labelled by incubating Transcription Master Mix, containing the cyanine 3-CTP dye, with the cDNA at 40°C on a thermocycler for two hours. The RNeasy Mini Kit was used to purify the amplified cRNA samples according to the manufacturer's protocol of Agilent. Subsequently, the cRNA was quantified using a spectrophotometer with the Microarray Measurement function. The yield and specific activity of Cy3 bound to the cRNA was determined using the formulas in the manufacturer's protocol of Agilent.

After incubating cRNA samples with Gene Expression Blocking Agent and Fragmentation Buffer (Agilent Technologies) at 60°C for 30 minutes, hybridization was performed on SurePrint G3 Human GE 8x60k V2 slides and a hybridization oven (Shel Lab, United States) was used at 65°C for 17 hours. After hybridization, the microarray slides were washed with Gene Expression wash buffers (Agilent Technologies, The Netherlands) and scanned using an Agilent DNA Microarray Scanner with Surescan High-resolution Technology (Agilent Technologies, The Netherlands) with scanner settings to Dye Channel:

G, Profile: AgilentG3_GX_1Color, Scan region: Agilent HD (61 x 21.3 mm), Scan resolution 3 µm, Tiff file dynamic range: 20 bit, Red PMT gain: 100%, and Green PMT gain: 100%.

II-6- Pre-processing and data analysis of microarrays

Pre-processing methods used were described previously (14). In short, all samples met the quality criteria of the Feature extraction software (FES) (version 10.7.3.1) from Agilent. An in-house QC pipeline was developed and published (github.com/BiGCAT-UM/arrayQC_Module) to thoroughly check the quality and normalize the data as follows: local background correction, flagging of bad spots, controls and spots without adequate intensity, log2 transformation and quantile normalization. Five samples out of 71 did not pass the quality control the first time. These samples were re-run and were validated by the QC the second time. Raw data that has both expression values and genes were selected for data analysis based on flags and missing values (GEO accession: GSE110410; token: ojstcgeczhktzgx).

First pre-processing was performed with the samples of the time course experiment with NPs. For this, six groups were defined: NPs 2h, 4h, and 24h for the exposed samples and control 2h, 4h, and 24h for the controls. The second pre-processing was split in 2 parts in which the first part was a pre-processing of the NPs 24h with its time-matched control and the second part was a pre-processing of E171 24h and MPs 24h with their time-matched control. The second pre-processing was split in 2 because the experiments were performed independently.

After defining the different groups for the pre-processing, the next steps were exactly the same for all groups. Within each group, probes were flagged for bad spots and at least 30% of all samples had to have good spots. Spot identifiers were deleted when more than 40% of samples in each group had a missing value. Background correction was performed by removing the spot identifiers that had an average expression less than four in all groups. Missing values were imputed by k-nearest neighbours using the standard settings of the GenePattern ImputeMissingValues.KNN module v13 (30). Spot identifiers were annotated to Agilent probe identifiers and merging of exact same probe identifiers with the median method for pre-processing data was performed in Babelomics 5 (31). Next, Agilent probe identifiers were re-annotated to EntrezGeneIDs. Merging of the expression data for all genes with an identical EntrezGeneIDs was done with Babelomics 5 using the median method for pre-processing data.

Differentially expressed genes (DEG) were identified by using a Linear Mixed Model Analysis for Microarrays (LIMMA) (version 1.0) R-script with cut-off values of a fold-change (Log2FC) of 1.2, 1.5, and 1.8 and a p-value of 0.05 (32). The data was paired for replicates. Furthermore, according to the Benjamini-Hochberg method with a threshold at 0.05, the false discovery rate was calculated. With the LIMMA analysis, the number of DEG were identified from each sample; data of the exposed samples were corrected to the data from its time matched control sample.

II-7- Pathway analyses

Over-representation gene set analysis (ORA) was performed with Consensus Pathway Database (CPDB) with the DEG of each time point (33). CPDB is an aggregate of 16 different databases developed by the Max Planck institute and its functionalities have been explained in Nature Protocols (34). CPDB has a focus on molecular interactions, and identifies pathways associated with DEG. For computing the significance of the over-representation of the annotation sets with respect to user-input molecules, CPDB applies Fisher's exact test. For each annotation set, a p-value is calculated. As many annotation sets are tested, CPBD corrects for multiple hypothesis testing using the false discovery rate procedure within each type of annotation set (33,34). All the available databases from CPDB were used (release 32, 1 Nov. 2017) with settings in the “pathways as defined by pathway databases” with a minimum overlap of input list of 2 and a p-value cut-off of $p<0.01$. As shown previously, the pathway analysis is limited to the number of genes that can be mapped to a pathway which is often less than 50% of the input list (14). In order to retrieve the maximal amount of relevant biological information from our gene lists, the corresponding GO terms were also determined.

II-8- Gene Ontology (GO) term classification

GO categories related to the DEG were identified by CPBD. In order to retrieve more biological information, GO terms of level 2, 3, 4, and 5 were selected with a p-value cut off of 0.01. Biological processes of each GO term were retrieved based on GO terminology.

III- Results

III-1- Time course responses to TiO_2 NPs exposure

We first exposed Caco-2 cells to TiO_2 NPs for 2, 4, and 24h to identify what time point would show the most abundant and pronounced transcriptomic response.

III-1-1- Differentially expressed genes (DEG)

After LIMMA, DEG were identified per time point and shown in Table 1 including different fold changes (Log2FC) cut-offs. With a Log2FC ≥ 1.5 and a p-value <0.05, a gradual increase of the number of DEG was observed. This increase was absent with the other Log2FC. Furthermore, when using a less stringent Log2FC like 1.2, noise might be introduced to the gene expression data. With a more stringent Log2FC (1.8), part of the biological effect might be lost. Therefore, the value of 1.5 was used as a cut-off value for Log2FC. Due to the absence of DEG when including an adjusted p-value, the analysis was further performed with a regular p-value of 0.05 and a Log2FC ≥ 1.5. Under these conditions, 234 DEG were found after 2h exposure, which slightly increased after 4h to 242 DEG to increase again after 24h to 281 DEG.

Table 1: DEG per time point after Caco-2 cells exposure to TiO_2 NPs.
A LIMMA test was used in R with a fold change (Log2FC) of >= 1.2, 1.5 or 1.8 and a p-value < 0.05. DEG used for the analysis are shown in bold. |FC| = Fold Change, p.val = p-value, adj.p.val = adjusted p-value.

	Log2FC ≥ 1.2			**Log2FC ≥ 1.5**			**Log2FC ≥ 1.8**		
	2h	**4h**	**24h**	**2h**	**4h**	**24h**	**2h**	**4h**	**24h**
|FC|	3827	5220	3916	806	797	623	253	155	248
Upregulated	2004	2051	1978	595	503	234	214	63	169
Downregulated	1823	3169	1938	211	294	389	39	92	79
p.val < 0.05	532	1991	470	532	470	1991	532	1991	470
adj.p.val < 0.05	0	3	0	0	0	3	0	3	0
|FC| and p.val	434	1532	432	**234**	**242**	**281**	121	88	129
|FC| and adj.p.val	0	3	0	0	0	1	0	1	0

The overlap of DEG between the three time points was visualized using Venn diagrams, showing the overlap of all DEG (Figure 1A), the overlap of upregulated DEG (Figure 1B), and downregulated DEG (Figure 1C) after exposure to TiO_2 NPs for 2, 4, and 24 hours. Not a single gene was differentially expressed at all time points (Figure 1A). There were 11 DEG overlapping between 2 and 4h of exposure, all of which were upregulated (Figure 1B). Two DEG were overlapping between 4 and 24h of which 1 was upregulated and 1 downregulated (Figure 1C) at both time points. Three DEG were overlapping between 2 and 24h of exposure, none of these genes were expressed in the same direction at both time points. All the other DEG were time specific.

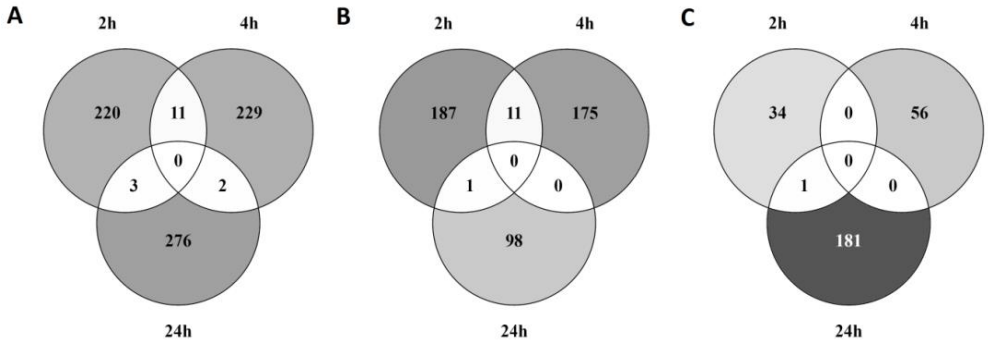

Figure 1: Overlap of DEG over time after exposure to TiO_2 NPs for 2, 4 or 24 hours.
Venn diagrams representing the overlap of (A) all DEG, (B) upregulated DEG and (C) downregulated DEG

III-1-2- Pathway and gene analyses

Using CPDB, the DEG for each time point were integrated in known pathways from different databases. The exposure to TiO_2 NPs led to changes in gene expression that indicate different types of biological processes (Table 2). The result of this analysis is further described below.

After 2h of exposure to TiO_2 NPs, ORA showed that the modulated DEG were involved in pathways related to signal transduction with 7 pathways involved in olfactory, G protein-coupled receptor (GPCR) and other signal transduction. In addition, 2 pathways were associated with the innate immune system containing genes coding for C-type lectin domain, Fc fragment, HLA, and complement system. Two other pathways, vitamin A and retinol metabolism were affected after 2h exposure. These 2 pathways were also implicated in increasing oxidative stress (35). DEG after 2h exposure were also involved in transport of molecules with HTR3B, GABRG2, and 2 solute carrier genes.

After 4h of exposure to TiO_2 NPs, 30 pathways associated to the DEG were observed after ORA. Different biological processes were identified such as signal transduction with 15 pathways involved in olfactory, GPCR, and VEGF signalling and metabolism with 8 pathways related to serotonin, bile acid, peptide hormones, and angiotensin metabolism. In addition, neuronal system was observed with 3 pathways associated to serotonin activity and neuroactive ligand-receptor interaction. Transport of small molecules was a biological function observed after 4h exposure and contained 4 pathways involved in ligand-gated ion channel transport, transport of organic anion, and transport of glucose and other sugars, bile salts and organic acids, metal ions and amine compounds.

After 24h exposure, ORA identified 18 pathways affected after exposure to TiO_2 NPs. These pathways were involved in a various number of biological processes such as signal transduction with 4 pathways related to gastrin-CREB, peptide ligand binding, and GPCR signalling. Metabolism was also observed with 5 pathways including 2 pathways (creatinine and prostaglandin metabolism) involved in a response to oxidative stress (36,37). Neuronal system biological function was also detected with 2 pathways containing genes involved in HCN channels. In addition, 2 pathways were observed in developmental biology including endoderm differentiation, 1 in immune system: negative regulation of MAPK pathway, 1 in cancer: photodynamic therapy-induced HIF-1 survival signalling, 1 in haemostasis, 1 in gene expression (transcription): TP53 regulates transcription of cell cycle genes, and 1 in transport of small molecules: bile salt and organic anion SLC transporters.

Table 2: Pathway over-representation analysis (ORA) of the DEG

Pathways related to the DEG after ORA with ConsensusPathDB. The pathways were grouped per time points and per biological function.

Time of exposure	Biological function	Name of pathway	p-value
2h	Signal Transduction	- Olfactory receptor activity	3.03E-09
		- Olfactory transduction	4.73E-09
		- Olfactory Signalling Pathway	8.72E-09
		- GPCR downstream Signalling	6.47E-07
		- Signalling by GPCR	1.60E-06
		- GPCRs, Class A Rhodopsin-like	0.00518
		- Signal Transduction	0.0125
	Immune system	- *Staphylococcus aureus* infection	0.0113
		- Dectin-2 family	0.0125
	Metabolism	- Vitamin A and Carotenoid Metabolism	0.0297
		- Retinol metabolism	0.0468
	Transport	- Cation-coupled Chloride cotransporters	0.0125
4h	Signal Transduction	- Olfactory Signalling Pathway	1.57E-05
		- Olfactory receptor activity	9.53E-05
		- Olfactory transduction	9.53E-05
		- GPCR downstream Signalling	0.000714
		- Signalling by GPCR	0.000807
		- GPCR Signalling-G alpha i	0.0223
		- GPCR Signalling-pertussis toxin	0.0223
		- VEGF binds to VEGFR leading to receptor dimerization	0.0223
		- VEGF ligand-receptor interactions	0.0223
		- GPCR Signalling-cholera toxin	0.0234
		- GPCR Signalling-G alpha s Epac and ERK	0.0234
		- GPCR Signalling-G alpha q	0.0234
		- VEGF and VEGFR Signalling network	0.0234
		- Signal Transduction	0.0234
		- GPCR Signalling-G alpha s PKA and ERK	0.0234
	Metabolism	- Serotonin and melatonin biosynthesis	0.0127
		- Bile acid and bile salt metabolism	0.029
		- Peptide hormone metabolism	0.029

		-	Synthesis of bile acids and bile salts via 24-hydroxycholesterol	0.029
		-	Biogenic Amine Synthesis	0.037
		-	Metabolism of Angiotensinogen to Angiotensins	0.0389
		-	Primary bile acid biosynthesis	0.0407
		-	Amine-derived hormones	0.044
	Transport	-	Ligand-gated ion channel transport	0.00701
		-	Transport of organic anions	0.0234
		-	Transmembrane transport of small molecules	0.029
		-	Transport of glucose and other sugars, bile salts and organic acids, metal ions and amine compounds	0.0389
	Neuronal system	-	Serotonin and anxiety	0.029
		-	Serotonergic synapse	0.0407
		-	Neuroactive ligand-receptor interaction	0.0446
24h	Signal Transduction	-	Gastrin-CREB Signal Transduction pathway via PKC and MAPK	0.108
		-	Peptide ligand-binding receptors	0.108
		-	Class A/1 (Rhodopsin-like receptors)	0.108
		-	G alpha (i) Signal Transduction events	0.128
	Immune system	-	Negative regulation of MAPK pathway	0.131
	Metabolism	-	Glucocorticoid Receptor Pathway	0.00221
		-	Glycine, serine, alanine and threonine metabolism	0.0207
		-	Creatine metabolism	0.108
		-	Prostaglandin Synthesis and Regulation	0.108
		-	Metabolism of polyamines	0.128
	Transport	-	Bile salt and organic anion SLC transporters	0.128
	Neuronal system	-	TarBasePathway	0.128
		-	HCN channels	0.03
	Cancer	-	Photodynamic therapy-induced HIF-1 survival Signalling	0.128
	Gene expression (Transcription)	-	TP53 Regulates Transcription of Cell Cycle Genes	0.128
	Developmental biology	-	Endoderm Differentiation	0.128
		-	Developmental Biology	0.108
	Haemostasis	-	Haemostasis	0.0382

III-1-3- Comparison of the different time points

No pathways after ORA were common to all time points but 7 were overlapping between 2 and 4h of exposure to TiO_2 NPs and were all related to signal transduction and transport of small molecules (Table 2). No affected pathways were overlapping between 4 and 24h and between 2 and 24h of exposure. Pathways classified according to their biological function showed that signal transduction, metabolism and transport of small molecules were common to all time points. In addition, between 2 and 24h molecular changes were observed in the immune system.

The same affected biological processes were observed when the GO terms associated to the DEG were analysed. Over time, the number of GO terms observed increased from 43 GO terms after 2h of exposure, to 54 GO terms after 4h and 111 GO terms after 24h (Figure 2A). Overlap was observed between 2 and 4h with 20 GO terms involved in cellular response to stimulus, membrane, nervous system, receptor activity, signal transduction, and system process. Only one GO term was overlapping between 4 and 24h, regulation of secretion. However, when the GO terms were classified according to their biological function, more overlap was observed. Figure 2B shows the different biological processes per time point with 12 after 2h exposure, 12 after 4h and 26 after 24h. Of these 26 biological processes after 24h exposure, 5 were in common with 2 and 4h: cellular response to stimulus, nervous system, membrane, metabolism, immune system, 4 GO terms between 4 and 24h: transport of small molecules, response to stress, secretion, and response to stimulus, and 1 GO term between 2 and 24h: reproduction.

The results show the most abundant and diverse gene expression and pathway changes after 24h exposure, for which reason we choose this time point to establish gene expression responses following MPs and E171 exposure.

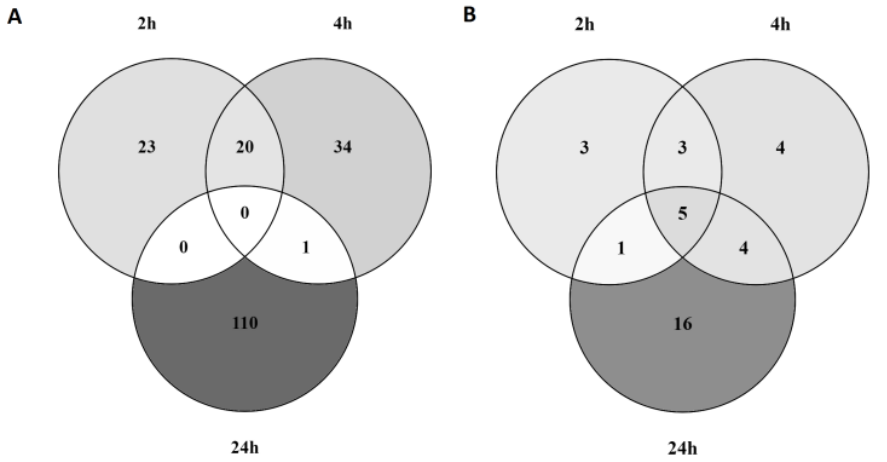

Figure 2: Overlap of GO terms and their biological processes over time.
Venn diagram representing A: the number of GO terms in common between 2, 4, and 24h exposure to TiO_2 NPs, and B: the associated biological processes to the GO terms in common between 2, 4, and 24h exposure to TiO_2 NPs.

III-2- Comparison of responses to different sizes of TiO_2

III-2-1- Differentially expressed genes (DEG)

In order to compare the gene expression responses induced by different fractions of E171, Caco-2 cells were also exposed to E171 and MPs for 24h. Table 3 shows the number of DEG identified after LIMMA with the same Log2FC and p-value cut-offs used for the time course with TiO_2 NPs. After exposure to E171, the number of DEG was 3 times greater than after MPs and NPs exposure. As explained in the Materials and Methods, a new pre-processing was done on NPs with its time-matched control.

Figure 3 shows that the DEG after exposure to the different sizes of TiO_2 were mostly specific to each fraction, only a few genes were in common. One DEG was in common after MPs and NPs exposure: LGALS14, a galectin gene. Two DEG were in common between the NPs and E171 exposure: TCP11X2, a T-complex family gene and KCCAT333, a renal clear cell carcinoma-associated transcript but the exact function of these 2 genes remains unknown. When comparing the DEG after MPs and E171 exposure, 3 DEG were observed: WDR78, LOC401478, and ANKRD26P3. WDR78 gene is shown to be a target of the hedgehog activity. LOC401478 and ANKRD26P3 have unknown functions.

Table 3: DEG after exposure of Caco-2 cells to different TiO_2 particles for 24h.
A LIMMA test was used in R with a fold change (Log2FC) of >= 1.5 and a p-value < 0.05 after *in vitro* exposure to E171, MPs, and NPs of TiO_2. The number of DEG used for further analysis is shown in bold.
|FC| = Log2 Fold Change, p.val = p-value, adj.p.val = adjusted p-value.

	NPs	MPs	E171
|FC| >= 1.5	415	365	1040
Upregulated	148	136	63
Downregulated	267	229	977
p.val < 0.05	664	459	1198
adj.p.val < 0.05	0	0	0
|FC| and p.val	**121**	**121**	**365**
|FC| and adj.p.val	0	0	0

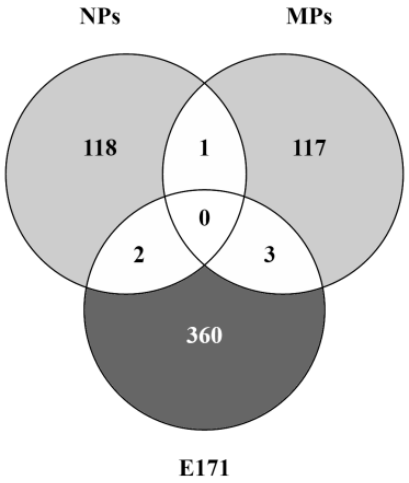

Figure 3: Unique and common DEG between E171 and the different size fractions of TiO_2.
Venn diagram showing the overlap of DEG after exposure of Caco-2 cells to E171, MPs, and NPs for 24h.

III-2-2- Pathway and gene analyses

III-2-2-1- E171 exposure

ORA showed that after E171 exposure, 9 pathways involved in signal transduction were observed; 4 of them were related to GPCR, 3 to olfactory signalling, 1 to signal transduction and 1 to bone morphogenic protein signalling (Table 4). In addition, gene expression was affected in one pathway involved in haemostasis (endothelins), one in neuronal system (dopaminergic neurogenesis), one in metabolism of proteins (insulin processing), and another one in transport of small molecules (zinc efflux by solute carriers family). In addition, gene analysis showed biological effects on the immune system with 34 DEG including BCL10, CD274, COLEC10, defensin, and IFI27 genes. Gene expression in metabolism was also influenced by E171 exposure with a total of 22 DEG including genes involved in ATP binding, cytochrome P450, bile acid, and prostaglandin. With 13 DEG involved in cholinergic receptor, calcium channels, potassium channels, and glutamate receptor, neuronal system was also affected by E171 exposure. The gene expression (transcription) biological function was altered by 12 DEG such as MTERF1 (mitochondrial transcription), SMURF1 (ubiquitin related gene), HIST1H3I (histone cluster), zinc finger genes, and TP53I11 (tumour protein p53 inducible protein 11). With 10 DEG each, 2 biological processes were modulated, cellular responses to external stimuli with genes coding for prostaglandin protein, histone cluster, and heat shock protein and disease with NAG20, NRG1, SLA2, CSNK1A1L (signalling by WNT in cancer). E171 exposure also affected, with less than 10 DEG each, gene expression in other biological processes such as metabolism of RNA, DNA repair, cell cycle, muscle contraction, extracellular matrix organization, organelle biogenesis and maintenance, cell-cell communication, chromatin organization, circadian clock, DNA replication, programmed cell death, and reproduction.

III-2-2-2- MPs exposure

ORA showed that after MPs exposure, signal transduction was affected by the modulation of gene expression in 2 olfactory pathways. In addition, pathways involved in developmental biology were observed, mostly involved in the myogenesis (Table 4). Gene analysis showed that after exposure to MPs for 24h, gene expression was also affected in the immune system with defensins, interleukins, THRIL, BTC, TIMP4, and MPEG1 genes. In addition, 8 genes were related to transport of small molecules and vesicle-mediated transport (solute carriers, ABCG4, CLIC2, KIF25, MYH13 and LCN9). One DEG, up-regulated after MPs exposure, was found to be up-regulated in presence of oxidative stress (UCP1) (38). Cancer development was observed by the modulation of genes involved in cell death (HIST1H1T, CASP14, and DNAJC3), cancer related genes (WNT8A and CASC8), gene expression (transcription) (ZNF570 and ZFP42), and metabolism of proteins (CALB2 and

KLHDC3). Three DEG were found to be related to the extracellular matrix organisation (COL17A1, ARC, and TIMP4). Six others were modulated in the developmental biology biological function (CDH4, KRT14, POU3F3, NTN3, RGMA, and HFE2), 3 DEG in metabolism (ARG1, TPH2, and PNPLA2), and one DEG in neuronal system (CHRNA3).

III-2-2-3- NPs exposure

As shown in Table 3, the new pre-processing was statistically more stringent. More than 90% of the DEG of the pre-processing of 24h only was also present in the time course analysis. A pathway and gene analysis were performed with the 121 DEG of the new pre-processing and compared to the one performed with the 281 DEG of the time course analysis. The biological response after NPs exposure after 24h exposure was similar to the 24h time point described in the time course with pathways involved in HCN channels, transport of small molecules, and 5 metabolism pathways including creatinine and prostaglandin also involved in response to oxidative stress response (Table 4).

Table 4: Pathways associated with the DEG after NPs, MPs and E171 exposure
ORA analysis performed with CPDB on all the DEG after NPs, MPs and E171 exposure *in vitro* for 24h.

Time of exposure	Biological function	Name of pathway	p-value
E171	Signal Transduction	- GPCR downstream signalling	1.09E-08
		- Signalling by GPCR	3.75E-07
		- Olfactory Signalling Pathway	2.05E-06
		- Olfactory transduction - Homo sapiens (human)	3.36E-05
		- Olfactory receptor activity	6.69E-05
		- GPCR ligand binding	0.000236
		- Signal Transduction	0.000461
		- G alpha (q) signalling events	0.00222
		- Bone Morphogenic Protein (BMP) Signalling and Regulation	0.00845
	Transport of small molecules	- Zinc efflux and compartmentalization by the SLC30 family	0.00406
	Neuronal system	- Dopaminergic Neurogenesis	0.0004

	Developmental Biology	-	Interaction between L1 and Ankyrins	0.0041
	Haemostasis	-	Endothelins	0.00989
	Metabolism of proteins	-	Insulin processing	0.00406
MPs	Signal Transduction	-	Olfactory Signalling Pathway	0.0579
		-	Olfactory transduction	0.0579
	Developmental Biology	-	CDO in myogenesis	0.0654
		-	Myogenesis	0.0654
		-	Netrin-1 signalling	0.0775
NPs	Metabolism	-	Glycine, serine, alanine and threonine metabolism	0.000543
		-	Creatine metabolism	0.000789
		-	Urea cycle and metabolism of amino groups	0.00514
		-	Glucocorticoid Receptor Pathway	0.00541
		-	Prostaglandin Synthesis and Regulation	0.00861
	Neuronal system	-	HCN channels	8.60E-05
		-	TarBasePathway	0.00126
		-	Potassium Channels	0.00689
	Transport of small molecules	-	Amino acid transport across the plasma membrane	0.00926

III-2-3- Common and specific biological reactions

Pathways extracted after ORA showed no common response between all the particles, all pathways were specific to each fraction. However, Figure 4A shows that, after E171 and NPs exposure, 2 biological processes were in common: transport of molecules and neuronal system. After E171 and MPs exposure, signal transduction and developmental biology were common processes affected by gene expression changes. Both signal transduction pathways are related to the olfactory transduction.

Specific biological processes related to the DEG were also observed after NPs exposure: metabolism and response to stress. All biological processes after MPs exposure were common to E171 exposure. After E171 exposure, 2 specific biological reactions were observed: haemostasis and metabolism of proteins.

Figure 4B shows that one biological process extracted from the GO terms was common between the different types of TiO_2, which is cellular response to stimuli. Furthermore, after E171 and NPs exposure gene expression was affected in 2 common biological processes: Transport and Membrane. Other common effects on gene expression were identified after E171 and MPs exposure in signal transduction, system processes, and neuronal system. After MPs and NPs exposure DEG were observed in the Binding biological process.

After NPs exposure, specific biological processes extracted from the GO terms of the DEG were related to metabolism, haemostasis, oxidative stress, and regulation of biological process. Two specific biological processes were observed after MPs exposure: reproduction and extracellular matrix organisation. The number of biological processes observed after E171 exposure was increased compared to NPs and MPs with receptor activity, immune system, DNA repair, muscle adaptation, catalytic activity, organ development, and transcription factor.

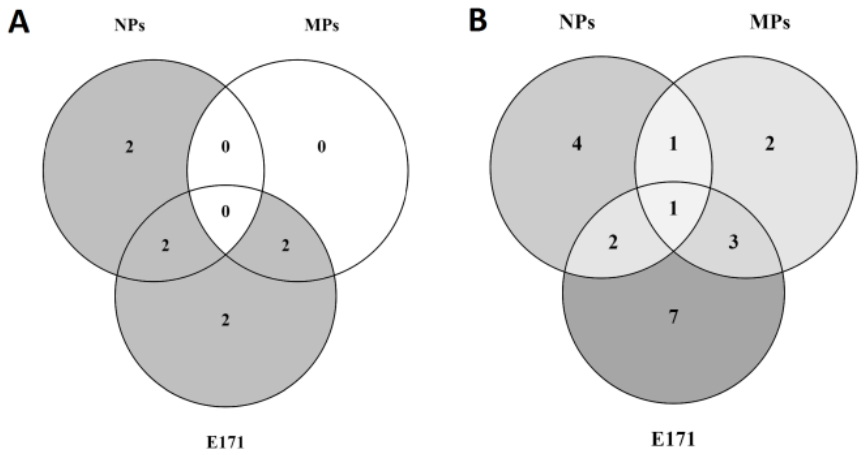

Figure 4: Overlap of the biological processes between the different sizes of TiO_2
Venn diagram showing after exposure of Caco-2 cells to E171, MPs, and NPs for 24h A: the overlap of biological processes after ORA, B: the overlap of the biological processes related to the GO terms.

IV- Discussion

The aim of this study was to assess the gene expression changes in colonic cells after *in vitro* exposure to E171 and the contribution of the NPs and MPs fractions to these changes based on transcriptome analysis in Caco-2 cells. First the optimal time point for the evaluation of gene expression responses was established to be 24 hours because this time point showed the highest number of DEG and affected pathways. Subsequently, cells were also exposed for 24 hours to MPs and E171.

IV-1- Time course responses to TiO_2 NPs exposure

Previous studies showed the capacity of TiO_2 NPs to induce significant levels of oxidative stress in a cell-free environment as well as *in vitro* in Caco-2 and in human amnion epithelial (WISH) cells (8,10,23-25). After exposure of colonic cells to NPs, we observed gene expression changes related to oxidative stress and oxidative stress response. These genes were observed after 4h with the up-regulation of a protein coding gene (GML) involved in cellular response to stress and heat shock response and after 24h with 2 DEG (TUBB2B and SCML4) involved in cellular response to stress, oxidative stress induced senescence and in a heat shock protein (HSP90) chaperone cycle. Oxidative stress is one of the factors that can induce DNA damage. Previously, we reported that TiO_2 NPs induced significant levels of DNA damage after exposure to TiO_2 NPs in Caco-2 cells, Caco-2/HT29-MTX co-culture system, and WISH cells (8,10,23-25). In line with previous studies, the present study shows that, after 4h exposure, 4 DEG (HAP1, GML, SPIDR, and REM1) were found to be involved in DNA damage and DNA repair. Two DEG were involved in the mechanisms of DNA repair activity either via a p53-target gene (GML) (39) or via homologous recombination (SPIDR). Furthermore, HAP1 is known to be activated after DNA damage (40) and REM1 expression is also shown to be modulated in CRC samples (41).

Exposure to TiO_2 NPs induced gene expression changes related to the immune system. These changes start to manifest after 2h of exposure with the modulation of the expression of C4B and C3AR1 genes from the complement system as well as HLA-DRB5 gene involved in TCR signalling. After 4h of exposure, no pathways involved in immune system were associated with the DEG, however, at the GO term level, cytokine production and tumour necrosis factor were observed. After exposure to TiO_2 NPs for 24h, similar effects to 2 and 4h exposure on the immune system were observed like on the innate immune system. In addition, specific gene expression changes related to IL-1 production, leukocyte migration, and chemokine signalling were observed. This suggests an impact of

the exposure on the innate and adaptive immune system. Regarding the effects of TiO_2 NPs on the immune system, 24h exposure was the most pronounced time point by including a majority of the 2 and 4h exposure effects including additional 24h effects. Effects of TiO_2 NPs *in vivo* demonstrated that these NPs impact the immune response via a potent Th1/Th17 immune response after exposure to 10 mg/kg_{bw}/day in rats of P25 TiO_2 (13), or via a spleen injury in mice resulting from the reduction of the immune capacity (17), or via a thymus injury in mice via a reduction of WBC in blood and CD3+, CD4+, CD8+, B cells and NK cells in thymus (42). Our results show that the induction of the immune response by TiO_2 NPs might not only be induced in immune related organs as seen *in vivo* but also as a consequence of direct exposure of intestinal epithelium cells.

Gene expression changes in transport of small molecules and vesicle-mediated transport were observed by changes in gene expression of solute carrier genes from 2h exposure with 3 DEG, to 4h and 24h exposure with 7 DEG each. In addition, 2 cadherin genes, which play a role with cargo proteins in clathrin-independent endocytosis (43), differentially expressed (4h: CDH18, 24h: PCDH9). Induction of genes in transport pathways may be explained by the small size and high surface area of TiO_2 NPs. Previous experiments showed that TiO_2 NPs can enter the cells as well as the nucleus (24,25,44) and suggest that solute carriers and endocytosis might be two mechanisms by which the particles enter the cells (44-46).

Overall, Figure 2 shows that after 24h exposure to TiO_2 NPs, the gene expression changes were partly similar to other time points but also more diverse. Therefore, 24h exposure was chosen to be the optimal time of exposure for the comparison of the different particles of TiO_2. Effects of MPs and E171 at the molecular levels as well as the contribution of each fraction in these effects will be described below.

IV-2- Gene expression responses to MPs of TiO_2

Like for the NPs, we have shown that MPs also induce oxidative stress after 1h exposure in a cellular environment (10). In our current study we find a significant up-regulation of UCP1, a gene with a very strong link to mitochondrial oxidative stress and DNAJC3, related to endoplasmic reticulum stress. UCP encodes for uncoupling proteins which limits ROS production in the mitochondrial respiratory chain after being stimulated by superoxide anions(47,48). DNAJC3 encodes for a protein involved in the unfolded protein response during endoplasmic reticulum stress (49). Oxidative stress and cellular stress observed after MPs exposure might explain the induction of DNA damage previously observed after exposure of Caco-2 cells to TiO_2 MPs (10). In the current study, a gene expression change of one histone gene (HIST1H1T) was observed, which is involved

in DNA repair (50,51). In addition, after exposure to TiO_2 MPs, DEG related to cancer, cell death, and gene expression (transcription) were observed like WNT8A and CASC8 which are highly correlated with CRC development and progression (52,53). Furthermore, CASP14, a potent pro-apoptotic gene but also potentially involved in cell differentiation (54) and RD3 a down-regulated gene normally expressed in the colon while loss is associated with the development of neuroblastoma and potentially other cancers (55) were observed. After exposure to TiO_2 MPs, gene expression changes seem to point towards facilitation of cancer.

Like exposure to TiO_2 NPs, also the MPs affected gene expression changes in relation to the immune system with the down-regulation of pro-inflammatory cytokine receptor IL-6R involved in the MAPK1 and MAPK3 activation and also in response to oxidative stress (56). Other genes involved in the innate immune system such as defensins, interleukins, THRIL, BTC, TIMP4, and MPEG1 were up- or down-regulated after exposure to TiO_2 MPs. TiO_2 MPs ingested in the diet via E171 were previously suspected to induce a pro-inflammatory and immune response which could increase the symptoms of inflammatory bowel disease via the NLRP3 inflammasome (57) or when MPs are bound to Pathogen Associated Molecular Patterns (PAMPs) in the gastrointestinal lumen (58).

Gene expression changes were observed in transport of small molecules and vesicle-mediated transport with 7 DEG. Within these 7 DEG, ABCG4, a gene coding for a protein in the ATP-binding cassette (ABC) transporter superfamily which transport various molecules across extra- and intra-cellular membranes, and LCN9 gene which is involved in the transport of glucose and other sugars, bile salts and organic acids, metal ions and amine compounds pathway were down- and up-regulated respectively. The results suggest a misbalance of the efflux pumps which, correlated to induction of oxidative stress, may lead to accumulation of superoxide in exposed cells (59).

IV-3- Responses to E171

Also after exposure to E171, the modulation of 2 genes (PTGES3 and HIST1H3I) related to cellular response to stress, oxidative stress induced senescence and cellular response to heat stress was observed. The exposure to E171 induced gene expression changes towards the development of inflammation which can also lead to DNA damage. Like for the NPs and MPs, DNA damage was previously described after exposure to E171 (10). In the present study, 4 DEG (POLB, NEIL3, POLD2 and LIG4) involved in DNA repair were modulated like POLB involved in base excision and repair and POLD2 in DNA replication and repair. NEIL3 encodes for DNA glycosylases which cleaves bases damaged

by ROS (60). The protein coded by LIG4 is essential in DNA double-strand break repair through non-homologous end joining. In our study, cancer related genes, which can be modulated as a consequence of DNA damage, were also observed like down-regulation of CELF2, a putative tumour suppressor, which is normally expressed in normal intestinal tissues but downregulated in colon tumour tissues (61). In addition, NRG1 is involved in constitutive signalling by aberrant PI3K in cancer, CSNK1A1L in signalling by WNT in cancer, and MUCL1 in defective GALNT12 causes colorectal cancer.

Exposure to E171 affected resulted in 31 DEG that were associated with the immune system. These DEG were involved in innate and adaptive immune system. The effects of E171 on the expression of genes of the immune system *in vitro* are in line with previous *in vivo* studies in which impairment of the immune system was observed. After ingestion of 5 mg/kg_{bw}/day of E171 for 2, 7, 14, and 21 days, BALB/c mice showed an impairment of the immune system based on gene expression (14). One immune related gene was commonly down-regulated in both *in vitro* and in the *in vivo* experiment, BCL10. It is involved not only in different processes in the immune system but also in protein ubiquitination and haemostasis. Another study described an impairment of the immune system via a Th1/Th7 response after exposure to 10 mg/kg_{bw}/day in rats for 7 and 100 days (13). The dysregulation of the immune system is a known factor that can lead to the development of cancer.

IV-4- Contribution of each TiO_2 fraction to the gene expression changes after E171 exposure

As shown above, several biological processes observed after E171 exposure were commonly induced by the MPs and NPs fraction such as gene expression changes in oxidative stress, DNA repair, immune system, and transport. Furthermore, some other effects observed after E171 were also identified after NPs and MPs exposure and associated to signal transduction.

In addition to common effects in gene expression in the immune system with the 3 types of TiO_2, specific effects of NPs and E171 were observed in TLR cascade, advanced glycolysation, the MHC class I antigen processing and presentation and MHC class II presentation, and cytokine signalling with IL-1, IL-17, and IL-20. In addition, 3 DEG involved in potassium channels were modulated. Changes in potassium channel expression are associated with colon carcinogenesis, however, it is not clearly defined whether those changes are inducing the development of cancer or a consequence reflecting dedifferentiation and ongoing proliferation (62).

GO term analysis showed that Membrane was also observed as a common biological process after the NPs and E171 exposure. Within this biological process, 1 DEG after NPs and 1 DEG after E171 exposure were both coding for a late cornified envelope protein and both down-regulated. The cornified envelope is a structure which is responsible for the major barrier function of the skin (63). Whether it plays a role in other epithelia barrier functions such as in the intestines is unknown. A dysregulation of the genes coding for these proteins might have a consequence on the integrity of the barrier in the gut and allow particles to pass through.

Exposure to NPs and E171 also induced gene expression changes in the cell cycle. The up-regulation of TUBB1 after NPs exposure involved in G2-G2/M and M phases and the down-regulation of HIST1H3I after E171 exposure also involved in M phase show a potential incidence of the TiO_2 exposure on the regulation of cell cycle. Effects of titanium dioxide on the G2/M phase were already observed by Wu et al. who showed that anatase TiO_2 NPs (25, 50, 100, and 200 µg/ml) in neuronal cells induced p53 and JNK activation in G2/M cell cycle arrest and apoptosis (64).

After E171 and MPs exposure, specific biological processes and 3 DEG were commonly observed. Two out of three DEG have unknown function but WDR78 gene is shown to be a target of the Hedgehog activity and a promotor of FOXJ1 activity in zebrafish (65). FOXJ1 is involved in the production of the motile cilia. In relation to the immune system, MPs and E171 affected gene expression in relation with the α-defensins including DEFA6 after MPs exposure and DEFA4 after E171 exposure were up- and down-regulated respectively. Normally present in epithelial cells, the defensins are antimicrobial peptides contributing to the mucosal host defence by the action of permeabilization of the microbe membrane (66). Gene expression changes after MPs and E171 exposure were associated with signalling, notably olfactory signalling. After MPs exposure, 2 DEG involved in cell junction organisation were modulated and 1 DEG after E171 exposure. More precisely 2 DEG (E171: CDH18 and MPs: CDH4) were both coding for cadherin surface proteins. These proteins not only play an important role in endocytosis but also cellular adhesion and intercellular liaison between the cells (67). These results might identify one of the mechanisms by which TiO_2 can enter the cell. In the neuronal system, 2 CHRNA genes, 1 after MPs and 1 after E171 exposure, were modulated and coding for cholinergic receptors. Cholinergic receptors are normally present in Caco-2 cells and after production of acetylcholine by the cells, a common effect in colorectal cells, the cholinergic receptor are affected and its dysregulation might be associated with inflammation and tumour development (68,69).

A majority of the effects after exposure to E171 could be associated to the effects of the NPs and MPs fractions. However, some effects could only be attributed to the E171 itself. At the pathway level, metabolism of proteins with the insulin processing pathway and haemostasis were specific to E171 exposure. Effects in the expression of insulin genes were also observed *in vivo* by several groups (14,70). At the GO term level, receptor activity, muscle adaptation, catalytic activity, organ development, and transcription factor were specific to E171 exposure. In addition, at the gene expression level, changes were observed in metabolism of RNA, chromatin organization, circadian clock, and programmed cell death. For these specific effects of E171, it should be taken into consideration that the NPs and MPs used do not fully cover the range of E171.

IV-5- Comparison to the previous in vivo transcriptomics study

Common to the *in vitro* exposure to E171, a study on ingestion of E171 in the mouse (14) also found an effect on the mRNA levels in the colon related to oxidative stress, DNA repair, immune system, transport as well as signal transduction, neuronal system, and extracellular matrix organisation. In addition, the expression of seven orthologue genes affected after *in vivo* exposure were also found *in vitro* and were representative of the major effects of E171: immune system (BCL10, TNFAIP8L2, LRRC15), inflammation (LRRC15), signal transduction (TAS2R3), metabolism (BAAT, TNFAIP8L2, and BCL10), and cancer (WDR78). The WDR78 gene has been shown to be in the top 20 of hypermethylated genes in CRC (71). The downregulation of the mRNA of WDR78 in our study corresponds to hypermethylation of the gene. Furthermore, WDR78 is also significantly downregulated after exposure to TiO_2 MPs. The fraction of TiO_2 which affect this gene might be the MPs fraction indicating that despites the higher size of MPs, MPs could also induce gene expression changes in relation to cancer.

V- Conclusion

The present study provides an overview of the major effects on gene expression after exposure to E171 and its different fractions. These effects include signalling, inflammation, immune system, transport, and cancer. The gene expression changes associated with the immune system and inflammation induced by E171, MPs, and NPs suggest the creation of a favourable environment for cancer development. Gene expression changes associated with oxidative stress are in line with previous observation of ROS formation in Caco-2 cells and *in vivo* transcriptomics analysis on colons of mice after oral administration of E171 (14). Taken together, these results indicate that the classification of E171 as an inert particle is not valid and that NPs induce a more pronounced effect at the transcriptome level than MPs.

References

1. Weir, A., Westerhoff, P., Fabricius, L., Hristovski, K., and von Goetz, N. (2012) Titanium dioxide nanoparticles in food and personal care products. *Environmental science & technology*, **46**, 2242-2250.
2. Peters, R.J., van Bemmel, G., Herrera-Rivera, Z., Helsper, H.P., Marvin, H.J., Weigel, S., Tromp, P.C., Oomen, A.G., Rietveld, A.G., and Bouwmeester, H. (2014) Characterization of titanium dioxide nanoparticles in food products: analytical methods to define nanoparticles. *J Agric Food Chem*, **62**, 6285-6293.
3. Lomer, M.C.E., Thompson, R.P.H., Commisso, J., Keen, C.L., and Powell, J.J. (2000) Determination of titanium dioxide in foods using inductively coupled plasma optical emission spectrometry. *Analyst*, **125**, 2339-2343.
4. EU (2012) Regulation No 231-2012 on food additives. *Official Journal of the European Union*.
5. FAO, and WHO (1969) TOXICOLOGICAL EVALUATION OF SOME FOOD COLOURS, EMULSIFIERS, STABILIZERS, ANTI-CAKING AGENTS AND CERTAIN OTHER SUBSTANCES. *FAO Nutrition Meetings Report Series* **No. 46A WHO/FOOD ADD/70.36**.
6. FAO, and WHO (1970) Specification for the identity and purity of food additives and their toxicological evaluation. *World Health Organization technical report series No. 445, FAO nutrition meetings report series No. 46*.
7. FDA (2014) Listing of color additives exempt from certification. TITLE 21--FOOD AND DRUGS; CHAPTER I--FOOD AND DRUG ADMINISTRATION. *Code of Federal Regulations*, **21CFR73.1575**.
8. Dorier, M., Beal, D., Marie-Desvergne, C., Dubosson, M., Barreau, F., Houdeau, E., Herlin-Boime, N., and Carriere, M. (2017) Continuous in vitro exposure of intestinal epithelial cells to E171 food additive causes oxidative stress, inducing oxidation of DNA bases but no endoplasmic reticulum stress. *Nanotoxicology*, 1-54.
9. Dudefoi, W., Moniz, K., Allen-Vercoe, E., Ropers, M.H., and Walker, V.K. (2017) Impact of food grade and nano-TiO2 particles on a human intestinal community. *Food Chem Toxicol*, **106**, 242-249.
10. Proquin, H., Rodriguez-Ibarra, C., Moonen, C.G., Urrutia Ortega, I.M., Briede, J.J., de Kok, T.M., van Loveren, H., and Chirino, Y.I. (2017) Titanium dioxide food additive (E171) induces ROS formation and genotoxicity: contribution of micro and nano-sized fractions. *Mutagenesis*, **32**, 139-149.
11. Yang, Y., Doudrick, K., Bi, X.Y., Hristovski, K., Herckes, P., Westerhoff, P., and Kaegi, R. (2014) Characterization of Food-Grade Titanium Dioxide: The Presence of Nanosized Particles. *Environmental science & technology*, **48**, 6391-6400.
12. Urrutia-Ortega, I.M., Garduno-Balderas, L.G., Delgado-Buenrostro, N.L., Freyre-Fonseca, V., Flores-Flores, J.O., Gonzalez-Robles, A., Pedraza-Chaverri, J., Hernandez-Pando, R., Rodriguez-Sosa, M., Leon-Cabrera, S., Terrazas, L.I., van Loveren, H., and Chirino, Y.I. (2016) Food-grade titanium dioxide exposure exacerbates tumor formation in colitis associated cancer model. *Food Chem Toxicol*, **93**, 20-31.
13. Bettini, S., Boutet-Robinet, E., Cartier, C., Comera, C., Gaultier, E., Dupuy, J., Naud, N., Tache, S., Grysan, P., Reguer, S., Thieriet, N., Refregiers, M., Thiaudiere, D., Cravedi, J.P., Carriere, M., Audinot, J.N., Pierre, F.H., Guzylack-Piriou, L., and Houdeau, E. (2017) Food-grade TiO2 impairs intestinal and systemic immune homeostasis, initiates preneoplastic lesions and promotes aberrant crypt development in the rat colon. *Sci Rep*, **7**, 40373.
14. Proquin, H., Jetten, M.J., Jonkhout, M.C.M., Garduno-Balderas, L.G., Briede, J.J., de Kok, T.M., Chirino, Y.I., and van Loveren, H. (2018) Gene expression profiling in colon of mice exposed to food additive titanium dioxide (E171). *Food Chem Toxicol*, **111**, 153-165.

15. Hu, R., Zheng, L., Zhang, T., Gao, G., Cui, Y., Cheng, Z., Cheng, J., Hong, M., Tang, M., and Hong, F. (2011) Molecular mechanism of hippocampal apoptosis of mice following exposure to titanium dioxide nanoparticles. *J Hazard Mater*, **191**, 32-40.
16. Yang, J., Luo, M., Tan, Z., Dai, M., Xie, M., Lin, J., Hua, H., Ma, Q., Zhao, J., and Liu, A. (2017) Oral administration of nano-titanium dioxide particle disrupts hepatic metabolic functions in a mouse model. *Environ Toxicol Pharmacol*, **49**, 112-118.
17. Sheng, L., Wang, L., Sang, X., Zhao, X., Hong, J., Cheng, S., Yu, X., Liu, D., Xu, B., Hu, R., Sun, Q., Cheng, J., Cheng, Z., Gui, S., and Hong, F. (2014) Nano-sized titanium dioxide-induced splenic toxicity: a biological pathway explored using microarray technology. *J Hazard Mater*, **278**, 180-188.
18. Wang, J., Zhou, G., Chen, C., Yu, H., Wang, T., Ma, Y., Jia, G., Gao, Y., Li, B., Sun, J., Li, Y., Jiao, F., Zhao, Y., and Chai, Z. (2007) Acute toxicity and biodistribution of different sized titanium dioxide particles in mice after oral administration. *Toxicology letters*, **168**, 176-185.
19. Brun, E., Barreau, F., Veronesi, G., Fayard, B., Sorieul, S., Chaneac, C., Carapito, C., Rabilloud, T., Mabondzo, A., Herlin-Boime, N., and Carriere, M. (2014) Titanium dioxide nanoparticle impact and translocation through ex vivo, in vivo and in vitro gut epithelia. *Particle and fibre toxicology*, **11**, 13.
20. Chen, Z., Wang, Y., Wang, X., Zhuo, L., Chen, S., Tang, S., Zhao, L., Luan, X., and Jia, G. (2018) Effect of titanium dioxide nanoparticles on glucose homeostasis after oral administration. *J Appl Toxicol*.
21. Ruiz, P.A., Moron, B., Becker, H.M., Lang, S., Atrott, K., Spalinger, M.R., Scharl, M., Wojtal, K.A., Fischbeck-Terhalle, A., Frey-Wagner, I., Hausmann, M., Kraemer, T., and Rogler, G. (2017) Titanium dioxide nanoparticles exacerbate DSS-induced colitis: role of the NLRP3 inflammasome. *Gut*, **66**, 1216-1224.
22. Nogueira, C.M., de Azevedo, W.M., Dagli, M.L., Toma, S.H., Leite, A.Z., Lordello, M.L., Nishitokukado, I., Ortiz-Agostinho, C.L., Duarte, M.I., Ferreira, M.A., and Sipahi, A.M. (2012) Titanium dioxide induced inflammation in the small intestine. *World J Gastroenterol*, **18**, 4729-4735.
23. Gerloff, K., Albrecht, C., Boots, A.W., Forster, I., and Schins, R.P.F. (2009) Cytotoxicity and oxidative DNA damage by nanoparticles in human intestinal Caco-2 cells. *Nanotoxicology*, **3**, 355-364.
24. Saquib, Q., Al-Khedhairy, A.A., Siddiqui, M.A., Abou-Tarboush, F.M., Azam, A., and Musarrat, J. (2012) Titanium dioxide nanoparticles induced cytotoxicity, oxidative stress and DNA damage in human amnion epithelial (WISH) cells. *Toxicol In Vitro*, **26**, 351-361.
25. Shukla, R.K., Sharma, V., Pandey, A.K., Singh, S., Sultana, S., and Dhawan, A. (2011) ROS-mediated genotoxicity induced by titanium dioxide nanoparticles in human epidermal cells. *Toxicol In Vitro*, **25**, 231-241.
26. Faust, J.J., Doudrick, K., Yang, Y., Westerhoff, P., and Capco, D.G. (2014) Food grade titanium dioxide disrupts intestinal brush border microvilli in vitro independent of sedimentation. *Cell Biol Toxicol*, **30**, 169-188.
27. Qiagen (2012) RNeasy Mini Handbook. *https://www.qiagen.com/us/resources/resourcedetail?id=14e7cf6e-521a-4cf7-8cbc-bf9f6fa33e24&lang=en*.
28. Agilent (2015) One-Color Microarray-Based Gene Expression Analysis. *http://www.agilent.com/cs/library/usermanuals/Public/G4140-90040_GeneExpression_OneColor_6.9.pdf*.
29. Jiang, J., Mathijs, K., Timmermans, L., Claessen, S.M., Hecka, A., Weusten, J., Peters, R., van Delft, J.H., Kleinjans, J.C.S., Jennen, D.G.J., and de Kok, T.M. (2017) Omics-based identification of the combined effects of idiosyncratic drugs and inflammatory cytokines on the development of drug-induced liver injury. *Toxicol Appl Pharmacol*, **332**, 100-108.

30. Reich, M., Liefeld, T., Gould, J., Lerner, J., Tamayo, P., and Mesirov, J.P. (2006) GenePattern 2.0. *Nature genetics*, **38**, 500-501.
31. Alonso, R., Salavert, F., Garcia-Garcia, F., Carbonell-Caballero, J., Bleda, M., Garcia-Alonso, L., Sanchis-Juan, A., Perez-Gil, D., Marin-Garcia, P., Sanchez, R., Cubuk, C., Hidalgo, M.R., Amadoz, A., Hernansaiz-Ballesteros, R.D., Aleman, A., Tarraga, J., Montaner, D., Medina, I., and Dopazo, J. (2015) Babelomics 5.0: functional interpretation for new generations of genomic data. *Nucleic Acids Res*, **43**, W117-121.
32. Smyth, G.K. (2005) Limma: linear models for microarray data. *Bioinformatics and computational biology solutions using R and Bioconductor*. Springer, pp. 397-420.
33. Kamburov, A., Stelzl, U., Lehrach, H., and Herwig, R. (2013) The ConsensusPathDB interaction database: 2013 update. *Nucleic Acids Res*, **41**, D793-800.
34. Herwig, R., Hardt, C., Lienhard, M., and Kamburov, A. (2016) Analyzing and interpreting genome data at the network level with ConsensusPathDB. *Nat Protoc*, **11**, 1889-1907.
35. Dal-Pizzol, F., Klamt, F., Benfato, M.S., Bernard, E.A., and Moreira, J.C.F. (2001) Retinol supplementation induces oxidative stress and modulates antioxidant enzyme activities in rat sertoli cells. *Free Radical Res*, **34**, 395-404.
36. Basu, S., Michaelsson, K., Olofsson, H., Johansson, S., and Melhus, H. (2001) Association between oxidative stress and bone mineral density. *Biochem Bioph Res Co*, **288**, 275-279.
37. Araujo, M.B., Moura, L.P., Vieira, R.C., Junior, M.C., Dalia, R.A., Sponton, A.C., Ribeiro, C., and Mello, M.A.R. (2013) Creatine supplementation and oxidative stress in rat liver. *J Int Soc Sport Nutr*, **10**.
38. Bouillaud, F., Alves-Guerra, M.C., and Ricquier, D. (2016) UCPs, at the interface between bioenergetics and metabolism. *Bba-Mol Cell Res*, **1863**, 2443-2456.
39. Tanaka, H., Arakawa, H., Yamaguchi, T., Shiraishi, K., Fukuda, S., Matsui, K., Takei, Y., and Nakamura, Y. (2000) A ribonucleotide reductase gene involved in a p53-dependent cell-cycle checkpoint for DNA damage. *Nature*, **404**, 42-49.
40. Walker, L.J., Craig, R.B., Harris, A.L., and Hickson, I.D. (1994) A role for the human DNA repair enzyme HAP1 in cellular protection against DNA damaging agents and hypoxic stress. *Nucleic Acids Res*, **22**, 4884-4889.
41. Barresi, V., Castorina, S., Musso, N., Capizzi, C., Luca, T., Privitera, G., and Condorelli, D.F. (2017) Chromosomal instability analysis and regional tumor heterogeneity in colon cancer. *Cancer Genet-Ny*, **210**, 9-21.
42. Hong, F., Zhou, Y., Zhou, Y., and Wang, L. (2017) Immunotoxic effects of thymus in mice following exposure to nanoparticulate TiO2. *Environ Toxicol*, **32**, 2234-2243.
43. Grant, B.D., and Donaldson, J.G. (2009) Pathways and mechanisms of endocytic recycling. *Nature reviews. Molecular cell biology*, **10**, 597-608.
44. Cai, K., Hou, Y., Hu, Y., Zhao, L., Luo, Z., Shi, Y., Lai, M., Yang, W., and Liu, P. (2011) Correlation of the cytotoxicity of TiO2 nanoparticles with different particle sizes on a sub-200-nm scale. *Small*, **7**, 3026-3031.
45. Steffansen, B., Nielsen, C.U., Brodin, B., Eriksson, A.H., Andersen, R., and Frokjaer, S. (2004) Intestinal solute carriers: an overview of trends and strategies for improving oral drug absorption. *Eur J Pharm Sci*, **21**, 3-16.
46. des Rieux, A., Fievez, V., Garinot, M., Schneider, Y.J., and Preat, V. (2006) Nanoparticles as potential oral delivery systems of proteins and vaccines: A mechanistic approach. *J Control Release*, **116**, 1-27.
47. Rial, E., and Zardoya, R. (2009) Oxidative stress, thermogenesis and evolution of uncoupling proteins. *J Biol*, **8**, 58.
48. Robbins, D., and Zhao, Y. (2011) New aspects of mitochondrial Uncoupling Proteins (UCPs) and their roles in tumorigenesis. *Int J Mol Sci*, **12**, 5285-5293.

49. Petrova, K., Oyadomari, S., Hendershot, L.M., and Ron, D. (2008) Regulated association of misfolded endoplasmic reticulum lumenal proteins with P58/DNAJc3. *EMBO J*, **27**, 2862-2872.
50. Hunt, C.R., Ramnarain, D., Horikoshi, N., Iyengar, P., Pandita, R.K., Shay, J.W., and Pandita, T.K. (2013) Histone modifications and DNA double-strand break repair after exposure to ionizing radiations. *Radiat Res*, **179**, 383-392.
51. Rossetto, D., Avvakumov, N., and Cote, J. (2012) Histone phosphorylation: a chromatin modification involved in diverse nuclear events. *Epigenetics*, **7**, 1098-1108.
52. Yao, K.H., Hua, L., Wei, L.S., Meng, J.M., and Hu, J.H. (2015) Correlation Between CASC8, SMAD7 Polymorphisms and the Susceptibility to Colorectal Cancer An Updated Meta-Analysis Based on GWAS Results. *Medicine*, **94**.
53. Polakis, P. (2007) The many ways of Wnt in cancer. *Current opinion in genetics & development*, **17**, 45-51.
54. Pistritto, G., Jost, M., Srinivasula, S.M., Baffa, R., Poyet, J.L., Kari, C., Lazebnik, Y., Rodeck, U., and Alnemri, E.S. (2002) Expression and transcriptional regulation of caspase-14 in simple and complex epithelia. *Cell Death Differ*, **9**, 995-1006.
55. Aravindan, S., Somasundaram, D.B., Kam, K.L., Subramanian, K., Yu, Z., Herman, T.S., Fung, K.M., and Aravindan, N. (2017) Retinal Degeneration Protein 3 (RD3) in normal human tissues: Novel insights. *Sci Rep*, **7**, 13154.
56. Atreya, R., Mudter, J., Finotto, S., Mullberg, J., Jostock, T., Wirtz, S., Schutz, M., Bartsch, B., Holtmann, M., Becker, C., Strand, D., Czaja, J., Schlaak, J.F., Lehr, H.A., Autschbach, F., Schurmann, G., Nishimoto, N., Yoshizaki, K., Ito, H., Kishimoto, T., Galle, P.R., Rose-John, S., and Neurath, M.F. (2000) Blockade of interleukin 6 trans signaling suppresses T-cell resistance against apoptosis in chronic intestinal inflammation: evidence in crohn disease and experimental colitis in vivo. *Nature medicine*, **6**, 583-588.
57. Becker, H.M., Bertschinger, M.M., and Rogler, G. (2012) Microparticles and their impact on intestinal immunity. *Dig Dis*, **30 Suppl 3**, 47-54.
58. Powell, J.J., Thoree, V., and Pele, L.C. (2007) Dietary microparticles and their impact on tolerance and immune responsiveness of the gastrointestinal tract. *Brit J Nutr*, **98**, S59-S63.
59. Dorier, M., Brun, E., Veronesi, G., Barreau, F., Pernet-Gallay, K., Desvergne, C., Rabilloud, T., Carapito, C., Herlin-Boime, N., and Carriere, M. (2015) Impact of anatase and rutile titanium dioxide nanoparticles on uptake carriers and efflux pumps in Caco-2 gut epithelial cells. *Nanoscale*, **7**, 7352-7360.
60. Bandaru, V., Sunkara, S., Wallace, S.S., and Bond, J.P. (2002) A novel human DNA glycosylase that removes oxidative DNA damage and is homologous to Escherichia coli endonuclease VIII. *DNA Repair (Amst)*, **1**, 517-529.
61. Ramalingam, S., Ramamoorthy, P., Subramaniam, D., and Anant, S. (2012) Reduced Expression of RNA Binding Protein CELF2, a Putative Tumor Suppressor Gene in Colon Cancer. *Immunogastroenterology*, **1**, 27-33.
62. Heitzmann, D., and Warth, R. (2008) Physiology and pathophysiology of potassium channels in gastrointestinal epithelia. *Physiol Rev*, **88**, 1119-1182.
63. Kalinin, A.E., Kajava, A.V., and Steinert, P.M. (2002) Epithelial barrier function: assembly and structural features of the cornified cell envelope. *Bioessays*, **24**, 789-800.
64. Wu, J., Sun, J.A., and Xue, Y. (2010) Involvement of JNK and P53 activation in G2/M cell cycle arrest and apoptosis induced by titanium dioxide nanoparticles in neuron cells. *Toxicology letters*, **199**, 269-276.
65. Yu, X., Ng, C.P., Habacher, H., and Roy, S. (2008) Foxj1 transcription factors are master regulators of the motile ciliogenic program. *Nature genetics*, **40**, 1445-1453.
66. Bevins, C.L., Martin-Porter, E., and Ganz, T. (1999) Defensins and innate host defence of the gastrointestinal tract. *Gut*, **45**, 911-915.

67. Shapiro, L., and Weis, W.I. (2009) Structure and biochemistry of cadherins and catenins. *Cold Spring Harb Perspect Biol*, **1**, a003053.
68. Cheng, K., Samimi, R., Xie, G., Shant, J., Drachenberg, C., Wade, M., Davis, R.J., Nomikos, G., and Raufman, J.P. (2008) Acetylcholine release by human colon cancer cells mediates autocrine stimulation of cell proliferation. *Am J Physiol Gastrointest Liver Physiol*, **295**, G591-597.
69. M. Pelissier-Rota, M. Lainé, B. Ducarouge, and, B.B., and M. Jacquier-Sarlin (2013) Role of Cholinergic Receptors in Colorectal Cancer: Potential Therapeutic Implications of Vagus Nerve Stimulation? *Journal of Cancer Therapy*, **4**, 1116-1131.
70. Hu, H., Guo, Q., Wang, C., Ma, X., He, H., Oh, Y., Feng, Y., Wu, Q., and Gu, N. (2015) Titanium dioxide nanoparticles increase plasma glucose via reactive oxygen species-induced insulin resistance in mice. *J Appl Toxicol*, **35**, 1122-1132.
71. Kim, Y.H., Lee, H.C., Kim, S.Y., Yeom, Y.I., Ryu, K.J., Min, B.H., Kim, D.H., Son, H.J., Rhee, P.L., Kim, J.J., Rhee, J.C., Kim, H.C., Chun, H.K., Grady, W.M., and Kim, Y.S. (2011) Epigenomic analysis of aberrantly methylated genes in colorectal cancer identifies genes commonly affected by epigenetic alterations. *Ann Surg Oncol*, **18**, 2338-2347.

Chapter 7

Summary and general discussion

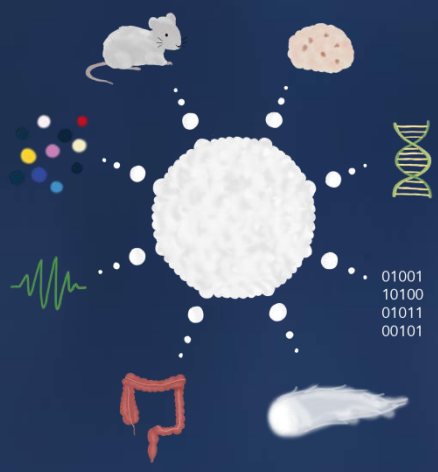

Colorectal cancer (CRC) is the second most prevalent cancer in women with 614,000 cases (9.2% of the total number of cancer cases) and the third in men with 746,000 cases (10.0% of the total number of cancer cases) in 2012 worldwide (1). Strong evidence was found between dietary factors and cancer risks (2). The consumption of milk and whole grains products may have a protective role against CRC (2) whereas consumption of red and processed meat may increase cancer risks by stimulating the endogenous formation of carcinogenic N-nitroso compounds (NOCs) and the presence of pyrolysis products like polycyclic aromatic hydrocarbons (PAHs) heterocyclic amines (3). In recent years, concerns about the potential adverse effects of titanium dioxide (TiO_2) as food additive are rising in scientific literature. Two different crystal forms are authorised in food products: anatase and rutile. Due to lower production costs, anatase is the form the most commonly used in food and mostly studied. The anatase TiO_2 food additive is designated E171. The food additive E171 comprises between 25-40% of NPs (<100 nm) and 60-75% of microparticles (MPs) (>100 nm) (4-7).

Exposure to TiO_2 by ingestion of food and products containing TiO_2 occurs on a daily basis and several studies showed that people of all ages from infant to elderly are exposed (7-10). Exposure to TiO_2 happens as a consequence of the ingestion of many food products like dairy products (milk, cheese, and ice cream), milk replacements (powdered milk), sweets (M&M's®, Mentos®, chewing-gums, and cookies), drinks (soft drinks, sport drinks, and syrups), dressings and sauces (salad dressings), and food supplements (multivitamin pills) (7-11).

In vivo studies after ingestion of E171 show an increased tumour formation and the growth of aberrant crypt foci in a chemically induced CRC mouse and rat models respectively (12,13). Furthermore, in normal BALB/c mice exposed to 5 mg/kg_{bw}/day of E171, dysplastic changes in the colonic epithelium and a decrease of goblet cells were observed (13). In addition, after ingestion of 10 mg/kg_{bw}/day of E171 in rats for 7 days a Th1/Th17 immune deviation as well as an impairment of the intestinal homeostasis was observed (12). In the same study, the identical effects on the immune response and intestinal homeostasis were observed after ingestion of 10 mg/kg_{bw}/day of anatase TiO_2 nanoparticles (NPs). The NPs have a smaller size (<100 nm) and a higher surface area, therefore, these particles are assumed to have the most adverse effects. Consequently, a majority of the studies on adverse effects of TiO_2 have been performed with the anatase NPs fraction. After *in vivo* and *in vitro* exposure to TiO_2 NPs, observations of effects towards a facilitation of the development of cancer were supported by findings of an increased oxidative stress (4,14), an induction of DNA damage (4,15-17), and an

impairment of the immune system (18,19). In addition, an *in vivo* study on the adverse effects of rutile NPs showed an inflammatory response via cytokine production or NLRP3 inflammasome in the gut (20).

Emerging evidence of adverse effects of TiO_2 have raised concerns about the safe use of TiO_2. Therefore, the International Agency for Research in Cancer (IARC) evaluated TiO_2 in 2010 based on new findings (21). Human epidemiological studies on inhalation were assessed and the agency decided that the data available was inadequate to draw a conclusion whether or not TiO_2 causes cancer in humans. Animal studies on inhalation were also evaluated and the IARC concluded that there was convincing evidence of an increase of lung tumours. Other routes of administration (ingestion and dermal contact) did not show an increase incidence of tumours. Subsequent to the results of these studies, the IARC classified TiO_2 as possible carcinogen to humans (Group 2B). The modes of action underlying these adverse effects like kinetics, *in vivo* and *in vitro* genotoxicity, cytotoxicity, presence of inflammation, and penetration of TiO_2 through the skin have also been taken into consideration for the evaluation. The evidence was not strong enough to warrant classification other than Group 2B.

Traditionally toxicity testing of products and compounds was only based on only animal testing with a specific end-point. Currently, *in silico* methods are added to the animal testing to evaluate mechanistic changes in biological processes using biopsies, cells, and organs. Advances in bioinformatics, epigenetics, toxicogenomics, systems biology, and computational toxicology are transforming the toxicological assessment of compounds. The combination of these scientific advances with animal testing with a specific end-point are expected to generate more robust data on the potential risks to humans and offering the prospect of improved risk-based regulatory decision (22,23). Therefore, elucidating the molecular mechanisms behind the adverse effects of E171 is becoming an important step for food safety evaluation. Mechanistic toxicology or toxicogenomics, through the identification and interpretation of significant gene expression changes, may play an important role in linking cellular response to toxicological endpoints (22,23). Within the realm of toxicogenomics, a technique available is the high-throughput analysis of biological systems: whole-genome mRNA microarrays used for transcriptomics analysis.

We aimed in this thesis to 1) better understand the potential risks of the TiO_2 food additive E171 by studying the molecular mechanisms of facilitation of CRC as well as the histopathological changes observed after exposure to E171 *in vivo* and 2) to assess the relative contribution of the different fractions of E171 to the adverse effects *in vitro*. For these purposes, we applied transcriptomics analyses in combination with markers of cytotoxicity, genotoxicity and oxidative stress.

I- Potential risks of ingestion of TiO_2

I-1- In vivo studies

In order to answer the first research question of this thesis, gaining insight in the mechanisms of facilitation of CRC as well as the pathological changes observed after exposure to E171, 3 *in vivo* studies were performed. All *in vivo* experiments were performed with the food additive E171. To optimise the evaluation of the mechanisms behind the adverse effects of E171, common conditions of exposure *in vivo* were chosen in this thesis i.e. sample preparation, type of ingestion, time points of sampling, and types of samples for microarray analysis. The time points chosen were based on the long term exposure performed by Urrutia-Ortega et al. (13). A significant increased number of tumours in the distal colon was observed in the chemically induced CRC mouse model with azoxymethane (AOM) and dextran sodium sulphate (DSS) additionally exposed to 5 mg/kg_{bw}/day of E171 for 10 weeks. In the same study, in the mice solely exposed to E171, dysplastic changes in colonic epithelium and a decrease of goblet cells were observed. The tumours arise after 3 weeks of exposure to E171 in combination with AOM/DSS, therefore, 4 time points were chosen before tumours arise at 2, 7, 14, and 21 days. Transcriptomics changes were determined in the distal colon of mice at each time point, where the tumours were previously found. All *in vivo* experiments were performed in these conditions with the same concentration of E171 given by intragastric administration: 5 mg/kg_{bw}/day. Only in the mouse model of **Chapter 4**, 2 additional concentrations 1 and 2 mg/kg_{bw}/day were used. Three mouse models were chosen: a normal BALB/c model (**Chapter 2**), a chemically induced CRC model with AOM/DSS (**Chapter 3**), and a transgenic Cre-LoxP with Car-1 promoter model (**Chapter 4**).

In the study described in **Chapter 2**, we aimed to unravel the mechanisms underlying the pathological changes observed by Urrutia-Ortega et al. after sole exposure to E171 (13). Normal BALB/c mice were exposed to E171 and gene expression changes were observed as well as histopathology in the distal colons. Histopathological analysis showed alteration and disruption in the normal structure of crypts inducing a hyperplastic

epithelium. At the mRNA level, significant gene expression changes were observed in oxidative stress, the immune system, the olfactory/GPCR receptor family and of cancer related genes.

A majority of the biological effects observed in the normal BALB/c mice (**Chapter 2**) were also observed in the experiment described in **Chapter 3**, a study aiming to understand the mechanisms behind the development of tumours observed by Urrutia-Ortega et al. (13) in a chemically induced CRC model after E171 ingestion. Similar affected biological processes in normal BALB/c (**Chapter 2**) and in the CRC mouse models (**Chapter 3**) were observed including the downregulation of genes involved in the immune system, suggesting an impairment of this system. Also changes in the oxidative stress and olfactory/GPCR receptor family were found in both normal and CRC models. In addition, in the experiment in which mice were stimulated to form tumours by AOM/DSS described in **Chapter 3**, significant changes in the mRNA levels were identified for genes involved in biotransformation of xenobiotics which can form reactive intermediates resulting in toxicological effects.

In the study described in **Chapter 4** which was aiming to confirm the results observed in normal BALB/c (**Chapter 2**) and in the CRC mouse models (**Chapter 3**) in a transgenic mouse model that spontaneously develops colorectal tumours, similar biological processes affected after E171 exposure were observed. In this model the Cre-LoxP with Car-1 promoter leads to spontaneous colon cancer formation in 26% of the animals. An increase of the number of tumours per mice and the number of mice with tumours was observed after exposure to 5 mg/kg_{bw}/day. Furthermore, after exposure to 1 mg/kg_{bw}/day of E171, gene expression changes were observed genes involved in cell cycle, signalling, cancer, DNA repair, gene expression (transcription), the immune system, and inflammation pathways.

Gene expression changes related to signal transduction, immune system, oxidative stress, and cancer-related genes reflect early biological responses induced by E171 which precede tumour formation in an AOM/DSS mouse model (13) and are in line with the pathological changes observed in the colon of rats and mice after E171 exposure (12,13). In addition, modulation of genes involved in the immune system is in line with a recent study which described an impairment of the intestinal immune homeostasis after oral exposure to E171 for one week (12).

It should be mentioned that transcriptomics analysis is still limited to the current knowledge of the functionality of genes and their involvement in pathways. Indeed, in this thesis, we report changes in genes that have thus far not been classified in known pathways but may induce functional changes by interacting with other genes involved in known biological pathways. Moreover, accumulation of E171 in other organs than the gastrointestinal tract can induce diverse effects like reduced fertility (24), decreased glucose levels in blood (25,26), and formation of ROS and DNA damage in different organs (15-17).

I-2- in vitro studies

In order to address the second aim of this thesis, the relative contribution of the different fractions of E171 to the adverse effects, 2 *in vitro* studies were performed. Effects of the MPs and NPs fraction of E171 have been assessed *in vitro* using Caco-2 cells in **Chapter 5 and 6**. From the biological effects observed, the relative contribution of the different sizes *in vivo* may be inferred. First, in **Chapter 5**, the cytotoxicity of the E171, NPs, and MPs was studied with a Trypan blue test, the genotoxicity with comet assay and micronucleus test, and the capacity to induce oxidative stress by electron spin spectroscopy. Results showed that E171 was cytotoxic to Caco-2 cells from a concentration of 14.3 µg/cm² whereas NPs and MPs was cytotoxic at a concentration of 143 µg/cm² suggesting that the combination of NPs and MPs in E171 was more cytotoxic than the NPs and MPs separately. In addition, E171 and NPs induced reactive oxygen species (ROS) formation in a cell-free environment whereas MPs induced ROS in presence of Caco-2 cells after 1h exposure. Chromosome damage was shown to be induced by E171, as tested with the micronucleus assay. In addition, single-strand DNA damage was observed for all 3 different TiO_2 suggesting that both NPs and MPs fractions contribute to the adverse effects of E171. In line with our results, MPs were also found to induce oxidative stress in RAW 264 cells after 4h of exposure (27). More recently, the capacity of E171 to induce ROS formation and DNA damage was confirmed in Caco-2 and Caco-2/HT29-MTX cells (4). In addition, the capacity of TiO_2 NPs to induce oxidative stress is also reported in several cell lines like mouse fibroblast, mouse peritoneal macrophages (RAW 264), goldfish skin cells (GFSk-S1), human bronchial epithelial (BEAS-2B) cells, human bronchial fibroblasts (IMR 90), human foetal osteoblast cell, human amnion epithelial (WISH), glial, brain microglia, and human epidermal cells (16,27-39). In addition, Charles et al. evaluated a number of studies that had an appropriate level of confidence suitable for regulatory context i.e. studies with adequate characterization of TiO_2, adequate description of the dispersion and genotoxicity protocols, evidence of cytotoxicity, inclusion of positive and negative results, and use of replicates or independent experiments (27).

The 36 studies assessed showed that 58% of the comet assays reported positive results as well as 56% of the micronucleus assay after exposure to anatase TiO_2 NPs. These results show that potential *in vivo* genotoxic effects might be underestimated, therefore, further evaluation needs to be performed by *in vivo* studies in combination with genotoxic tests on different organs.

Because of its small size and higher surface area, the NPs fraction is suspected to be the most active fraction. Therefore, after a time course exposure with TiO_2 NPs *in vitro* to determine the best exposure time, exposure to E171 and MPs was performed in **Chapter 6**. At the optimal time point, 24h, gene expression changes in Caco-2 cells exposed to NPs, MPs and E171 were established. Overall effects after E171, NPs, or MPs exposure *in vitro* were gene expression changes related to signalling, inflammation, immune system, and cancer. The results showed that E171 induces more changes at the mRNA level than the MPs or NPs fractions. In addition, in **Chapter 6,** effects of NPs and E171 exposure suggested that some similar biological processes were affected: TLR cascade, MHC class I and II presentation, late cornified envelope, potassium channels and cell cycle. In addition, after exposure to MPs and E171, identical affected biological processes were observed: Hedgehog family, α-defensins, cadherin and cholinergic receptors. Most studies on TiO_2 are based on the NPs fraction of E171, but as shown in the *in vitro* studies on the relative contribution of the NPs and MPs fraction to the effects of E171 (**Chapter 5 and 6)**, the MPs fraction can also induce adverse effects. Even if the NPs induced more pronounced effect at the transcriptome level compared to the MPs, both fractions included in E171 should be assessed. The gene expression changes related to signalling, inflammation, immune system, and cancer confirm previous findings described in normal BALB/c mice (**Chapter 2**), CRC mouse model (**Chapter 3**), and transgenic mouse model (**Chapter 4**). Furthermore, the immune response genes affected after exposure to TiO_2 in Caco-2 cells shows that this biological process might not only be induced in combination with other organs as seen *in vivo* in BALB/c mice, CRC mouse model, and transgenic mouse model but also as a consequence of direct exposure of intestinal epithelium cells.

I-3- Additional biological processes

In the studies described in this thesis, we have also demonstrated that the adverse effects induced by E171 are very diverse. In addition to processes mentioned above in normal BALB/c mice (**Chapter 2**), in CRC mouse model (**Chapter 3**), and in transgenic mouse model (**Chapter 4**), we also describe gene expression changes in Cyp450 genes, metabolism, insulin metabolism, transport of molecules, and bone development. In the colon of normal BALB/c mice exposed to E171, mRNA was described to be modulated in pathways indicating calcium mobilisation, cell cycle, and metabolism of RNA. In the colon of CRC mice exposed to E171, transcriptome changes in bile metabolism, digestive system, haemostasis, metabolism of xenobiotics, extracellular matrix organisation, muscle contraction, and translocation were also observed. In the colon of the transgenic mice exposed to E171, gene expression changes identified related to circadian clock, endocrine system, cell cycle, haemostasis, metabolism of xenobiotics, and extracellular matrix organisation. Furthermore, in the *in vitro* experiment with Caco-2 cells exposed to E171, NPs, or MPs (**Chapter 6**) additional biological processes were also observed. Gene expression changes in neuronal system and transport of small molecules were also reported after NPs exposure. After MPs exposure, additional affected biological processes were in developmental biology. After E171 exposure, modulation of mRNA levels in metabolism of proteins, developmental biology, transport of small molecules and haemostasis were observed.

Overall, the diversity of molecular mechanisms influenced by E171 in colon shows that E171 is not inert and the adverse effects may not only contribute to cancer development in colon but may also aggravate inflammatory bowel diseases.

II- Relevance to the human situation

The concentrations used during the *in vivo* and *in vitro* studies described in this thesis and aimed to represent the actual human exposure. Weir et al. showed that adults (>10 years old) are exposed to 0.2-0.7 mg/kg_{bw}/day in the US and 1 mg/kg_{bw}/day in the UK (7). A Dutch study estimated an average exposure of 0.17 mg/kg_{bw}/day of TiO_2 (11). A higher exposure has been estimated by the EFSA in their re-evaluation of TiO_2: 2.4 mg/kg_{bw}/day (8). The quantity of TiO_2 ingested in children is higher than in adults because of the higher quantities of sweets and cookies eaten by the children as well as ingestion of toothpaste. The estimated ingestion of TiO_2 for children (<10 years old) in US is 1-2 mg TiO_2/kg_{bw}/day and in UK 2-3 mg TiO_2/kg_{bw}/day (7). In addition, the Dutch estimation was of 0.67 mg TiO_2/kg_{bw}/day between 2-6 years old (11) and the EFSA estimated the ingestion at 5.5 mg/kg_{bw}/day for children between 3-9 years old (8).

The highest concentration used in this thesis was 5 mg/kg_{bw}/day which is in the same range as the human exposure, closer to the children exposure. In the study described in **Chapter 4**, 3 different concentrations of E171 were studied and the strongest effects were observed with the lowest concentration (1 mg/kg_{bw}/day) compared to 2 and 5 mg/kg_{bw}/day. The lowest concentration used in this **Chapter 4** is the closest to the US, UK, and Dutch estimation for adults and lower than the one from the EFSA.

As for the relevance of the *in vitro* concentrations to the human situation, a conservative estimate was performed in **Chapter 5**. In this scenario, a 70 kg adult was assumed to eat 1 mg/kg_{bw}/day. In the 250 g faeces excreted, the concentration of E171 would be 0.28 mg/g of faeces. As faeces contain 75% of water and if we consider the density of faeces to be similar as water, the concentration of E171 would be 0.28 mg/mL of faeces. By assuming that 1% of this is biologically available, 0.0028 mg/mL would be potentially the concentration in contact with the gut cells. The concentration used in **Chapter 5 and 6** were 0.01 and 0.001 mg/mL. These concentrations are in the same order of magnitude as the estimated concentration in humans and were first tested to be non-cytotoxic in Caco-2 cells (**Chapter 5**).

The estimated daily exposure and the conservative scenario do not include exposure to TiO_2 via the ingestion of pharmaceutical pills. Depending on the properties of the pill, they could dissolve in very different parts of the gastrointestinal track. One can therefore assume that the intestinal epithelium can be exposed to higher concentration of TiO_2 depending on the pill ingested in addition to E171.

III- Conclusions and future perspectives

The results of this thesis show the complexity of the response to the exposure to E171. Whole-genome gene expression analysis on colonic tissue as well as in vitro testing indicated mechanisms by which E171 may enhance tumour formation (13). Transcriptome changes have demonstrated the presence of oxidative stress, DNA damage, impairment of the immune system, and activation of cancer-related genes as a consequence of exposure to E171, which may collectively represent the molecular mode of action that explains the stimulation of colorectal tumour formation. Moreover, the information provided by this thesis indicates that the relative contribution of each fraction to these effects is different. The NPs fraction by its small size and higher surface area seems to induce more adverse effects than the MPs. Yet, the fact that MPs have an effect on ROS, DNA damage, and gene expression changes implies that potential health risks cannot be eliminated by increasing the proportion of MPs in E171.

The results of this thesis generated more insight of the potential adverse effects following oral exposure to E171. However, for a full risk assessment, additional experiments should be performed. It is important to establish causality between the gene expression changes and processes leading to CRC development, which requires the *in vivo* investigation of the functionality of the immune system, inflammation, oxidative stress, and DNA damage. Such studies may be also done according to the Organisation for Economic Co-operation and Development (OECD) guidelines for regulatory purposes. Repeated dose 28-day and 90-day oral toxicity studies in rodents should be performed. In order to have more insight in the effects of exposure on the immune system, an extended one generation reproductive toxicity study should be performed, which includes exposure during all life stages of the animals, and includes a specific cohort of animals tested for developmental immunotoxicity.

Additional *in vitro* and *in vivo* experiments would help to extrapolate the enhancement of tumour growth observed in the animal studies to real life exposures, i.e. consumers ingesting E171. Additional *in vitro* models like co-cultures of different cells and cell lines (e.g. Caco-2 and macrophages) or 3D models with normal human colon organoids and spheroids can serve for this purpose. The consistency found between different *in vitro* models with the combination of several human cell lines allows a closer understanding of the human situation and therefore improving the extrapolation. Eventually, a randomized controlled intervention study in humans on E171 ingestion should be performed, in which gene expression profiles in the colon would be analysed. Such information would

substantiate the relevance of the *in vitro* findings and animal data, and provide the definitive proof of adverse effects of ingestion in the population. The totality of the evidence, including dose response relationships of the endpoint and intermediate measures in animals, *in vitro* studies, and studies on early effects in humans will provide a more solid base for estimating the risk of colon tumour enhancement after intake of E171.

In order to further advance our insight in mechanisms underlying the effects, novel technologies could be applied. All finding described in this thesis are based on microarray analysis, however, the use of technologies such as sequencing may be instrumental for this purpose. This technique allows more in depth as well as quantitative analyses of effects of TiO_2 on the expression of mRNA, transcript isoforms, non-coding RNA, and circular RNA. In addition, modulation of miRNAs expression can lead to upregulation of miRNA involved in cancer or downregulation of tumour suppressors which would enhance cancer development (39). Such regulators of cancer-related processes can be identified by miRNA-sequencing in blood and colon tissue of animals and humans after exposure to E171 and would contribute to the understanding of mechanisms behind the enhancement of CRC by E171. Furthermore, time-series analysis would help to identify gene expression patterns over time and dose which allows for evaluation the mechanisms underlying the effects following oral exposure to E171. Applying Dose-Time Network Identification (DTNI) tool for data analysis would provide more in depth information on inferring molecular key events and may detect novel interaction which can be studied experimentally by silencing these genes (40).

Based on the new information presented in this thesis, we conclude that the classification of E171 as free from toxic effects on the account of its insolubility and inertness is no longer valid. Furthermore, the results of this thesis indicate the presence of inflammation that was found in animal models after E171 ingestion could aggravate inflammatory bowel diseases and potential adverse effects towards enhancement of colorectal cancer. Therefore, we recommend that the experiments described here above, with an emphasis on actual testing in humans, should be performed for a further evaluation of E171 on its potential adverse effects on the enhancement of cancer, dysregulation of the immune system, and inflammation. These new data would provide insight on the effects on humans for a full risk assessment which can lead to a modification of the use of E171 in food products. These modifications may be a reduction of the quantity of NPs, establishing a maximum level of use in food products, a stricter limitation in the types of products it can be used in, or a banishment of the product itself.

References

1. Globocan (2012) CANCER FACT SHEETS: COLORECTAL CANCER.
2. Vieira, A.R., Abar, L., Chan, D.S.M., Vingeliene, S., Polemiti, E., Stevens, C., Greenwood, D., and Norat, T. (2017) Foods and beverages and colorectal cancer risk: a systematic review and meta-analysis of cohort studies, an update of the evidence of the WCRF-AICR Continuous Update Project. *Ann Oncol*, **28**, 1788-1802.
3. Aykan, N.F. (2015) Red meat subtypes and colorectal cancer risk. *International journal of cancer. Journal international du cancer*, **137**, 1788.
4. Dorier, M., Beal, D., Marie-Desvergne, C., Dubosson, M., Barreau, F., Houdeau, E., Herlin-Boime, N., and Carriere, M. (2017) Continuous in vitro exposure of intestinal epithelial cells to E171 food additive causes oxidative stress, inducing oxidation of DNA bases but no endoplasmic reticulum stress. *Nanotoxicology*, 1-54.
5. Dudefoi, W., Moniz, K., Allen-Vercoe, E., Ropers, M.H., and Walker, V.K. (2017) Impact of food grade and nano-TiO2 particles on a human intestinal community. *Food Chem Toxicol*, **106**, 242-249.
6. Yang, Y., Doudrick, K., Bi, X.Y., Hristovski, K., Herckes, P., Westerhoff, P., and Kaegi, R. (2014) Characterization of Food-Grade Titanium Dioxide: The Presence of Nanosized Particles. *Environmental science & technology*, **48**, 6391-6400.
7. Weir, A., Westerhoff, P., Fabricius, L., Hristovski, K., and von Goetz, N. (2012) Titanium dioxide nanoparticles in food and personal care products. *Environmental science & technology*, **46**, 2242-2250.
8. EFSA (2016) Scientific Opinion on the re-evaluation of titanium dioxide (E 171) as a food additive. *EFSA Journal*, **14**, 4545-4638.
9. Lomer, M.C.E., Thompson, R.P.H., Commisso, J., Keen, C.L., and Powell, J.J. (2000) Determination of titanium dioxide in foods using inductively coupled plasma optical emission spectrometry. *Analyst*, **125**, 2339-2343.
10. Peters, R.J., van Bemmel, G., Herrera-Rivera, Z., Helsper, H.P., Marvin, H.J., Weigel, S., Tromp, P.C., Oomen, A.G., Rietveld, A.G., and Bouwmeester, H. (2014) Characterization of titanium dioxide nanoparticles in food products: analytical methods to define nanoparticles. *J Agric Food Chem*, **62**, 6285-6293.
11. Rompelberg, C., Heringa, M.B., van Donkersgoed, G., Drijvers, J., Roos, A., Westenbrink, S., Peters, R., van Bemmel, G., Brand, W., and Oomen, A.G. (2016) Oral intake of added titanium dioxide and its nanofraction from food products, food supplements and toothpaste by the Dutch population. *Nanotoxicology*, **10**, 1404-1414.
12. Bettini, S., Boutet-Robinet, E., Cartier, C., Comera, C., Gaultier, E., Dupuy, J., Naud, N., Tache, S., Grysan, P., Reguer, S., Thieriet, N., Refregiers, M., Thiaudiere, D., Cravedi, J.P., Carriere, M., Audinot, J.N., Pierre, F.H., Guzylack-Piriou, L., and Houdeau, E. (2017) Food-grade TiO2 impairs intestinal and systemic immune homeostasis, initiates preneoplastic lesions and promotes aberrant crypt development in the rat colon. *Sci Rep*, **7**, 40373.
13. Urrutia-Ortega, I.M., Garduno-Balderas, L.G., Delgado-Buenrostro, N.L., Freyre-Fonseca, V., Flores-Flores, J.O., Gonzalez-Robles, A., Pedraza-Chaverri, J., Hernandez-Pando, R., Rodriguez-Sosa, M., Leon-Cabrera, S., Terrazas, L.I., van Loveren, H., and Chirino, Y.I. (2016) Food-grade titanium dioxide exposure exacerbates tumor formation in colitis associated cancer model. *Food Chem Toxicol*, **93**, 20-31.
14. Nogueira, C.M., de Azevedo, W.M., Dagli, M.L., Toma, S.H., Leite, A.Z., Lordello, M.L., Nishitokukado, I., Ortiz-Agostinho, C.L., Duarte, M.I., Ferreira, M.A., and Sipahi, A.M. (2012) Titanium dioxide induced inflammation in the small intestine. *World J Gastroenterol*, **18**, 4729-4735.

15. Trouiller, B., Reliene, R., Westbrook, A., Solaimani, P., and Schiestl, R.H. (2009) Titanium dioxide nanoparticles induce DNA damage and genetic instability in vivo in mice. *Cancer research*, **69**, 8784-8789.
16. Shi, Z.Q., Niu, Y.J., Wang, Q., Shi, L., Guo, H.C., Liu, Y., Zhu, Y., Liu, S.F., Liu, C., Chen, X., and Zhang, R. (2015) Reduction of DNA damage induced by titanium dioxide nanoparticles through Nrf2 in vitro and in vivo. *Journal of Hazardous Materials*, **298**, 310-319.
17. Sycheva, L.P., Zhurkov, V.S., Iurchenko, V.V., Daugel-Dauge, N.O., Kovalenko, M.A., Krivtsova, E.K., and Durnev, A.D. (2011) Investigation of genotoxic and cytotoxic effects of micro- and nanosized titanium dioxide in six organs of mice in vivo. *Mutation research*, **726**, 8-14.
18. Vandebriel, R.J., Vermeulen, J.P., van Engelen, L.B., de Jong, B., Verhagen, L.M., de la Fonteyne-Blankestijn, L.J., Hoonakker, M.E., and de Jong, W.H. (2018) The crystal structure of titanium dioxide nanoparticles influences immune activity in vitro and in vivo. *Particle and fibre toxicology*, **15**, 9.
19. Cui, Y., Liu, H., Ze, Y., Zhang, Z., Hu, Y., Cheng, Z., Cheng, J., Hu, R., Gao, G., Wang, L., Tang, M., and Hong, F. (2015) Corrigendum: Gene Expression in Liver Injury Caused by Long-Term Exposure to Titanium Dioxide Nanoparticles in Mice. *Toxicol Sci*, **146**, 202.
20. Ruiz, P.A., Moron, B., Becker, H.M., Lang, S., Atrott, K., Spalinger, M.R., Scharl, M., Wojtal, K.A., Fischbeck-Terhalle, A., Frey-Wagner, I., Hausmann, M., Kraemer, T., and Rogler, G. (2017) Titanium dioxide nanoparticles exacerbate DSS-induced colitis: role of the NLRP3 inflammasome. *Gut*, **66**, 1216-1224.
21. IARC (2010) IARC MONOGRAPHS ON THE EVALUATION OF CARCINOGENIC RISKS TO HUMANS: Carbon Black, Titanium dioxide and Talc. **Volume 93**.
22. Council, N.R. (2007) Toxicity testing in the 21st century: a vision and a strategy. *National Academies Press, Washington, DC*.
23. Krewski, D., Acosta, D., Jr., Andersen, M., Anderson, H., Bailar, J.C., 3rd, Boekelheide, K., Brent, R., Charnley, G., Cheung, V.G., Green, S., Jr., Kelsey, K.T., Kerkvliet, N.I., Li, A.A., McCray, L., Meyer, O., Patterson, R.D., Pennie, W., Scala, R.A., Solomon, G.M., Stephens, M., Yager, J., and Zeise, L. (2010) Toxicity testing in the 21st century: a vision and a strategy. *J Toxicol Environ Health B Crit Rev*, **13**, 51-138.
24. Zhao, X., Sheng, L., Wang, L., Hong, J., Yu, X., Sang, X., Sun, Q., Ze, Y., and Hong, F. (2014) Mechanisms of nanosized titanium dioxide-induced testicular oxidative stress and apoptosis in male mice. *Particle and fibre toxicology*, **11**, 47.
25. Chen, Z., Wang, Y., Wang, X., Zhuo, L., Chen, S., Tang, S., Zhao, L., Luan, X., and Jia, G. (2018) Effect of titanium dioxide nanoparticles on glucose homeostasis after oral administration. *J Appl Toxicol*.
26. Hu, H., Guo, Q., Wang, C., Ma, X., He, H., Oh, Y., Feng, Y., Wu, Q., and Gu, N. (2015) Titanium dioxide nanoparticles increase plasma glucose via reactive oxygen species-induced insulin resistance in mice. *J Appl Toxicol*, **35**, 1122-1132.
27. Kang, J.L., Moon, C., Lee, H.S., Lee, H.W., Park, E.M., Kim, H.S., and Castranova, V. (2008) Comparison of the biological activity between ultrafine and fine titanium dioxide particles in RAW 264.7 cells associated with oxidative stress. *J Toxicol Env Heal A*, **71**, 478-485.
28. Park, E.J., Yi, J., Chung, K.H., Ryu, D.Y., Choi, J., and Park, K. (2008) Oxidative stress and apoptosis induced by titanium dioxide nanoparticles in cultured BEAS-2B cells. *Toxicology letters*, **180**, 222-229.
29. Chen, Z., Wang, Y., Ba, T., Li, Y., Pu, J., Chen, T., Song, Y., Gu, Y., Qian, Q., Yang, J., and Jia, G. (2014) Genotoxic evaluation of titanium dioxide nanoparticles in vivo and in vitro. *Toxicology letters*, **226**, 314-319.
30. Zijno, A., De Angelis, I., De Berardis, B., Andreoli, C., Russo, M.T., Pietraforte, D., Scorza, G., Degan, P., Ponti, J., Rossi, F., and Barone, F. (2015) Different mechanisms are involved in

oxidative DNA damage and genotoxicity induction by ZnO and TiO nanoparticles in human colon carcinoma cells. *Toxicol In Vitro*, **29**, 1503-1512.

31. Saquib, Q., Al-Khedhairy, A.A., Siddiqui, M.A., Abou-Tarboush, F.M., Azam, A., and Musarrat, J. (2012) Titanium dioxide nanoparticles induced cytotoxicity, oxidative stress and DNA damage in human amnion epithelial (WISH) cells. *Toxicol In Vitro*, **26**, 351-361.
32. Jin, C.Y., Zhu, B.S., Wang, X.F., and Lu, Q.H. (2008) Cytotoxicity of titanium dioxide nanoparticles in mouse fibroblast cells. *Chem Res Toxicol*, **21**, 1871-1877.
33. Shukla, R.K., Sharma, V., Pandey, A.K., Singh, S., Sultana, S., and Dhawan, A. (2011) ROS-mediated genotoxicity induced by titanium dioxide nanoparticles in human epidermal cells. *Toxicol In Vitro*, **25**, 231-241.
34. De Angelis, I., Barone, F., Zijno, A., Bizzarri, L., Russo, M.T., Pozzi, R., Franchini, F., Giudetti, G., Uboldi, C., Ponti, J., Rossi, F., and De Berardis, B. (2013) Comparative study of ZnO and TiO(2) nanoparticles: physicochemical characterisation and toxicological effects on human colon carcinoma cells. *Nanotoxicology*, **7**, 1361-1372.
35. Long, T.C., Saleh, N., Tilton, R.D., Lowry, G.V., and Veronesi, B. (2006) Titanium dioxide (P25) produces reactive oxygen species in immortalized brain microglia (BV2): implications for nanoparticle neurotoxicity. *Environmental science & technology*, **40**, 4346-4352.
36. Bhattacharya, K., Davoren, M., Boertz, J., Schins, R.P., Hoffmann, E., and Dopp, E. (2009) Titanium dioxide nanoparticles induce oxidative stress and DNA-adduct formation but not DNA-breakage in human lung cells. *Particle and fibre toxicology*, **6**, 17.
37. Huerta-Garcia, E., Perez-Arizti, J.A., Marquez-Ramirez, S.G., Delgado-Buenrostro, N.L., Chirino, Y.I., Iglesias, G.G., and Lopez-Marure, R. (2014) Titanium dioxide nanoparticles induce strong oxidative stress and mitochondrial damage in glial cells. *Free Radic Biol Med*, **73**, 84-94.
38. Niska, K., Pyszka, K., Tukaj, C., Wozniak, M., Radomski, M.W., and Inkielewicz-Stepniak, I. (2015) Titanium dioxide nanoparticles enhance production of superoxide anion and alter the antioxidant system in human osteoblast cells. *Int J Nanomed*, **10**, 1095-1107.
39. Reeves, J.F., Davies, S.J., Dodd, N.J., and Jha, A.N. (2008) Hydroxyl radicals (*OH) are associated with titanium dioxide (TiO(2)) nanoparticle-induced cytotoxicity and oxidative DNA damage in fish cells. *Mutation research*, **640**, 113-122.
40. Krauskopf, J., Verheijen, M., Kleinjans, J.C., de Kok, T.M., and Caiment, F. (2015) Development and regulatory application of microRNA biomarkers. *Biomark Med*, **9**, 1137-1151.
41. Hendrickx, D.M., Souza, T., Jennen, D.G.J., and Kleinjans, J.C.S. (2017) DTNI: a novel toxicogenomics data analysis tool for identifying the molecular mechanisms underlying the adverse effects of toxic compounds. *Arch Toxicol*, **91**, 2343-2352.

Addendum I

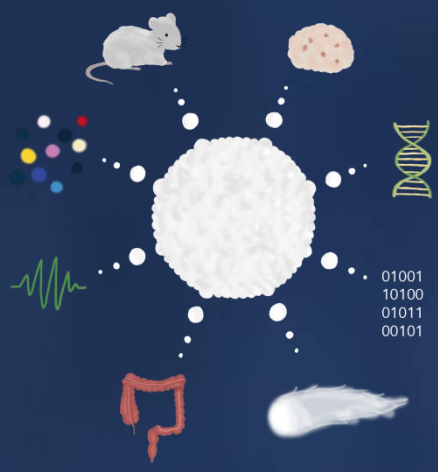

The focus of this thesis is to study the facilitation of colorectal cancer (CRC) development after ingestion of food additive titanium dioxide (E171) and extend the current knowledge by investigating mechanisms that underlie these effects. The results showed that E171 induces oxidative stress in an acellular environment, DNA damage *in vitro*, gene expression changes *in vitro* and *in vivo* towards an impairment of the immune system, DNA repair, induction of oxidative stress, dysregulation of olfactory/GPCR receptor family, and facilitation of development of CRC. In addition, the relative contribution of the nanoparticle (NPs) (<100 nm) fraction (40% of E171) and the microparticle (MPs) (>100 nm) fraction (60% of E171) were investigated *in vitro*. Results showed that NPs also induce oxidative stress in an acellular environment whereas MPs induced oxidative stress *in vitro*. Both MPs and NPs provoked DNA damage and gene expression changes indicating effects in signalling, inflammation, immune system, transport, and cancer. This valorisation chapter reflects on how the scientific results described in this thesis can be applied to create societal value.

I- Societal and economic relevance

The societal relevance of the present thesis is regarding the consumers. E171 is present in a large number of products as shown in Chapter 1 and the exposure is occurring every day for all age groups. Recently, consumers have become more insistent over the need for greater transparency in their food and drinks. These changes have propelled the movement to simpler and natural ingredients affecting product formulation and consumer purchase interest. The consumers are looking for more information and can easily find them on the internet. However, the related information is not necessary scientific based conclusions and this has an impact on the consumers. It is important that they can find the scientific based conclusions about the possible risks engendered by the ingestion of these products as shown in this thesis.

Additionally, this thesis indicates a link between ingestion of E171 and enhancement of CRC. CRC is, worldwide, the second most common cancer in women and the third in men (1). With a morbidity of 614,000 cases for women and 740,000 for men, CRC represents 9.2% and 10% of all cancers respectively (1). CRC is also the fourth leading cause of cancer death in the world accounting for about 700,000 deaths in 2012. While taking into account the demographic projection, the global burden of CRC is estimated to increase by 60% to more than 2.2 million new cases and 1.1 million deaths by 2030 (1). The distribution of CRC burden varies around the world with almost 55% of all cases and about 60% of all death occurring in developed regions. Indeed, incidence rates are

estimated to be the highest in Australia/New Zealand (32.2 and 44.8 per 100,000 women and men respectively) and the lowest in Western Africa (3.8 and 4.5 per 100,000 women and men respectively). In view of these figures and studies on the effects of diet, CRC has been strongly associated with the adverse effects of lifestyle and diet (2).

The economic burden of CRC was recently estimated in Spain between €20,478 and 27,000€ per patient for 5 years after diagnosis (3). A rough estimation according to the number of cancer worldwide (1.4 million in 2012) would show a global economic burden between €5.5 and 7.3 billion per year for the year 2012 and between €9.0 and 11.9 billion per year for the year 2030. This estimation does not include extra costs due to the side effects of the chemotherapy which were estimated monthly in US per patient at $1,480 for hematologic, $1,253 for respiratory, and $1,213 for endocrine and metabolic adverse effects (4).

The results of this thesis contribute to both goals, more knowledge and transparency over food additive E171 and contributing in identifying underlying causes of the western diet leading to an increase of development of CRC.

II- Target group

Outside of the academic community, the industries using TiO_2 in their products are interested by our research results. Due to the pressure of the consumers, certain industries are investigating the potential adverse effects of TiO_2 and opting for alternatives. Indeed, because of the incertitude regarding the potential adverse effects of TiO_2, some big companies have already claimed that they stopped using TiO_2 in all or some of their products like Lutti®, Verquin®, and Dunkin' Brands, Inc®. Furthermore, the possible changes in the regulation of E171 are well monitored by the industries and E171 is considered as an example of what could also happen with other food additives.

Additionally, the national organisation like Anses (Agence nationale de sécurité sanitaire de l'alimentation, de l'environnement et du travail), NVWA (Nederlandse Voedsel- en Warenautoriteit), BfR (Bundesinstitut für Risikobewertung), and FDA (Food and Drug Administration) as well as regulators are also interested by the results of this thesis. Following the change of classification of TiO_2 by the IARC in 2010 from non-carcinogen to possible carcinogen (group 2B) concerns of the different routes of exposure like ingestion rose. Therefore, in 2016, the EFSA made a re-evaluation of TiO_2 as a food additive (5). Based on the available genotoxicity database, EFSA concluded that,

absorption, distribution, and excretion of micro- and nanosized TiO_2 particles after oral exposure are unlikely to represent a genotoxic hazard *in vivo*. In addition, in June 2017, the risk assessment committee of the European Chemical Agency (ECHA) classified TiO_2 as a suspected human carcinogen (category 2) via inhalation (6). Furthermore, national organisation could include the results of this thesis in a risk assessment which could lead to possible changes of the use of TiO_2 in food products.

The research presented in this thesis is of interest to the whole population for all age groups. Indeed, TiO_2 is present in various food products from dairy products (milk, cheese, and ice cream), milk replacements (powdered milk), sweets (M&M's®, Mentos®, chewing-gums, and cookies), drinks (soft drinks, sport drinks, and syrups), dressings and sauces (salad dressings), and food supplements (multivitamin pills) (7-11). The exposure varies depending on the age group. Children are the most exposed to TiO_2 due to their higher ingestion of sweets and toothpaste. Depending on the diet (US, UK, Dutch or a global European diet) the estimation ranged from 0.67 mg TiO_2/kg_{bw}/day in the Netherlands (children between 2-6 years old) to 5.5 mg/kg_{bw}/day as estimated by the European Food Safety Authority (EFSA) (children between 3 and 9 years old). For the adults, the estimated concentrations were lower from 0.17 mg TiO_2/kg_{bw}/day between 7-69 years in the Netherlands to 4.1 and 4.0 mg TiO_2/kg_{bw}/day for adolescents (10-17 years old) and adults (18-64 years old) respectively as estimated by the EFSA (5,10,11).

III- Translation of the results

The results from this thesis provide an opportunity for further research and a basis for a future risk assessment of TiO_2 as food additive. Following new evidence provided in the last 2 years, the European Commission asked the EFSA to include 4 new studies in their re-evaluation of titanium dioxide as food additive. In addition, due to the new evidence about the adverse effects of E171, the French government asked the Anses to perform more research about potential adverse effects of ingestion of E171.

IV- Innovation of the research

When the IARC decided, in 2010, to re-evaluate TiO_2 to assess its potential impact on development of cancer, enough evidence was found from the inhalation route where tumours in the lungs of rats were observed (12). Based on these results, the IARC decided to change the classification of TiO_2 from non-carcinogen to possible carcinogen to humans. During this evaluation, the IARC stated that there was not enough evidence regarding the other routes of exposure (dermal contact and ingestion) as well as the modes of action of TiO_2 underlying these adverse effects (kinetics, *in vivo* and *in vitro* genotoxicity, cytotoxicity, presence of inflammation, and penetration of TiO_2 through the skin).

Since the change of classification by the IARC, the ingestion route via the ingestion of food products containing E171 has been studied. Within these studies, a collaborative group has observed that after ingestion of 5 mg/kg_{bw}/day of E171 for 10 weeks in a chemically induced colorectal cancer mouse model with azoxymethane (AOM) and dextran sodium sulphate (DSS), the number of tumour was increased when E171 was also orally administrated (13). From the results of this study, the mechanisms behind this development of tumours were studied. **Chapter 2, 3, and 4** present the first whole-genome mRNA analysis of the colon of mice after oral exposure to E171 in 3 different mouse models: a normal BALB/c, a chemically induced CRC with AOM/DSS, and a transgenic model. These analyses provide potential underlying molecular mechanisms modulated after oral exposure to E171. The mechanisms of *in vitro* genotoxicity, cytotoxicity and oxidative stress on a human colon cell line (Caco-2) in **Chapter 5** confirmed previous findings of other cells lines. Additionally, the contribution of each fraction of E171 was identified and shows that the NPs and the MPs fraction contribute to these adverse effects. The mechanisms were also investigated *in vitro* in Caco-2 cells in **Chapter 6** to assess the contribution of the MPs and NPs at the mRNA level. To the best of our knowledge, this was the first time that the contribution of each fraction of E171 was assessed.

V- Implementation of the valorisation

The knowledge acquired in this thesis offers a potential mechanistic explanation of the enhancement of tumours in the colon of mice and can be used for further translational and applied purposes, for instance for risk assessment in food safety of food additive E171. With this risk assessment, competent regulatory authorities could decide if policy changes are necessary. Risk assessments may set conditions for more healthy food. Consumers will be better informed regarding products that are added in the food.

References

1. Globocan (2012) CANCER FACT SHEETS: COLORECTAL CANCER.
2. Arnold, M., Sierra, M.S., Laversanne, M., Soerjomataram, I., Jemal, A., and Bray, F. (2017) Global patterns and trends in colorectal cancer incidence and mortality. *Gut*, **66**, 683-691.
3. Andrade, P., Sacristan, J.A., and Dilla, T. (2017) The Economic Burden of Cancer in Spain: A Literature Review. *Health Economics & Outcome Research: Open Access*, **3**.
4. Latremouille-Viau, D., Chang, J., Guerin, A., Shi, S., Wang, E., Yu, J., and Ngai, C. (2017) The economic burden of common adverse events associated with metastatic colorectal cancer treatment in the United States. *J Med Econ*, **20**, 54-62.
5. EFSA (2016) Re-evaluation of titanium dioxide (E 171) as a food additive. *EFSA Journal*, **14**, e04545-n/a.
6. Charles, S., Jomini, S., Fessard, V., Bigorgne-Vizade, E., Rousselle, C., and Michel, C. (2018) Assessment of the in vitro genotoxicity of TiO2 nanoparticles in a regulatory context. *Nanotoxicology*, 1-18.
7. EFSA (2016) Scientific Opinion on the re-evaluation of titanium dioxide (E 171) as a food additive. *EFSA Journal*, **14**, 4545-4638.
8. Lomer, M.C.E., Thompson, R.P.H., Commisso, J., Keen, C.L., and Powell, J.J. (2000) Determination of titanium dioxide in foods using inductively coupled plasma optical emission spectrometry. *Analyst*, **125**, 2339-2343.
9. Peters, R.J., van Bemmel, G., Herrera-Rivera, Z., Helsper, H.P., Marvin, H.J., Weigel, S., Tromp, P.C., Oomen, A.G., Rietveld, A.G., and Bouwmeester, H. (2014) Characterization of titanium dioxide nanoparticles in food products: analytical methods to define nanoparticles. *J Agric Food Chem*, **62**, 6285-6293.
10. Weir, A., Westerhoff, P., Fabricius, L., Hristovski, K., and von Goetz, N. (2012) Titanium dioxide nanoparticles in food and personal care products. *Environmental science & technology*, **46**, 2242-2250.
11. Rompelberg, C., Heringa, M.B., van Donkersgoed, G., Drijvers, J., Roos, A., Westenbrink, S., Peters, R., van Bemmel, G., Brand, W., and Oomen, A.G. (2016) Oral intake of added titanium dioxide and its nanofraction from food products, food supplements and toothpaste by the Dutch population. *Nanotoxicology*, **10**, 1404-1414.
12. IARC (2010) IARC MONOGRAPHS ON THE EVALUATION OF CARCINOGENIC RISKS TO HUMANS: Carbon Black, Titanium dioxide and Talc. **Volume 93**.
13. Urrutia-Ortega, I.M., Garduno-Balderas, L.G., Delgado-Buenrostro, N.L., Freyre-Fonseca, V., Flores-Flores, J.O., Gonzalez-Robles, A., Pedraza-Chaverri, J., Hernandez-Pando, R., Rodriguez-Sosa, M., Leon-Cabrera, S., Terrazas, L.I., van Loveren, H., and Chirino, Y.I. (2016) Food-grade titanium dioxide exposure exacerbates tumor formation in colitis associated cancer model. *Food Chem Toxicol*, **93**, 20-31.

Addendum II

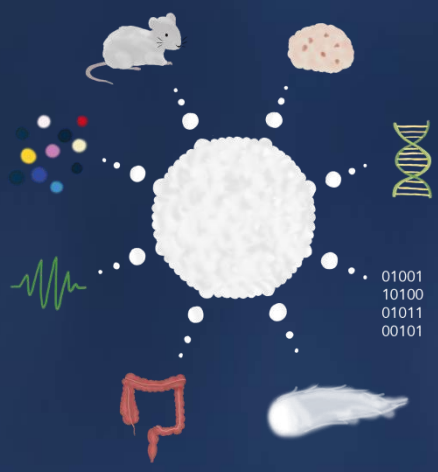

I would like to use the last pages of this thesis to express my thanks to all the people that have helped to make this thesis possible.

First I would like to give my sincere thanks to my promotion team. I would like to thank Prof. dr. Henk van Loveren to allow me to participate in this amazing project that was to show that a food additive was not as safe as we thought it was. We faced many challenges during this project and I am very grateful for all the scientific knowledge and help you gave me to overcome these. I would also like to thank my second promotor Prof. dr. Theo de Kok for all the help you provided me and also all the tips and tricks in how to make your way in this scientific world. I would also like to thank my co-promotor Dr. Jacco Briedé for your advice especially with the ESR where I had the joy to work with diskettes again. I would also like to thank Prof. dr. Jos Kleinjans to include me in his team, your questions during the team meetings were always very interesting.

In this project we also collaborated with a group in Mexico. I would like to first thank Prof. dr. Yolanda Chirino for all her knowledge on E171, her help with planning experiments and sending samples. I am very happy I have met you in person and I wish we can still work together in the future. I would like to also thank the team over there, Luis Garduño Balderas, Carolina Rodríguez Ibarra, and Ismael Urrutia Ortega who I have unfortunately never met in person but your help in this project was very valuable and I am grateful for the experiments you have performed to make this thesis happen.

During this thesis I also had the opportunity to go to the RIVM and meet Margriet Park who I thank for teaching me a lot on the functionality of nanoparticles. I would like to thank Wendy Rodenburg and Conny van Oostrom for their help to find the transgenic mouse model as well as Minne Heringa and Agnes Oomen for the nice explanation about the daily intake of TiO_2. I would also like to thank Liset de la Fonteyne, Rob Vandebriel, Wim de Jong, Wout Slob, and Eric Gremmer for all the different help you provided for me. I would also like to thank the PhD students there, Hedwig Braakhuis and Christina Giannakou, for the nice discussions when I was there.

For helping and giving good feedback for the preparation of the METC, I would like to thank Dr. Ad van Bodegraven.

I would also like to thank members of the assessment committee Prof. dr. J.C.S. Kleinjans, Prof. dr. A. Opperhuizen, Prof. dr. C.T.A. Evelo, Dr. M.B. Heringa, and Dr. A. van Bodegraven for reading and allowing me to defend my thesis.

After 4 years in the TGX team I would like to thank everybody for the nice time, discussion, and help. I would like to thank Christa, Sandrien, Rob, René R., Danyel, Tom, Daniël, Maarten, and Tilman for the help in the IT- and administrative work. I would also like to thank Twan, Simone, Florian, Juma, and Sacha for the constructive discussions. I would also like to thank the PhD students, current or graduated, Rajinder, Evelyn, Terezinha, Jarno, Jian, Juan, Manon for the fun times, the knowledge we shared to help each other, and the support. I would like to thank Jason too, you were almost part of our team too, thank you for all the cakes you baked for us.

I would also like to thank the technicians Yannick, Marcel, Jolanda, and Harm-Jan who helped me to order products and figure out some details of my experiments. I would like to specially thank Yannick for helping me with my mouse experiment, I don't see how I could have dissected all these mice without you. I would also like to thank the people that already left the department, Dennie, Karen, Rachel, Penny, Wim, Lize, and Linda. I hope we can see each other again in the future. I would like to give a special thanks to Marlon for teaching me the data analysis of the microarrays, for helping me with some experiments, I am very grateful you were here to help me with all this. I would like to thank all the people joining for lunch for the nice discussion, for the tasting of all the different types of food, for making me discover your cultures, these times have been very rich.

After spending 4 years in the same room, I would like to thank my roommates Almudena, Julian, and Daniela for all the help we provided to each other in the good and bad times. Almudena, I will always remember you saying "lunch time" in your own way every day and regularly singing "Lemon tree". Julian, we had very interesting discussions and you were always there when I needed you, thank you for that. Daniela, we haven't been roommates for long but I enjoyed working with you to succeed in growing organoids, it was nice to have you for a roommate.

I would like to give a special thanks to my paranymphs René S. and Marcha, both of you are my best friends and I would like to tell you how much I appreciate that you are there on my defence day to support me. You have been supporting me my whole thesis and were there for me for all steps of it. Marcha, you have been my roommate since day 1 (+ 1 month) and we have lived our theses at the same time. We helped each other, we figured how to do things together, and we learned a lot about each other subjects. This was great to do that together. René S, I've met you during my studies and not only you

helped me there but also during my thesis. Your support, your friendship, and all the fun times really helped me through these 4 years.

I would also like to thank my 2 Master students Carolyn and Marloes. I was very pleased to teach you in the lab and you both did a very good job. I am happy to see now that you are both very busy with your own PhD. I look forward to come to your own defences. Carolyn, aka minion number 1, aka maid of honour, you have been a very independent student. I will always remember all the times you came to the room panicking because you thought that the cells were infected! I am also very pleased you have been my maid of honour to my wedding and this will remain an amazing memory. Marloes, aka minion number 2, we have done a lot of different work together but especially with mice. You really helped me with that and we managed to have a great time preparing all this. I am very happy I have met you.

Je souhaite dédier ma thèse à 3 de mes grands-parents qui m'ont vu la commencer mais qui malheureusement nous ont quittés entre temps. À mon papy Roger qui m'a toujours montré que c'est en travaillant dur que l'on obtenait ce qu'on voulait. À ma mamy Paulette qui n'a jamais cru que j'arriverai jusque là mais qui était très fière de me voir sur la voie de devenir docteur. À mon papy Michel que j'imagine faire une petite danse pour montrer qu'il est content pour moi et dire toutes les 5 min qu'il est fier. À vous tous, j'aurai aimé que vous soyez là pour me voir finir. Je suis heureuse que ma mamy Odette soit encore là pour partager ce moment avec moi. J'aurai aimé que tu puisses venir pour ma soutenance.

Je voudrais remercier mes parents, mon frère Nicolas, ma sœur Adeline, ma belle-sœur Céline, et mon beau-frère Antoine pour m'avoir aidée et soutenue dans les moments de joie et les moments difficiles. Votre soutien m'a été des plus précieux surtout avec la distance qui nous sépare. J'espère qu'après ma soutenance vous aurez compris sur quoi j'ai travaillé pendant ces 4 ans. Un petit merci aussi pour mes petites nièces Aimy, Louise et Charline et mon petit neveu Amael, continuez à être aussi mignons. Je voudrais remercier encore plus mes parents qui sans eux et leur soutien moral et financier pour me payer des études, je n'aurais jamais pu faire cette thèse. Merci d'avoir fait en sorte que l'on puisse faire les études que l'on voulait et où on le voulait.

Ik wil ook mijn schoonfamilie, René B., Ina, Jaron en Nienke bedanken voor hun steun en om te proberen te begrijpen wat ik heb gedaan de laatste 4 jaren.

Pour bien finir, Leon, mon mari, je voudrais te remercier de tout mon cœur. J'aurai jamais cru y'a plus de 13 ans que nous serions là aujourd'hui, et que je te dirais « oui » deux fois avec 6 mois d'écart ! Sans toi, ton soutien à la maison dans les bons comme les mauvais moments, on ne serait pas là aujourd'hui.

Addendum III

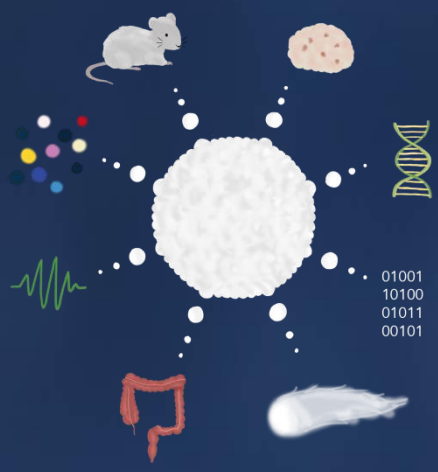

Héloïse Proquin was born in La Roche-sur-Yon, France on September 7th 1988. In 2006, she started her studies to become a private laboratory technician in biology and biochemistry in Laval, France and graduated in 2008. She finished her Bachelor in the University of Nantes in biology, biochemistry and molecular biology in 2010. That same year, she did an internship at Danone research in Wageningen before starting her Master in Toxicology and Environmental Health at the University of Utrecht.

In March 2014, she started her PhD at the department of Toxicogenomics at Maastricht University under the supervision of Prof. dr. Henk van Loveren, Prof. dr. Theo de Kok, and Dr. Jacco Briedé. The aims of this thesis were to understand the molecular mechanisms after oral exposure to food additive E171 on the development of colorectal cancer and the contribution of each fraction of E171 (the nanoparticle and microparticle fractions). The results obtained during these 4 years are presented in this thesis.

Addendum IV

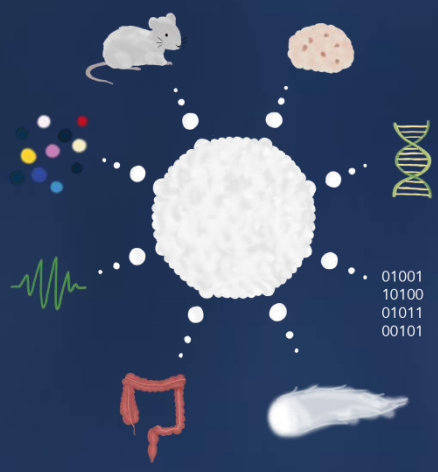

Full papers

Titanium dioxide food additive (E171) induces ROS formation and genotoxicity: contribution of micro and nano-sized fractions.
Héloïse Proquin, Carolina Rodríguez-Ibarra, Carolyn G. J. Moonen, Ismael M. Urrutia Ortega, Jacob J. Briedé, Theo M. de Kok, Henk van Loveren, Yolanda I. Chirino
Mutagenesis, January 2017; 32 (1): 139-149. doi: 10.1093/mutage/gew051

Corrigendum: Titanium dioxide food additive (E171) induces ROS formation and genotoxicity: contribution of micro and nano-sized fractions.
Mutagenesis, August 2018, gey011, https://doi.org/10.1093/mutage/gey011

Gene Expression Profiling in Colon of Mice Exposed to Food Additive Titanium Dioxide (E171)
Héloïse Proquin, Marlon J. Jetten, Marloes C.M. Jonkhout, Luis G. Garduño-Balderas, Jacob J. Briedé, Theo M. de Kok, Yolanda I. Chirino, Henk van Loveren
Food and Chemical Toxicology, January 2018, Volume 111, Pages 153-165.
doi: 10.1016/j.fct.2017.11.011

Time course gene expression data in colon of mice after exposure to food-grade E171
Héloïse Proquin, Marlon J. Jetten, Marloes C.M. Jonkhout, Luis G. Garduño-Balderas, Jacob J. Briedé, Theo M. de Kok, Yolanda I. Chirino, Henk van Loveren
Data in Brief, February 2018, Volume 16, Pages 531-600. doi: 10.1016/j.dib.2017.11.067

Transcriptomics analysis reveals new insights in E171-induced molecular alterations in a mouse model of colon cancer
Héloïse Proquin, Marlon J. Jetten, Marloes C.M. Jonkhout, Luis G. Garduño-Balderas, Jacob J. Briedé, Theo M. de Kok, Henk van Loveren, Yolanda I. Chirino
Scientific Reports, December 2018, Volume 8 (1):9738. doi:10.1038/s41598-018-28063-z

Abstracts and conferences

Effect of E171 (titanium dioxide nanoparticles) on the development of colorectal cancer
Héloïse Proquin, Carolyn Moonen, Jacob J. Briedé, Theo M. de Kok, Henk van Loveren
Poster and speed presentations at the annual meeting of the Netherlands Society of Toxicology (NVT), June 2015, Soesterberg, The Netherlands.

Effect of E171 (titanium dioxide nanoparticles) on the development of colorectal cancer
Héloïse Proquin, Carolyn Moonen, Jacob J. Briedé, Theo M. de Kok, Henk van Loveren
Poster presentation at the ESF-EMBO Conference on Interaction Between the Immune System and Nanomaterials: Safety and Medical Exploitation, October 2015, Pultusk, Poland.

Effect of E171 (titanium dioxide nanoparticles) on the development of colorectal cancer
Héloïse Proquin, Carolyn Moonen, Jacob J. Briedé, Theo M. de Kok, Henk van Loveren
Poster presentation at the faculty GROW science day, Maastricht University, November 2015, Maastricht, The Netherlands.

Oral exposure of E171 in Balb/c mice induces gene expression changes in the colon
Héloïse Proquin, Marloes C.M. Jonkhout, Marlon J. Jetten, Luis G. Garduño Balderas, Jacob J. Briedé, Theo M. De Kok, Yolanda I. Chirino, Henk van Loveren
Poster and platform presentations at the annual meeting of the Netherlands Society of Toxicology (NVT), June 2016, Soesterberg, The Netherlands.

Oral exposure of E171 in Balb/c mice induces gene expression changes in the colon
Héloïse Proquin, Marloes C.M. Jonkhout, Marlon J. Jetten, Luis G. Garduño Balderas, Jacob J. Briedé, Theo M. De Kok, Yolanda I. Chirino, Henk van Loveren
Toxicology Letters 2016; 258, Supplement, S277. doi: 10.1016/j.toxlet.2016.06.1968
Poster presentation at the 52nd European Congress of the European Societies of the Toxicology (EUROTOX), September 2016, Sevilla, Spain. Poster number: P17-048

Transcriptomics approach reveals increase of drug metabolism and downregulation of immune system induced by food additive E171 (titanium dioxide) in an AOM/DSS mouse model

Héloïse Proquin, Marloes C.M. Jonkhout, Marlon J. Jetten, Luis G. Garduño Balderas, Jacob J. Briedé, Theo M. De Kok, Yolanda I. Chirino, Henk van Loveren

Poster and speed presentations at the faculty GROW science day, Maastricht University, November 2016, Maastricht, The Netherlands.

Analysis of the contribution of the micro- and nanoparticles in food-grade titanium dioxide (E171) on the transcriptome in Caco-2 cells and potential impact on colon cancer development

Jacco J. Briedé, ***Héloïse Proquin***, Theo M. de Kok, Henk van Loveren

Toxicology Letters 2018. doi: 10.1016/j.toxlet.2018.06.727